Identification of the metalloproteinase Adamts1 and Nitric Oxide as new therapeutic targets in aortic diseases

Universidad Autónoma de Madrid
Programa de Doctorado en
Biociencias Moleculares

Jorge Oller Pedrosa
Madrid 2017

Universidad Autónoma de Madrid

Departamento de Biología Molecular
Facultad de Ciencias

Tesis doctoral

Identification of the metalloproteinase Adamts1 and Nitric Oxide as new therapeutic targets in aortic diseases

Jorge Oller Pedrosa

Madrid 2017

Universidad Autónoma de Madrid

Departamento de Biología Molecular
Facultad de Ciencias

Identification of the metalloproteinase Adamts1 and Nitric Oxide as new therapeutic targets in aortic diseases

Tesis doctoral presentada por:

Jorge Oller Pedrosa

Licenciado en Bioquímica y Biología por la Universidad Autónoma de Madrid

Máster en Biomedicina Molecular por la Universidad Autónoma de Madrid

Bajo la dirección de los Doctores:

Juan Miguel Redondo Moya
Miguel Campanero García

Grupo de Regulación de la Expresión Génica en el Remodelado Vascular

Centro Nacional de Investigaciones Cardiovasculares (CNIC)

Los doctores: **Juan Miguel Redondo**, Profesor de investigación en el Centro Nacional de Investigaciones Cardiovasculares (CNIC) y **Miguel Ramón Campanero García,** científico titular del CSIC

CERTIFICAN

Que Don J**orge Oller Pedrosa**, licenciado en Bioquímica y Biología por la Universidad Autónoma de Madrid, ha realizado bajo su dirección el trabajo titulado "Identification of the metalloproteinase Adamts1 and Nitric Oxide as new therapeutic targets in aortic diseases"**,** presenta como Tesis Doctoral para alcanzar el grado de Doctor por la Universidad Autónoma de Madrid.

Revisado el presente trabajo, expresamos nuestra conformidad para la presentación del mismo en el departamento de Biología Molecular de la Universidad Autónoma de Madrid, por considerar que reúne los requisitos necesarios para ser sometido a evaluación ante el tribunal correspondiente para optar al grado de Doctor en Biociencias Moleculares.

Y para que conste, firmamos el presente certificado; en Madrid a 3 mayo del 2017.

Esta tesis ha sido realizada en el Centro Nacional de Investigaciones Cardiovasculares (CNIC) bajo la dirección de los Drs. Juan Miguel Redondo Moya y Miguel Ramón Campanero García.

Jorge Oller Pedrosa ha disfrutado de una beca de Formación de Personal Investigador (FPI-MICINN) 2010-2014 BES-2010-034552 asociada al proyecto SAF2009-10708 del Dr. Juan Miguel Redondo.

A mis padres y a mi abuelo Domingo

Imagination will often carry us to worlds that never were.

Carl Sagan

It is not the strongest of the species that survives, nor the most intelligent that survives. It is the one that is most adaptable to change.

Ignorance more frequently begets confidence than does knowledge. It is those who so positively assert that this or that problem will never be solved by science.

Charles Darwin

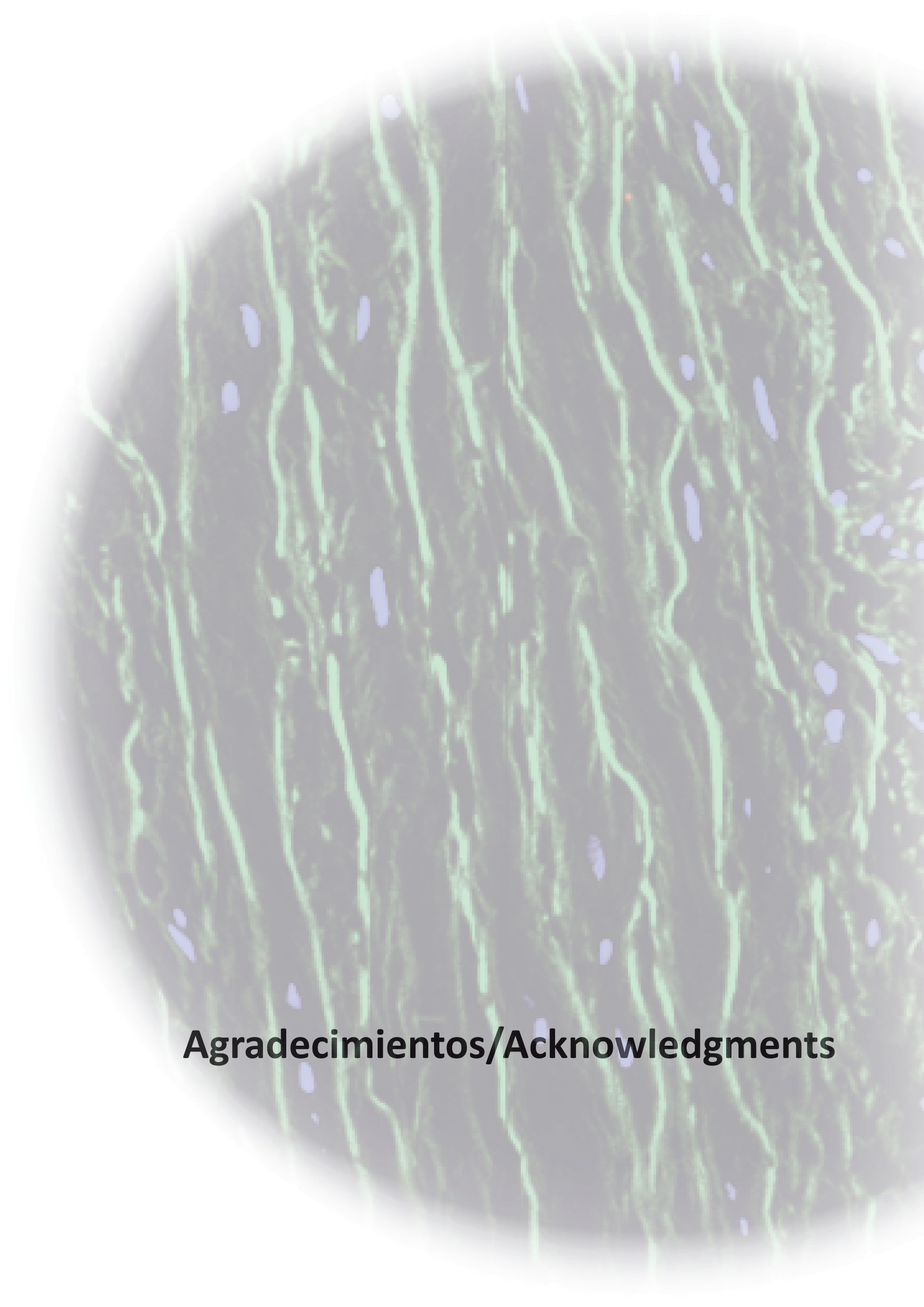

Agradecimientos/Acknowledgments

Parece mentira que tras tanto tiempo, haya llegado la hora de escribir el trabajo que hemos hecho durante todos estos años.

Aún recuerdo como si fuese ayer mismo mi llegada al labo, con mucha ilusión pero desorientado y sin saber muy bien cómo iba a acabar todo ésto. Reflexionando durante estos días puedo decir que estoy muy orgulloso del resultado. Nuestro trabajo como científicos está basado principalmente para crear, romper, refutar paradigmas e hipótesis. Tras mirar con perspectiva, creo que hemos aportado un granito más de arena a la ciencia.

Desde bien pequeño siempre he sido un "perro verde", me encantaba leer y aprender cosas de "bichos". Aunque parezca extraño, siempre que me preguntaban qué quería ser de mayor, respondía que biólogo para estar en el Amazonas descubriendo nuevas especies de peces; todo un potencial Frank de la Jungla. Pero tiempo después, la biología molecular me sedujo y no pude resistirme a seguir profundizando más sobre ella. Aún así, mis padres no entienden cómo acabé dedicándome a ésto, pero saben que me apasiona y la verdad, no podría dedicarme a otra cosa. La gente que me conoce bien sabe que no podría vivir sin mis "bichos". Todos estos años desde que me mudé a Madrid desde mi pequeño pueblo en Valladolid, han sido sumamente intensos. Han estado llenos de retos, grandes esfuerzos, ilusiones y decepciones; miles de horas trabajando con experimentos algunos exitosos y otros muchos fallidos; he conocido a grandes personas y amigos, que han hecho que estos años hayan estado llenos de vivencias y experiencias que han hecho que crezca como persona, profesional y en los que he sido muy feliz. Hoy escribiendo estas páginas, me siento que estoy un pasito más cerca de alcanzar mis sueños.

Es imposible escribir en pocas palabras todo el agradecimiento a la gente que me ha acompañado en este tiempo y que han contribuido en mayor o menor parte a convertirme en lo que soy hoy en día.

Tengo que empezar a dar gracias a la persona que permitió que empezase este trabajo, a mi mentor, el Dr. Juan Miguel Redondo, "**JuanMi**". Sin su apoyo no podría haber llegado hasta aquí, no hubiera aprendido tanto, ni llegado a buen puerto. Gracias por invertir un montón de horas desinteresadamente en enseñarme a pensar y planear los experimentos de manera óptima.

Gracias también a mi co-director de tesis el Dr. Miguel Campanero "**Campi**", por sus consejos, a enseñarme a ser detallista y meticuloso; y sobre todo, en las largas reuniones de los "peques" en las que ha participado en los numerosos y largos "brain-stormings". Por ayudarnos a organizar los experimentos y poner los controles adecuados. Sin mis dos directores de tesis sería imposible haber terminado este trabajo.

Es de obligación, dar miles de gracias a “mamá molecular” **Arantza**, quien fue mi mentora cuando aterricé por el CNIC. Casi todo lo que sé de técnicas de biología molecular es gracias a ella. Gracias a tu inmensa y “santísima” paciencia y a tu buena ciencia. Por todo esto, he crecido profesionalmente, he aprendido a pensar y en parte, soy lo que soy. Gracias por estar siempre disponible incluso en la distancia, por escuchar y discutir las ideas descabelladas que me rondaban la cabeza. Gracias por tirar del carro cuando se atascaban los experis e incluso mejorar y aclarar aún más los resultados. Siempre te estaré agradecido.

También tengo que agradecer a mi “mamá aórtica” **Nere**. Sin ti no hubiera sido capaz de hacer ni una “eco”. Por todas las inhalaciones de anestésico, los pinchazos de virus; por las interminables horas que hemos pasado en el animalario, que estábamos coordinados como una “cinta de montaje”. Gracias a ti he aprendido un montón en modelos animales. Me has transmitido un montón de energía y motivación para seguir adelante. Muchísimas gracias de verdad, siempre me acordaré de esos momentos. Sin ti hubiera sido imposible terminar.

Angel Luis, tengo que agradecerte que me invitases a participar en tu proyecto de PMCA y de acogerme en tu casa durante el congreso de UK. ¡Muchas gracias!

Gracias a **Lizet**, sin tu ayuda hubiera sido imposible. Gracias por tu motivación, la energía que has puesto, todo el curro que has sacado adelante y tus sugerencias. Además, tu punto de vista clínico me ha enseñado un montón. Me has hecho mucho más amenas las largas jornadas de trabajo con nuestras anécdotas y vivencias. Me has enseñado que, aunque la vida puede darte palos, hay luz al final del túnel. ¡Ánimo! Sé que llegarás lejos.

Muchísimas gracias **Bea**. Llegamos prácticamente a la vez, y aunque, compartimos “bench” que durante meses no llegamos a las manos :). Gracias por tus sugerencias y tus conocimientos en histología me han ayudado muchísimo. Eres una gran profesional, te fijas en todos los mínimos detalles. Gracias también a **Silvia** por echarme una mano cuando estaba a tope. Y gracias a las dos por las risas y las charlas escatológicas a la hora de comer. Sólo puedo decir que: ¡Sed fuertes y mirar para delante!.

Tengo mucho que agradecer a **Noe** que aunque ya no esté por el labo, me sacó un montón de trabajo con los virus cuando no daba abasto. Siempre creíste en mí, ¡muchas gracias!.

A **Rut**, gracias por sacarme un montón de trabajo y pasarte muchísimas tardes en el microtomo, sin ti todo ésto no hubiera sido posible.

A **María Jesús**, que en poco tiempo recibirás mi “legado” con toneladas de datos y experimentos. Tengo que decirte que tienes madera de científica. Solo te digo que fuerza y ¡a por la tesis!.

A todos los partícipes de las reuniones de los ”peques”, gracias por aportar ideas y soluciones a los experimentos fallidos y a hacer un poco más amenas las largas tardes de los martes.

Gracias al resto del laboratorio porque he aprendido muchísimo de ellos. A **Paula, Antonio, Josué, Sara, Alicia, Raquel, a Loli y a Pablo,** por enseñarme técnicas que no conocía y por echar una mano cuando lo necesitaba. Siempre me acordaré de vosotros.

Tengo que agradecer muchísimo a nuestras expertas en ecografía **Ana Vanesa y Lorena,** y también a **Luis Jesús Borreguero** por toda la dedicación y atención que habéis puesto en nuestro trabajo, todas las horas que habéis gastado en nuestros experimentos; vuestras ideas y el punto de vista clínico; las cancelaciones y reservas de última hora… además de ser grandísimas personas, por todo esto, ¡Mil gracias!.

I have to give thanks to **Dr. Nistal, Dr. Milewicz and Dr. De Bacquer** for human samples and advices, thanks a lot!

Muchas gracias a **Ana Briones y Mercedes Salaices** por sus consejos y los experimentos sobre contractilidad y de óxido nítrico.

Gracias también a **Alicia García Arroyo** por sus consejos sobre las metaloproteasas y zimografía. Nos has aportado otro punto de vista y un montón de ayuda.

Gracias a toda la gente del ala primera norte, a los **"Alicios" y "Miguelangeles"**, que hacen un ambiente excepcional. Gracias especialmente a **Cris y Antonio,** por todas las risas y charlas. Siempre me acordaré con cariño de los buenos momentos.

A nuestros managers y secretarios **Antonio Jesús, Laura, Almudena y Eduardo** por todos los trámites, gestiones y papeleos que nos solucionáis rápidamente y nuestras charlas en la hora de la comida.

A mis compañeros de la Uni: a **Isa, Sandra y Alberto**, añoro muchísimo nuestros viajes a cualquier sitio. Aunque nos podamos ver unas pocas veces al año por la distancia, siempre me acuerdo de vosotros. Sobre todo por las charlas, risas, vivencias y tiempo que pasamos juntos. Hicisteis que mi paso por la universidad fuese inolvidable. Gracias por vuestra amistad y apoyo incondicional. ¡Sandra, ahora te toca a ti leer tu tesis!.

Gracias al grupo de las "**Zordas**" por apoyarme y poder contar todos mis proyectos, éxitos y frustraciones aunque a veces os suene a "chino" y os lo tenga que "traducir". Por esas interminables cenitas en "Yellowstone". Gracias por ayudarme a desconectar cuando más lo he necesitado, sin vosotros sobrevivir a la tesis hubiese sido mucho más difícil. Tengo que agradecer muchísimo a **Luis** ¡Qué vale un Potosí!, a parte de lo buenísima y genuina persona que eres, nos has hecho reír hasta decir basta. Mil gracias por ayudarme con el inglés de la tesis, siempre te deberé una.

Aunque sólo nos conocemos desde hace poco más de un año, tengo que agradecer a **Raúl**, toda su ayuda prestada para nuestras pequeñas bestias, cuando nos diste a **Ella** nos cambió la vida para bien, y ahora tenemos a **Yoel** educándose contigo. Sin lugar a dudas nos has marcado en nuestra vida con tus consejos, tu gran corazón, lo buena persona que eres y tu gran sentido del humor. Seguiremos preguntándote cientos de veces ¡Muchas gracias!.

Tengo que agradecer también a mi familia política que va en aumento: a **Mariví, Fernando, Carlos y Naomi** por sentirme uno más desde el primer día. Sois un autentico modelo de superación y trabajo duro. Gracias por los detalles que marcan la diferencia.

A toda mi familia, que siempre se ha interesado en todos los pasos que he dado. Gracias por aconsejarme y escucharme; gracias de verdad. Especialmente quiero agradecer a mi abuelo **Domingo**, que aunque ya no está entre nosotros, me inculcó unos valores como son la perseverancia y el trabajo. Siempre me acordaré de las tardes en las que me contabas tus aventuras y las enfermedades que lidiabas día a día, que por fortuna ahora son raras. Has sido una fuente de inspiración en mi vida. A mi tío **Matías** que aunque no estés cerca, me indicaste con tu humildad y respeto a trabajar para conseguir mis sueños. Además tengo que agradecer a **Pili,** que me ha guiado durante toda mi carrera científica, diciéndome los pros y los contras. Aunque muchas veces no he querido hacerte caso … Aún así, ¡muchas gracias!.

Tengo que agradecer muchísimo a mis **padres**, sin ellos hubiera sido imposible llegar hasta aquí. Siempre habéis creído en mí y ofrecido una vida llena de posibilidades. Nunca me habéis puesto límites en mis ambiciones pero siempre con los pies en la tierra. Marché del pueblo muy joven y sin conocer a nadie no me pusisteis ninguna traba. Muchas gracias por los días que habéis gastado en ayudarme con mis estudios y mis problemas. Sois todo un ejemplo a seguir. Siempre me habéis aconsejado e intentado guiar, sin vosotros no sería quién soy. Os agradezco muchísimo todo lo que me habéis enseñado y lo que me enseñaréis.

A **Fer**, por ser mi pilar de apoyo y nunca permitir que tirase la toalla, mi fuente de desconexión y de equilibrio. Gracias por darme otro punto de vista de la vida fuera de la ciencia y poner los pies en la tierra y en la realidad. Sin ti hubiera sido imposible sobrevivir a la tesis. Gracias por entender que algunos días me ausentaba tanto física como mentalmente, e intentar que volviese a tierra.... En resumen, gracias por hacerme feliz.

Seguramente me deje a alguien en el tintero… Muchas gracias a todo el mundo que de una manera u otra ha influido o participado en esta etapa de mi vida.

Lo que parece ser el final, suele ser en realidad un nuevo comienzo.

Jorge

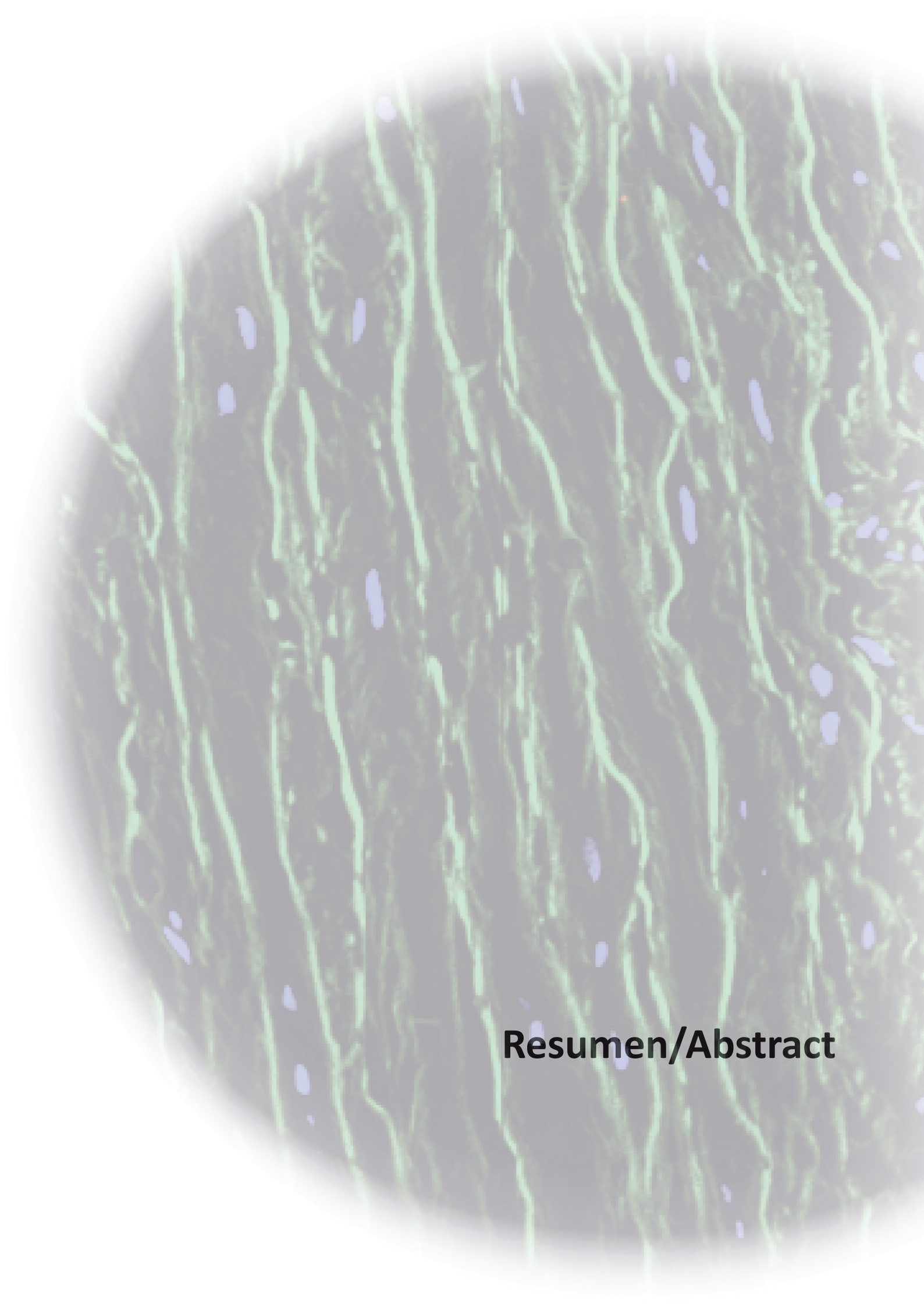

Resumen/Abstract

El principal origen de las enfermedades cardiovasculares es el **remodelado vascular patológico.** Este proceso es el causante de la degeneración quística de la media, que produce un debilitamiento de la pared aórtica y, por lo tanto, un aumento del riesgo de aneurismas. **Un aneurisma** es una dilatación localizada de una arteria y puede ser causa de una disección arterial. Algunos desórdenes genéticos, como es el caso del Síndrome de Marfan, tienen predisposición a padecer aneurismas aórticos. Actualmente no existe ningún tratamiento farmacológico para frenar o disminuir el tamaño del aneurisma y prevenir su disección. Trabajos previos indican que las metaloproteasas de matriz extracelular tienen un papel clave durante el proceso de remodelado vascular. Por otra parte, estudios anteriores muestran que la **metaloproteasa extracelular Adamts1** podría tener un papel importante en la homeostasis y patología vascular. Sin embargo, el papel específico de Adamts1 en la homeostasis vascular y en el desarrollo de aneurismas aórticos es desconocido.

El objetivo principal de este trabajo ha sido determinar, por una parte, los mecanismos y agentes moleculares por los cuales Adamts1 se expresa en la vasculatura y, por otra parte, las funciones de esta metaloproteasa en la homeostasis vascular y en el desarrollo de la patología de aneurismas aórticos.

En primer lugar, dilucidamos que diferentes agentes remodeladores como son **VEGF, Ang-II, IL1-β y TNF-α, inducen la expresión de Adamts1 de manera diferencial** en células vasculares dependiente de estímulo. Esta regulación es debida a una activación diferencial de los factores de transcripción, de tal manera que, la activación de la ruta de señalización de Calcineurina-NFAT por VEGF y de la fosforilación de C/EBPβ por Ang-II, IL1β y TNF-α inducen el aumento de la expresión de Adamts1 en células vasculares *in vitro* e *in vivo*. Finalmente, hemos descrito el **papel funcional de Adamts1** en la pared vascular. En este caso, hemos observado que los ratones deficientes en *Adamts1* poseen características similares al Síndrome de Marfan como son: mayor longitud de huesos largos, hipercifosis, enfisema pulmonar y una mayor incidencia de aneurismas aórticos. Por otra parte, hemos analizado en detalle los mecanismos moleculares en los que esta metaloproteinasa está involucrada en aneurismas. En este caso, hemos comprobado que la deficiencia de *Adamts1* produce un aumento de expresión de la óxido nítrico sintasa inducible (NOS2) y un aumento de óxido nítrico (NO). Posteriormente, hemos descrito que tanto el modelo de ratón del Síndrome de Marfan estudiado, como los pacientes con este desorden presentan niveles disminuidos de Adamts1 que correlacionan con niveles aumentados de NOS2 y NO. Además, hemos probado que la actividad de NOS2 sería la responsable de la aortopatía inducida en ambos modelos, tanto en los ratones con Síndrome de Marfan como en los deficientes para *Adamts1*, ya que inhibidores específicos de NOS2 reducen la dilatación aórtica y la degeneración de la media en ambos modelos de ratón.

Por lo tanto, **en este trabajo hemos descrito nuevos mecanismos moleculares y dianas terapéuticas que están presentes en enfermedades aórticas**, y que hoy en día no tienen tratamiento. Todos estos resultados aportan nuevos mediadores como son ADAMTS1 y NOS2 en enfermedades aórticas, especialmente en el Síndrome de Marfan.

The main cause of cardiovascular diseases is the **pathological vascular remodeling**. This process is the cause of the cystic medial degeneration of the aortic wall that produces a weakening and, therefore, an increased risk of aneurysms. **An aneurysm** is a localized dilation of an artery and may be causative of an arterial dissection. Some genetic disorders such as Marfan Syndrome are prone to aortic aneurysms. Currently, there is no pharmacological treatment to slow or decrease the size of the aneurysm and to prevent its dissection. Previous studies indicate that extracellular matrix metalloproteinases play a key role during the vascular remodeling process. Moreover, previous reports show that **extracellular metaloprotease Adamts1** could play an important role in homeostasis and vascular pathology. However, the specific role of Adamts1 in vascular homeostasis and in the development of aortic aneurysm is unknown.

The main objective of this work was to determine, on one hand, the mechanisms and molecular mediators by which Adamts1 is expressed in the vasculature and, on the other hand, the functions of this metalloprotease in vascular homeostasis and in the development of aortic aneurysm.

First, we elucidate that different remodeling agents such as **VEGF, Ang-II, IL1-β and TNF-α induce the expression of Adamts1 differentially in stimulus-dependent vascular cells.** This regulation is due to a differential activation of transcription factors: VEGF through Calcineurin-NFAT pathway and the phosphorylation of C/EBPβ by Ang-II, IL1β and TNF-α induce a increase in the expression of Adamts1 in vascular cells *in vitro* and *in vivo*. Finally, we have described **the functional role of Adamts1** in the vascular wall. In this case, we have observed that *Adamts1*-deficient mice have characteristics similar to Marfan Syndrome such as: longer bone length, hyperkinesis, and pulmonary emphysema and a higher incidence of aortic aneurysms. On the other hand, we have analyzed in detail the molecular mechanisms in which this metalloproteinase is involved in aneurysms. In this case, we have found that *Adamts1* deficiency induces an increase of expression of inducible nitric oxide synthase (NOS2) and in Nitric Oxide (NO). Subsequently, we have found that both, mice and patients with Marfan Syndrome have decreased levels of Adamts1 that correlate with increased levels of NOS2 and NO. The activity of NOS2 would be responsible for the induced aortopathy in both models, since specific inhibitors of NOS2 reduce the aortic dilation and the degeneration of the Tunica Media in Marfan and *Adamts1*-deficient mice.

Therefore, **in this work we have described new molecular mechanisms and therapeutic targets that are present in aortic diseases**, that nowadays have no treatment. All these results provide new mediators targets such as ADAMTS1 and NOS2 in aortic diseases, specifically in Marfan Syndrome.

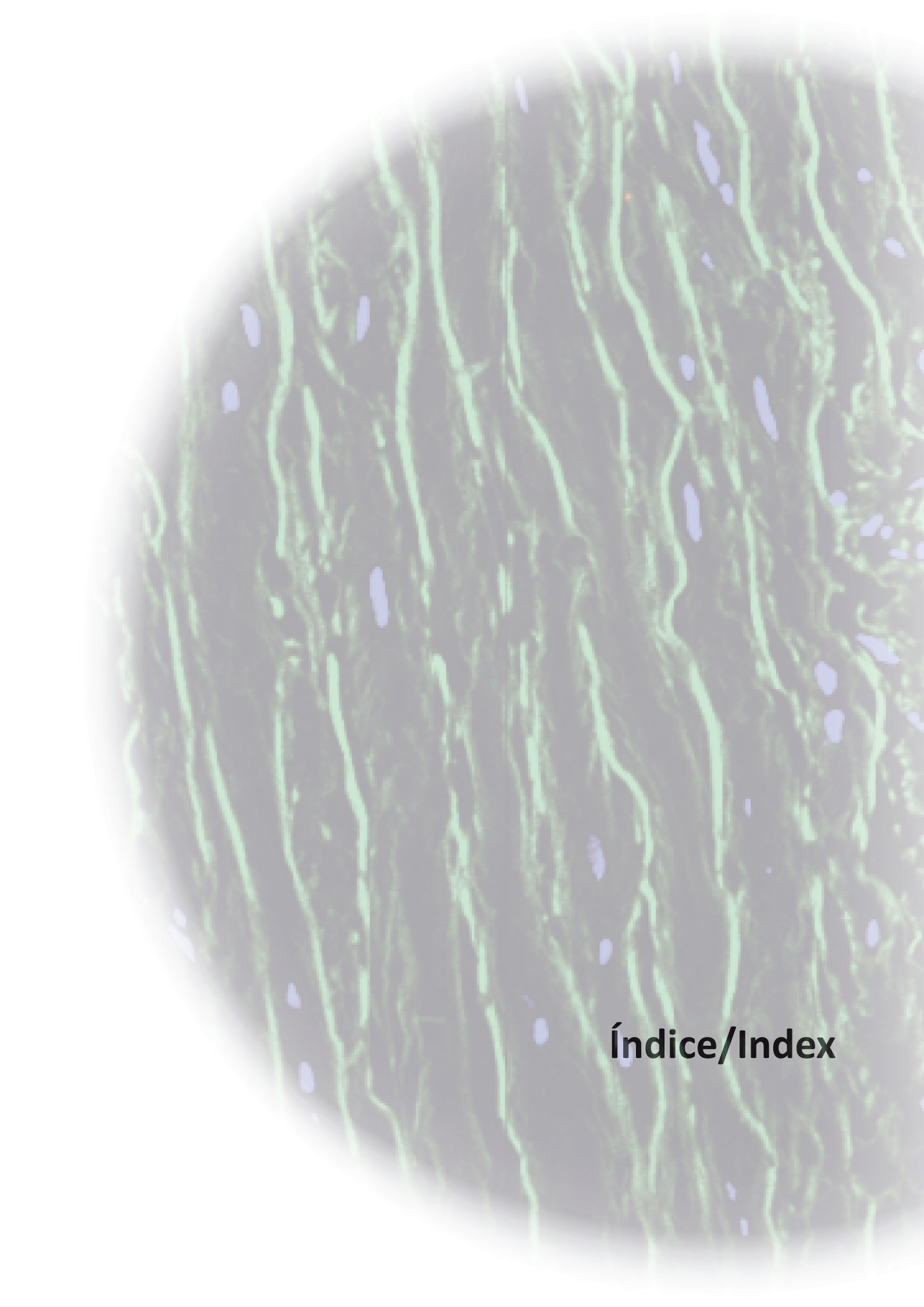

Índice/Index

Abbreviations 1

Introduction 6

1. General aspects of the cardiovascular system 6

1.2. Arteries 7

1.3. Aorta 8

2. Aortic Aneurysms (AA) 9

2.1. Hereditary disorders that course with aortic aneurysm 10

2.2.1. Marfan Syndrome (MFS) 10

2.2.2. Loeys-Dietz Syndrome (LDS) 11

2.2.3. Cutis Laxa Syndrome (CLS) 11

2.2.4. Vascular type Enhlers-Danlos Syndrome (EDS-IV) 11

2.2.5. Bicuspid aortic valve (BAV) 11

2.2.6. Non-syndromic familial forms of TAA with dissection (FTAAD) 12

3. Pathological vascular wall remodeling 14

3.1. Molecular pathways implicated in vascular wall remodeling 15

3.1.1. Transforming Growth Factor beta (TGFb) pathway 15

3.1.2. Angiotensin-II (Ang-II) signaling 16

3.1.3. Vascular Endothelial Growth Factor (VEGF) 17

3.1.4. Nitric Oxide (NO) 18

4.Extracellular Matrix (EMC) role in AA 21

4.1. Ground or amorphous substance 21

4.2. Fibrous proteins 21

5. ECM metalloproteinases 21

5.1. Matrix Metalloproteinases (MMPs) 23

5.2. ADAM proteases 23

5.3. ADAMTS and ADAMTSL family members 23

5.4.1. Hereditary connective tissue diseases related to ADAMTS(L) family members 25

5.4.2. ADAMTS1 26

Justification and Objectives 29

Results 33

» **Article 1:** C/EBPβ and Nuclear Factor of Activated T Cells Differentially Regulate Adamts-1 Induction by Stimuli Associated with Vascular Remodeling 34

» **Article 2:** Nitric oxide mediates aortic disease in mice deficient in the metalloprotease Adamts1 and in a mouse model of Marfan syndrome 49

Discussion 83

Conclusiones/Conclusions 96

Bibliography 101

Appendix 115

» **Article 3:** Plasma Membrane Calcium ATPase Isoform 4 Inhibits Vascular Endothelial Growth Factor–Mediated Angiogenesis Through Interaction With Calcineurin 116

» **Article 4:** PLK1 regulates contraction of postmitotic smooth muscle cells and vascular homeostasis 117

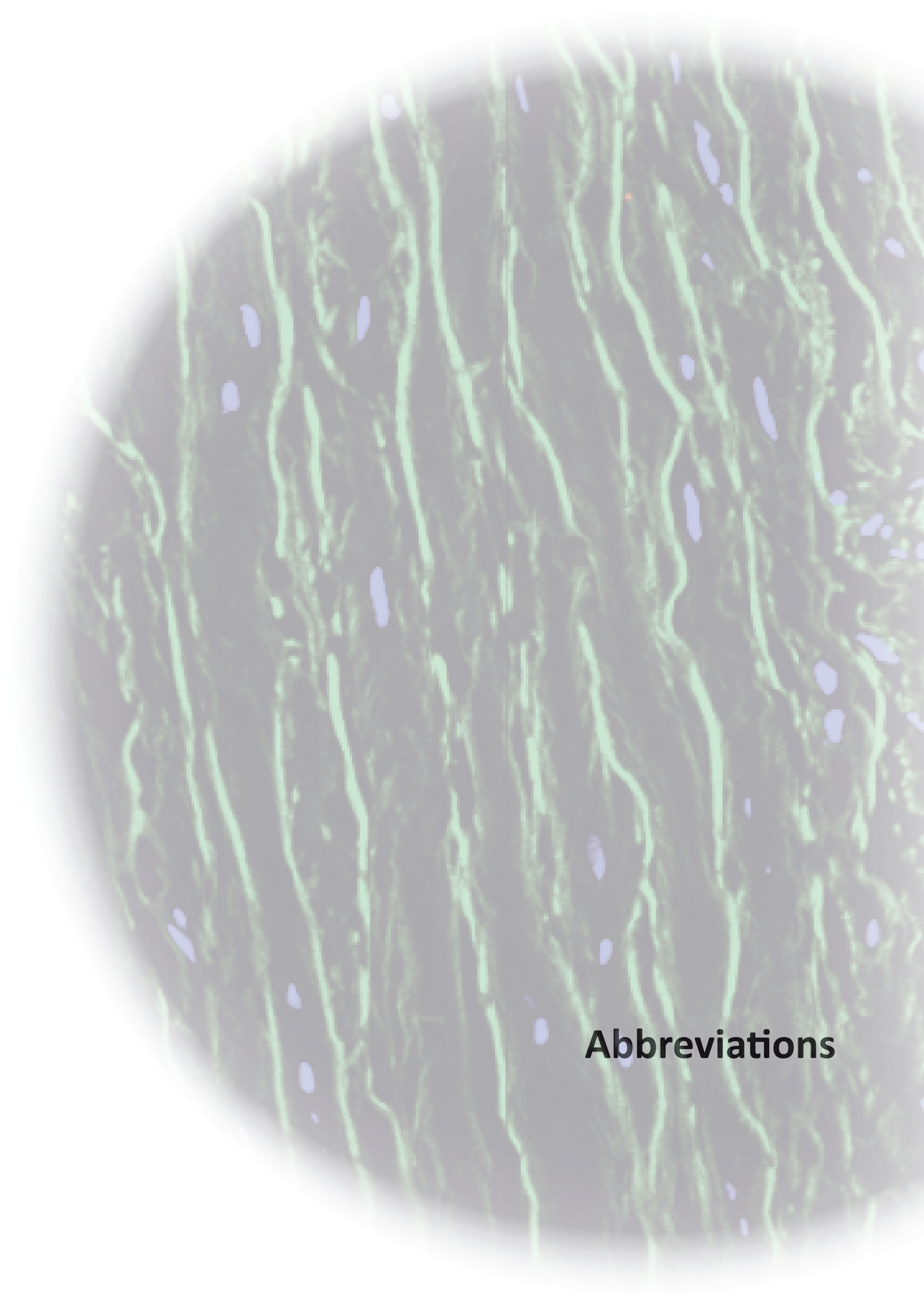

Abbreviations

- **AA:** Aortic Aneurysm
- **AAA:** Abdominal Aortic Aneurysm
- **AbAo:** Abdominal Aorta
- **ACTA2:** Actin Alpha 2, Smooth Muscle Aorta
- **ADAM:** A Disintegrin and Metalloproteinase
- **ADAMTS:** A Disintegrin and Metalloproteinase with Thrombospondin motifs
- **ADAMTSL:** ADAMTS-Like
- **AKT:** RAC-alpha serine/threonine-protein kinase
- **Ang-II:** Angiotensin-II
- **AR:** Aortic Ring
- **AsAo:** Ascending Aorta
- **BAV:** Bicuspid Valve
- **BGN:** Biglycan
- **BH_4:** Tetrahydrobiopterin
- **C/EBPβ:** CCAAT-Enhancer-Binding Protein Beta
- **cGMP:** Cyclic Guanosine Monophosphate
- **CLS:** Cutis Laxa syndrome
- **CN:** Calcineurin
- **COL3A1:** Collagen Type III Alpha 1 Chain
- **COMP:** Oligomeric Cartilage Protein
- **Cox-2:** Cyclooxigenase type 2
- **CsA:** Cyclosporine-A
- **DAG:** Diacylglycerol
- **DNA:** Deoxyribonucleic Acid
- **DSCR1:** Down syndrome critical region 1
- **ECM:** Extracellular matrix
- **ECs:** Endothelial Cells or endothelium
- **EDS:** Enhlers-Danlos Syndrome
- **EDRF:** Endothelium Derived Relaxing Factor
- **EFEMP2:** EGF Containing Fibulin Like Extracellular Matrix Protein 2 or Fibullin4.
- **EGF:** Epidermal Growth Factor

Abbreviations

- **ELN:** Elastin gene
- **FAD:** Flavin Adenine Dinucleotide
- **FBN1:** Fibrillin type 1
- **FMN:** Flavin Mononucleotide
- **FTAAD:** non-syndromic Familial forms of Thoracic Aortic Aneurysm and Dissections
- **GC:** Guanylyl Cyclase
- **GD:** Geleophysic Dysplasia
- **HUVECs:** Human Umbilical Vein Endothelial Cells
- **IFNγ:** Interferon gamma
- **IL-13:** Interleukin 13
- **IL1-β:** Interleukin 1 beta
- **IP3:** Inositol Triphosphate
- **JAK:** Janus Kinase
- **KDR:** Kinase insert Domain Receptor
- **L-NAME:** L-N-nitro-Arginine Methyl Ester
- **L-NMA:** L-N-Mono-Methyl Arginine
- **LAP:** Latency Associated Protein
- **LAP (C/EBPβ isoform):** Liver-enriched Transcriptional Activator Protein
- **LDS:** Loeys-Dietz Syndrome
- **LIP (C/EBPβ isoform):** Liver-enriched Inhibitory Protein
- **LOX:** Lysyl oxidase
- **LPS:** Lipopolysaccharide
- **LTBP:** Latent TGFβ Binding Protein
- **MAPK:** Mitogen Activated Kinases
- **MAT2A:** Methionine Adenosyltransferase 2A
- **MFAP5:** Microfibrillar Associated Protein 5
- **MFS:** Marfan Syndrome
- **MLC:** Myosin Light Chain
- **MLCP:** Myosin Light Chain Phosphatase
- **MLECs:** Mouse Lung Endothelial Cells
- **MMCAT:** Microcornea Chorioretinal Myopathy Atrophy and Telecanthus syndrome
- **MMP:** Matrix Metalloproteinases

- **mRNA:** Messenger Ribonucleic Acid
- **MT-MMP17:** Membrane-Type Matrix Metallopeptidase type 17
- **mTOR:** Mammalian target of Rapamycin
- **MYH11:** Myosin Heavy Chain type 11
- **MYLK:** Myosin light chain kinase
- **NADPH:** Nicotinamide Adenine Dinucleotide Phosphate
- **NF-κB:** Nuclear Factor of Kappa light polypeptide gene enhancer in B cells
- **NO:** Nitric oxide
- **NOS**: Nitric Oxide Synthase
- **NOS1/nNOS:** Nitric Oxide Synthase type 1 / neural Nitric Oxide Synthase.
- **NOS2/iNOS:** Nitric Oxide Synthase type 2 / inducible Nitric Oxide Synthase.
- **PGs**: Proteoglycans
- **PLC:** Phospholypase-C
- **PMCA:** Plasma Membrane Ca2+ ATPase
- **PRKG1:** Protein Kinase, cGMP-Dependent, Type I
- **PYK2:** Protein tyrosine kinase type 2 beta
- **RCAN1:** Regulator of Calcineurin type 1
- **RHO:** ras homolog family member
- **ROS:** Reactive oxygen species
- **SMAD:** Similar to Drosophila gene Mothers Against Decapentaplegic (Mad)
- **SRC:** Scruffy protein kinase
- **STAT:** Signal-Transducer and Activator of Transcription protein
- **TAA:** Thoracic Aortic Aneurysm
- **TAAD:** Thoracic Aortic Aneurysm and dissections
- **TGFR:** Tumor Growth Factor beta Receptor
- **TGFβ:** Tumor Growth Factor beta
- **TNF-α:** Tumor Necrosis Factor Alfa
- **VEGF:** Vascular Endothelial Growth Factor
- **VEGFR:** VEGF Receptor
- **VSMCs**: Vascular Smooth Muscle Cells
- **WMS:** Weill-Marchesani Syndrome
- **vWF:** von-Willebrand coafulation Factor

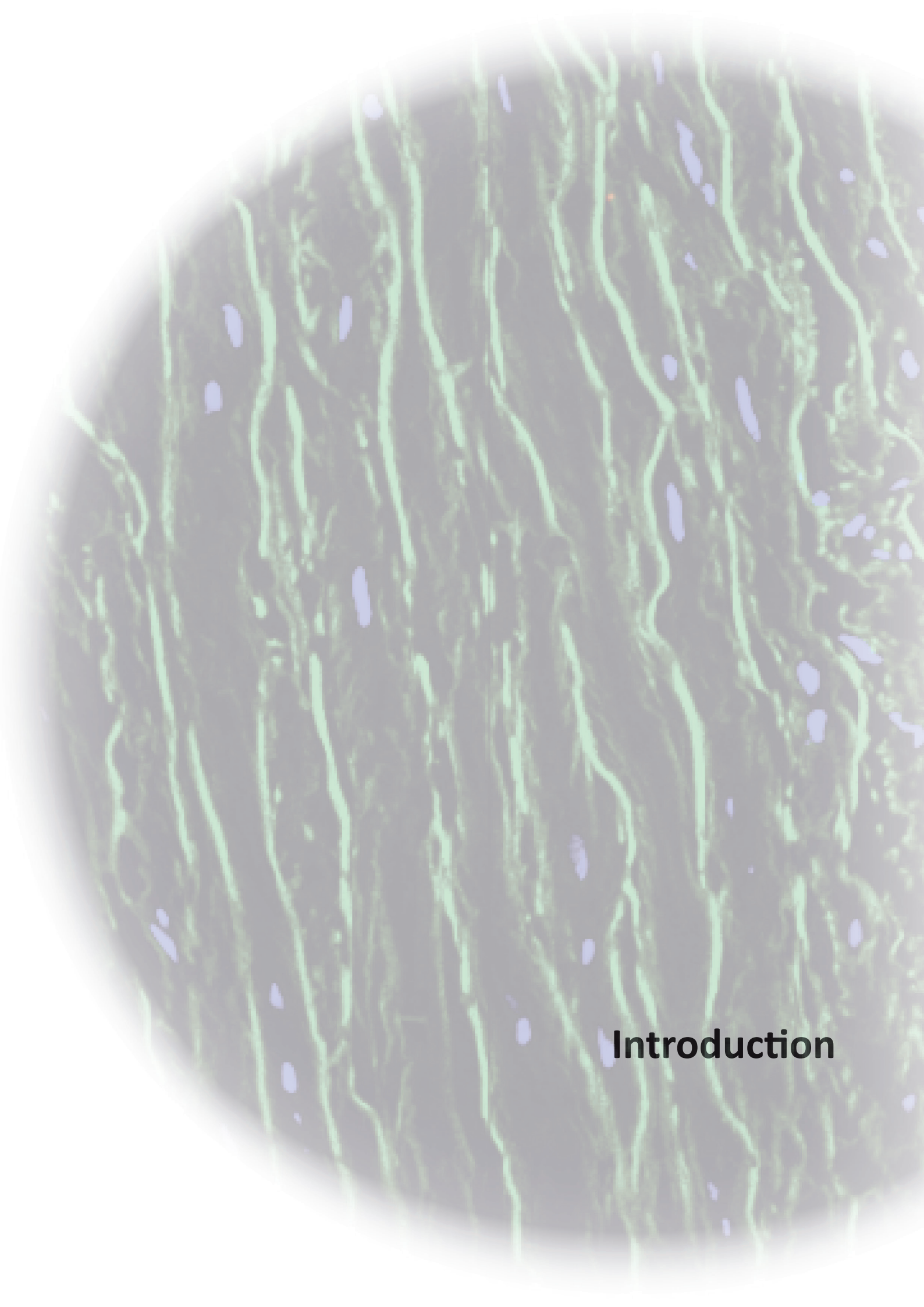

Introduction

1. General aspects of the cardiovascular system

Most of the different groups of animals of certain size and complexity have developed mechanisms for the transport of substances between the different regions of their body. The presence of a true circulatory system, that is, one in which the blood travels through the interior of hollow vessels, is necessary to get adequate rates of transport within the body which can no longer be achieved by diffusion. A closed and well-developed circulatory system is present in chordates, with a number of complementary components (a propulsive organ, arterial distribution system; capillary and venous store and return systems). On these animals, during embryonic development, the cardiovascular system is the first to be developed, highlighting its important role as maintainer of homeostasis[1,2]. In a closed circulation system, blood flows in a continuous circuit of tubes from arteries to veins through capillaries, impulsed by a propulsive organ. In mammals and birds, the heart acts as a pump that pushes blood to the major artery of the body: the aorta, which branches into smaller arteries that pass through body tissues where they branch again into smaller vessels called arterioles. Arterioles, in turn, branch into capillaries that are thin-walled vessels, allowing a high rate of transfer of substances; therefore, they are responsible for supplying oxygen and nutrients directly to the cells through the blood. The circulatory system carries blood unidirectionally towards all parts of the body. Deoxygenated blood, loaded with waste materials, is transported from the capillaries into wider vessels called venules. Venules join to form veins, and then carry the blood back to the heart to be driven into the pulmonary arteries to oxygenate blood through pulmonary capillaries[1-3].

With the evolution of pulmonary respiration, and the elimination of the gills between the heart and the aorta, tetrapods have developed a double high and low pressure circulatory system, with a systemic or high-pressure circuit which provides oxygenated blood to the capillaries of body organs and a lower-pressure pulmonary circuit. In crocodilians, mammals, and birds, both types of movement are completely separated by the presence of two independent cardiac ventricles[4].

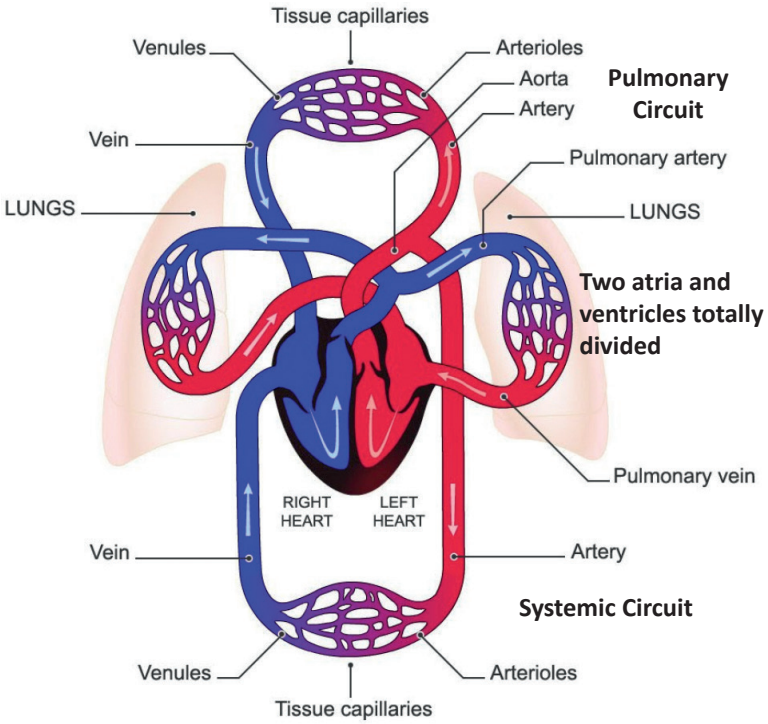

Figure 1: Model depicting the closed double circulatory system present in crocodilians, birds and mammals. (Modified from http://humananatomylibrary.com/diagram-circulatory-system).

1.2. Arteries

All blood vessels leaving the heart are called arteries, regardless whether the blood they are carrying is oxygenated or not. Their main feature is their histological structure, since they need a certain structure to withstand high pressures generated during ventricular contraction. Therefore, large arteries have layers of smooth muscle tissue coated with a series of layers of elastic fibers, which in turn is covered with a thick layer of connective tissue. Thus, the arterial wall is at the same time resilient and elastic. The elasticity of the main arteries allows them to expand after receiving a pulse of blood from the heart after systole, and then contract during ventricular diastole. This aspect is essential for the physiological maintenance of vascular tone. In this way, the pressure change is regulated and continuous blood flow is maintained by the elastic and pulsatile nature of the vessel wall[1,2].

The artery wall consists of **three concentric histological layers**[5]:

- **Internal layer or Tunica Intima:** Constituted by a monolayer of endothelial cells (ECs) and a basal lamina. In the case of large arteries of large animals as in the case of human aorta, there is a subendothelial layer constituted by connective tissue.
- **Tunica Media:** Composed of vascular smooth muscle cells (VSMCs) arranged concentrically, elastic fibers and collagen fibers, in varying proportions depending on the type of artery.
- **Tunica Externa or Adventitia:** Formed by connective tissue, composed mainly of fibroblasts, collagen fibers and resident leukocytes. In arteries greater than 1mm diameter, nutrition of these internal layers is done by the *vasa vasorum*; innervation of the arteries is done by *nervi vasorum*; both cross the Adventitia to the Tunica Media.

The boundaries between the three layers are generally well defined in the arteries. They always have an internal elastic lamina separating the Intima from Media, and have an external elastic lamina that separates the Tunica Media of the Adventitia.

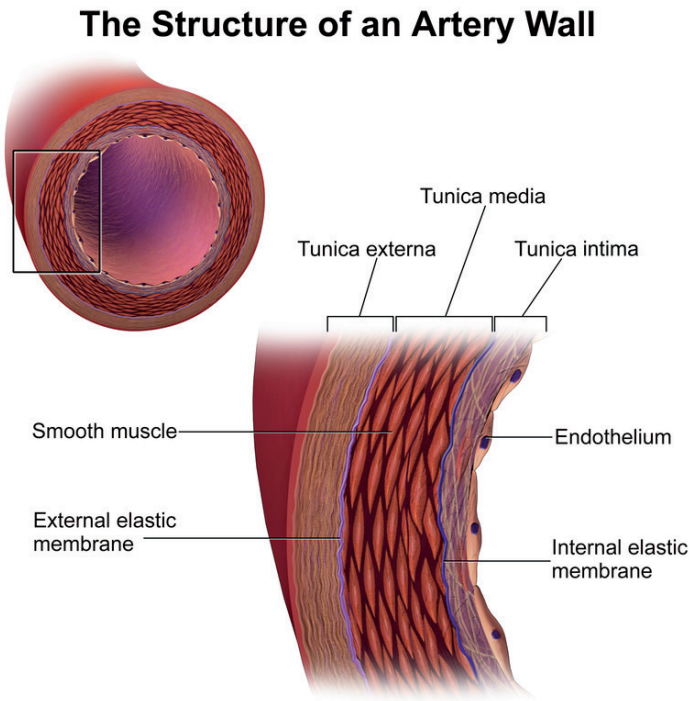

Figure 2: The arterial wall is composed by three concentric histological layers: Tunica intima, Tunica media and Tunica adventitia or externa. (From Wikipedia).

1.3. Aorta

The aorta is the main artery of the body. It begins at the left ventricle and then divides into all the arteries of the circulatory system, except for the pulmonary arteries that are born in the right ventricle. The aorta, besides being a tube with elastic properties, has an active function, dilating during systole to store part of the ejection volume and using its capacity of elastic recoil during diastole driving the remaining blood forward, ensuring the maintenance of continuous blood flow in the periphery during diastole. The aortic wall is in a balance between elasticity from the elastic bands and the rigidity provided by the collagen layers. This artery has to withstand continuous exposure to blood pressure and shear forces from the contractile heart movements. Therefore, the aortic wall is particularly liable to being injured due to loss of elasticity caused by the rupture of elastin bands or increase/loss of stiffness caused by alterations of the extracellular matrix. This imbalance tends to produce abnormal protrusions that may give rise to aneurysms[1,2].

The aorta is divided into different anatomical parts[6]:

- **Ascending Aorta**: The first portion of aorta that covers the stretch from the aortic valve to the aortic arch, from it the left and right coronary arteries originate. Originally, it presents a convexity called aortic root containing the three aortic sinuses that connect to the aortic valve that prevents the reverse flow of blood during diastole.

- **Arc or aortic arch**: Due to its inverted U-shape in its central portion is traditionally called Aortic Arch. It gives rise to the first three aortic branches: brachiocephalic, left common carotid and left subclavian arteries.

- **Descending Aorta**: The section from the Aortic Arch to the common iliac arteries. It is divided into two regions:

    - **Descending thoracic aorta**: It is named the half of the descending aorta from the end of the aortic arch to diaphragm.

    - **Abdominal aorta**: Get the name half of the descending aorta that extends from the diaphragm to the bifurcation of the iliac arteries.

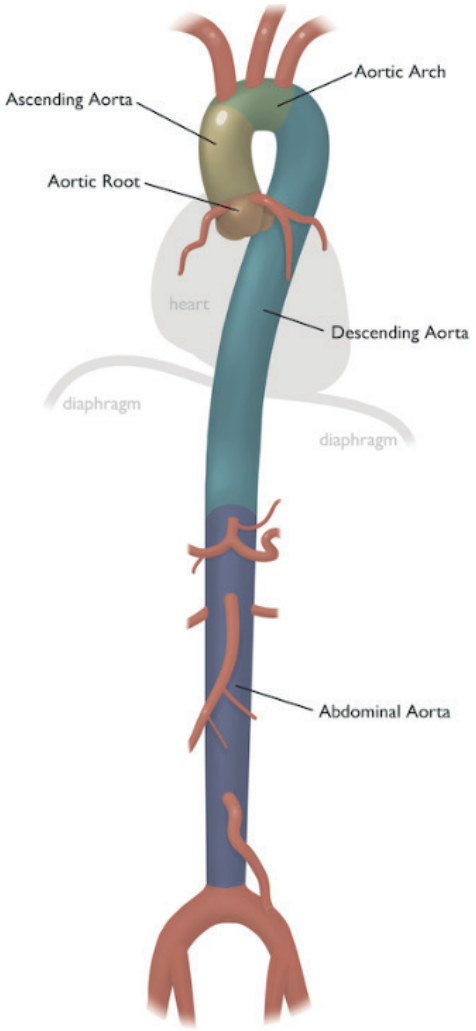

Figure 3: Anatomy of the aorta. Diagram showing the different regions along the aorta. (From https://m.ufhealth.org/uf-health-aorta-center/aorta-anatomy).

The maximum aortic diameter in adult humans corresponds to 3 cm in Ascending Aorta and gradually decreasing to 2.5cm in Thoracic Descending aorta, and then decreases to 1.8-2cm in the abdominal portion. An aneurysm is considered when 50% of the value of normal arterial diameter is exceeded[6].

2. Aortic Aneurysms (AA)

The term aneurysm comes from Greek: *ἀνεύρυσμα*, *aneurysma*, "dilation", and from *ἀνευρύνειν, aneurynein,* "to dilate". A definition accepted in Johnston *et al*. in 1991, **"Aneurysm is a focal dilatation of the artery which is an increase of more than 50% of the expected diameter"**[7]. Aneurysms are common in the abdominal and thoracic regions of the aorta. While generally asymptomatic, the progression of aneurysms is associated with the devastating consequences of aortic rupture. AA and dissections rushes being 1-2% of deaths in industrialized countries. While thoracic aneurysms (TAA) are closely associated with high-penetrance genetic predisposition, about 70%; this is not the case with abdominal aneurysms (AAA) whose main etiology is degenerative-atherosclerotic[8,9]. In the general, the proportion of abdominal/ thoracic aneurysms is about 7/1 for males and 3/1 for females[10]. The evolution of the aneurysm includes the continuous expansion of the arterial wall by degradation of elastin and collagen deposition and massive neovascularization[8,9]. All of these cause destabilization and rupture or dissection of the artery wall, causing a quick death of the patient due to an extensive hemorrhage.

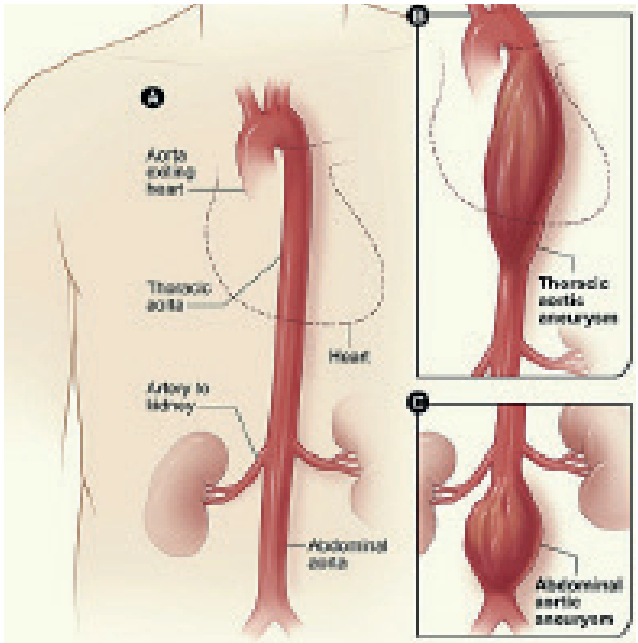

Figure 4: Diagram depicting the most common location of human aortic aneurysms. (A) Shows a normal aorta, in (B) shows a thoracic aortic aneurysm (TAA) and in (C) an abdominal aortic aneurysm (AAA) located below the renal arteries. In mice models the AAA typically occurs above the renal arteries. (From http://vascular.surgery.ucsf.edu/).

There are numerous factors related to the pathogenesis of AA, both intrinsic and extrinsic factors to the vessel wall. Intrinsic factors include changes in the extracellular matrix and the contractile apparatus of the VSMCs as a result of genetic alterations in some congenital connective tissue disorders such as Marfan Syndrome (MFS). Extrinsic factors of aneurysm formation encompass several factors that increase the expansion forces of the aortic wall or decrease the capacity to withstand these forces[11-13]. Thus, diabetes, obesity, hypertension, tobacco use, alcoholism, high cholesterol, copper deficiency, increasing age, and tertiary syphilis are risk factors most often associated with AA[9]. These factors lead to degenerative or atherosclerotic aneurysms, the most common cause of AAA[8].

2.1. Hereditary disorders that course with aortic aneurysm

Up to 20% of individuals with Thoracic Aortic Aneurysm and Dissections (TAAD) have an affected relative[14]. Heritable TAA diseases are due to mutations in a number of genes that affect the aorta and other arteries with differing severity. They can be classified in two different ways depending on the methodology. Clinically they could be divided into syndromic and non-syndromic AA depending on whether they show other systemic symptoms than aneurysm or not; whereas if we look at the genetic origin we can distinguish between mutations that go with genes that code for proteins related to ECM and others with the contractile apparatus of the smooth muscle.

There are six major **autosomal dominant diseases**[15-21]:

1. **Marfan Syndrome (MFS)**
2. **Loeys-Dietz Syndrome (LDS)**
3. **Autosomal dominant, Cutis Laxa Syndrome (CLS)**
4. **Vascular type Enhlers-Danlos Syndrome (EDS-IV)**
5. **Bicuspid Aortic valve (BAV)**
6. **Non-syndromic Familial forms of TAA with Dissection (FTAAD)**

Moreover, there are mutations with **recessive inheritance of Cutis Laxa syndrome (CLS)**.

2.2.1. Marfan Syndrome (MFS)

MFS is the most common genetic disorder associated with aneurysm, affecting 1/3000-5000 people. Mutations in the *FIBRILLIN1* gene (FBN1) are behind most cases (70%) of MFS. In this case, in addition to AA, patients present oculo-musculo-skeletal characteristics such as: high stature, long fingers (arachno-dactyly), widening and sinking of the chest (*pectum excavatum*), scoliosis and kyphosis, hypermobility and elasticity of the joints. In addition, they present other characteristics like dislocation of the lens (*ectopia lentis*) and pulmonary emphysema with spontaneous pneumothorax. FBN1 is a large protein of about 350 kDa that forms a fibrillar framework of microfibers. In addition, FBN1 participates in the assembly of the elastic fibers[22].

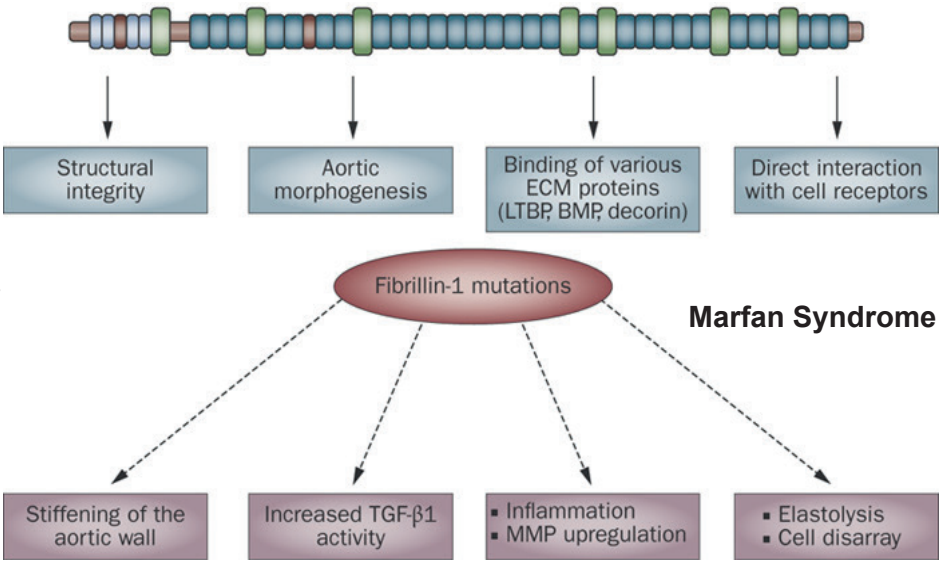

Figure 5: *FBN1* mutations are involved in MFS. (Modified from Hamamasy et al 2009[23]).

In normal individuals, FBN1 is an important structural component of the aortic wall, forming a lattice around elastic fibers. FBN1 has pivotal regulatory functions by sequestering cytokines and growth factors such as Tumor Growth Factor beta (TGFβ). Moreover, FBN1 can interact directly with integrin receptors on VSMCs and FBN1 links to components of the extracellular matrix like proteoglycans to the cells. Mutations in *FBN1* lead to structural changes in the aorta, increased bioavailability and activity of TGFβ, chemotaxis, inflammation and expression of MMPs. These changes result in elastic fibers fragmentation, cell apoptosis and disarray of the aortic wall.

2.2.2. Loeys-Dietz Syndrome (LDS)

In the case of LDS, it partially phenocopies some skeletal characteristics of the MFS. Moreover, it usually goes with other symptoms such as vascular tortuosity and cleaved palate. This disease is more severe than MFS because the patients usually suffer from aortic aneurysm and dissections in childhood. LDS is caused by mutations with loss of function of TGFβ pathway components such as mutations in ***TGFβ Receptor 1 and 2 (TGFR1-2)***, ***TGFβ1-3 and SMAD3*** response transcription factor (causing a disease known as Osteoarthritis with Aneurysm)[21].

2.2.3. Cutis laxa syndrome (CLS)

Autosomal dominant forms of CLS are caused by mutations in ***ELASTIN gene*** *(ELN)*, Nevertheless mutations in the Elastin-associated protein ***FIBULIN4*** *(EFEMP2)* are causative of recessive CLS. Fibulins are extracellular proteins that form part of elastic bands and connect Elastin to Fibrilin microfibers. Thus, loss of Fibulin4 produces elastic fibers disarray and promotes AA. This syndrome is characterized by virtually no skin elasticity, vascular tortuosity, aneurysm with excessive elastolysis, emphysema, concave palate, craniofacial signs and *pectus excavatum*. Aortic aneurysm appears at an early age, often requiring an aortic prosthesis in neonatal stages. The deficient mice for *EFEMP2* die by a severe elastolysis and aneurysm recapitulating the aortic phenotype of the patients[24,25].

2.2.4. Vascular type Enhlers-Danlos Syndrome (EDS-IV)

EDS-IV is caused by mutations in the ***COLLAGEN3*** **gene** (*COL3A1*) that produce hyperelasticity of the skin and joints, short stature with a slim build, and typically have thin, pale, translucent skin with very easy bruising and propensity to develop ecchymoses (bruising without trauma); arterial, intestinal, and uterine fragility. Vascular dissection or rupture, gastrointestinal perforation, or organ rupture are the presenting signs in the majority of adults. Arterial rupture may be preceded by aneurysm but also may occur spontaneously. The mean age of death in this population is about 50 years old[26]. *Col3a1* deficient mice die by aortic dissection without previous aneurysm formation[27].

2.2.5. Bicuspid aortic valve (BAV)

BAV is a congenital disease of the aortic valve, in which two of the aortic valvular leaflets fuse during development resulting in a valve that is bicuspid, instead of the normal tricuspid configuration. BAV is an autosomal dominant condition with incomplete penetrance with mutations associated in ***Smooth Muscle***

Actin (ACTA2) and ***NOTCH1*** as high as 89%. Other congenital heart defects are associated with bicuspid aortic valve at various frequencies, including coarctation of the aorta. In this disease, due to this anatomical malformation, hemodynamics in the ascending aorta changes, increasing the shear-stress and promoting TAA development[28].

2.2.6. Non-syndromic familial forms of TAA with dissection (FTAAD)

Approximately 30% families with heritable-TAAD, without clinical diagnosis of syndromic disease have a causative pathogenic variant in one of the known genes described on table 1. In the case of patients with FTAAD, they do not present any evident musculo-skeletal and ocular features. In contrast of sporadic TAAs, FTAAD are typically present earlier, have a higher growth rate, and do not demonstrate association with traditional risk factors for aortic diseases. Cases of non-syndromic TAA mainly involve the thoracic aorta and specially the ascending aorta. The genes that cause this disease are divided in two different categories: **those affecting the smooth muscle contractile apparatus and those affecting ECM proteins**. To date, 14 genes are known to be causative of FTAAD (Table 1). Note that many families (about 70-80%) with a familial history of TAAD do not have a pathogenic variant in one of these known genes[30].

Gene	Proportion of Families in FTAAD	Other Findings Observed
ACTA2	12%-21%	Multisystemic Smooth Muscle Dysfunction
FBN1	3%	Variable Marfanoid features
MAT2A	1%	Bicuspid aortic valve (BAV)
MFAP5	0.25%	Atrial fibrillation, mitral valve prolapse and arterial tortuosity in some patients
MYH11	1%	Patent *ductus arteriosus*
MYLK	1%	
PRKG1	1%	Coronary artery aneurysm/dissection and arterial tortuosity in some patients
TGFB2	1%	Variable LDS features with abdominal aortic aneurysms and/or intracranial and other arterial aneurysms and/or dissections.
TGFB3	2%	
TGFBR1	3%	
TGFBR2	5%	
MT-MMP17	Rare	
LOX	Rare	
BGN	Rare	X-linked disease

Table 1: Summary of genes related with FTAAD

Some affected genes that encode contractile proteins produce other symptoms than aortic aneurysm. This is the case of **patent *ductus arteriosus*** in *MYH11* mutations (encoding Smooth Muscle Myosin Heavy Chain). Recently, Milewicz *et al.* (2010) described new mutations in *ACTA2* (encoding Smooth Muscle Actin)[31]. This disease was referred to as **Multisystemic Smooth Muscle Dysfunction**. This pathology includes: congenital mydriasis (fixed dilated pupils), patent *ductus arteriosus*, aortic coarctation, intestine hypoperistalsis, hypotonic bladder with hydronephrosis, *livedo reticularis* (Skin-reticulated vascular pattern), small vessel infarcts and aneurysms, pulmonary artery dilation and hypertension, tachypnea (abnormally rapid breathing), and cryptorchidism (absence of one or both testes from the scrotum).

Other mutations that affect the contractile apparatus of VSMCs are: mutations in the ***Myosin Light Chain Kinase*** (*MYLK)* and gain-of-function mutations in ***Protein Kinase cGMP-dependent*** (*PRKG1)*. This protein is a downstream target of Nitric Oxide (NO). *PRKG1* mutations are present in 4 different families affected by TAA, suggesting that NO might be also essential in non-syndromic familial TAAD[32].

Moreover, the **genes that affect ECM are**: the metalloproteinase ***MT-MMP17***[33], ***Lysyl Oxidase*** (*LOX*) cross-linker of collagen and elastin[34], proteoglycan ***Biglycan*** (*BGN*)[35], ***Microfibrillar Associated Protein-5*** (*MFAP5*)[36].

Furthermore, some non-syndromic patients harbor mutations in *FBN1, TGFB2,3 TGFBR1, TGFBR2* genes that do not cause any oculo-skeletal manifestation. It has been estimated that in nearly 70-80% of the FTAAD cases the genetic origin remains unknown[37,38]. In addition, some mutations in the *FBN1* gene that will be described below, cause connective tissue disorders without vascular phenotype.

Disorder	Genes	Mode of inheritance	Discriminating clinical features
Marfan syndrome	*FBN1* *TGFBR2*	AD	• thoracic aortic aneurysms/dissections, ectopia lentis, high myopia, arachnodactyly, camptodactyly, pes planus, pectus excavatum or carinatum, scoliosis, joint hypermobility
Loeys-Dietz syndrome	*TGFBR1* *TGFBR2* *SMAD3*	AD	• generalized arterial tortuosity, aortic and peripheral arterial aneurysms/dissections, bifid uvula/cleft palate, hypertelorism, craniosynostosis, contractures, translucent skin, easy bruising • osteoarthritis
Ehlers-Danlos type IV	*COL3A1*	AD	• aneurysms of middle-sized arteries, translucent skin, easy bruising, abnormal wound healing, hypertrophic scar formation, bowel rupture, uterine rupture
Ehlers-Danlos type VIA	*PLOD1*	AR	• hyperextensible skin, easy bruising, hypertrophic scars, joint hypermobility, progressive scoliosis
fTAAD	*TGFBR2* *TGFBR1* *ACTA2* *MYH11* *MYLK*	AD	• thoracic aortic aneurysms/dissections without other MFS features • premature coronary artery diease and/or stroke, livedo reticularis • patent ductus arteriosus
Ectopia lentis syndrome	*FBN1* *LTBP2* *ADAMTSL4*	AD	• ectopia lentis without aortic aneurysm/dissection
Cutis laxa, AR type 1	*FBLN4*	AR	• loose, hypoelastic skin, arterial tortuosity, aneurysms, emphysema
Bicuspid aortic valve with calcification	*NOTCH1*	AD	• bicuspid aortic valve with calcification, aortic aneurysm/dissection
Sphrintzen-Goldberg syndrome	?	?	• marfanoid skeletal features, mild-to-moderate intellectual disability, craniosynostosis, brain abnormalities
Weill-Marchesani syndrome	*ADAMTS10* *ADAMTS17* *FBN1 (rare)*	AR AD	• ectopia lentis, microspherophakia, severe myopia, glaucoma, short stature, joint stiffness, brachydactyly
Stiff skin syndrome	*FBN1*	AD	• thick skin, joint contractures
Geleophysic and acrophysic dysplasia	*FBN1*	AD	• short stature, short extremities, stiff joints, distinct facial features
Congenital contractural arachnodactyly	*FBN2*	AD	• multiple joint contractures, arachnodactyly, severe kyphoscoliosis, muscular hypotonia, crumpled ears
Homocystinuria	*CBS*	AR	• marfanoid skeletal features, ectopia lentis, severe myopia, mild-to-moderate intellectual disability, thromboembolism

AD = Autosomal dominant; AR = autosomal recessive; fTAAD = familial thoracic aortic aneurysms/dissections.

Table 2. Genes involved in Marfan syndrome and related connective tissue disorders. (From Hoffjan *et al.* 2012).

All these disorders course with **cystic medial degeneration**, a histological abnormality characterized by fragmentation of elastic fibers, fibrosis, accumulation of amorphous matrix (proteoglycans) and loss of VSMCs. This histological change is commonly seen in patients with dilatation, aneurysm, or dissection of the ascending aorta associated with hereditary diseases, such as MFS. This condition was recognized as the etiology of aortic aneurysm and dissection. Thus, the presence of big amount of proteoglycans in the aortic media accompany by a loss and fragmentation of elastic fibers involves a profound change in the extracellular matrix leading to structural inhomogeneity, enhanced circumferential wall and shear stress, leading to a weakness of the aortic wall, which is susceptible to rupture in time. A pathological vascular remodeling process causes this histological abnormality.

3. Pathological vascular wall remodeling

Substantial vascular wall remodeling occurs during AA formation. Vessel wall remodeling is an active process that alters the structure and arrangement of blood vessels through cell growth, cell death, cell migration, and production or degradation of the extracellular matrix. Pathological vessel wall remodeling is the leading cause of morbidity and mortality in the Western World and the primary cause of AA, myocardial infarction, stroke, and ischemia.

Vascular wall remodeling is a complex and active process of structural alterations that involves changes in, at least, four cellular processes: cell growth, cell death, cell migration, and ECM synthesis or degradation. This remodeling leads to changes in the thickness of the Medial Layer, which produces the reduction or increase of the vessel lumen[39]. In 1987, Glagov *et al.* have reported that the narrowing of the arterial lumen by atherosclerotic plaques is no as simple as the result of the enlargement of atherosclerotic lesions[40]. Instead, the arteries undergo many changes to maintain the blood flow, including the enlargement of the outside diameter. Indeed, the arterial wall appears to be highly plastic to prevent irreversible damage. Recently, it has been suggested that the incapacity to remodel vessels properly might be a way of "**vascular insufficiency**," similar to that observed in the heart during heart failure. This inability to respond and compensate by exhaustion might be the cause of the terminal vascular disease.

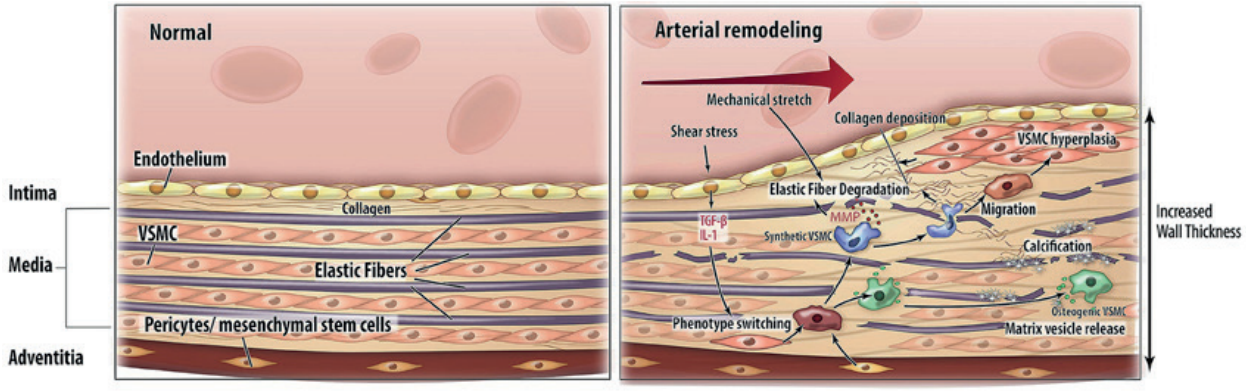

Figure 6: Pathological mechanisms of arterial remodeling. Schematic view of the arterial wall. (A) Normal situation. (B) Arterial remodeling. Arterial remodeling is characterized by thickening of the wall, elastic fiber degradation, extracellular matrix and collagen deposition. (From van Varik *et al.* 2009) [46].

The proper functioning of the vascular system depends on a complex network of interactions at mechanical, cellular and molecular level. This process depends on the dynamic interaction between local factors such as Transforming Growth Factor beta (TGFβ), Vascular Endothelial Growth Factor (VEGF), the pro-inflammatory cytokines: Interleukin-1β (IL1β) and Tumor Necrosis Factor-α (TNF-α), Angiotensin-II (Ang-II) and vasoactive substances, such as Nitric Oxide (NO). All cells of the vascular wall can participate in the remodeling process. Under normal physiological conditions, the VSMCs are quiescent and contractile, which are able to contract or relax maintaining vascular tone by contraction or expansion[41,42]. However, in pathological or vascular remodeling situations, VSMCs switch to a secretory phenotype. In this case, cells are no longer quiescent, lose some of the contractile apparatus and come to be migratory, proliferative and increase the secretion of extracellular matrix components and protein metalloproteinases (MMPs), thus, represent a critical hallmark of this process[43-47].

3.1 Molecular pathways implicated in vascular remodeling

3.1.1. Tansforming Growth Factor (TGFβ) pathway

The TGFβ pathway plays a central role in these pathologies. In both, syndromic and non-syndromic aneurysms this signaling pathway is hyper-activated. However, it is unclear whether TGFβ activation is cause or consequence of TAA. Chaudhry *et al*. described in 2007 that aoric samples from MFS show a significantly increase of TGFβ protein level in the extracellular space[48]. TGFβ is a paracrine regulatory molecule of several processes, including embryonic development, cell growth and apoptosis induction[49]. TGFβ is produced in dimer form in the cells and is bound with Latency-Associated Protein (LAP) to form Small Latent Complex (the inactive form of TGFβ). This secreted complex is bound to extracellularly to Latent TGFβ Binding Protein (LTBP) to form Large Latent complex. LTBP is then attached to microfibrils. Therefore, under normal conditions the TGFβ complexes are sequestered in the extracellular matrix, by FBN1. Nevertheless, in MFS result in aberrant formation of FBN1 microfibers that are not able to sequester LTBP in the ECM. This situation promotes the release of TGFβ and binding to its receptors TGFBR1 and TGFBR2, forming a complex which induces a phosphorylation cascade. The final step of the signaling cascade is the phosphorylation of the transcription factors SMAD2 and 3 and their translocation to the nucleus. Therefore, they induce the transcription of target genes related to fibrosis, apoptosis, cell proliferation, growth and differentiation. Accordingly, these syndromes are characterized by an increase in fibrosis, degeneration of the media with accumulation of PGs, disorganization and rupture of elastic bands; de-differentiation of VSMCs, weakness of the vascular wall and its rupture. TGFβ is thought to be an inducer of these processes. Paradoxically, mutations with loss of function in the TGFβ pathway occur in LDS, resulting in hyperactivation of the TGFβ pathway in a non-canonical way[50,51]. Consistent with a pathogenic role of TGFβ in TAA, neutralizing anti-TGFβ antibodies prevent aortic dilation and inhibit elastic lamellae fragmentation in a mouse model of MFS[52,53].

3.1.2 Angiotensin-II (Ang-II) signaling

Ang-II is an oligopeptide and an hormone that causes vasoconstriction and a subsequent increase in blood pressure. It is part of the Renin-Angiotensin System, which is a major regulator of blood pressure and balance of electrolytes. Molecularly, Ang-II acts through two different receptors coupled to G proteins: type-I and type-II Angiotensin Receptors (AT1R, AT2R)[54]. They are expressed in organs involved in the regulation of blood pressure such as the heart, vessels, kidney and some parts of the brain[55,56]. AT1R receptor is involved in the increasing blood pressure via vasoconstriction. The AT1R receptor, by activating G proteins, activates different molecular pathways triggering a multifactorial and complex response. Among the activated pathways is the activation of **Mitogen-Activated Kinases** (MAPK), in addition to the **PYK2, SRC, JAK/STAT** kinases[57,58]; or the regulation pathway of the actin cytoskeleton organization via the RhoA/Rho kinase pathway and the activation of the **NAD(P)H oxidase** producing Reactive Oxygen Species (ROS) that will give rise to cellular oxidative stress and inflammation[59].

On one hand, the binding of Ang-II to its AT1R receptor activates the signaling cascade initiated by **Phospholypase-C** (PLC) that produces **Inositol Triphosphate** (IP3) / **Diacylglycerol** (DAG), which result in the increase of Ca^{2+}. This increase in intracellular Ca^{2+} causes calcium-coupled Calmodulin to induce the activation of **Myosin Light Chain Kinase** (MLCK) and consequently the phosphorylation of the **Myosin Light Chain** (MLC) is induced, eliciting smooth muscle contraction.

On the other hand, the binding of Ca^{2+} to Calmodulin activates the phosphatase **Calcineurin** (CN)[60]. Activated CN dephosphorylates the family of **NFAT transcription factors** (nuclear factors of activated T cells). NFAT dephosphorylation induces a conformational change resulting in exposure of a nuclear localization domain. This results in translocation of NFAT to the nucleus, where they interact with specific DNA sequences[61]. Finally, the NFATs are hyperphosphorylated and re-located in the cytoplasm. Some of the target genes of CN-NFAT are: *Cyclooxygenase-2* (*Cox-2*) and the inducible isoform of *Regulator of Calcineurin-1* (*RCAN1.4*)[60,62,63]. CN pharmacological inhibitors such as Cyclosporine-A (CsA) and a blocking peptide based on the NFAT Calcineurin binding site, LxVP; inhibit Ang-II induced abdominal aortic aneurysms in ApoE-deficient mice[60]. There are also endogenous regulators of CN activity such as RCAN1 and the plasma membrane calcium pump PMCA4[64], to mention some of them.

In a mouse model of MFS that carry a point mutation on Fbn1 (*Fbn1*$^{C1039G/+}$), the aortic dilation and medial degeneration is slowed by Losartan, an AT1R-antagonist that inhibits TGFβ signaling in a non-canonical way[11,13,50,52,65,66]. Losartan treatment in mouse models of MFS and LDS improves aortic wall architecture and inhibits aortic growth.

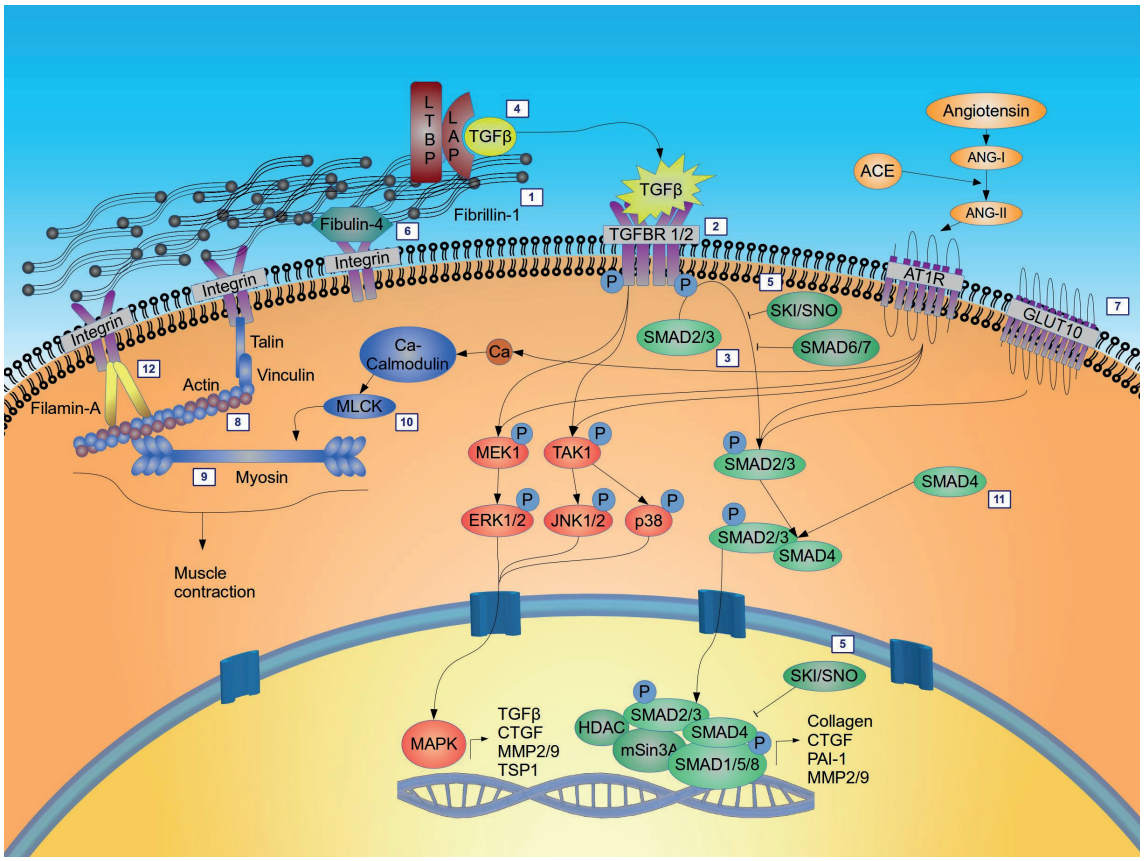

Figure 7: TGFβ and Ang-II Pathways implicated in TAA. Numbers indicate the corresponding syndrome caused by mutations in the protein. 1, Marfan syndrome; 2 and 3 Loeys–Dietz syndrome, 6 Cutis laxa; 7, Arterial tortuosity syndrome; 8 to 10,Familial thoracic aortic aneurysms and dissections; 12, Ehlers–Danlos– related syndrome. (From Gillis *et al.*2013 [13]).

3.1.3. Vascular Endothelial Growth Factor (VEGF)

The AA are associated with remodeling of the vascular wall by angiogenesis as well as proteolysis. Vascular Endothelial Growth Factor (VEGF) is known to be a regulator of angiogenesis and to simultaneously stimulate elastolytic proteinases. It has been shown that VEGF is overexpressed in human aneurysm samples[67,68]. Members of the VEGF family are extracellular proteins involved in **vasculogenesis** (*de novo* vessel formation, which occurs primarily during genesis of the embryonic circulatory system) and in **angiogenesis** (growth of blood vessels from pre-existing ones). VEGF actions have been studied in vascular ECs, although it also has effects on other cell types (such as in the migration of macrophages, neurons, renal epithelial cells and tumor cells). VEGF has been shown to stimulate the division, survival and migration of ECs. VEGF is also a vasodilator and increases vascular permeability. The major member of VEGF involved in angiogenesis and cell permeability is VEGF-A.Therefore, VEGF-A is an important target for preventing excessive angiogenesis in different diseases such as cancer, retinopathies or neovascularization present in aortic aneurysms[69]. The molecular mechanism by which members of the VEGF family perform their function in the target cells is through three types of receptors with intrinsic kinase activity: VEGFR-1, VEGFR-2 and VEGFR-3, located mainly in endothelial cells. The most important one in angiogenesis is VEGFR-2 also called KDR which is activated primarily by the binding of VEGF-A. VEGFR-2 activates different pathways such as the **MAPK pathway** (inducing cell survival and proliferation). Moreover, it activates the PLC/IP3/DAG pathway, producing an increase in intracellular Ca^{2+} and activating the **CN-NFAT pathway**[70].

Both activating the expression of target genes such as *Cox-2* and *RCAN1.4*. Inhibition of this pathway blocks the induction of VEGF angiogenesis *in vitro* and *in vivo* models[71]. Thus, the balance of VEGF pathway activation is crucially important for vascular pathophysiology.

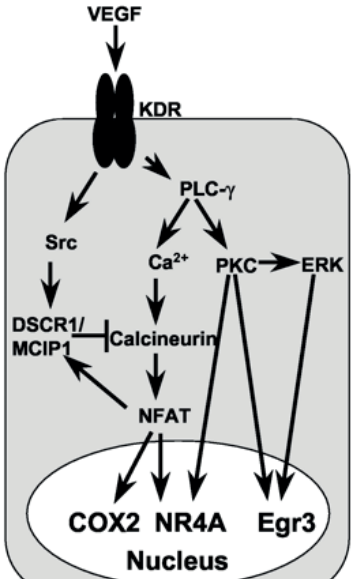

Figure 8: Signaling mechanisms mediating VEGF-regulated endothelial gene expression. Activation of phospholipase-C (PLC-γ) and subsequent increase of intracellular Ca^{2+}. Calcineurin-mediated activation of NFAT transcription factors has been reported to mediate VEGF-induced *RCAN1.4* (DSCR1) and *COX-2* expression. (From Liu *et al.* 2003)[72].

3.1.4 Nitric oxide (NO)

NO is a potently vasodilator gas, involved in the production of various physiological and pathological processes. In the first studies conducted in 1980 by Furchgott and Zawadzki, it was referred to as "the Endothelium Derived Relaxing Factor (EDRF)"[73]. Palmer *et al.* identified in 1987 EDRF as NO[73]. NO is produced biologically by the conversion of the amino acid L-Arginine into L-Citrulline, and two molecules of molecular oxygen and one of Nicotinamide Adenine Dinucleotide Phosphate (NADPH) are needed as an electron donor. Moreover, a haem iron and a molecule of Tetrahydrobiopterin (BH_4) are needed. This reaction is biologically catalyzed by the enzyme Nitric Oxide Synthase (NOS) and can be inhibited by structural derivatives of L-Arginine such as L-N-Mono-Methyl Arginine (L-NMMA) or L-N-Nitro-Arginine Methyl Ester (L-NAME)[74].

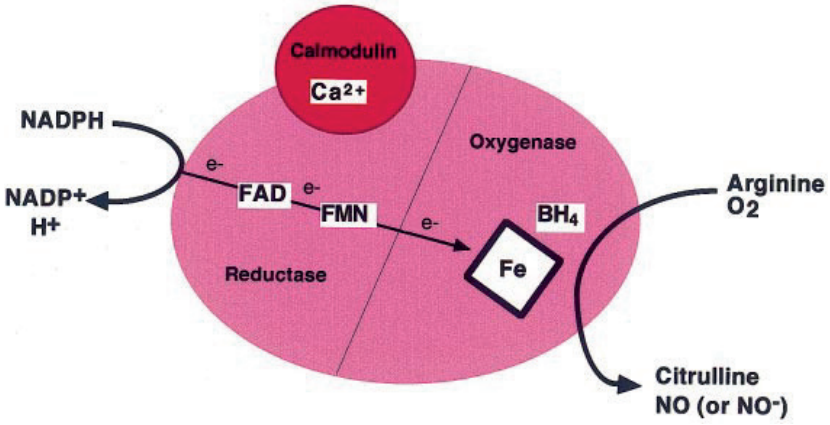

Figure 9: Scheme of reaction catalyzed by NOS. The reaction of NO biosynthesis is produced in two steps: in the reductase domain and oxygenase domain of NOS enzymes. Electrons (e^-) are donated by NADPH to the reductase domain of the enzyme and proceed via FAD and FMN redox carriers to the oxygenase domain. There they interact with the haem iron and BH_4 at the active site to catalyze the reaction of oxygen with L-Arginine, generating L-Citrulline and NO as products (From Alderton *et al.* 2001)[74].

There are also three different isoforms of NOS, classified according to their Ca^{2+}-dependence[75,76]. They are constituted by homodimeric subunits[74,77,78]:

•**Two Calcium-Calmodulin-dependent constitutive isoforms:** Endothelial NOS (eNOS or NOS3) and Neural NOS (nNOS or NOS1). They are constitutively expressed in different tissues (endothelial cells, muscle cells, neurons, glia and others) producing physiological NO amounts. They may be attached to the plasma membrane by palmitoylation. In the case of NOS3, in addition to the binding of Ca^{+2}/Calmodulin, the phosphorylation in the Serine-1777 by the AKT kinase produces an increase in its enzymatic activity[79].

• A calcium-independent isoform: **inducible NOS (iNOS)** or **NOS2**. The expression of NOS2 is inducible in different cell types such as macrophages, hepatocytes, neutrophils, smooth muscle and endothelium in response to different pro-inflammatory stimuli such as Interferon gamma (IFNγ), Tumor Necrosis Factor alpha (TNF–α) and bacterial Lipopolysaccharide (LPS)[80]. These molecular agents activate the major transcription factors involved in increasing the expression of NOS2, NF-κB and C/EBPβ. NOS2 is able to generate greater amounts of NO compared to the others isoforms (NOS3 and NOS1). This overload of NO becomes toxic to pathogens or to tumor cells[80-82].

The wide distribution of NOS helps to explain some of the effects in the organism associated with the release of nitric oxide. In general, NOS1 and NOS3 are present at relatively low levels and involved in the NO physiological regulation[83], whereas NOS2 is transcriptionally activated and it is able to produce 100- to 1000-fold more NO than its constitutive counterparts[84]. Conventional classification of NOS isoforms in neuronal, endothelial, and inducible NOS appears to reflect only characteristics of the original tissue where they were described. However, the expression of the three NOS isoforms in the same tissue, such as myocardium or skeletal muscle, has been found by immunodetection techniques[85]. The biosynthesis of NO in vascular tissue was traditionally restricted exclusively to the endothelium[73]. However Buchwalow *et al.* described in 2002 that smooth muscle cells expresses the three NOS-isoforms in a constitutive way and under physiological conditions. Thus, NOS expression could modulate vascular functions independently of the endothelium[86].

The molecular mechanism, by which NO exerts a vasodilator role, is based on the activation of the enzyme **Guanylyl Cyclase** (GC) and this causes the intracellular increase of cyclic guanosine monophosphate (cGMP). This in turn activates the **Protein Kinase G** (PKG), which induces the recapture of intracellular Ca^{+2} and opening the calcium-dependent potassium channels, producing hyperpolarization of the cells as well as phospholylation and inhibition of **MLCK**, and **RhoA** to activate **Myosin light Chain Phosphatase** (MLCP). In this way, it causes the inhibition of MLCK. Resulting in the inhibition of MLC-phosphorylation and in the **relaxation of smooth muscle**[87].

Under normal physiological conditions, NO is produced in the vasculature at low levels by NOS3 to maintain vascular tone[88]. Alterations in NO production in the vasculature are thought to contribute to the pathogenesis of atherosclerosis, hypertension, heart failure and diabetes[89,90]. However, data on role of NO in AA and the contribution of NOS2 and NOS3 to this disease are limited and, in many cases, contradictory[91-94]. An overload of NOS activity produces a mixture of superoxide (O_2^-) anions and NO that result in peroxynitrite ($ONOO^-$) and as a result, cytotoxicity may occur as they may react with the amino acids of the proteins producing nitrosylation. Also, NO-overload mediates lipid-oxidation and inhibition of the mitochondrial respiration (blocking the Complex-I and II), hypoxia (stabilizing Hypoxia-Inducible Factors) and DNA damage[95]. NO is unstable, and its half-life is short (few minutes); its final products are nitrite (NO_2^-) and nitrate (NO_3^-). All this molecules increase the cellular oxidative stress. In addition, an excess of NO produces muscle relaxation that would contribute to the loss of the contractile phenotype of VSMCs[96,97]. Moreover, the increase of NO has been related to the activation of extracellular matrix metalloproteinases (MMPs). In fact, the elastase activity of MMP9 is activated by nitrosylation[98]. Thus, the increase of NO could imply elastolysis and cell toxicity and, therefore, the degeneration of the medial layer[98-104]. In summary, NO levels in the vascular system are basic to maintain control of vascular tone; although an excess of NO implies a change in the contractile capacity of the arteries both by a change of the mechanical and elastic properties of the arterial wall.

All these factors influence the remodeling of the vascular wall, producing changes at the cellular and molecular level.

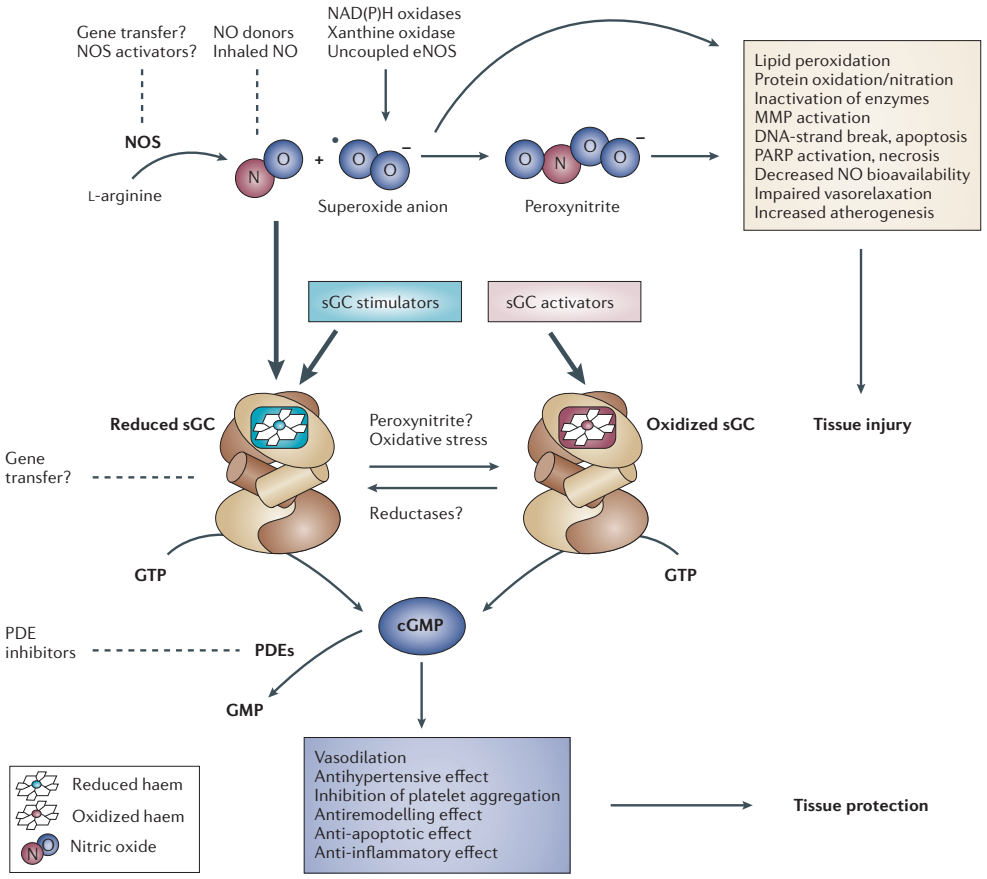

Figure 10: Scheme of pato-physiological effects of the NO production. (From Poulos *et al.* 2006)[104].

4. Extracellular matrix (ECM) role in AA.

The ECM is the main component by weight of the arterial wall. It is part of the basic structure of the vessels and provides part of the mechanical and structural support thanks to the elasticity, stiffness and intercellular communication that determines the physical properties of the tissue. Therefore, alterations in the ECM can contribute to the pathogenesis of AA. The ECM is formed by an interlaced network of non-soluble fibers such as collagens, elastin and FBN that provide elasticity and resistance; in addition to an amorphous or fundamental matrix that fixes water molecules and provides resistance to compression. The elements of the matrix are secreted locally and assembled into an organized network in close contact with the cells that produce it in an integrin-dependent or independent manner[46,47].

The two most important **types of extracellular components** that form the matrix are[105]:

4.1 Ground or amorphous substance

It is an amorphous gel-like substance surrounding the cells. Ground substance is primarily composed of water, **glycosaminoglycans, proteoglycans (PGs), and glycoproteins**. Proteoglycans are glycoproteins that form linear chains of polysaccharides covalently bound to a protein center. PGs have less than 10% by weight of protein, with the remainder being carbohydrates. The most common in the arteries are **chondroitin sulfate** (Versican, Biglican, Perlecan, Syndecan), **heparan sulfate** (Aggrecan, Decorin, Perlecan) and **dermatan sulfate**. By the carbohydrates chains, containing sulfate groups, they have high negative charge density that attract osmotically active cations like Na^+; thus forming hydrated gels, which resist compressive forces and allow the rapid diffusion of nutrients. Many of them trap a wide variety of cellular modulators; therefore, they act as a local store and control the release of growth factors in a paracrine manner. The accumulation of proteoglycans, as can be visualized by Alcian Blue staining, is characteristic in the pathological process of cystic degeneration of the tunica media that occurs in mainly in TAA [7,45,106-108].

4.2. Fibrous proteins

They can be classified according to their properties into two types:

A) **Structural** such as collagen, fibrillin and elastin.
B) **Adhesive** such as fibronectin and laminin.

Collagens are fibrous proteins secreted by fibroblasts and VSMCs. The mature collagen molecule forms a triple helix. Unlike the fibers of proteoglycans that resist compressive forces, collagen fibrils form structures that resist tensile forces. There are at least five different types of collagen in the blood vessels. The most important for the maintenance of the structure of blood vessels are types I and III, which form long fibers. Type IV, however, is also an important structural component that forms a network of molecules in the basal membranes of ECs and VSMCs. There are genetic disorders with presence in mutations of *COLLAGEN3* gene that produce aneurysms and aortic dissections such as the vascular type **Enhlers Darlos syndrome** (EDS-IV)[109].

Elastin: once secreted, these fibers are highly intertwined and form an extensive network of strongly hydrophobic fibers. They are rich in proline and lysine and have the property of being five times more extensible than a rubber band of equal diameter. The elastic fiber is covered, in addition to elastin, by a sheath of microfibrils composed of a glycoprotein called Fibrillin1 that are essential for its integrity and whose genetic defect causes medial degeneration, due to the alteration in the elastin assembly in MFS[110,111].

The interaction of ECM with cells is basic for vessel integrity, mechanotransduction and cell survival. Alteration of ECM binding to cells or cell-cell contacts produces apoptosis, migration, proliferation, and phenotypic changes[112]. In summary, different physiological and pathological conditions induce changes in the ECM components of the vascular wall, such as expression, assembly, entanglement and degradation. These changes are of vital importance during the vascular remodeling process[8,9].

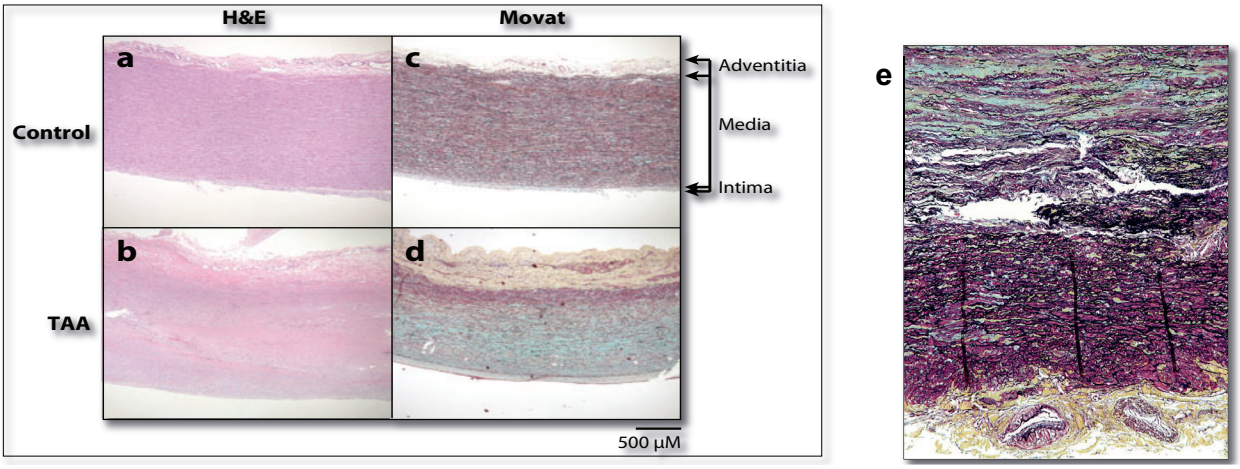

Figure 11. ECM changes in Familial TAAD produces cystic medial degeneration by vascular remodeling process. a-b (H&E) and c-e Movat pentachrome staining of aortic sections from (a-c) a normal subject and (b-e) a patient with FTAA, illustrating medial degeneration. Movat staining shows fragmentation of elastic fibers (stained black), loss of VSMCs (cells stained red and nuclei stained violet), and accumulation of proteoglycans (stained blue) and collagens (yellow), in the medial layer. (Modified from Milewicz *et al.* 2008[38].

5. ECM Metalloproteinases

They regulate the renewal, maintenance and remodeling of the ECM. Therefore, they are of extreme importance for the homeostasis and pathology of the vascular wall[113-115]. There are five metalloproteinase superfamilies, classified according to the sequence of the peptides. In vascular remodeling the **Metzincin** superfamily is an angular stone by their high expression. All metzincins show a highly conserved HEXXHXXGXXH motif with three histidines coordinating a Zn^{+} and a conserved methionine close to the catalytic site required for catalytic activity. The metzicine family is subdivided into four multigenic families, such as **Matrix Metalloproteinases (MMP) and Adamalysins (ADAM, ADAMTS)**. The expression of these metalloproteinases is prominent in macrophages, but they are also present in vascular smooth muscle and endothelial cells. The structure is similar and is organized into domains or modular regions[116,117].

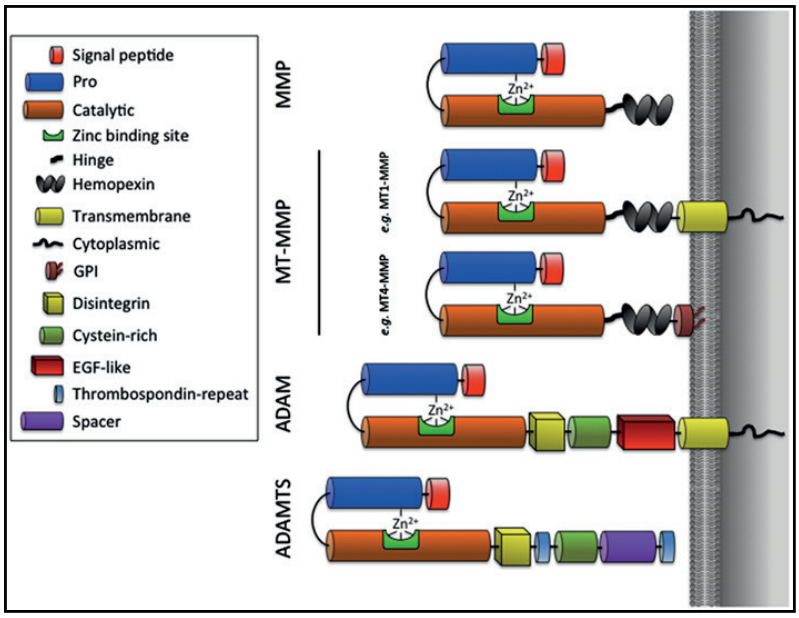

Figure 12: Schematic representation of the metzincin proeases: MMPs, MT-MMPs, ADAMs, and ADAMTS. (From Daevic *et al.* 2016) [119].

5.1. Matrix Metalloproteinases (MMPs)

The basic structure of the MMPs presents common domains: a signal peptide, a pro-peptide in the N-terminal sequence with inhibitory activity, which is deleted by the protease Furin in the Golgi-apparatus; and a carboxy-terminal catalytic metalloprotease domain. Several variants of this basic structure appear such as a hemopexin-like domain mediating substrate specificity and interactions with endogenous inhibitors, or a transmembrane domain in the case of plasma membrane-associated MMP (MT-MMP)[98].

5.2. ADAM proteases

The **ADAM (disintegrin and metalloproteinase)** family comprises membrane multifunctional proteins, similar to the snake venom metalloproteinases with disintegrin domain. In their structure, they show a complex domain organization consisting of: metalloprotease domain, disintegrin domain with integrin-binding capacity, cysteine-rich region, epidermal growth factor receptor (EGF) domain, transmembrane region, and a cytoplasmic domain. 25 different genes encoding ADAMs have been described in humans. Its activity has been associated with spermatogenesis, fertilization, modulation of cell migration and adhesion during neurogenesis, activation of signaling pathways, and release of cytokines and extracellular growth factors. In the cardiovascular system, ADAM 17 and 19 have essential functions in the development of the heart and valves; and ADAM10 and 15 are involved in angiogenesis and neovascularization[118].

5.3. ADAMTS and ADAMTSL family members

The **ADAMTS family (disintegrin and metalloprotease with thrombospondin domains)** members are ADAM-related extracellular proteases that lack the transmembrane domain and the EGF domain. Instead, they contain several domains of Thrombospondin Type-I (TS) repeats. They may also have other types of domains that together with the TS domains confer specific binding to substrates and ECM. It has been reported that other proteases such as MMPs or ADAMTS themselves are able to process these domains by participating in the maturation or degradation process. 19 different ADAMTS have been identified in humans.

ADAMTS proteins have specific functions in normal and pathological processes, such as angiogenesis, coagulation, atherosclerosis, stenosis, arthritis, cancer, wound closure and embryonic development[119].

ADAMTS proteins in mammals can be subdivided into 8 different clades based on their sequence, known functions, and organization of their functional domains. The first of them would be the ADAMTS clade with **aggrecanase and proteoglycanase function**. These proteins are ADAMTS1,4,5,8,9,15, and 20[120]. They are able to digest PGs such as Aggrecan, Versican, Brevican and Neurocan. Some members of this subgroup have angioinhibitory activity. For example, ADAMTS1 and 8 are able to inhibit angiogenesis since they are capable of sequestering and blocking VEGF[122]. Another group consisting of ADAMTS2, 3 and 14 is called pro-collagen peptidases. These proteins are essential for the **maturation of the collagen triple helix**. ADAMTS13 is the member of the family that is able to proteolize von-Willebrand (vWF) coagulation Factor. Mutations in this gene cause **Thrombocytopenia Purpurea (TPP)**. Another clade would consist of the ADAMTS7 and 12, which are capable of processing the **oligomeric cartilage protein (COMP)**. The rest of the members of the family are considered as "orphans" because their function and substrates have not been clearly identified. Their classification is established according to sequence similarity and the presence of functional domains. Thus, the ADAMTS6,10; ADAMTS16,18 and ADAMTS17,19 subclasses have been proposed. Of note, some of these orphan ADAMTS members have been related to hereditary connective tissue disorders[118,121,123,124].

In addition, **7 members of the ADAMTSL (ADAMTS-like) subfamily**, lacking the metalloprotease domain, have been found. Their function seems to be related to the assembly of the ECM because, for example, ADAMTSL2, 4, 6, aid in the assembly of fibrillin microfibers[121].

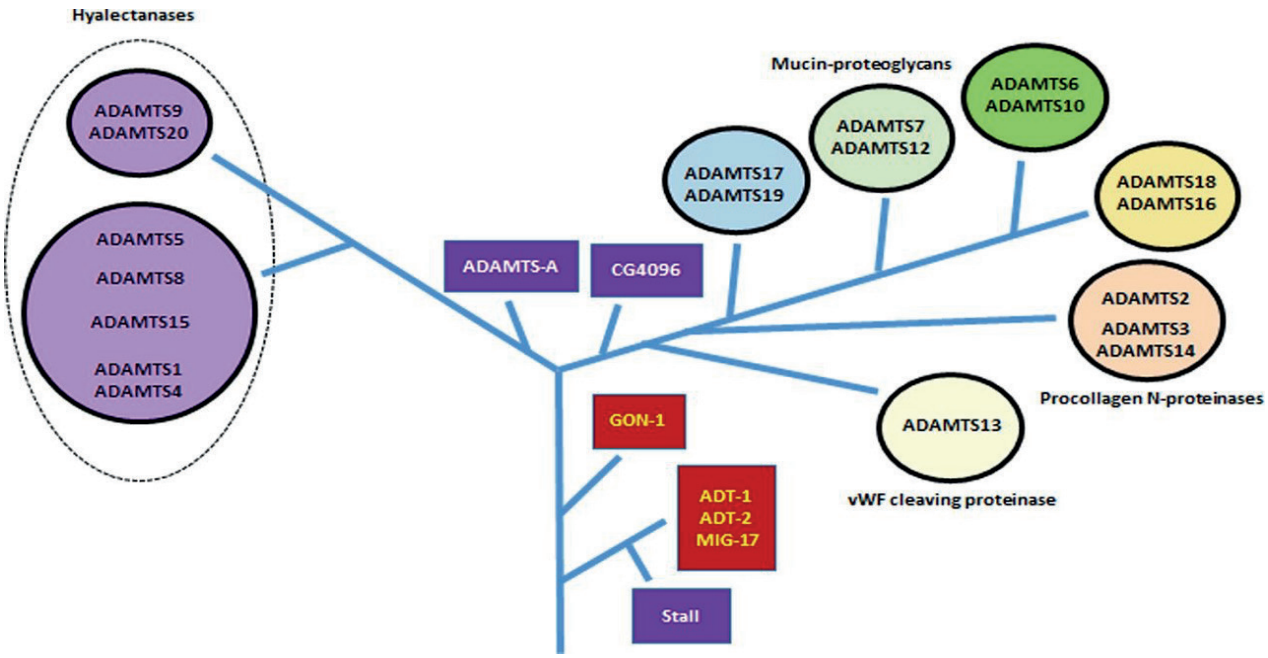

Figure 13: Evolution of the ADAMTS family. C. elegans has four ADAMTS family members, MIG-17, GON-1, ADT-1 and ADT-2, Drosophila has three, ADAMTS-A, CG4096 and Stall, and mammals have 19 members, ADAMTS1–10 and 12–20. Different clades and functions is discribed in the squeme (From Daevic *et al.* 2016)[120]

5.4.1. Connective hereditary diseases related to members of the family ADAMTS(L).

Recent works have identified that some members of the family of ADAMTS and ADAMTSL are essential for the formation and assembly of the extracellular matrix, such as in the maturation processes of collagens, the formation of fibrillin microfibers, and the activation of the TGFβ pathway. Several mutations have been found in members of the ADAMTS/ADAMTSL family and have been related to connective tissue diseases without vascular phenotype. Some of them phenocopy part of the characteristics of MFS patients, mainly ocular signs. For example, mutations with recessive inheritance in *ADAMTS10/17/19* "orphans" members cause a rare syndrome called **Weill-Marchesani syndrome (WMS)**. This syndrome is characterized phenotypically because it is opposed to MFS: short stature, achromatic chondrodysplasia with short fingers and limbs, and thick and low elasticity of the skin. However, as in MFS, *ectopia lentis* is present. Surprisingly, mutations with dominant inheritance in specific regions of the *FBN1* gene also produce WMS. It has been described that the mutated regions of FBN1 in WMS interact with ADAMTS10/17/19[15,121,125]. It has been reported recently that some cases of WMS also present TAAD[126]. WMS is molecularly characterized by loss of organization of microfibers and increased TGFβ activity in the connective tissues[127-129].

Another syndromic disease called **Geleophysic Dysplasia (GD)** is present in humans, dogs and sheep. GD is caused by mutations in *ADAMTSL2* with recessive inheritance. In this case, patients show a characteristic facial phenotype with a "happy" expression; short stature; shortening of arms, legs, hands, and feet; thickening of the skin and heart valves; aortic, tracheal, and pulmonary stenosis; and bronchopulmonary insufficiency with premature death. Moreover, mutations in specific regions of *FBN1* that cause GD with dominant inheritance, have been shown. The GD phenotype has been related to deficient binding of ADAMTSL2 to FBN1 and TGFβ[129-131] Cultured fibroblasts from GD patients have disorganized FBN1 microfibers and a hyperactivated TGFβ-pathway, with increased phosphorylation of SMAD2. *Adamtsl2* deficient mice die after birth by a severe bronchial epithelial dysplasia resembling the cellular anomalies described previously in GD. Moreover, there are patients with ***ectopia lentis*** that have recessive inherited mutations in *ADAMTSL4* and dominant mutations in *FBN1* genes.

However, the precise functions of ADAMTS10/17/19 and ADAMTSL2/4 are unknown. Therefore, there is evidence supporting the binding of ADAMTSL3, ADAMTSL5 and ADAMTSL6 to FBN1, promoting the assembly of Fibrillin microfibers *in vitro* and *in vivo*. In fact, the administration of recombinant Adamtsl6 improves microfiber organization in MFS mouse model[132,133].

Recessive mutations of the collagenase *ADAMTS2* produce **Ehnlers-Danlos Syndrome dermatoparaxis (EDS-VIIC).** Both humans and the deficient mice for *Adamts2* have extremely fragile skin and severe distal lung emphysema due to lack of maturation of collagen fibers, but no vascular phenotype has been reported[134-136].

Other rare genetic disease called **Microcornea, chorioretinal myopathy atrophy and telecanthus** (shortening of pupillary to tear), MMCAT, is caused by mutations with recessive inheritance in *ADAMTS18*. The *Adamts18* deficient mice recapitulate the features of MMCAT disease with lung and vaginal developmental problems[137-139].

In addition, there are different animal models that clarify a possible functional roles of different ADAMTS in the cardiovascular system. For example, ***Adamts9*$^{+/-}$ mice** (homozygosis is lethal during embryogenesis) present valvular thickening and aortic anomalies such as accumulation of PGs and collagen, elastolysis, and aortic dissection[140]; whereas ***Adamts5*$^{-/-}$ mice** show valvular thickening (valvular myxomatosis) by accumulation of PGs (mainly Versican), and *Adamts5*$^{-/-}$*;Smad2*$^{+/-}$ mice develop bicuspid aortic and pulmonary valves with total penetrance[141].

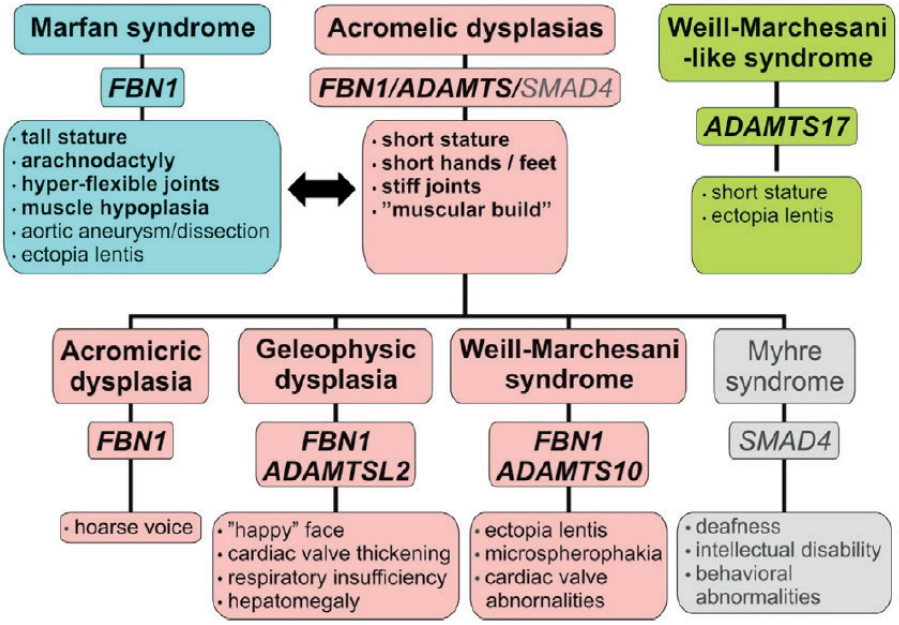

Figure 14. Disorders caused by mutations in ADAMTS family or in FBN1. Musculoskeletal presentations of Marfan syndrome (blue boxes) and the acromelic dysplasias (pink boxes). Myhre syndrome (gray boxes), caused by SMAD4 mutations. Weill–Marchesani-like syndrome (green boxes) (From Hubmacher *et al.* 2015)[125].

5.4.2 ADAMTS1

Adamts1 gene expression was first described in a murine model of cachexic-colorectal adenocarcinoma. Moreover, the authors showed that *Adamts1* mRNA was induced in response to acute inflammation *in vivo* [142]. Adamts1 binds to Fibulin1 as co-factor and degrades Collagen and some PGs such as Nidogen, Aggrecan, Syndecan, Versican, and Brevican[123]. Moreover, Adamts1 facilitates the cleavage of latent TGFβ to its active form[143]. Adamts1 mRNA expression increases in proliferating/migrating VSMCs[144] and in ECs treated with VEGF or subjected to hypoxia or to high wall shear stress[146,147].

Adamts1 has a potential role in the vascular pathophysiology. On the one hand, it has been widely described as an antiangiogenic molecule. Indeed, Adamts1 directly binds VEGF-A and blocks VEGFR2 phosphorylation, with consequent suppression of EC proliferation[148,149]. Accordingly, the suppression of endogenous *Adamts1* expression enhances endothelial cell proliferation[148,]. On the other hand, it is known that Adamts1 is expressed during aortic development and in adult vascular tissue, specifically in ECs and VSMCs; that it processes aortic Versican and Aggrecan; and that its expression is increased in atherosclerotic plaques and in degenerative thoracic aortic aneurysms (TAA)[144,150-152]. It seems therefore that Adamts1 expression is essential for vascular physiology. However, the role of Adamts1 in AA development remained unknown.

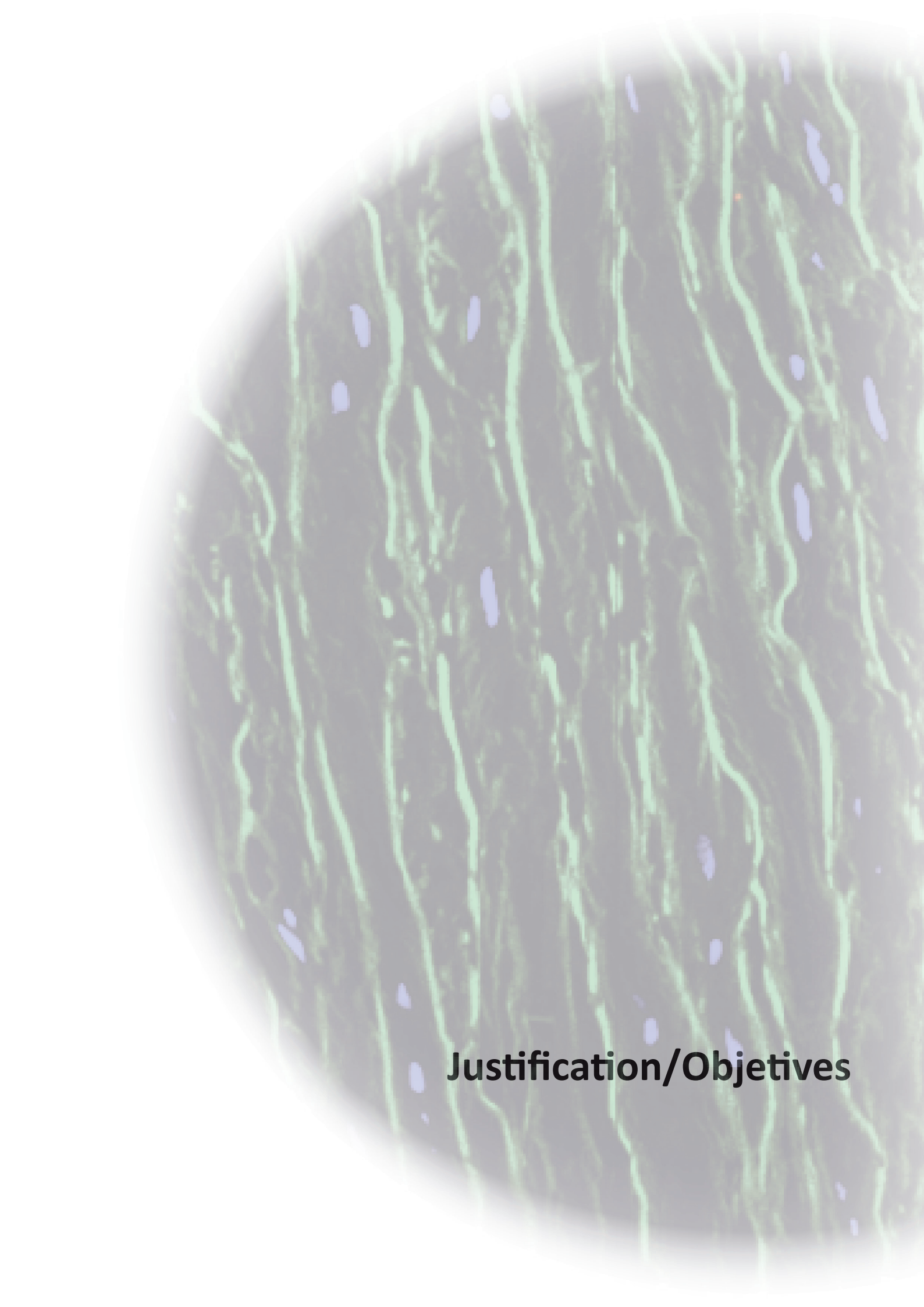

Justification/Objetives

High Adamts1 levels have been found in diseases associated to vascular remodeling, such as degenerative aneurysm, atherosclerosis and acute inflammation. However, the molecular mechanisms underlying *Adamts1* up-regulation and the potential role of this metalloprotease in these pathologies have not been elucidated.

Thus, the main objective of this thesis was to identify the molecular mediators involved in Adamts1 transcriptional regulation in vascular cells and to investigate the role of this extracellular metalloproteinase in vascular homeostasis and disease.

The specific objectives were:

1. To study the molecular mechanisms implicated in Adamts1 induction by stimuli associated with vascular remodeling

1.1. To evaluate *Adamts1* induction in vascular cells by different stimuli implicated in vascular remodeling, including VEGF, Ang-II, IL-1β, and TNF-α.

1.2. To investigate the regulation of the *Adamts1* promoter by vascular pro-remodeling agents.

1.3. To identify the specific signaling pathways involved in *Adamts1* induction.

1.4. To determine the relative contribution of each signaling pathway in vascular cells *in vitro* and in aortic tissue *in vivo*.

2. To determine the role of Adamts1 in vascular homeostasis, pathological vessel remodeling, and Marfan Disease.

2.1. To analyze the aortic phenotype of *Adamts1*-deficient mice under homeostatic conditions and after Ang-II stimulation.

2.2. To determine whether *Adamts1*-deficient mice develop a syndromic aortic disease.

2.3. To develop an inducible model of TAA in adult mice.

2.4. To unveil the molecular mechanisms that mediate TAA induction by *Adamts1* deficiency.

2.5. To assess Adamts1 expression in MFS aortic tissue.

2.6. To identify common molecular mechanisms involved in MFS and the aortic disease caused by *Adamts1* deficiency.

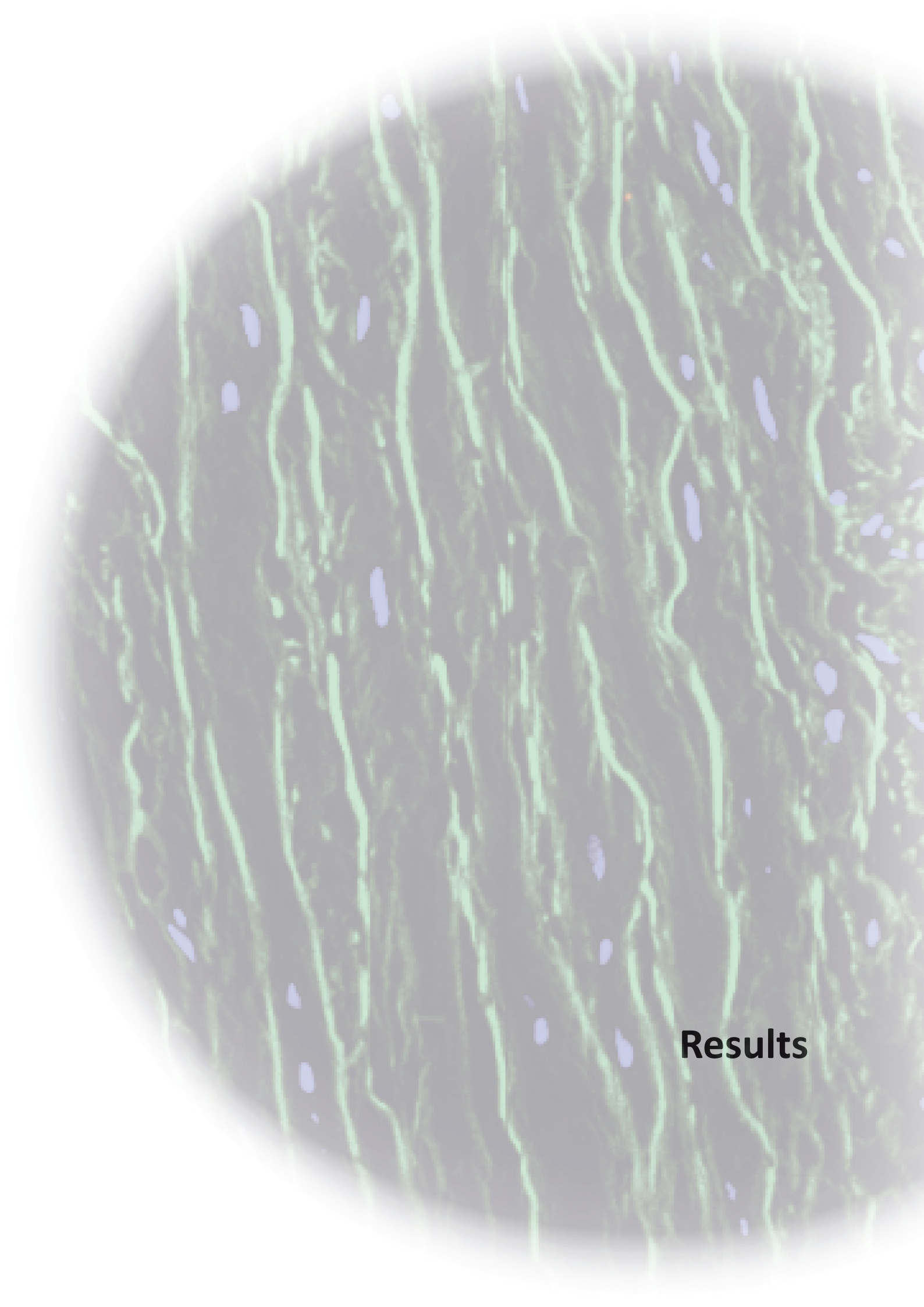

Results

Artículo 1: C/EBPβ and Nuclear Factor of Activated T Cells Differentially Regulate Adamts-1 Induction by Stimuli Associated with Vascular Remodeling.

Autores: Jorge Oller, Arántzazu Alfranca, Nerea Méndez-Barbero, Silvia Villahoz, Noelia Lozano-Vidal, Mara Martín-Alonso, Alicia G. Arroyo, Amelia Escolano, Angel Luis Armesilla, Miguel R. Campanero, Juan Miguel Redondo.

Publicado en: *Molecular and Cellular Biology*, Octubre 2015.

Resumen:

El remodelado de la pared vascular está producido por diversos agentes, entre los cuales se encuentran las fuerzas hemodinámicas, factores endocrinos o paracrinos tales como el factor de crecimiento endotelial vascular (VEGF) o Angiotensina-II (Ang-II) y las citoquinas proinflamatorias IL-1β y TNF-α. Estos factores producen proliferación y migración de células de músculo liso vascular (VSMCs), neovascularización, disfunción endotelial e infiltración de células inflamatorias. Además, inducen profundos cambios en la matriz extracelular de la pared aórtica debido a la secreción de diferentes componentes de la matriz extracelular y metaloproteinasas. Todos estos procesos son clave durante el desarrollo del remodelado vascular. Existen trabajos previos que indican que la metaloproteinasa Adamts1 podría jugar un papel significativo en la fisiopatología del remodelado vascular ya que ésta se expresa durante el desarrollo de la aorta, en tejido aórtico adulto y sus niveles se encuentran aumentados en diferentes patologías vasculares, como son: la aterosclerosis, el aneurisma aórtico degenerativo y la formación de neoíntima, pero apenas se conoce las vías de señalización que controlan la expresión de Adamts1.

En este trabajo hemos demostrado que tanto, VEGF, Ang-II, como IL-1β y TNF-α, aumentan la expresión de Adamts1 en VSMCs y en células endoteliales. El posterior análisis de la señalización intracelular implicada en este proceso reveló que VEGF y Ang-II inducen la expresión de Adamts1 a través de la activación diferencial de las vías de señalización que, en última instancia, promueven respectivamente la activación y unión de los factores de transcripción NFAT o C/EBPβ al promotor *Adamts1*. Por otra parte, hemos descrito que la infusión de Ang-II en ratones desencadena la fosforilación y translocación nuclear de C/EBPβ, concomitantemente con un aumento en la expresión de *Adamts1*. De forma similar, la infusión de VEGF promovió la activación de NFAT y la regulación de Adamts1 en la pared aórtica de manera dependiente de Calcineurina. Un análisis en profundidad de la regulación de estas vías de señalización podría ser útil en el tratamiento de enfermedades que cursan con remodelado vascular.

Aportación Personal al trabajo: He participado tanto en la parte de diseño y realización experimental, así como en la escritura del artículo.

MCB
Journals.ASM.org

C/EBPβ and Nuclear Factor of Activated T Cells Differentially Regulate Adamts-1 Induction by Stimuli Associated with Vascular Remodeling

Jorge Oller,[a] Arántzazu Alfranca,[a,b] Nerea Méndez-Barbero,[a] Silvia Villahoz,[a] Noelia Lozano-Vidal,[a] Mara Martín-Alonso,[a] Alicia G. Arroyo,[a] Amelia Escolano,[a] Angel Luis Armesilla,[c] Miguel R. Campanero,[d] Juan Miguel Redondo[a]

Department of Vascular Biology and Inflammation, Centro Nacional de Investigaciones Cardiovasculares Carlos III, Madrid, Spain[a]; Unidad de Biotecnología Celular, Instituto de Investigación en Enfermedades Raras, Instituto de Salud Carlos III, Madrid, Spain[b]; Research Institute in Healthcare Science, School of Pharmacy, Faculty of Science and Engineering, University of Wolverhampton, Wolverhampton, United Kingdom[c]; Department of Cancer Biology, Instituto de Investigaciones Biomédicas Alberto Sols, CSIC-UAM, Madrid, Spain[d]

Emerging evidence indicates that the metalloproteinase Adamts-1 plays a significant role in the pathophysiology of vessel remodeling, but little is known about the signaling pathways that control Adamts-1 expression. We show that vascular endothelial growth factor (VEGF), angiotensin-II, interleukin-1β, and tumor necrosis factor α, stimuli implicated in pathological vascular remodeling, increase Adamts-1 expression in endothelial and vascular smooth muscle cells. Analysis of the intracellular signaling pathways implicated in this process revealed that VEGF and angiotensin-II upregulate Adamts-1 expression via activation of differential signaling pathways that ultimately promote functional binding of the NFAT or C/EBPβ transcription factors, respectively, to the *Adamts-1* promoter. Infusion of mice with angiotensin-II triggered phosphorylation and nuclear translocation of C/EBPβ proteins in aortic cells concomitantly with an increase in the expression of Adamts-1, further underscoring the importance of C/EBPβ signaling in angiotensin-II-induced upregulation of Adamts-1. Similarly, VEGF promoted NFAT activation and subsequent Adamts-1 induction in aortic wall in a calcineurin-dependent manner. Our results demonstrate that Adamts-1 upregulation by inducers of pathological vascular remodeling is mediated by specific signal transduction pathways involving NFAT or C/EBPβ transcription factors. Targeting of these pathways may prove useful in the treatment of vascular disease.

Hemodynamic mechanical forces, endocrine or paracrine cellular factors such as vascular endothelial growth factor (VEGF) or angiotensin-II (Ang-II), and the proinflammatory cytokines interleukin-1β (IL-1β) and tumor necrosis factor-α (TNF-α) are strongly implicated in vascular remodeling, including vascular smooth muscle cell (VSMC) proliferation and migration, neovascularization, endothelial cell (EC) dysfunction, and/or inflammatory cell infiltration (1–4). Furthermore, profound changes in the extracellular matrix of the aortic wall, mediated by cellular secretion of extracellular matrix components and protein metalloproteinases, represent a critical hallmark of this process (5, 6).

Emerging evidence suggests that increased expression of the metalloproteinase Adamts-1 is associated with remodeling of the extracellular matrix in the aortic wall (7–10). Adamts-1 is a member of the ADAMTS (A disintegrin and metalloproteinase with thrombospondin motifs type I) family of proteases, which degrades the proteoglycans nidogen, aggrecan, syndecan, versican, and brevican (11). The expression of *Adamts-1* mRNA has been reported to increase in proliferating/migrating VSMCs (7) and in ECs treated with VEGF (12) and high wall shear stress (13, 14). However, the intracellular signaling pathways involved in its upregulation by these stimuli are poorly understood.

Here, we report that the expression of Adamts-1 in endothelial and vascular smooth muscle cells is induced by a broad range of stimuli associated with vascular remodeling, including VEGF, Ang-II, IL-1β, and TNF-α. We provide evidence supporting the alternative involvement of either NFAT or C/EBPβ in *Adamts-1* transcriptional activation by these stimuli and show *in vivo* activation of these transcription factors by VEGF and Ang-II, respectively, which might be involved in Adamts-1 induction in the aorta.

MATERIALS AND METHODS

Cell culture and reagents. Human umbilical vein ECs (HUVECs) were isolated from umbilical veins (15). Cells were cultured in 0.5% gelatin-coated plates in medium 199 supplemented with 20% fetal calf serum (FCS), 50 μg/ml bovine brain extract, 100 μg/ml heparin, and 1% penicillin-streptomycin. Cells were used between passages 4 and 6. Murine VSMCs were isolated and grown as described previously (16). Murine lung ECs (MLECs) were purified and cultured by previously published methods (17).

Cells were stimulated with 50 ng/ml recombinant human $VEGF_{165}$, 100 ng/ml IL-1β, or 50 ng/ml TNF-α (all from Peprotech). Ang-II (10^{-6} M for MLECs or VSMCs or 10^{-5} M for HUVECs) and phorbol myristate

Received 14 May 2015 **Returned for modification** 8 June 2015
Accepted 22 July 2015
Accepted manuscript posted online 27 July 2015
Citation Oller J, Alfranca A, Méndez-Barbero N, Villahoz S, Lozano-Vidal N, Martín-Alonso M, Arroyo AG, Escolano A, Armesilla AL, Campanero MR, Redondo JM. 2015. C/EBPβ and nuclear factor of activated T cells differentially regulate Adamts-1 induction by stimuli associated with vascular remodeling. Mol Cell Biol 35:3409–3422. doi:10.1128/MCB.00494-15.
Address correspondence to Miguel R. Campanero, mcampanero@iib.uam.es, or Juan Miguel Redondo, jmredondo@cnic.es.
J.O. and A.A. contributed equally to this work.
M.R.C. and J.M.R. contributed equally as senior authors.

doi:10.1128/MCB.00494-15

acetate (10 ng/ml) were purchased from Sigma-Aldrich. Calcium ionophore A23187 (1 μM) was obtained from EMD, Tocris Bioscience. Where indicated, cells were treated with 200 ng/ml cyclosporine (CsA) for 30 min prior to stimulation.

Western blot analysis. Cell extracts were obtained as described previously (16). Proteins were separated on SDS-polyacrylamide gels and transferred to nitrocellulose membranes. Membranes were incubated with the corresponding primary antibody. Primary antibodies were detected by incubation with either a 1:5,000 dilution of peroxidase-conjugated goat anti-mouse immunoglobulin antibody (Sigma) or a 1:5,000 dilution of peroxidase-conjugated goat anti-rabbit immunoglobulin antibody (GE Healthcare), depending on the origin of the primary antibody. All antibody dilutions were carried out in 1% bovine serum albumin (BSA) in Tris-buffered saline–Tween 20. Bound antibodies were detected by enhanced chemiluminescence detection (Millipore).

The antibodies used in this study were mouse anti-ADAMTS1 monoclonal antibody (1:1,000), mouse anti-NFATc1 monoclonal antibody (1:500), rabbit anti-NFATc3 polyclonal antibody (1:1,000), and rabbit anti-NFATc4 polyclonal antibody (1:1,000) (all from Santa Cruz), mouse anti-human Cox-2 monoclonal antibody (Cayman; 1:4,000), rabbit anti-mouse Cox-2 polyclonal antibody (Cayman; 1:1,000), rabbit anti-C/EBPβ polyclonal antibody (Santa Cruz; 1:1,000), rabbit phospho-specific anti-C/EBPβ polyclonal antibody (Cell Signaling; 1:1,000), rabbit anti-CNA polyclonal antibody (Chemicon, Ab-1695; 1:1,000), mouse anti-CNB monoclonal antibody (Upstate; 1:4,000), rabbit anti-RCAN1 polyclonal antibody (Sigma; 1:500), mouse antitubulin monoclonal antibody (Sigma; 1:40,000), mouse anti-glyceraldehyde phosphate dehydrogenase monoclonal antibody (Abcam; 1:10,000), and mouse anti-polypyrimidine tract-binding protein-associated splicing factor (anti-PSF) monoclonal antibody (Sigma; 1:1,000).

Reverse transcription and RT-qPCR analysis. RNA was extracted with the TriPure kit (Roche), and cDNA synthesis was performed with 2 μg of total RNA (16). Quantification of RNA levels was carried out by real-time quantitative PCR (RT-qPCR) with the following TaqMan assays (Applied Biosystems): human *ADAMTS-1* (Hs00199608_m1), human *TFCR* (Hs00951083_m1), mouse *Adamts-1* (Mm00607939_s1), and mouse *Hprt1* (Mm00446968_m1). RT-qPCR assays were performed as described previously (16). Analysis of RT-qPCR data was carried out by the comparative $2^{-\Delta\Delta CT}$ method.

Plasmids. Luciferase-based reporter vectors containing the human *ADAMTS-1* proximal promoter region −706/+207 and −342/+207 (18) were generously provided by Y. Ninomiya (Okayama University, Okayama, Japan). To generate pMetLuc(−274/+207), the corresponding region of the *ADAMTS-1* promoter was amplified by PCR with Adamts-1 hPromoter−274 sense and Adamts-1 hPromoter+207 antisense oligonucleotides and cloned into pMet-Luc (Clontech). To generate luciferase-based reporter vectors containing the −539/+41 and −269/+41 regions of the murine *Adamts-1* promoter, the corresponding regions were amplified by PCR from mouse genomic DNA isolated from MLECs as a template with either Adamts-1 mPromoter−539 sense or Adamts-1 mPromoter−269 sense oligonucleotides in combination with the Adamts-1 mPromoter+41 antisense primer. Amplified products were cloned into pGL3-Basic (Promega), generating plasmids pGL3(−539/+41) and pGL3(−269/+41), respectively. Construct pGL3(−325/+41) was generated by digestion of pGL3(−539/+41) with PstI and XhoI and subcloning into pGL3-Basic. The oligonucleotides used for cloning were Adamts-1 hPromoter+207 antisense (5′-GCAGGCAGAGTGGCTC-3′), Adamts-1 hPromoter−274 sense (5′-CGGTGGAAGGGAGAGTC-3′), Adamts-1 mPromoter−539 sense (5′-GGTACCGAGAAGCGCAGAATCAAC-3′), Adamts-1 mPromoter−269 sense (5′-GGTACCCCGAGAGATGAAGTT AAAGG-3′), and Adamts-1 mPromoter+41 antisense (5′-CTCGAGCT TGCGATAGCACCTAG-3′).

Site-directed mutagenesis was performed with the QuikChange mutagenesis kit (Stratagene). The fidelity of all amplified products was confirmed by sequencing. The oligonucleotides used for site-directed mutagenesis were (the mutated positions are underlined) GGGGAGAAAAG GAATGTCGAGGTTTCTTTTCAATTCGACC (to mutate the C/EBPβ binding site at position −365 of the murine promoter region), CAGG ATAGGGAAATGTCGAAGTTGGGACTGCGTTCTCC (to mutate the C/EBPβ binding site at position −410 of the human promoter region), GTGGGGAGGAAGGGTGTTGTAGGAAACCGGCGAGG (to mutate the binding site for NFAT at position −302 of the human promoter region), GGGGAGGAAGGGTGGTCCATTACACCGGCGAGG (to mutate the binding site for NFAT at position −294 of the human promoter region), and GAGGAAGGGTGTTGTATTACACCGGCGAGGGAGA AAAG (to mutate both binding sites for NFAT at positions −302 and −294 of the human promoter region).

Transient transfection and luciferase assay. HUVECs (5×10^4) were transfected with 0.6 μg of luciferase reporter vector by the calcium phosphate method (15). Murine VSMCs (10^4) were transfected with 0.6 μg of luciferase reporter vector with Lipofectamine (16). In cotransfection experiments, pcDNA3.1-LIP or the pCDNA3.1-Empty control expression vector was transfected together with the corresponding luciferase reporter plasmid at a ratio of 3:1. Differences in cell survival or changes in global translation rate due to different treatments were ruled out through the parallel transfection of the corresponding empty luciferase vector (basal activity, 10,000 to 30,000 relative light units). Luciferase activity was measured with the luciferase assay kit (Promega) or the Ready to Glow kit (Clontech) for pGL3- or pMetLuc-derived plasmids, respectively.

Formaldehyde cross-linking and ChIP assays. Chromatin immunoprecipitation (ChIP) assays were performed essentially as described previously (19). HUVECs (1.5×10^7) were stimulated with 50 ng/ml VEGF or 10^{-5} M Ang-II for 30 min and then fixed with 1% formaldehyde for 5 min at 4°C. Fixation was quenched by the addition of 0.125 M glycine and incubation for 10 min at 4°C. Cells were washed three times with cold phosphate-buffered saline (PBS) and scraped into PBS containing proteinase inhibitors. After a centrifugation step, cells were suspended in lysis buffer 1 (50 mM HEPES-KOH [pH 7.5], 1 mM EDTA, 10% glycerol, 0.5% NP-40, 0.25% Triton X-100, 140 mM NaCl, proteinase inhibitors) for 10 min at 4°C. Nuclear pellets were washed in lysis buffer 2 (10 mM Tris-HCl [pH 8], 200 mM NaCl, 1 mM EDTA, 0.5 mM EGTA), lysed in lysis buffer 3 (10 mM Tris-HCl [pH 8], 200 mM NaCl, 1 mM EDTA, 0.5 mM EGTA, 0.5% SDS), and sonicated with a Bioruptor sonicator (Diagenode). Before immunoprecipitation, the size of DNA fragments was confirmed to be 200 to 600 bp by reverse cross-linking (3 volumes of Tris-EDTA [TE] buffer and 0.3 M NaCl at 65°C overnight) of an aliquot of chromatin sample and subsequent electrophoresis in a 2% agarose gel. A portion (5%) of the total chromatin sample was saved for input detection. For each immunoprecipitation, 50 μl of protein A Dynabeads (Invitrogen) was blocked with 0.5% BSA-PBS for 1 h and incubated overnight in 0.5% BSA-PBS with 6 μg of control mouse or rabbit IgG (Santa Cruz), a rabbit anti-C/EBPβ polyclonal antibody (Santa Cruz), or an anti-NFATc1 monoclonal antibody (kindly provided by T. Minami, Research Center for Advanced Science and Technology, University of Tokyo, Tokyo, Japan). Chromatin was diluted 1/6 in TE buffer containing 50 mM NaCl and 1% Triton X-100 (Sigma) and incubated with rocking overnight at 4°C with antibody-coupled Dynabeads. The beads were washed three times with low-salt washing buffer (20 mM Tris-HCl [pH 8], 2 mM EDTA, 150 mM NaCl, 1% Triton X-100, 0.1% SDS, 0.3% sarcosyl, 0.5% sodium deoxycholate), three times with high-salt buffer (20 mM Tris-HCl [pH 8], 2 mM EDTA, 500 mM NaCl, 1% Triton X-100, 0.1% SDS), three times with high-salt radioimmunoprecipitation assay buffer (20 mM Tris-HCl [pH 7.5], 500 mM NaCl, 1 mM EDTA, 1 mM EGTA, 1% NP-40, 1% sodium deoxycholate), and twice with TE buffer containing 150 mM NaCl. Finally, chromatin bound to Dynabeads was eluted in 200 μl of 10 mM Tris-HCl [pH 8]–10 mM EDTA–2% SDS buffer by rocking at 65°C for 45 min, followed by vortexing for 5 min. Reverse cross-linking was performed by incubation with 600 μl of TE buffer containing 300 mM NaCl at 65°C overnight. DNA samples were treated with 0.2 μg/ml RNase (Sigma-Aldrich) for 1 h at 37°C and 0.2 μg/ml proteinase K (Sigma-Aldrich) for 1 h

at 50°C. DNA was extracted with phenol-chloroform, precipitated, and resuspended in 50 μl of water. One-third of the final volume was analyzed by Sybr green real-time PCR with the oligonucleotides ADAMTS-1 promoter C/EBPβ site (sense, CCTAGCTCATCTCCTAGATTG; antisense, GGTTCGGTTGGAGAACGC), ADAMTS-1 NFATs sites (sense, GGAAG GGTGGTCCAGGAAA; antisense, CGCCACTGCTCGTCAATC), ADAMTS-1 3′ UTR (sense, GACAAGTGATCTCAATGTCCCC; antisense, GAGCTTAGTACCTCCAACTTCCT), and COX-2 promoter (sense, GG TTTCCGATTTTCTCATTTCCG; antisense, CACTGCAAGTCGTATGA CAATTG).

Animals. Animal studies were performed in accordance with the guidelines of the European Union on animal care and approved by the Animal Care and Ethics committee at the Centro Nacional de Investigaciones Cardiovasculares. Calcineurin (CN) B1 (*Cnb1*$^{\Delta/fl}$) conditional knockout mice (20) were kindly provided by Gerald R. Crabtree (Howard Hughes Medical Institute, Stanford University School of Medicine, Stanford, CA). Mice were administered VEGF or Ang-II by subcutaneous osmotic minipump (Alzet Corp) infusion at 25 μg/kg/day and 1 μg/kg/min, respectively. Where indicated, minipumps loaded with CsA (Novartis; 5 mg/kg/day) were implanted 24 h before VEGF or Ang-II administration. The AT_1R blocker losartan (Fluka) was administered at 10 mg/kg/day by minipumps implanted 24 h before the administration of Ang-II.

Lentivirus production and infection. Lentivirus production was performed as described previously (16). Lentiviruses encoding Cre recombinase, green fluorescent protein (GFP)-LXVP, and GFP-LXVP Mutant have been previously described (21, 22). Lenti-LIP, a lentivirus encoding LIP (liver inhibitor protein), was generated by subcloning mouse C/EBPβ (LIP) from pcDNA3.1-C/EBPβ (LIP) (a gift from Peter Johnson; Addgene plasmid 12561) into lentiviral plasmid pHRSIN-IRES-GFP. VSMCs, HUVECs, and MLECs were infected at a multiplicity of infection of 3.

Histological analysis. Aortas were fixed in 4% paraformaldehyde overnight at 4°C. Paraffin cross sections (5 μm) from fixed aortas were used for immunohistochemistry analysis. Heat-induced epitope retrieval was performed in citrate buffer (10 mM sodium citrate [pH 6], 0.05% Tween 20) at 125°C for 5 min. The antibodies used for immunohistochemistry analysis were anti-C/EBPβ (1/100; Santa Cruz Biotechnology), anti-p-C/EBPβ (1/25; Cell Signaling), rabbit polyclonal anti-Adamts-1 (1/100; Santa Cruz), and anti-NFATc4 (1/100; Santa Cruz). Substrate staining was developed with diaminobenzidine (Vector Laboratories), and sections were counterstained with hematoxylin, dehydrated, and mounted in DPX (Fluka).

Statistical analysis. Results are expressed as mean values ± standard deviations (SD). Differences were evaluated by one-way analysis of variance with the *post hoc* Newman-Keuls comparison test. Statistical significance was assigned at P values of <0.05.

RESULTS

Different signal transduction pathways regulate VEGF- and Ang-II-induced Adamts1 gene expression in vascular cells. Because Adamts-1 expression increases in response to the activation of ECs with VEGF (12) and shear stress (13, 14), we hypothesized that other extracellular inducers of vascular remodeling may also regulate Adamts-1 expression. We used Ang-II to test this hypothesis. Treatment of HUVECs, murine VSMCs, and MLECs with Ang-II resulted in a strong increase in Adamts-1 protein and mRNA levels (Fig. 1A and B), with maximal expression occurring at approximately 6 h poststimulation.

Because VEGF and Ang-II activate the CN/nuclear factor of activated T cells (NFAT) signaling pathway in ECs and VSMCs (16, 23, 24), we investigated the involvement of this pathway in the upregulation of the *Adamts-1* gene by these stimuli. Vascular cells were preincubated with the CN inhibitor CsA (25), and Adamts-1 expression was analyzed by Western blot and RT-qPCR analyses. VEGF-dependent upregulation of Adamts-1 expression at the

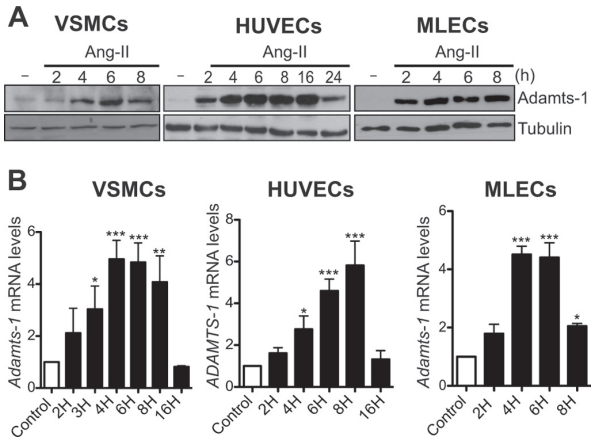

FIG 1 Ang-II induces the expression of Adamts-1 in vascular cells. (A) Western blot analysis of Adamts-1 expression in protein extracts from primary VSMCs, HUVECs, and MLECs stimulated with Ang-II. (B) *Adamts-1* gene expression was measured by qPCR in VSMCs, HUVECs, and MLECs treated with Ang-II as indicated. Values are expressed as fold increases relative to nonstimulated cells (Control). Histograms represent means ± SD of at least three independent experiments. *, $P < 0.05$; **, $P < 0.01$; ***, $P < 0.001$ (versus the control).

mRNA and protein levels was markedly reduced by inhibition of the CN/NFAT pathway with CsA (Fig. 2A). In contrast, induction of Adamts-1 expression in response to Ang-II was unchanged in the presence of CsA (Fig. 2B), despite efficient blockade of CN signaling by CsA, as confirmed by CsA-mediated inhibition of the genes for cyclooxygenase 2 (Cox-2) and RCAN1.4 (Fig. 2), two known CN/NFAT targets (19, 24). These results suggest that CN signaling is implicated in VEGF-dependent induction of Adamts-1 expression but not in Ang-II-promoted Adamts-1 upregulation.

In addition to inhibiting CN, CsA can exert additional effects on the cell, such as activation of the transforming growth factor β1 pathway (26) or stabilization of the RNA encoding VEGF (27). To confirm that the CsA-mediated reduction of Adamts-1 expression by VEGF was not the result of off-target effects of CsA, we transduced ECs and VSMCs with lentiviral vectors encoding LXVP, a peptide that inhibits CN phosphatase activity and blocks its docking site for NFAT (28). Consistent with the data obtained with CsA, LXVP expression in vascular cells abrogated *Adamts-1* gene upregulation in response to VEGF, but not in response to Ang-II (Fig. 3A to D). As expected, the LXVP peptide inhibited Cox-2 upregulation induced by both stimuli (Fig. 3A, B, E, and F), demonstrating efficient impairment of CN signaling in all cases, whereas an LXVP mutant had no effect on either Adamts-1 or Cox-2 upregulation by these stimuli (Fig. 3A to F). The participation of CN-independent signal transduction pathways in the regulation of Adamts-1 expression by Ang-II led us to investigate whether other stimuli that operate in a CN-independent fashion, such as the proinflammatory cytokines TNF-α and IL-1β, might also induce Adamts-1. Stimulation of HUVECs and VSMCs with TNF-α or IL-1β led to a time-dependent increase in Adamts-1 levels in both cell types, peaking at 6 to 8 h poststimulation (Fig. 4A and B). CN inhibition with CsA or the LXVP peptide failed to block TNF-α- or IL-1β-induced upregulation of Adamts-1 ex-

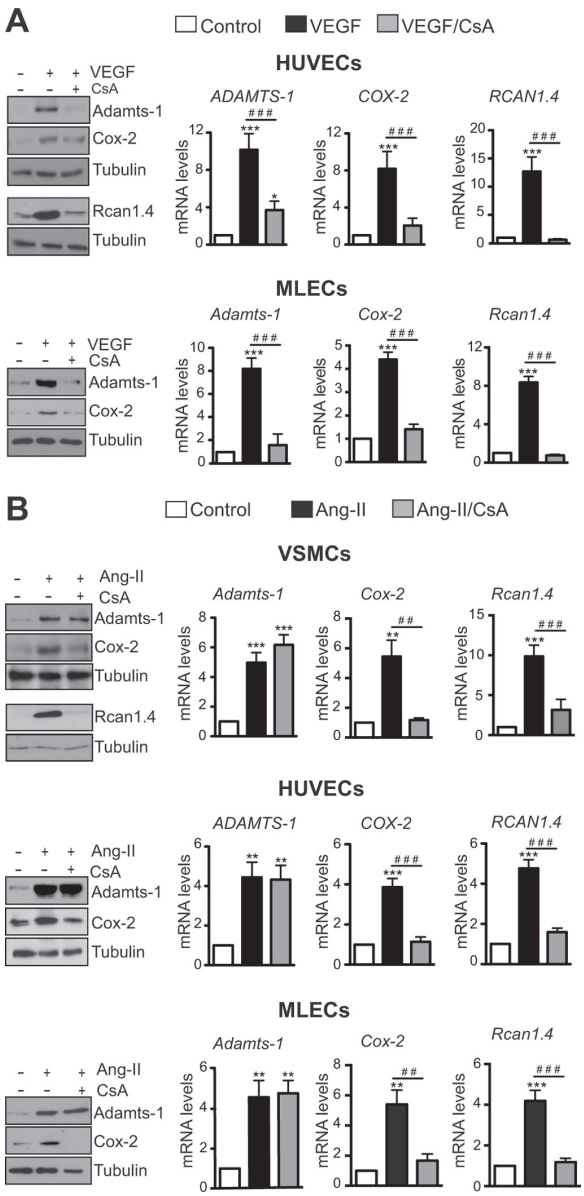

FIG 2 Ang-II and VEGF upregulate Adamts-1 expression in vascular cells via differential signaling mechanisms. Western blot and qPCR analyses of *Adamts-1*, *Cox-2*, and *RCAN1.4* expression in HUVECs and MLECs treated with CsA or the vehicle 1 h before stimulation with VEGF for 4 h (A) and VSMCs, HUVECs, and MLECs treated with CsA or the vehicle 1 h before stimulation with Ang-II for 4 h (B). In all Western blot assays, the expression of tubulin was analyzed as a loading control. The immunoblot assays shown are representative of three independent experiments. In qPCR analyses, mRNA levels were normalized to hypoxanthine phosphoribosyltransferase expression. Data are expressed as fold increases relative to nonstimulated cells (Control) and shown as means ± SD of three independent experiments. *, $P < 0.05$; **, $P < 0.01$; ***, $P < 0.001$ (versus control); ##, $P < 0.01$; ###, $P < 0.001$ (versus CsA-pretreated cells).

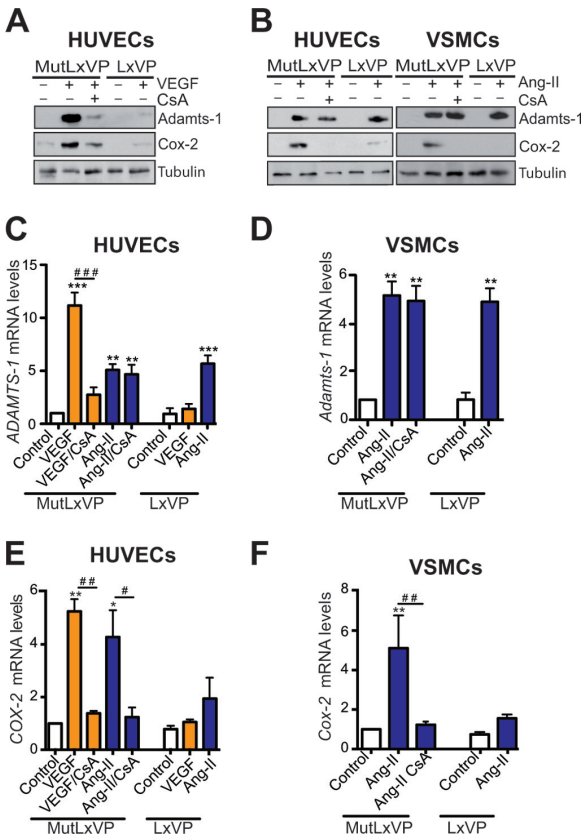

FIG 3 Blockade of CN activity with the NFAT-derived peptide LXVP inhibits Adamts-1 upregulation by VEGF but not Ang-II in vascular cells. (A and B) Western blot analysis of Adamts-1 and Cox-2 expression in the indicated vascular cells transduced with lentiviral particles expressing GFP tagged with the CN inhibitory peptide LXVP (LxVP) or a mutant version unable to inhibit CN (MutLxVP). Infected cells were stimulated with VEGF (A) or Ang-II (B) for 4 and 6 h, respectively, in the absence or presence of CsA as indicated. Tubulin expression was analyzed as a loading control. The immunoblot assays shown are representative of at least two independent experiments. (C to F) *Adamts-1* (C and D) and *Cox-2* (E and F) mRNA expression was measured by qPCR in cells infected with lentiviruses as described above and stimulated as indicated. Values are expressed as fold increases relative to nonstimulated cells (Control). Data are shown as means ± SD of three independent experiments. **, $P < 0.01$; ***, $P < 0.001$ (versus the control); #, $P < 0.05$; ##, $P < 0.01$; ###, $P < 0.001$ (versus CsA-pretreated cells).

pression (Fig. 4C to F), suggesting that activation of the CN/NFAT pathway is not involved in this regulation. In parallel, we measured Cox-2 expression as a positive control for CN-independent TNF-α and IL-1β stimulation (24). As anticipated, Cox-2 induction by TNF-α and IL-1β was unaltered by inhibition of the CN/NFAT pathway (Fig. 4A to D, G, and H).

Finally, to further confirm the involvement of CN-dependent and -independent transduction mechanisms in the regulation of *Adamts-1* gene expression, we employed cells lacking CN. MLECs and VSMCs isolated from a conditional CN knockout mouse (20) were transduced with a lentivirus expressing Cre recombinase (Lenti-Cre) to promote deletion of the *Cnb1* gene. As shown in Fig. 5, Cnb1 deletion led to the destabilization of CN A in both cell

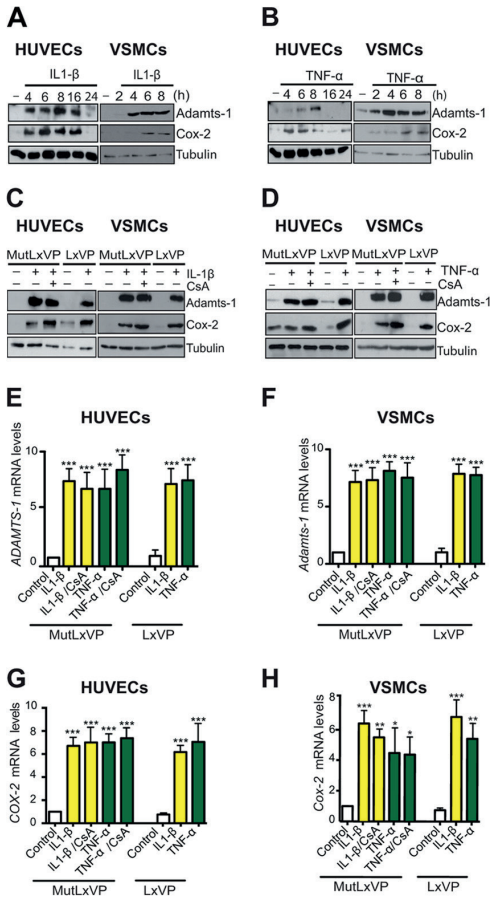

FIG 4 Upregulation of *Adamts-1* gene expression by the proinflammatory stimuli TNF-α and IL-1β does not require CN activation. (A to D) Western blot analysis of Adamts-1 and Cox-2 expression in vascular cells treated with IL-1β (A) or TNF-α (B) for the times indicated. (C and D) HUVECs and VSMCs were transduced with lentiviral particles expressing GFP tagged with the CN inhibitory peptide LXVP (LxVP) or a mutant version unable to inhibit CN (MutLxVP). Cells were stimulated with IL-1-β (C) or TNF-α (D) for 6 h in the absence or presence of CsA as indicated. In all cases, tubulin expression was analyzed as a loading control. The immunoblot assays shown are representative of at least two independent experiments. (E to H) *Adamts-1* and *Cox2* mRNA expression was measured by qPCR in HUVECs (E and G) or VSMCs (F and H) infected with lentiviruses as described above and stimulated as indicated. Values are expressed as fold increases relative to nonstimulated cells (Control). Data are shown as means ± SD of three independent experiments. *, $P < 0.05$; **, $P < 0.01$; ***, $P < 0.001$ (versus the control).

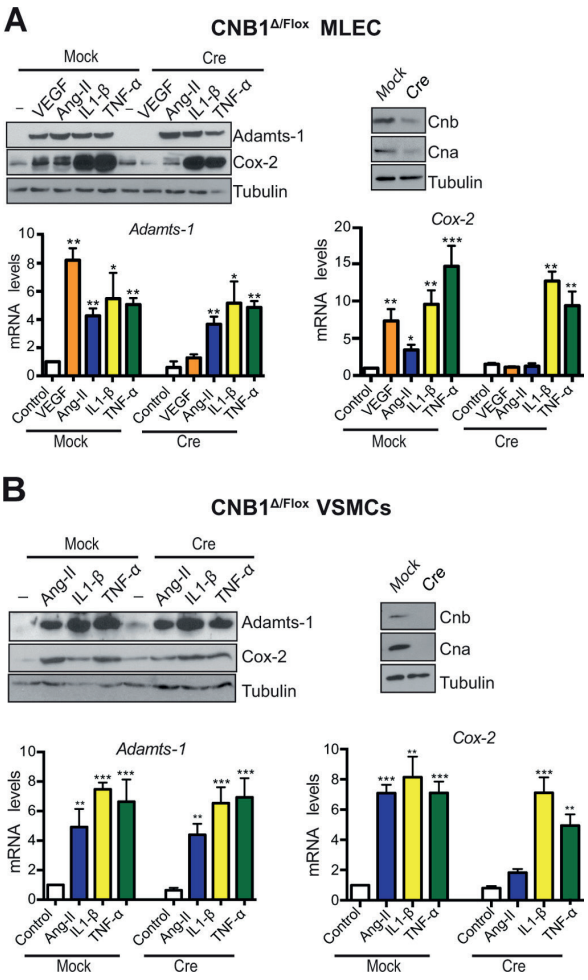

FIG 5 CN deletion impairs Adamts-1 upregulation by VEGF but not Ang-II, TNF-α, or IL-1β. To suppress CN expression in primary vascular cells, MLECs (A) and VSMCs (B) isolated from *Cnb1*$^{\Delta/fl}$ mice were infected with lentiviruses expressing the Cre recombinase (Cre) or GFP as a control and then stimulated as indicated. CN deficiency was assessed by Western blot analysis with antibodies specific for the CN B (Cnb) or A (Cna) subunit. Adamts-1 and Cox-2 protein levels were determined by Western blotting. In all cases, the expression of tubulin was analyzed as a loading control. Immunoblot assays are representative of at least three independent experiments. *Adamts-1* and *Cox2* mRNA expression was measured by qPCR in CN-deficient MLECs (A) or VSMCs (B) stimulated as indicated. Values are expressed as fold increases relative to nonstimulated cells (Control). Data are shown as means ± SD of three independent experiments. *, $P < 0.05$; **, $P < 0.01$; ***, $P < 0.001$ (versus the control).

types. VEGF stimulation was no longer able to induce Adamts-1 or Cox-2 gene expression in CN-deficient MLECs (Fig. 5A). In contrast, Adamts-1 upregulation by Ang-II, TNF-α, or IL-1β was unaffected by disruption of CN expression (Fig. 5). Consistent with the data obtained with CN inhibitors (Fig. 2 to 4), whereas Cox-2 induction by TNF-α or IL-1β was unaltered by CN deletion, Cox-2 upregulation by Ang-II was largely abolished in CN-deficient vascular cells (Fig. 5).

Collectively, these results indicate that stimulation of vascular cells induces *Adamts-1* gene expression via the activation of at least two different intracellular signaling pathways. Whereas VEGF-dependent upregulation of Adamts-1 requires CN activity, Ang-II, TNF-α, and IL-1β operate through the activation of an alternative signaling mechanism.

***Adamts-1* gene upregulation requires the binding of either NFAT or C/EBPβ to specific sequences located in its promoter region.** To identify the transcription factors that link signal transduction processes in vascular cells with upregulation of *Adamts-1* gene expression, we transfected HUVECs and VSMCs with luciferase-based reporter constructs containing the proximal

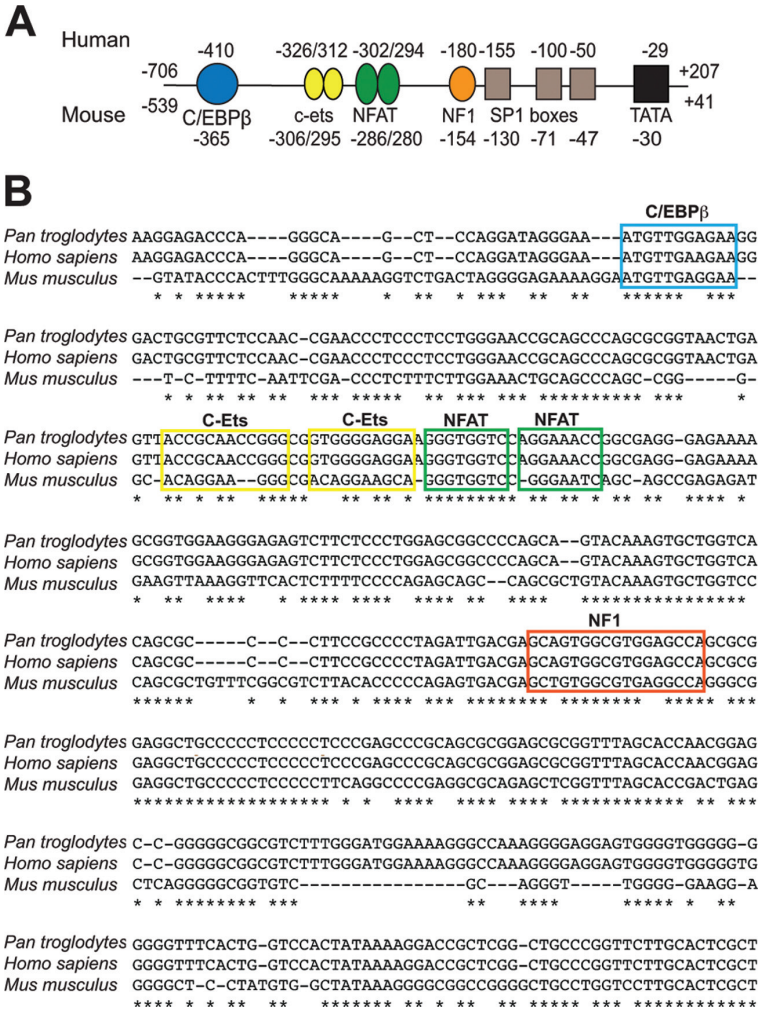

FIG 6 Sequence and putative regulatory elements of the *Adamts-1* proximal promoter region. (A) Diagram depicting putative *cis*-acting regulatory elements in the human and mouse promoter regions of *Adamts-1*. (B) Alignment of the proximal regions of the human (*Homo sapiens*), mouse (*Mus musculus*), and chimpanzee (*Pan troglodytes*) *Adamts-1* gene promoters. Nucleotides identical in the three species are indicated by stars. Putative transcription factor binding sites are boxed.

promoter regions of *Adamts-1*, pMetLuc(−706/+207) and pGL3(−539/+41), for the human and murine genes, respectively (Fig. 6). The presence of binding motifs for the transcription factors C/EBPβ, c-ets, NF-1, and SP1 in the *Adamts-1* proximal promoter (Fig. 6) has been previously reported (29), but no binding sites for NFAT have yet been identified in this region. A detailed *in silico* analysis of the human *ADAMTS-1* proximal promoter sequence revealed two potential NFAT binding sites at positions −302 and −294, corresponding to nucleotides −286 and −280 in the murine promoter (Fig. 6).

Stimulation of the transfected cells with VEGF, Ang-II, IL-1β, or TNF-α resulted in a significant increase in luciferase activity of the *Adamts-1* reporter vectors (Fig. 7), suggesting that this promoter region contains regulatory elements that mediate its transcriptional activation by these stimuli. In agreement with our results on protein and mRNA induction (Fig. 2), pretreatment of the transfected cells with CsA abolished the activation of the reporter in response to VEGF but not that in response to Ang-II, IL-1β, or TNF-α (Fig. 7). These results suggest that the −706/+207 region of human *ADAMTS-1* (−539/+41 in the mouse) contains CN-dependent and -independent regulatory elements that respond to stimulation by VEGF and Ang-II, IL-1β, or TNF-α, respectively.

We generated a series of deletion-containing versions of the promoter constructs to determine the functional relevance of the transcription factor-binding motifs identified in the *ADAMTS-1* proximal promoter. Deletion of the region encompassing the C/EBPβ-binding motif failed to alter the luciferase activity of the reporter vector in response to VEGF stimulation in HUVECs (Fig. 7A). Accordingly, preincubation of the cells with CsA prior to VEGF stimulation substantially inhibited the reporter activity of this construct (Fig. 7A). Conversely, loss of this region completely

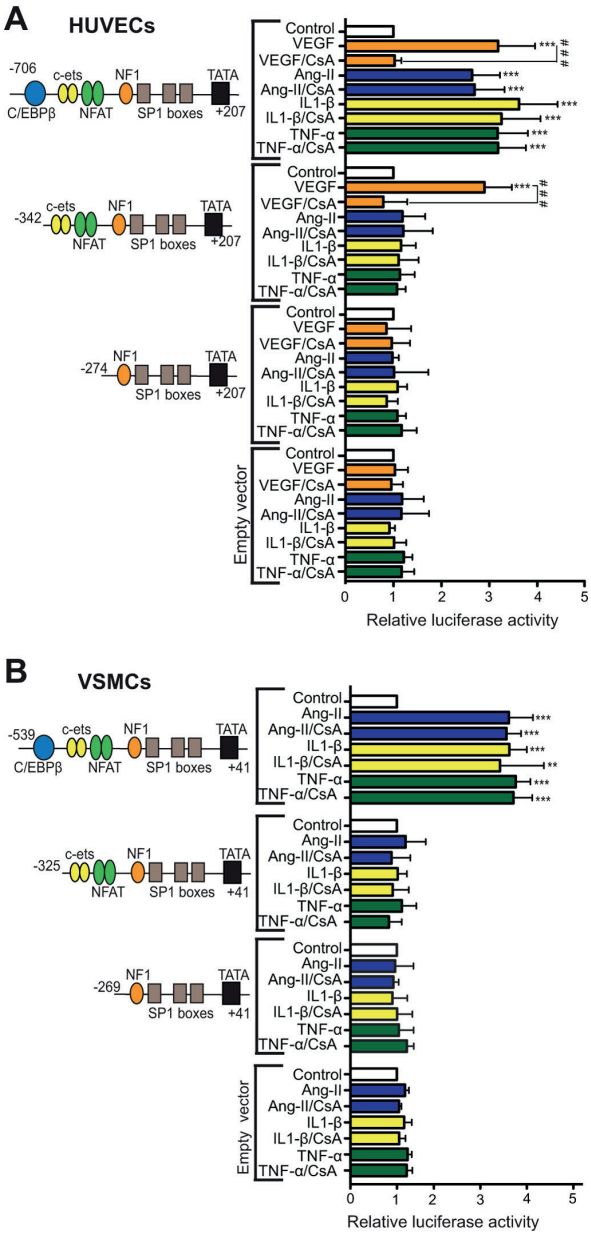

FIG 7 Functional analysis of *Adamts-1* promoter activity in response to VEGF, Ang-II, TNF-α, and IL-1β. HUVECs (A) or murine VSMCs (B) were transfected with luciferase-based reporter plasmids containing serial deletions of the human (A) or mouse (B) *Adamts-1* promoter region. Transfected cells were left unstimulated (Control) or stimulated with VEGF, Ang-II, IL-1-β, and TNF-α for 8 h. Where indicated, cells were treated with CsA for 1 h prior to stimulation. Luciferase activity is expressed as fold increases relative to the activity of the reporter in nonstimulated cells. Empty plasmids pMetLuc and pGL3 were used as negative controls. Histograms show data as means ± SD of at least five independent experiments. **, $P < 0.01$; ***, $P < 0.001$ (versus nonstimulated cells); ###, $P < 0.001$ (VEGF versus VEGF/CsA-stimulated cells).

blunted the upregulation of reporter gene activity in cells treated with Ang-II, IL-1β, or TNF-α (Fig. 7).

Further removal of the region containing the two potential binding sites for NFAT completely abrogated the VEGF-stimulated increase in reporter activity (Fig. 7A). As expected, this construct and the equivalent murine construct did not respond to Ang-II, TNF-α, or IL-1β treatment (Fig. 7). These results demonstrate that the −706/−343 region of the human *ADAMTS-1* promoter (−539/−326 in the mouse) contains CN-unrelated regulatory elements that control the transcriptional activation of the gene in response to Ang-II, TNF-α, and IL-1β, whereas the −342/−275 fragment (−325/−270 in the mouse) regulates VEGF-induced Adamts-1 expression in a CN-dependent fashion.

To test the possibility that the C/EBPβ and NFAT putative binding sites were implicated in *Adamts-1* promoter activation, we mutated these sequences and analyzed their transcriptional contribution by using luciferase reporter assays. Mutation of the C/EBPβ-binding site blunted the response of the human and mouse *Adamts-1* promoters to Ang-II, TNF-α, and IL-1β stimulation but did not affect their activation by VEGF (Fig. 8). Conversely, mutation of the two putative NFAT binding sites (either individually or together) blocked the transcriptional response to VEGF but not that to Ang-II, TNF-α, or IL-1β (Fig. 8A).

We next performed ChIP analysis to evaluate the functional occupancy of these motifs by the transcription factors C/EBPβ and NFAT in the endogenous *ADAMTS-1* promoter. ChIP assays of Ang-II-stimulated HUVECs with an antibody specific for C/EBPβ confirmed the recruitment of this factor (Fig. 9A). An identical experiment with an antibody specific for NFATc1 did not result in coprecipitation of the promoter region encompassing the NFAT binding sites (Fig. 9B), indicating that stimulation with Ang-II induces binding of C/EBPβ but not NFATc1 to the *ADAMTS-1* promoter. In contrast, ChIP assays of HUVECs stimulated with VEGF revealed the interaction of NFATc1 but not C/EBPβ with the corresponding promoter binding sites (Fig. 9A and B). Importantly, negative-control ChIP assays with anti-C/EBPβ or anti-NFATc1 antibodies on the 3′ untranslated region (UTR) of the *Adamts-1* mRNA excluded the possibility of coprecipitation of nonspecific DNA sequences (Fig. 9A and B). As a positive control, the *COX-2* promoter region was amplified in parallel in a ChIP assay to demonstrate C/EBPβ and NFATc1 recruitment upon Ang-II and/or VEGF treatment (Fig. 9C).

Taken together, these results establish the presence of functional binding sites for the transcription factors C/EBPβ and NFAT in the *ADAMTS-1* promoter region that play an essential role in the differential transcriptional activation of the gene in response to Ang-II/IL-1β/TNF-α or VEGF, respectively.

Ang-II and proinflammatory cytokines regulate *Adamts-1* gene expression through C/EBPβ. Alternative translation initiation sites in the C/EBPβ mRNA generate different protein isoforms designated LAP (liver activator protein) or LIP. LAP contains a conserved bZIP DNA-binding domain and a transactivation domain (and therefore is fully functional), whereas LIP lacks the transactivation domain and functions as a repressor (30). Phosphorylation of human C/EBPβ-LAP at residue Thr235 (Thr188 in the mouse) efficiently increases its transactivation activity (30). VSMCs stimulated with Ang-II resulted in a substantial increase in C/EBPβ-LAP phosphorylation at Thr235/188 after only 10 min of treatment, which persisted for 2 h (Fig. 10A). IL-1β

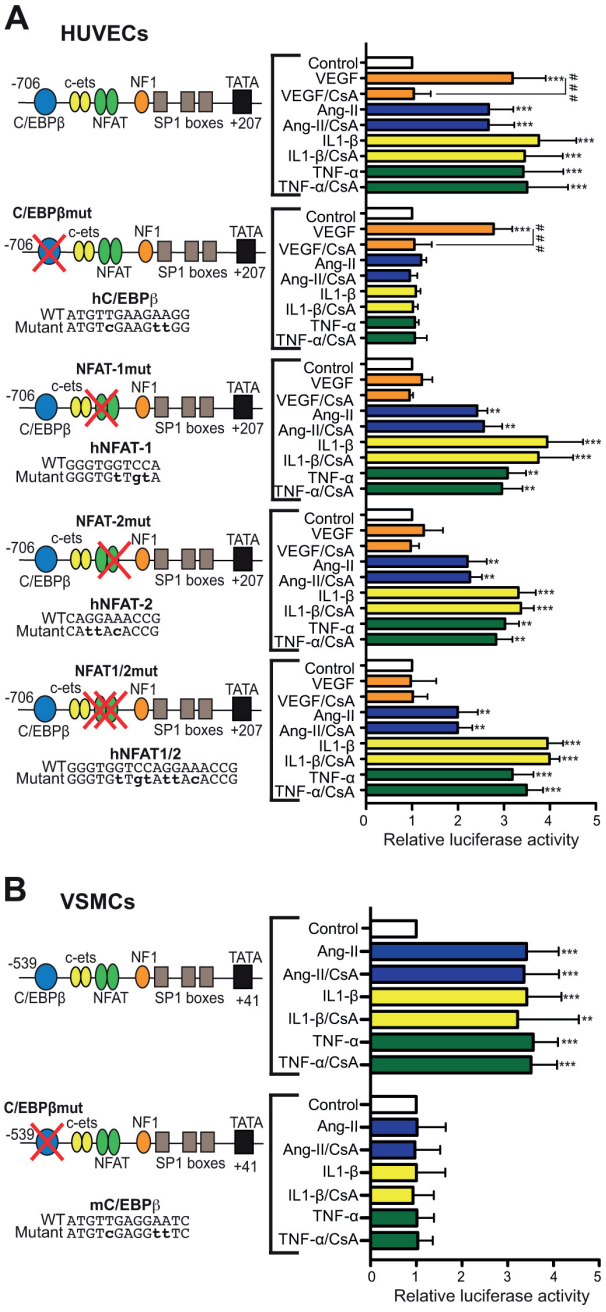

FIG 8 Integrity of NFAT- and C/EBPβ-binding sites is essential for *Adamts1* promoter activity in response to VEGF and Ang-II, TNF-α, or IL-1β, respectively. Mutant versions of the reporter vectors pMetLuc(−706/+207) (A) and pGL3(−539/+41) (B), where the putative binding sites for C/EBPβ and NFAT were abolished by site-directed mutagenesis (base substitutions are in bold), were transfected in HUVECs (A) or murine VSMCs (B). Transfected cells were left untreated (Control) or stimulated with VEGF, Ang-II, IL-1-β, or TNF-α for 8 h. Where indicated, cells were treated with CsA for 1 h prior to stimulation. Luciferase activity was expressed as fold increases relative to the activity of the reporter in nonstimulated cells. Histograms show data as means ± SD of at least three independent experiments. **, $P < 0.01$; ***, $P < 0.001$ (versus untreated cells); ###, $P < 0.001$ (VEGF versus VEGF/CsA-stimulated cells).

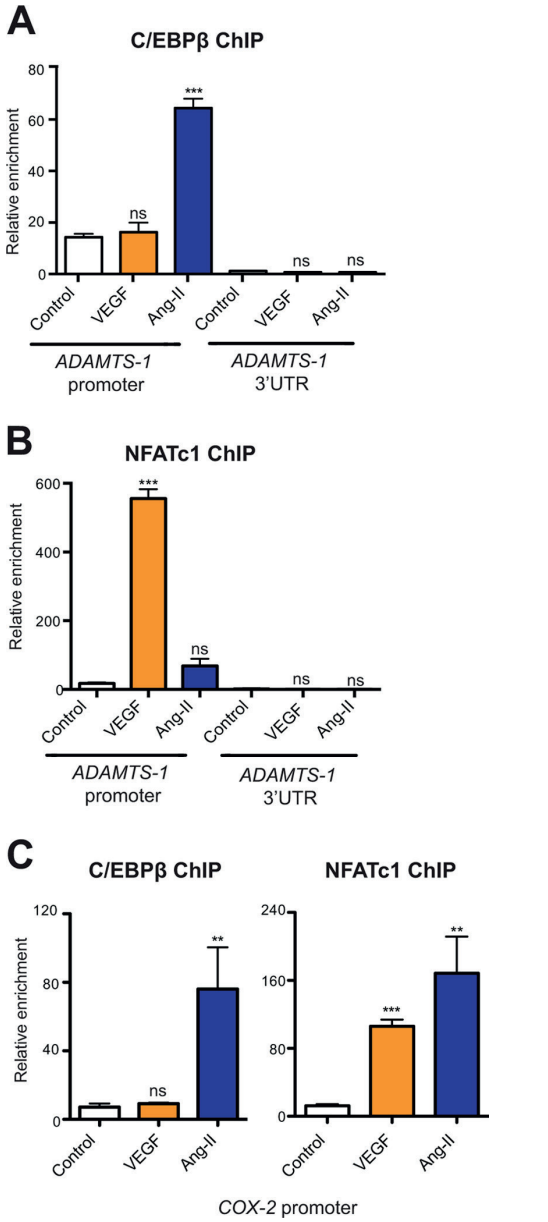

FIG 9 Recruitment of C/EBPβ and NFAT to the *Adamts-1* and *Cox-2* promoters is differentially induced by Ang-II and VEGF. ChIP assays of the promoter and 3′ UTR of *Adamts-1* (A and B) and the *Cox-2* promoter (C) performed with HUVECs left unstimulated (Control) or treated with either VEGF or Ang-II for 30 min, with antibodies specific for C/EBPβ or NFATc1 as indicated. Data are shown as enrichment of the amount of chromatin precipitated with anti-C/EBPβ or anti-NFATc1 antibody relative to the values obtained with an IgG control antibody. Histograms show means ± SD of three independent experiments. **, $P < 0.01$; ***, $P < 0.001$ (versus the control); ns, nonsignificant.

and TNF-α, but not VEGF, induced a similar increase in C/EBPβ-LAP phosphorylation (Fig. 10B and C). Analysis of the protein extracts with an antibody recognizing total C/EBPβ-LAP showed equivalent C/EBPβ-LAP expression levels in all cases (Fig. 10A to

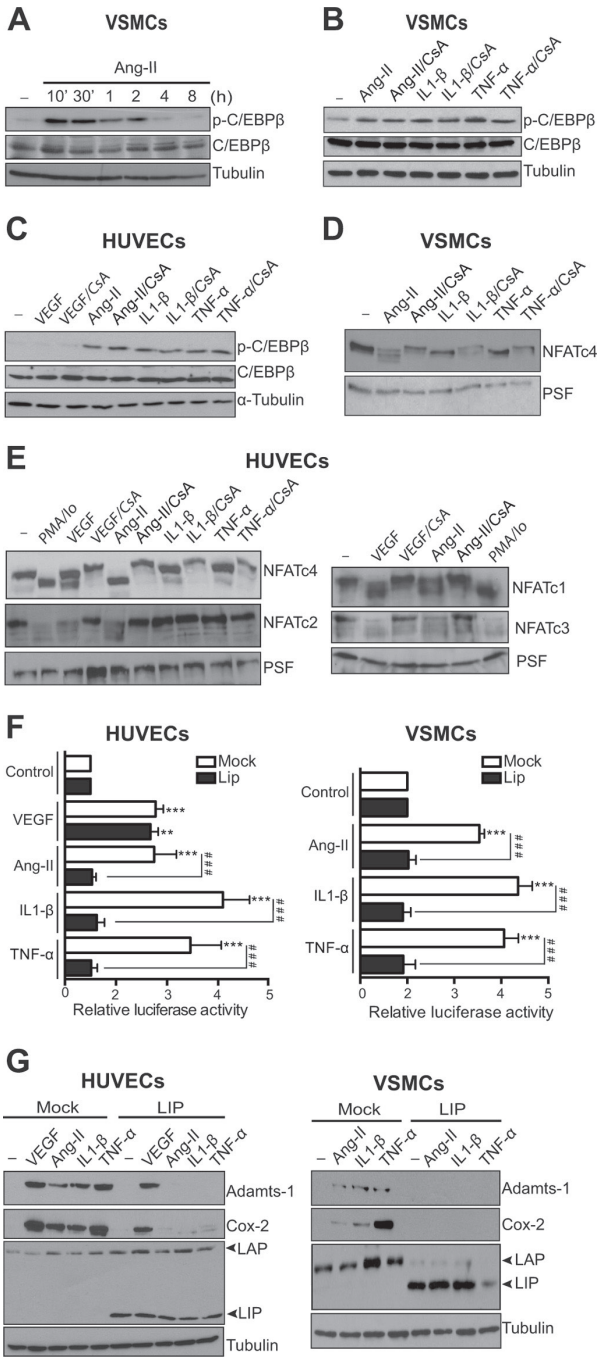

FIG 10 Ang-II, IL-1β, and TNF-α upregulate Adamts-1 in a C/EBPβ-dependent manner. (A to C) Immunoblot analysis of phospho-C/EBPβ and total C/EBPβ in protein extracts of VSMCs treated with Ang-II for the times indicated (A) and VSMCs and HUVECs treated with Ang-II, IL-1-β, TNF-α or VEGF for 15 min (B and C). Where indicated, cells were treated with CsA for 1 h prior to stimulation. Tubulin expression was analyzed as a loading control. (D and E) VSMCs and HUVECs were treated with the indicated stimuli for 30 min, and the activation (dephosphorylation) status of NFATc1 to -c4 transcription factors was analyzed by Western blotting. Where indicated, cells were treated with CsA for 1 h prior to addition of the stimulus. PSF expression was analyzed as a loading control. Immunoblot assays are representative of three independent experiments. (F) HUVECs and VSMCs were cotransfected with an expression vector encoding the C/EBPβ inhibitory isoform (LIP) or the empty plasmid (Mock), together with a luciferase-based reporter vector containing the human or mouse *Adamts-1* proximal promoter, pMetLucAdamts-1(−706/+207), or pGL3mAdamts-1(−539/+41), respectively. Transfected cells were left untreated (Control) or stimulated as indicated for 8 h. Luciferase activity was expressed as fold increases relative to the activity of the reporter in untreated cells. Histograms show data as means ± SD of four independent experiments. **, $P < 0.01$; ***, $P < 0.001$ (versus untreated cells); ###, $P < 0.001$ (versus CsA-pretreated cells). (G) HUVECs or VSMCs were infected with lentiviral particles expressing GFP or C/EBPβ-LIP (LIP). Transduced cells were stimulated with Ang-II, IL-1-β, or TNF-α for 6 h or with VEGF for 4 h, and Adamts-1 expression was analyzed by Western blotting. Successful expression of exogenous LIP was confirmed by Western blotting with an anti-C/EBP antibody that recognizes both the LAP and LIP isoforms of C/EBPβ. Cox-2 expression is shown as a positive control for stimulation, and tubulin is shown as a loading control. The immunoblot assays shown are representative of three independent experiments.

C). Whereas both VEGF and Ang-II induced significant dephosphorylation of all NFAT family members, neither IL-1β nor TNF-α activated these transcription factors (Fig. 10D and E). As expected, the observed increase in C/EBPβ-LAP phosphorylation was not affected by preincubation of the cells with CsA (Fig. 10B and C), which efficiently inhibited VEGF- and Ang-II-induced dephosphorylation of NFAT family members (Fig. 10D and E). These results indicate that Ang-II, IL-1β, or TNF-α, but not VEGF, triggers the activation of the C/EBPβ signal transduction pathway in vascular cells.

Given these results, we hypothesized that Ang-II-, IL-1β-, or TNF-α-dependent activation of the C/EBPβ pathway is implicated in the transcriptional activation of the *Adamts-1* gene. To explore this possibility, we cotransfected HUVECs or VSMCs with a luciferase reporter vector containing the *Adamts-1* proximal promoter region together with an expression plasmid encoding the C/EBPβ repressor C/EBPβ-LIP (pcDNA3.1-LIP) or the corresponding empty vector and measured promoter activation after stimulation. Whereas ectopic expression of C/EBPβ-LIP robustly inhibited the induction of luciferase activity by Ang-II, IL-1β, or TNF-α stimulation, induction by VEGF was not significantly affected by C/EBPβ-LIP (Fig. 10F). Confirming these observations, upregulation of endogenous Adamts-1 protein expression in vascular cells stimulated with Ang-II, IL-1β, or TNF-α was impaired with a lentivirus encoding LIP (Fig. 10G), whereas LIP ectopic expression did not affect the levels of Adamts-1 expressed in VEGF-treated cells (Fig. 10G).

These results support a selective participation of C/EBPβ signaling in the upregulation of Adamts-1 expression in cells treated with Ang-II, IL-1β, or TNF-α but not in cells treated with VEGF.

Regulation of Adamts-1 expression by VEGF and Ang-II in the aorta. Given the importance of NFAT and C/EBPβ activation in the regulation of Adamts-1 expression by VEGF and Ang-II *in vitro*, we studied whether these pathways are also operative *in vivo*. To this end, we infused VEGF or Ang-II into C57BL/6 mice and analyzed Adamts-1 expression in the aortas of control and treated animals. VEGF treatment promoted NFAT nuclear translocation and subsequent induction of Adamts-1 expression in the aorta, which was sensitive to CsA pretreatment (Fig. 11A). In contrast, the phosphorylation status of C/EBPβ was not modified by VEGF infusion into the aortic wall (Fig. 11B). Similarly, the expression of Adamts-1 in protein lysates of aortas isolated from animals in-

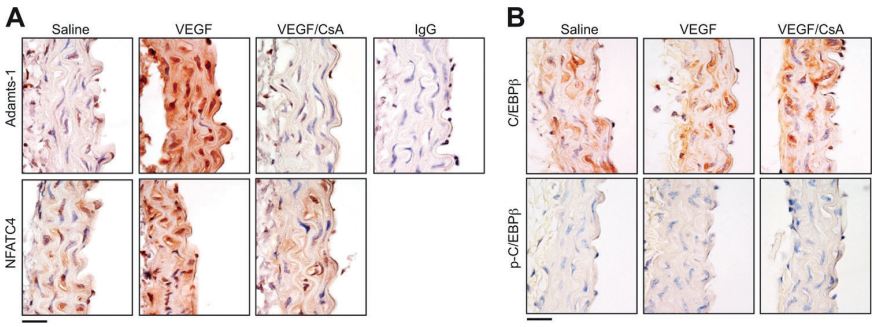

FIG 11 VEGF induces Adamts-1 expression and NFAT activation in the murine aorta. Representative immunostaining ($n = 3$) for Adamts-1 and NFATc4 (A) or total (C/EBPβ) and phosphorylated (p-C/EBPβ) C/EBPβ (B) proteins in aortic sections of mice treated with saline or VEGF at 25 μg/kg/day for 3 days or 1 day, respectively. Where indicated, mice were treated with CsA at 10 mg/kg/day for 1 day prior to VEGF administration. Bars, 20 μm. Staining of aortic sections with an IgG antibody was performed as a negative control.

fused with Ang-II for 1 to 21 days increased markedly (Fig. 12A). Correspondingly, *Adamts-1* mRNA levels increased significantly after only 5 h of Ang-II infusion and remained elevated for 21 days (Fig. 12A). Consistent with our *in vitro* findings, CsA did not inhibit Adamts-1 upregulation by Ang-II in the aorta (Fig. 12B). Moreover, immunostaining of Adamts-1 in murine aortic tissue sections revealed a significant induction of its expression by Ang-II (Fig. 12C), further supporting our observations.

Immunohistochemistry analysis of aortic tissue sections revealed that C/EBP-LAP staining was mainly cytoplasmic in the vasculature of saline-infused control animals but partially translocated to the nucleus upon activation by Ang-II (Fig. 12D). Concomitant with nuclear translocation, Ang-II induced a notable increase in C/EBP-LAP phosphorylation at Thr188 (Fig. 12D). Both Ang-II-induced Adamts-1 upregulation and C/EBPβ activation were prevented by the AT_1 receptor inhibitor losartan (Fig. 12C and D). These results demonstrate that aortic Adamts-1 expression increases after *in vivo* VEGF and Ang-II treatment and suggest that NFAT and C/EBPβ may mediate Adamts-1 upregulation induced by these stimuli in the murine aorta.

Altogether, our data show differential usage of signaling pathways in the regulation of Adamts-1 expression by stimuli associated with vascular remodeling and that Ang-II induces *in vivo* C/EBPβ phosphorylation and nuclear translocation, which could be involved in Ang-II-mediated Adamts-1 induction *in vivo*.

DISCUSSION

Emerging evidence indicates that the metalloproteinase Adamts-1 plays an important role in the pathophysiology of vascular disorders (7, 8, 10), but the intracellular mechanisms that control Adamts-1 expression during these processes remain poorly understood. In this work, we show that vascular expression of Adamts-1 is induced by mediators of vascular remodeling, such as VEGF, Ang-II, and the proinflammatory cytokines IL-1β and TNF-α. We have also characterized the coupling of specific signaling pathways and transcription factor activation in the regulation of Adamts-1 expression by these stimuli.

Using different approaches to block the CN/NFAT signal transduction pathway, we have identified this pathway as a critical mediator of the transcriptional activation of *Adamts-1* induced by VEGF in ECs. Previous reports have shown that VEGF upregulates *Adamts-1* mRNA (12, 31) and that NFATc1 binds the *Adamts-1* promoter upon VEGF treatment in ECs (32). Nevertheless, a detailed analysis of the transcriptional mechanisms involved in *Adamts-1* induction by VEGF had not been performed. Through our analysis, we have identified two novel NFAT binding sequences responsible for driving *Adamts-1* expression in response to VEGF. NFAT is known to activate transcription through functional cooperation with a variety of transcription factors, including AP1 (33, 34), CREB (35), FoxP3 (36), MyoD (37), and C/EBPβ (38); however, NFAT proteins may also bind DNA as monomers or dimers (39, 40). Thus, NFAT could be operating in our system without a heterologous partner, as is the case for TNF-α and IL-13 promoter activation (39). The possible requirement of NFAT dimers to mediate VEGF-induced *Adamts-1* expression would be in line with the abrogation of transcription upon the mutation of either NFAT site in the promoter. On the other hand, previous work has shown that VEGF upregulates endothelial Adamts-1 expression in a protein kinase C (PKC)-dependent manner (12). It is feasible that the increased expression of endothelial Adamts-1 triggered by VEGF requires the activation of both pathways. Accordingly, concomitant activation of CN and PKC signaling has been described during upregulation of the endothelial proteins RCAN1 to -4 (41, 42) and tissue factor (43) in activated ECs. Moreover, concerted activation of these two signaling pathways is a regulatory mechanism widely described for the regulation of gene expression in other cell types (44–46). Our data indicate that the CN/NFAT pathway not only participates in Adamts-1 induction by VEGF *in vitro* but is also required for VEGF-mediated Adamts-1 upregulation in the aortic wall (Fig. 11). In this context, we detected NFAT nuclear translocation and Adamts-1 induction in response to VEGF both in the endothelial layer and in VSMCs present in the tunica media. We cannot discard a paracrine effect exerted by an unidentified factor secreted by ECs, which activates the CN/NFAT pathway and Adamts-1 expression in VSMC in a secondary manner. Nonetheless, VEGF receptor expression in VMSCs *in vitro* and *in vivo* has been reported by several authors (47–50). VEGF might be therefore acting directly also on this cell type to promote Adamts-1 expression through the CN/NFAT pathway.

Stimulation of vascular cells *in vitro* and *in vivo* with Ang-II also induced a robust increase in the expression of Adamts-1, suggesting that this metalloproteinase is a molecular effector of Ang-II. Analogous to VEGF, Ang-II has been reported to trigger acti-

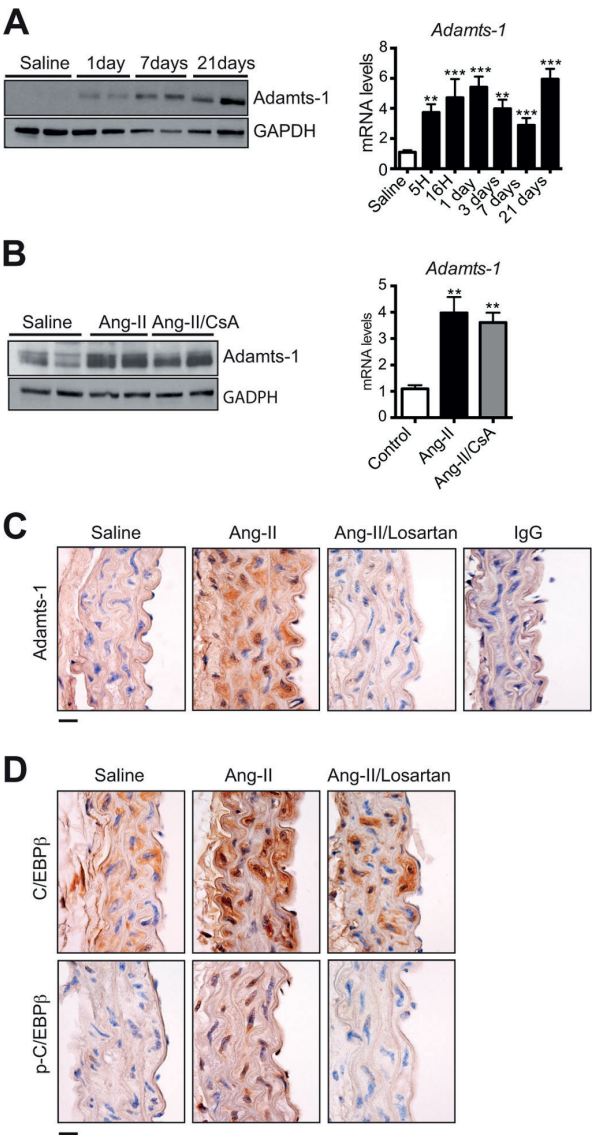

FIG 12 Ang-II induces Adamts-1 expression and C/EBPβ activation in the murine aorta. (A) Representative immunoblot ($n = 5$) and qPCR analyses of Adamts-1 expression in aortic extracts isolated from mice infused with saline or Ang-II (1 μg/kg/min) for the times indicated. Histograms show means ± SD of three independent experiments. **, $P < 0.01$; ***, $P < 0.001$ (versus the control). (B) Adamts-1 protein and mRNA expression was analyzed as described above in aortic samples isolated from mice infused with Ang-II for 3 days. Where indicated, mice were treated with CsA at 10 mg/kg/day for 1 day prior to Ang-II administration. Images are representative of four independent experiments. (C) Representative Adamts-1 immunostaining ($n = 3$) of aortic sections from mice treated with saline or Ang-II for 3 days. Where indicated, animals were infused with losartan (10 mg/kg/day) for 1 day before Ang-II administration. Bar, 20 μm. (D) Representative immunostaining ($n = 3$) of total (C/EBPβ) or phosphorylated (p-C/EBPβ) C/EBPβ proteins in aortic sections isolated from mice infused with Ang-II or saline for 1 day. Where indicated, animals were infused with losartan (10 mg/kg/day) for 1 day before Ang-II administration. Bar, 20 μm.

vation of the CN/NFAT pathway in vascular cells (16). Thus, we initially inferred that activation of CN/NFAT signaling would drive the transcriptional upregulation of *Adamts-1* by Ang-II. However, characterization of the intracellular pathways governing this process revealed a role for C/EBPβ proteins, and not for NFAT transcription factors. The C/EBPβ-binding sites in the *Adamts1* promoter have also been involved in its induction by progesterone receptor-mediated activation of granulosa cells (29), further supporting the relevance of C/EBPβ proteins in the regulation of Adamts-1 expression. Furthermore, active C/EBPβ proteins have been linked to the expression of other metalloproteinase proteins, including MMP-3, MMP-13, and Adamts-5, during arthritic tissue remodeling (51, 52).

ChIP analysis revealed the differential binding of NFATc1 to the *Adamts-1* promoter upon stimulation with VEGF or Ang-II (Fig. 9). The involvement of specific NFAT family members in the regulation of diverse target genes has been reported (19) and could underlie our data on the disparate role of NFAT on *Adamts-1* transcriptional regulation by VEGF and Ang-II. Alternatively, differential activation kinetics or selective activation of NFATs might also account for the differential response mediated by VEGF and Ang-II. However, both factors activate all of the NFAT family members (Fig. 10D and E), and we cannot conclude that VEGF and Ang-II activate NFAT proteins to different extents because we have observed variability in the response to the treatments. This is probably due to variations in receptor expression among batches or passages of HUVECs. Another possibility is that VEGF and Ang-II trigger stimulus-dependent epigenetic modifications of NFAT family members, further influencing their transcriptional activity (53, 54).

The *Cox-2* promoter region also contains C/EBPβ- and NFAT-binding sites (24). Unlike VEGF, C/EBPβ activation is essential not only for *Adamts-1* but also for *Cox-2* transcription induced by Ang-II, which is associated with functional occupancy of both C/EBPβ- and NFAT-binding motifs (Fig. 9C). It is well established that the C/EBPβ and NFAT transcription factors cooperate synergistically for DNA binding and gene activation (30, 55). Because the C/EBPβ and NFAT binding sites are in close proximity in the *Cox-2* promoter (24), both factors could hypothetically cooperate in Cox-2 induction by Ang-II, as suggested by our functional data. Conversely, C/EBPβ could drive *Adamts-1* transcription in response to Ang-II without functional cooperation with NFAT, which, as discussed above, would operate in a partner-independent manner upon VEGF activation. Hence, we hypothesize that cooperation with different partners might be responsible for the differential regulation of the *Adamts-1* and *Cox-2* promoters by the NFAT and C/EBPβ transcription factors (Fig. 13).

Unlike ECs, LIP overexpression in VSMCs leads to a decrease in endogenous LAP expression. LIP lacks a transactivation domain and is known to impair C/EBP function either through competition for C/EBP DNA binding sites or by forming inactive heterodimers with other C/EBPs. In addition, cross talk between tyrosine kinase receptors and LAP/LIP isoforms has been described, which could act in some cases as a regulatory loop of LAP-LIP equilibrium (55). Accordingly, LIP overexpression might initiate a cell-type-dependent regulatory circuit that directly or indirectly modulates LAP expression.

Metalloproteinases regulate diverse aspects of inflammatory processes and immune responses, either through the release and

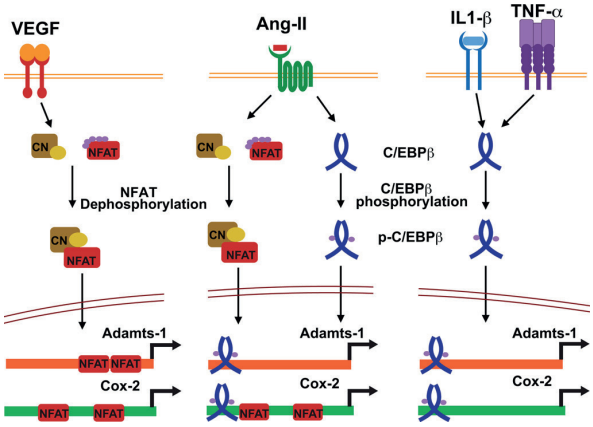

FIG 13 Differential transcriptional activation of the *Adamts-1* and *Cox-2* genes in response to VEGF, Ang-II, TNF-α, and IL-1β. The model shown represents the differential regulation of the *Adamts-1* and *Cox-2* promoters by the NFAT and C/EBPβ transcription factors during the stimulation of vascular cells by these factors. VEGF-induced upregulation of *Adamts-1* and *Cox-2* gene expression requires activation of the CN/NFAT signal transduction pathway. Although Ang-II also triggers the activation of CN-dependent signaling, Adamts-1 expression in response to Ang-II is mediated not by this pathway but instead by activation of C/EBPβ signaling. However, Ang-II-induced upregulation of Cox-2 requires activation of both the NFAT and C/EBPβ signaling pathways. Inflammatory stimuli induce Adamts-1 and Cox-2 upregulation via a molecular mechanisms that involves activation of C/EBPβ but not CN signaling.

activation of immune mediators (e.g., members of the TNF superfamily, epidermal growth factor, and Notch signaling pathways) or through a direct action on immune cells. Thus, Adamts-12 function is associated with neutrophil apoptosis and participates in inflammatory response control (56). Illustrated by atherosclerosis, many inflammatory diseases comprise extracellular matrix remodeling processes that are regulated at different levels by proinflammatory cytokines such as IL-1β and TNF-α and require metalloproteinase activity. IL-1β and TNF-α are known to induce *Adamts-1* mRNA in different cell types (57, 58); however, the precise transcriptional mechanism involved awaits identification. Similar to Ang-II, we have identified C/EBPβ as the chief mediator of Adamts-1 regulation by IL-1β and TNF-α in vascular cells. C/EBPβ is also implicated in the induction of Cox-2 expression by IL-1β and TNF-α. The convergence of signaling pathways triggered by disparate stimuli such as Ang-II and proinflammatory cytokines in C/EBPβ activation (Fig. 13) suggests a decisive role for this transcription factor in a broad range of pathophysiological processes. The role of matrix metalloproteinases in diseases that involve remodeling of the vessel wall, such as atherosclerosis, aortic aneurysm, and neointima formation in vascular restenosis, or genetic conditions, including familiar aortic diseases, indicates that Adamts-1 is a promising candidate for the development of novel therapeutic strategies for these disorders. Moreover, the prominent role of C/EBPβ in the induction of Adamts-1 by an array of stimuli, including Ang-II, IL-1, and TNF-α, suggests that pharmacological targeting of C/EBPβ may have utility in the treatment of vascular diseases of different origins.

ACKNOWLEDGMENTS

We thank Y. Ninomiya (Okayama University, Okayama, Japan) and T. Minami (University of Tokyo, Tokyo, Japan) for providing human *ADAMTS1* promoter constructs and the anti-NFATc1 monoclonal antibody, respectively, G. C. Crabtree (Stanford University, Stanford, CA) for providing the Cnb1 conditional knockout mouse, and Rut Alberca for technical assistance.

This work was funded by the Spanish Ministry of Economy and Competitiveness (Ministerio de Economía y Competitividad; SAF2012-34296 to J.M.R. and SAF2013-45258-P to M.R.C.), the Fundación La Marató TV3 (264/C/2012 to J.M.R.), the Spanish Ministry of Health (Ministerio de Sanidad y Consumo) Red de Investigación Cardiovascular (RIC) cofounded by FEDER (grants RD06/0042/0022 to J.M.R. and RD12/0042/0023 to A.G.A), and the Spanish Council for Scientific Research (CSIC; to M.R.C.). The Centro Nacional de Investigaciones Cardiovasculares Carlos III (CNIC) is supported by the Spanish Ministry of Economy and Competitiveness and the Pro-CNIC Foundation. J.O. is the holder of an FPI fellowship from the Spanish Ministry of Economy and Competitiveness (Ministerio de Economía y Competitividad; BES 2010-034552). The cost of this publication has been paid in part by FEDER funds.

We have no competing interests to declare.

REFERENCES

1. **Daugherty A, Manning MW, Cassis LA.** 2000. Angiotensin II promotes atherosclerotic lesions and aneurysms in apolipoprotein E-deficient mice. J Clin Invest **105:**1605–1612. http://dx.doi.org/10.1172/JCI7818.
2. **Hellenthal FA, Buurman WA, Wodzig WK, Schurink GW.** 2009. Biomarkers of abdominal aortic aneurysm progression. Part 2: inflammation. Nat Rev Cardiol **6:**543–552. http://dx.doi.org/10.1038/nrcardio.2009.102.
3. **Kaneko H, Anzai T, Takahashi T, Kohno T, Shimoda M, Sasaki A, Shimizu H, Nagai T, Maekawa Y, Yoshimura K, Aoki H, Yoshikawa T, Okada Y, Yozu R, Ogawa S, Fukuda K.** 2011. Role of vascular endothelial growth factor-A in development of abdominal aortic aneurysm. Cardiovasc Res **91:**358–367. http://dx.doi.org/10.1093/cvr/cvr080.
4. **Touyz RM.** 2005. Intracellular mechanisms involved in vascular remodelling of resistance arteries in hypertension: role of angiotensin II. Exp Physiol **90:**449–455. http://dx.doi.org/10.1113/expphysiol.2005.030080.
5. **Kuzuya M, Iguchi A.** 2003. Role of matrix metalloproteinases in vascular remodeling. J Atheroscler Thromb **10:**275–282. http://dx.doi.org/10.5551/jat.10.275.
6. **Lemarié CA, Tharaux PL, Lehoux S.** 2010. Extracellular matrix alterations in hypertensive vascular remodeling. J Mol Cell Cardiol **48:**433–439. http://dx.doi.org/10.1016/j.yjmcc.2009.09.018.
7. **Jönsson-Rylander AC, Nilsson T, Fritsche-Danielson R, Hammarström A, Behrendt M, Andersson JO, Lindgren K, Andersson AK, Wallbrandt P, Rosengren B, Brodin P, Thelin A, Westin A, Hurt-Camejo E, Lee-Søgaard CH.** 2005. Role of ADAMTS-1 in atherosclerosis: remodeling of carotid artery, immunohistochemistry, and proteolysis of versican. Arterioscler Thromb Vasc Biol **25:**180–185.
8. **Ren P, Zhang L, Xu G, Palmero LC, Albini PT, Coselli JS, Shen YH, LeMaire SA.** 2013. ADAMTS-1 and ADAMTS-4 levels are elevated in thoracic aortic aneurysms and dissections. Ann Thorac Surg **95:**570–577. http://dx.doi.org/10.1016/j.athoracsur.2012.10.084.
9. **Rodríguez-Manzaneque JC, Fernández-Rodríguez R, Rodríguez-Baena FJ, Iruela-Arispe LM.** 2015. ADAMTS proteases in vascular biology. Matrix Biol **44–46C:**38–45.
10. **Taketani T, Imai Y, Morota T, Maemura K, Morita H, Hayashi D, Yamazaki T, Nagai R, Takamoto S.** 2005. Altered patterns of gene expression specific to thoracic aortic aneurysms: microarray analysis of surgically resected specimens. Int Heart J **46:**265–277. http://dx.doi.org/10.1536/ihj.46.265.
11. **Porter S, Clark IM, Kevorkian L, Edwards DR.** 2005. The ADAMTS metalloproteinases. Biochem J **386:**15–27. http://dx.doi.org/10.1042/BJ20040424.
12. **Xu Z, Yu Y, Duh EJ.** 2006. Vascular endothelial growth factor upregulates expression of ADAMTS1 in endothelial cells through protein kinase C signaling. Invest Ophthalmol Vis Sci **47:**4059–4066. http://dx.doi.org/10.1167/iovs.05-1528.
13. **Bongrazio M, Baumann C, Zakrzewicz A, Pries AR, Gaehtgens P.** 2000. Evidence for modulation of genes involved in vascular adaptation by pro-

synergizes with PKC-theta to activate JNK and IL-2 promoter in T lymphocytes. EMBO J **17:**3101–3111. http://dx.doi.org/10.1093/emboj/17.11.3101.

47. **Ishida A, Murray J, Saito Y, Kanthou C, Benzakour O, Shibuya M, Wijelath ES.** 2001. Expression of vascular endothelial growth factor receptors in smooth muscle cells. J Cell Physiol **188:**359–368. http://dx.doi.org/10.1002/jcp.1121.
48. **Lash GE, Innes BA, Drury JA, Robson SC, Quenby S, Bulmer JN.** 2012. Localization of angiogenic growth factors and their receptors in the human endometrium throughout the menstrual cycle and in recurrent miscarriage. Hum Reprod **27:**183–195. http://dx.doi.org/10.1093/humrep/der376.
49. **Tedesco MM, Terashima M, Blankenberg FG, Levashova Z, Spin JM, Backer MV, Backer JM, Sho M, Sho E, McConnell MV, Dalman RL.** 2009. Analysis of in situ and ex vivo vascular endothelial growth factor receptor expression during experimental aortic aneurysm progression. Arterioscler Thromb Vasc Biol **29:**1452–1457. http://dx.doi.org/10.1161/ATVBAHA.109.187757.
50. **Wang H, Keiser JA.** 1998. Vascular endothelial growth factor upregulates the expression of matrix metalloproteinases in vascular smooth muscle cells: role of flt-1. Circ Res **83:**832–840. http://dx.doi.org/10.1161/01.RES.83.8.832.
51. **Hayashida M, Okazaki K, Fukushi J, Sakamoto A, Iwamoto Y.** 2009. CCAAT/enhancer binding protein beta mediates expression of matrix metalloproteinase 13 in human articular chondrocytes in inflammatory arthritis. Arthritis Rheum **60:**708–716. http://dx.doi.org/10.1002/art.24332.
52. **Tsushima H, Okazaki K, Hayashida M, Ushijima T, Iwamoto Y.** 2012. CCAAT/enhancer binding protein beta regulates expression of matrix metalloproteinase-3 in arthritis. Ann Rheum Dis **71:**99–107. http://dx.doi.org/10.1136/annrheumdis-2011-200061.
53. **Nayak A, Glockner-Pagel J, Vaeth M, Schumann JE, Buttmann M, Bopp T, Schmitt E, Serfling E, Berberich-Siebelt F.** 2009. Sumoylation of the transcription factor NFATc1 leads to its subnuclear relocalization and interleukin-2 repression by histone deacetylase. J Biol Chem **284:**10935–10946. http://dx.doi.org/10.1074/jbc.M900465200.
54. **Terui Y, Saad N, Jia S, McKeon F, Yuan J.** 2004. Dual role of sumoylation in the nuclear localization and transcriptional activation of NFAT1. J Biol Chem **279:**28257–28265. http://dx.doi.org/10.1074/jbc.M403153200.
55. **Zahnow CA.** 2009. CCAAT/enhancer-binding protein beta: its role in breast cancer and associations with receptor tyrosine kinases. Expert Rev Mol Med **11:**e12. http://dx.doi.org/10.1017/S1462399409001033.
56. **Khokha R, Murthy A, Weiss A.** 2013. Metalloproteinases and their natural inhibitors in inflammation and immunity. Nat Rev Immunol **13:**649–665. http://dx.doi.org/10.1038/nri3499.
57. **Cross AK, Haddock G, Stock CJ, Allan S, Surr J, Bunning RA, Buttle DJ, Woodroofe MN.** 2006. ADAMTS-1 and -4 are up-regulated following transient middle cerebral artery occlusion in the rat and their expression is modulated by TNF in cultured astrocytes. Brain Res **1088:**19–30. http://dx.doi.org/10.1016/j.brainres.2006.02.136.
58. **Ng YH, Zhu H, Pallen CJ, Leung PC, MacCalman CD.** 2006. Differential effects of interleukin-1beta and transforming growth factor-beta1 on the expression of the inflammation-associated protein, ADAMTS-1, in human decidual stromal cells in vitro. Hum Reprod **21:**1990–1999. http://dx.doi.org/10.1093/humrep/del108.

Artículo 2: Nitric oxide mediates aortic disease in mice deficient in the metalloprotease Adamts1 and in a mouse model of Marfan syndrome.

Autores: Jorge Oller, Nerea Méndez-Barbero, E Josue Ruiz, Silvia Villahoz, Marjolijn Renard, Lizet I Canelas, Ana M Briones, Rut Alberca, Noelia Lozano-Vidal, María A Hurlé, Dianna Milewicz, Arturo Evangelista, Mercedes Salaices, J Francisco Nistal, Luis Jesús Jiménez-Borreguero, Julie De Backer, Miguel R Campanero & Juan Miguel Redondo.

Publicado en: *Nature Medicine*, Enero 2017.

Resumen:

Los aneurismas y disecciones aórticas representan entre el 1-2% de todas las muertes en los países industrializados. El aneurisma torácico o TAA está asociado a una predisposición genética familiar e implica mutaciones genéticas. TAA y disecciones (TAAD) pueden aparecer aisladamente (familiar o FTAAD) o junto con características sistémicas del tejido conectivo (TAAD sindrómico), como ocurre en el Síndrome de Marfan (MFS). Actualmente el TAA carece de tratamiento y las mutaciones causales se han identificado solamente en una fracción de familias afectadas. Se ha descrito que en el modelo de ratón con Síndrome de Marfan la degeneración de la media y dilatación aórtica fueron inhibidos por Losartan, un antagonista del receptor de la Ang-II (AT1R). Losartan inhibe la señalización del TGFβ de manera no canónica. Sin embargo, en ensayos clínicos, Losartan no fue más eficaz para reducir la tasa de crecimiento de la raíz aórtica que el beta-bloqueador Atenolol. Poco se conoce sobre los mecanismos por los cuales Ang-II promueve aneurismas. Recientemente hemos descrito que Ang-II y otros estímulos asociados con la remodelación vascular inducen la expresión aórtica de Adamts1. Sin embargo, el papel de Adamts1 en el desarrollo del aneurisma es desconocido. En este trabajo, identificamos la metaloproteinasa Adamts1 y la enzima óxido nítrico sintasa inducible (NOS2) como dianas terapéuticas en individuos con TAAD. Por un lado, demostramos que Adamts1 es un mediador importante de la homeostasis vascular, dado que la haploinsuficiencia genética en ratones causa TAAD similar al MFS. Por otra parte, hemos visto que el óxido nítrico y los niveles de NOS2 fueron más altos en ratones deficientes en *Adamts1* y en un modelo de ratón de MFS. Además, comprobamos que los altos niveles de NOS2 son dependientes de la activación de la ruta de señalización mTOR2-AKT-NFκB. La actividad enzimática de NOS2 sería la responsable de la aortopatía presente en los ratones Marfan y en los deficientes en *Adamts1* ya que la inhibición farmacológica de NOS2 protegió ambos tipos de ratones de patología aórtica. Además, analizamos muestras de pacientes con MFS y comprobamos que la expresión de ADAMTS1 está disminuida y los niveles de NOS2 se mostraron elevados. Estos hallazgos revelan un posible papel causal para el eje ADAMTS1-NOS2 en el TAAD humano y justifican la evaluación de los inhibidores de NOS2 para la terapia en pacientes afectados con este tipo de enfermedades aórticas.

Aportación Personal al trabajo: He participado tanto en la parte de diseño y realización experimental, así como en la escritura del artículo.

nature medicine

ARTICLES

Nitric oxide mediates aortic disease in mice deficient in the metalloprotease Adamts1 and in a mouse model of Marfan syndrome

Jorge Oller[1,10], Nerea Méndez-Barbero[1,10], E Josue Ruiz[1], Silvia Villahoz[1], Marjolijn Renard[2], Lizet I Canelas[1], Ana M Briones[3], Rut Alberca[1], Noelia Lozano-Vidal[1], María A Hurlé[4], Dianna Milewicz[5], Arturo Evangelista[6], Mercedes Salaices[3], J Francisco Nistal[4], Luis Jesús Jiménez-Borreguero[7], Julie De Backer[3], Miguel R Campanero[8,11] & Juan Miguel Redondo[1,9,11]

Heritable thoracic aortic aneurysms and dissections (TAAD), including Marfan syndrome (MFS), currently lack a cure, and causative mutations have been identified for only a fraction of affected families. Here we identify the metalloproteinase ADAMTS1 and inducible nitric oxide synthase (NOS2) as therapeutic targets in individuals with TAAD. We show that Adamts1 is a major mediator of vascular homeostasis, given that genetic haploinsufficiency of *Adamts1* in mice causes TAAD similar to MFS. Aortic nitric oxide and Nos2 levels were higher in *Adamts1*-deficient mice and in a mouse model of MFS (hereafter referred to as MFS mice), and *Nos2* inactivation protected both types of mice from aortic pathology. Pharmacological inhibition of Nos2 rapidly reversed aortic dilation and medial degeneration in young *Adamts1*-deficient mice and in young or old MFS mice. Patients with MFS showed elevated NOS2 and decreased ADAMTS1 protein levels in the aorta. These findings uncover a possible causative role for the ADAMTS1–NOS2 axis in human TAAD and warrant evaluation of NOS2 inhibitors for therapy.

Aortic aneurysm (AA) and dissections account for 1–2% of all deaths in industrialized countries. Thoracic AA (TAA) is strongly associated with familial genetic predisposition and involves gene variants that show high penetrance. TAA and dissections (TAAD) can appear in isolation (familial TAAD) or together with features of a systemic connective tissue disorder (syndromic TAAD), such as that in MFS.

Syndromic and nonsyndromic TAAD are associated with increased transforming growth factor (TGF)-β signaling[1–3]. TGF-β activation has been proposed to cause aortic medial degeneration, a typical histopathological feature of TAAD, which is characterized by an enlarged and weakened medial layer, fibrosis, proteoglycan accumulation, and elastic fiber disorganization and fragmentation[4]. However, it is unclear whether TGF-β activation is a cause or a consequence of TAAD. Consistent with a pathogenic role of TGF-β in TAAD, neutralizing antibodies to TGF-β prevent aortic dilation and inhibit fragmentation of elastic lamellae in a mouse model of mild MFS[5]. In the same model, these processes are also inhibited by losartan, an angiotensin-II (Ang-II) type I receptor (AT1R) antagonist that inhibits TGF-β signaling[5,6]. However, in clinical trial, losartan was not more effective at reducing the rate of aortic root enlargement than the beta blocker atenolol, and dual therapy with both losartan and atenolol produced no additional benefit[7–9].

Little is known about the mechanisms by which Ang-II promotes aneurysms. We recently showed that Ang-II and other stimuli associated with vascular remodeling induce aortic expression of 'a disintegrin and metalloproteinase with thrombospondin motifs 1 (ADAMTS1)[10], raising the possibility that ADAMTS1 might mediate Ang-II-induced aneurysms. ADAMTS1, a member of the proteoglycan-degrading ADAMTS metalloproteinase family, is expressed in aortic endothelial cells and in vascular smooth muscle cells (VSMCs)[11,12]. It is also expressed in tissue from TAA lesions and is active in normal aortic tissue, where it cleaves versican and aggrecan[13,14]. However, the role of Adamts1 in aneurysm development is unknown.

RESULTS

A syndromic form of TAA is triggered by a constitutive *Adamts1* deficiency

To investigate the contribution of Adamts1 to Ang-II-elicited aortic dilation and aneurysm, we used *Adamts1*-deficient mice from the European Mouse Mutant Archive (EM:02291). Previously described

[1]Gene regulation in cardiovascular remodeling and inflammation group, Centro Nacional de Investigaciones Cardiovasculares (CNIC), Madrid, Spain. [2]Center for Medical Genetics Ghent, Ghent University Hospital, Ghent, Belgium. [3]Department of Pharmacology, Facultad de Medicina, Universidad Autónoma de Madrid, Madrid, Spain. [4]Cardiovascular Surgery and Department of Physiology and Pharmacology, Hospital Universitario Marqués de Valdecilla, IDIVAL, Facultad de Medicina, Universidad de Cantabria, Santander, Spain. [5]Division of Medical Genetics, University of Texas, Houston, USA. [6]Servei de Cardiologia, Hospital Vall d'Hebron, Barcelona, Spain. [7]Centro Nacional de Investigaciones Cardiovasculares and Hospital de la Princesa, Madrid, Spain. [8]Department of Cancer Biology, Instituto de Investigaciones Biomedicas Alberto Sols, Consejo Superior de Investigaciones Científicas–Universidad Autónoma de Madrid, Madrid, Spain. [9]Centro de Investigaciones Biomédicas en RED en Enfermedades Cardiovasculares (CIBERCV), Spain. [10]These authors contributed equally to this work. [11]These authors jointly directed this work. Correspondence should be addressed to M.R.C. (mcampanero@iib.uam.es) or J.M.R. (jmredondo@cnic.es).

Received 24 June 2016; accepted 13 December 2016; published online 9 January 2017; doi:10.1038/nm.4266

Adamts1$^{-/-}$ mice have congenital kidney malformations and high perinatal mortality[15], but no vascular phenotype has been reported. Our *Adamts1*$^{+/-}$ mice expressed lower levels of Adamts1 in the aorta than wild-type (WT) littermates (**Fig. 1a** and **Supplementary Fig. 1a**). We did not study *Adamts1*$^{-/-}$ mice because these mice had very low survival at the time of weaning (**Supplementary Fig. 1b**). By contrast, the survival of *Adamts1*$^{+/-}$ mice was similar to that of their WT littermates, and *Adamts1*$^{+/-}$ mice seemed to be healthy at this stage. Treatment of 8-week-old WT mice with Ang-II for 28 d promoted generalized aortic dilation, which was confirmed by ultrasonography of the aortic ring (AR), the ascending aorta (AsAo) and the abdominal aorta (AbAo) (**Fig. 1b**,**c**). In contrast to WT mice, untreated *Adamts1*$^{+/-}$ mice showed aortic dilation, which was exacerbated by Ang-II treatment (**Fig. 1b**,**c**). In addition, whereas Ang-II treatment induced AA or lethal aortic dissections in only 1 of 12 WT mice, this treatment rapidly triggered AA or lethal aortic dissections in 7 of 15 *Adamts1*$^{+/-}$ mice; this occurred in the AsAo in three mice and in the AbAo in four mice (**Fig. 1d**,**e**). No aneurysms or lethal dissections were detected in untreated *Adamts1*$^{+/-}$ mice at this age. Because Ang-II induces hypertension, we investigated whether *Adamts1* inactivation would also have a pro-hypertensive effect. However, unlike Ang-II treatment, *Adamts1* gene dose reduction led to a reduction in both systolic and diastolic blood pressure (BP) (**Fig. 1f**).

In line with previous observations of developmental kidney abnormalities in other *Adamts1*-targeted mice[15], we found that the kidneys of our *Adamts1*$^{+/-}$ mice had an enlarged caliceal space, indicative of hydronephrosis (**Supplementary Fig. 1c**). However, levels of urea and creatinine in the plasma were similar in WT and *Adamts1*$^{+/-}$ mice (**Supplementary Fig. 1d**,**e**), suggesting that renal function was not compromised.

The presence of renal abnormalities raised the possibility that the aortic pathology induced by Adamts1 deficiency might be syndromic. Syndromic aortic conditions in humans and mice, including MFS, involve alterations to the lungs and skeleton[16–19]. Examination of 3-month-old *Adamts1*$^{+/-}$ mice revealed a marked increase in distal airspace caliber, which is characteristic of emphysema (**Fig. 1g**). Moreover, kyphosis was detected in 44.4% of 3- to 4-month-old *Adamts1*$^{+/-}$ mice (**Fig. 1h**), which was associated with increased anteroposterior and transverse diameters of the chest due to overgrowth of the ribs (**Fig. 1i**). Other long bones (humerus, tibia and femur) were also longer in sex-matched *Adamts1*$^{+/-}$ mice than in WT mice, whereas there were no differences in cranial size and morphology between the *Adamts1*$^{+/-}$ and WT mice (**Fig. 1j**,**k**).

TAA is promoted by knockdown of *Adamts1* expression in the aorta

To investigate the direct effects of Adamts1 deficiency on aortic dilation, we knocked down its expression in the aorta of adult mice by using lentivirus encoding an *Adamts1*-specific siRNA. By screening candidate small interfering RNAs (siRNAs) specific for *Adamts1* in cultured VSMCs, we identified siRNA-27 as having high silencing capacity (**Supplementary Fig. 1f**,**g**). The siRNA-encoding lentivirus also encoded green fluorescent protein (GFP) to facilitate assessment of transduction efficiency. Intrajugular delivery of lentivirus encoding siRNA-27 (hereafter referred to as siAdamts1) into C57BL/6 mice[20] yielded efficient and long-term transduction of all aortic wall layers, as determined by GFP immunostaining of the AsAo, thoracic descending aorta and AbAo 7 weeks after lentiviral delivery (**Fig. 2a**,**b** and **Supplementary Fig. 1h**). *Adamts1* mRNA and Adamts1 protein expression was almost undetectable in aortic samples from mice that were inoculated with siAdamts1-expressing lentivirus (**Fig. 2b**,**c** and **Supplementary Fig. 1h**,**i**), even when the mice were treated with Ang-II for the last 4 weeks prior to the evaluation of Adamts1 expression (**Fig. 2c** and **Supplementary Fig. 1i**). Indeed, aortic *Adamts1* mRNA levels were lower in siAdamts1-transduced mice than in *Adamts1*$^{+/-}$ mice (**Supplementary Fig. 1i**). Silencing of *Adamts1* expression was confirmed in all layers of the AsAo, thoracic descending aorta and AbAo (**Fig. 2b** and **Supplementary Fig. 1h**). Consistent with the results obtained for *Adamts1*$^{+/-}$ mice, *Adamts1* silencing in the adult aorta led to decreased systolic and diastolic BP (**Fig. 2d**), as well as strong dilation of the AR, AsAo and AbAo; this dilation was further increased by treatment with Ang-II (**Fig. 2e** and **Supplementary Fig. 1j**). In addition, Ang-II treatment of siAdamts1-transduced mice caused aneurysms in 13 of 16 mice and lethal dissections in 4 of 16 mice, whereas Ang-II treatment of mice that were transduced with a control siRNA (siCtl) caused aneurysm in only 1 of 13 mice, and none developed lethal dissections. No aneurysms or lethal dissections were detected in siAdamts1-expressing mice at this age in the absence of Ang-II treatment.

Medial degeneration and activation of the TGF-β pathway in the aortic wall of *Adamts1* deficient mice

Reduction of Adamts1 levels in mice by either genetic inactivation or transduction of a lentivirus expressing siAdamts1 caused the characteristic features of medial degeneration: elastic fiber fragmentation and disarray, excessive collagen deposition and proteoglycan accumulation, as assessed by histologic analysis of the AsAo and the AbAo (**Fig. 2f–h** and **Supplementary Fig. 2a–e**). These features were exacerbated by Ang-II treatment of the mice (**Fig. 2f–h** and **Supplementary Fig. 2a–e**).

Figure 1 Induction of syndromic TAA by Adamts1 deficiency. (**a**) Representative images of Adamts1 immunostaining in aortic sections from the indicated strains of mice ($n = 3$ per group). Scale bar, 20 μm. (**b**,**c**) Representative ultrasound images (**b**) and maximal diameters (**c**) of AR, AsAo and AbAo from vehicle-treated (control) (*Adamts1*$^{+/+}$ (+/+), $n = 13$; *Adamts1*$^{+/-}$ (+/–), $n = 15$) and Ang-II-treated (*Adamts1*$^{+/+}$, $n = 11$; *Adamts1*$^{+/-}$, $n = 14$) mice for 28 d. In **b**, red dashed lines mark the lumen boundary, and the yellow dashed lines mark the lumen diameter. Data are presented as box-and-whisker plots, with 75th and 25th percentiles; bars represent maximal and minimal values. $^{*}P < 0.05$, $^{****}P < 0.0001$ (*Adamts1*$^{+/+}$ versus *Adamts1*$^{+/-}$ mice); $^{\#\#}P < 0.01$, $^{\#\#\#}P < 0.001$, $^{\#\#\#\#}P > 0.0001$ (vehicle- versus Ang-II-treated mice); by two-way analysis of variance (ANOVA). Scale bars, 1 mm. (**d**) Survival curve of Ang-II-treated (*Adamts1*$^{+/+}$, $n = 12$; *Adamts1*$^{+/-}$, $n = 15$) mice for 28 d. $^{*}P < 0.05$ by log-rank (Mantel–Cox) test. The numbers shown indicate the number of live mice versus the total number of mice at 28 d after the start of Ang-II treatment. (**e**) Aneurysm incidence in AsAo and AbAo in the Ang-II-treated cohorts of mice shown in **d**. (**f**) End-of-treatment systolic (left) and diastolic (right) BP in in the cohorts of mice shown in **c**. Data are presented as box-and-whisker plots, with 75th and 25th percentiles; bars represent maximal and minimal values. $^{***}P < 0.01$ and $^{****}P < 0.001$ (*Adamts1*$^{+/+}$ versus *Adamts1*$^{+/-}$ mice); $^{\#\#\#\#}P < 0.0001$ (control- versus Ang-II-treated mice); by two-way ANOVA. (**g**) Representative H&E-stained sections from formalin-fixed lungs of *Adamts1*$^{+/+}$ ($n = 10$) and *Adamts1*$^{+/-}$ ($n = 7$) mice. The asterisk marks the distal airspace, which is enlarged in lungs of *Adamts1*$^{+/-}$ mice. Scale bars, 500 μm (2×), 50 μm (20×). (**h**) Representative skeletal positron emission tomography–computed tomography (PET–CT) images of 16- to 20-week-old *Adamts1*$^{+/+}$ ($n = 10$) (top) and *Adamts1*$^{+/-}$ ($n = 9$) (bottom) mice. Red dashed lines, 1.67 cm; scale bar, 1 cm. Kyphosis incidence is indicated. (**i**–**k**) Quantification of the diameter of the anteroposterior (left) and transverse (right) thorax (**i**), and length of the cranium (**j**), humerus (left), femur (middle) and tibia (right) (**k**) from *Adamts1*$^{+/+}$ ($n = 20$) and *Adamts1*$^{+/-}$ ($n = 17$) mice. Data are mean ± s.e.m. $^{**}P < 0.01$; $^{***}P < 0.001$; n.s., not significant; by Student's *t*-test.

Aortic medial degeneration in Marfan and Loeys–Dietz syndromes is linked to activation of the TGF-β pathway[17,21]. Activation of this pathway leads to phosphorylation of the transcription factors Smad2 and Smad3, their subsequent translocation to the nucleus and transcriptional induction of their target genes, including connective tissue growth factor (*Ctgf*), collagen, type I, alpha 1 (*Col1a1*) and serine (or cysteine) peptidase inhibitor, clade E, member 1 (*Serpine1*; also called *Pai1*). Immunohistochemistry of aortic sections from *Adamts1*$^{+/-}$ mice revealed increased TGF-β1 and Smad2–Smad3 expression (**Fig. 2i**) and increased Smad2 activation, as seen by increased levels of phosphorylation and nuclear localization of Smad2, than in WT mice (**Fig. 2i**). Similarly, *Adamts1* knockdown in mice showed increased Smad2–Smad3 expression and Smad2 activation in the aorta (**Supplementary Fig. 3a**). Increased Smad2–Smad3 expression and Smad2 activation were also evident in sections from the AsAo of *Adamts1*$^{+/-}$ mice, as assessed by immunofluorescence

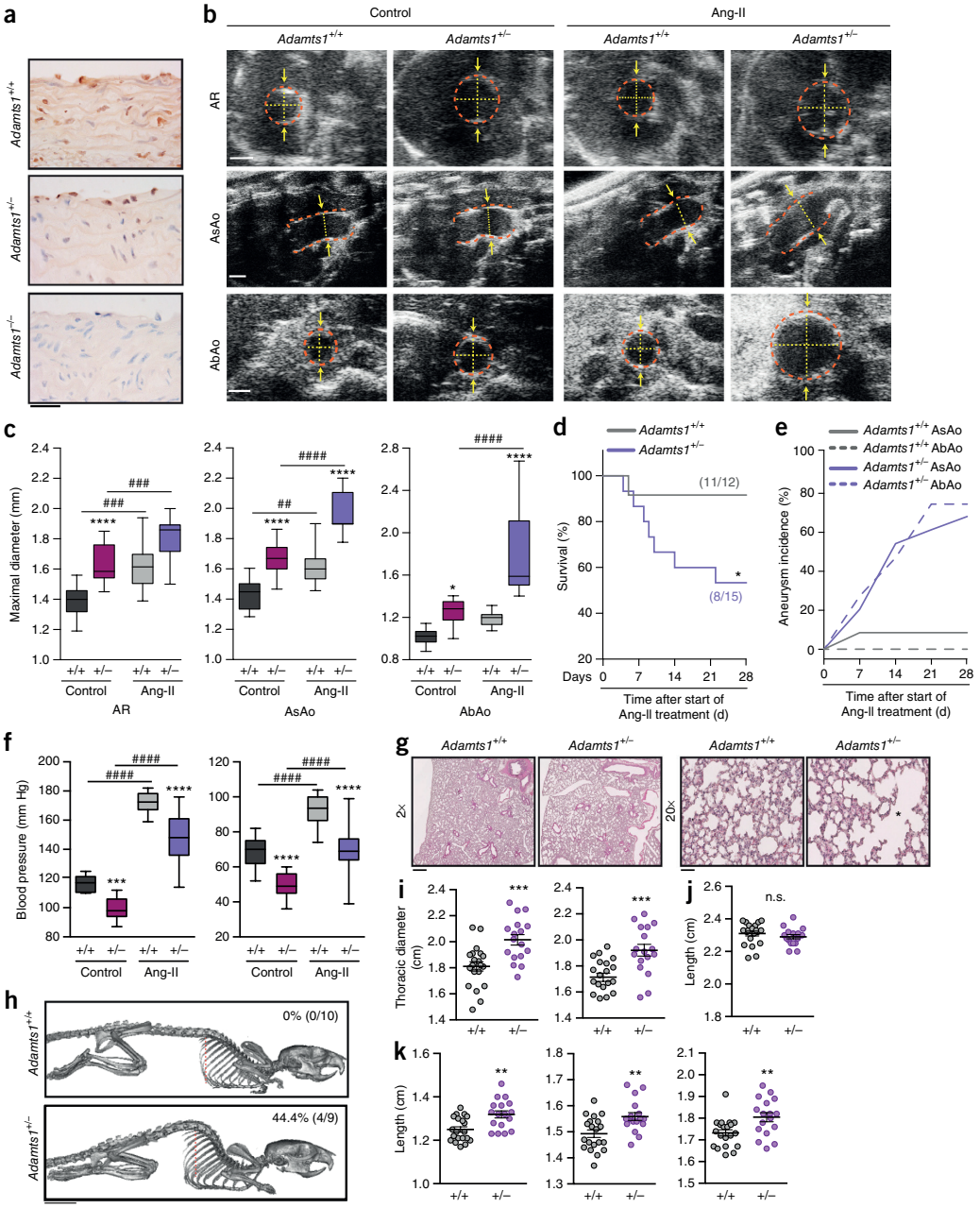

(**Supplementary Fig. 3b**). Moreover, we observed similar results in aortic sections from MFS mice (**Supplementary Fig. 3b**); this mouse strain is heterozygous for an allele of fibrillin 1 (*Fbn1*) containing a mutation (C1039G)[18] that is equivalent to a mutation frequently found in patients with MFS. Consistent with activation of TGF-β signaling, aortas from *Adamts1*$^{+/-}$ and siAdamts1-expressing mice had higher mRNA levels of the TGF-β transcriptional targets *Ctgf*, *Col1a1* and *Pai1* than aortas from WT and siCtl-expressing mice, respectively (**Supplementary Fig. 3c**,**d**).

Aortic dilation induced by *Adamts1* deficiency is rapid and independent of TGF-β

To assess the pathogenesis of aortopathy caused by an Adamts1 deficiency, we monitored AsAo and AbAo diameters and BP after intrajugular inoculation of the siCtl- or siAdamts1-expressing lentivirus (**Fig. 3a**). Levels of *Adamts1* mRNA and Adamts1 protein were decreased as early as 1–2 d after inoculation of mice with siAdamts1-expressing lentivirus than in mice inoculated with siCtl-expressing lentivirus (**Fig. 3b** and **Supplementary Fig. 4a**), which was followed immediately by a drop in BP and the induction of elastolysis (**Fig. 3c**,**d** and **Supplementary Fig. 4b**,**c**). There was no significant increase in aortic diameter until 3 d after inoculation (**Fig. 3e**), whereas collagen deposition in the aortic wall (**Fig. 3f**) and transcriptional activation of the TGF-β pathway (**Supplementary Fig. 4d**) did not occur until 1–2 weeks after inoculation. The early induction of elastolysis prompted us to assess the activities of matrix metallopeptidase 2 (Mmp2) and Mmp9, key elastolytic proteins in the aortic wall. Mmp9 activity but not Mmp2 activity was rapidly and markedly induced after *Adamts1* silencing (**Fig. 3g**), and increased levels of Mmp9 in smooth muscle actin (SMA)-positive cells of the tunica media were detected in AsAo sections by immunofluorescence (**Fig. 3h**). Notably, macrophages, a known source of Mmp9 in inflammatory diseases[22], were almost absent from these aortic sections (**Fig. 3h**) but were readily detected in atheroma plaques in mice deficient in apolipoprotein E (*Apoe*$^{-/-}$ mice)[23], which were used as a control for macrophage staining (**Fig. 3h**). These results therefore support the idea that VSMCs are the major source of Mmp9 in the diseased aorta of *Adamts1*-expressing mice.

Canonical and noncanonical pathways of TGF-β activation have critical roles in a mouse model of MFS, and treatment of such mice with a TGF-β-neutralizing antibody or the AT1R antagonist losartan can prevent aneurysm formation[5]. Although the timing of TGF-β activation after *Adamts1* silencing suggested a secondary role in aortopathy onset, we tested the contribution of the TGF-β pathway by treating siAdamts1-inoculated mice with losartan or a TGF-β-neutralizing antibody (**Fig. 3i**). Notably, neither treatment reduced siAdamts1-induced aortic dilation (**Fig. 3j** and **Supplementary Fig. 4e**), hypotension (**Supplementary Fig. 4f**), or elastic fiber fragmentation or fibrosis (**Fig. 3k**,**l**). As a confirmation that the neutralizing antibody was correctly administered and had neutralizing activity, we found that antibody treatment efficiently inhibited induction of the TGF-β transcriptional targets *Tgfb1*, *Pai1*, *Ctgf* and *Col1a1* (**Supplementary Fig. 4g**). Losartan treatment reduced BP in control mice, as expected (**Supplementary Fig. 4f**). These results support the conclusion that TGF-β pathway activation is secondary to aortic dilation, elastolysis and fibrosis in Adamts1-related aortopathy during disease onset.

Aortopathy induced by *Adamts1* deficiency is mediated by Nos2-derived nitric oxide

To further investigate the mechanism of Adamts1-related aortopathy, we focused on potential mediators of the hypotension induced by Adamts1 deficiency, because hypotension was the earliest effect that was detected after *Adamts1* silencing. A candidate factor is nitric oxide (NO), an endogenous vasorelaxant that relaxes smooth muscle and lowers BP. NO can be produced by the constitutively expressed NO synthase (NOS) of endothelial (eNOS; also called NOS3) or neuronal (nNOS; also called NOS1) origin or by inducible NOS (iNOS; also called NOS2)[24]. To test the contribution of NO to the induction of aortic dilation, we treated C57BL/6 mice with N_{ω}-nitro-L-arginine-methylesther (L-NAME), an inhibitor of all NOS enzymes (**Fig. 4a**). Despite its hypertensive effect (**Supplementary Fig. 5a**), L-NAME treatment prevented siAdamts1-induced dilation of the AsAo and the AbAo (**Fig. 4b**), blocked elastolysis (**Fig. 4c** and **Supplementary Fig. 5b**), decreased fibrosis (**Fig. 4d**) and prevented Mmp9 activation (**Fig. 4e**).

To further test the therapeutic potential of NOS activity inhibition, we administered L-NAME to *Adamts1*$^{+/-}$ mice. L-NAME treatment rapidly decreased the AsAo and AbAo diameters to normal levels (**Fig. 4f**), increased BP (**Fig. 4g** and **Supplementary Fig. 5c**), decreased elastic fiber fragmentation (**Fig. 4h**) and diminished fibrosis (**Fig. 4i**).

Under physiological conditions, vascular NOS3 produces low levels of NO to maintain vascular homeostasis[25], whereas under pathological conditions NOS2 can be transcriptionally activated and can produce 1,000-fold more NO than its constitutively active counterparts[26]. We therefore hypothesized that Nos2 levels might be increased in Adamts1-deficient mice and that high Nos2 levels could mediate aortic dilation and medial degeneration. *Nos2* mRNA expression was markedly induced as early as 2 d after inoculation with the

Figure 2 Knockdown of *Adamts1* expression in the aorta of adult mice causes an aortic disease similar to that induced by genetic deficiency of *Adamts1*. (**a**) Experimental design. 8-week-old C57BL/6 mice were inoculated (through the jugular vein) with lentivirus encoding GFP and either siCtl or siAdamts1. Eco-BP (ultrasound and BP analysis) was performed seven times (empty triangles). LVi, lentivirus inoculation; Ang-II, Ang-II minipump implantation. (**b**) Representative images of GFP (top) and Adamts1 (bottom) immunostaining in AsAo sections of uninfected (left), siCtl-expressing (middle) or siAdamts1-expressing (right) mice ($n = 4$ mice per group). Scale bar, 50 μm. (**c**) Immunoblot analysis for Adamts1 expression in aortic samples from mice that were transduced with lentivirus expressing the indicated siRNA and treated with vehicle (control) or Ang-II as indicated. Glyceraldehyde phosphate dehydrogenase (Gapdh) was used as a loading control. Each lane corresponds to an individual mouse. (**d**,**e**) End-of-treatment systolic (left) and diastolic (right) BP (**d**) and maximal AR (left) and AsAo (right) diameter (**e**) in control-treated siCtl-expressing mice ($n = 14$), control-treated siAdamts1-expressing mice ($n = 16$), Ang-II-treated siCtl-expressing mice ($n = 13$) and Ang-II-treated siAdamts1-expressing mice ($n = 16$). Data are presented as box-and-whisker plots, with 75th and 25th percentiles, and are pooled from two independent experiments; bars represent maximal and minimal values. $^{***}P < 0.01$, $^{****}P < 0.001$ (siCtl versus siAdamts1); $^{\#}P < 0.05$, $^{\#\#\#}P < 0.001$, $^{\#\#\#\#}P < 0.0001$ (control versus Ang-II treatment); by two-way ANOVA. (**f**) Representative images showing Masson's trichrome (Masson) (top), elastic van Gieson (EVG) (middle) and Alcian blue (bottom) staining in the AsAo from the indicated mice ($n = 4$ mice per group). Yellow arrowheads indicate elastin breaks. Scale bar, 50 μm. (**g**,**h**) Quantification of elastin breaks (left) and collagen content (right) in AsAo sections from the mouse cohorts shown in **d**,**e** (**g**) and in **Figure 1c** (**h**). $^{**}P < 0.01$, $^{***}P < 0.001$, $^{****}P < 0.0001$ (siCtl versus siAdamts1 or *Adamts1*$^{+/+}$ versus *Adamts1*$^{+/-}$ mice; $^{\#\#}P < 0.01$, $^{\#\#\#}P < 0.001$, $^{\#\#\#\#}P < 0.0001$ (control- versus Ang-II-treated mice); by two-way ANOVA. (**i**) Representative images showing staining for TGF-β1 (top), phosphorylated Smad2 (pSmad2) (middle), and total Smad2 and Smad3 (bottom) in AsAo sections from control- or Ang-II-treated *Adamts1*$^{+/+}$ and *Adamts1*$^{+/-}$ mice ($n = 3$ mice per group). Scale bar, 20 μm.

siAdamts1-expressing lentivirus, whereas *Nos3* mRNA expression was unaffected (**Supplementary Fig. 5d**). mRNA levels of endothelin 1 (*Edn1*), which encodes another BP regulator, was not affected by *Adamts1* silencing (**Supplementary Fig. 5d**). Immunostaining of aortic cross-sections from siAdamts1-expressing or *Adamts1*$^{+/-}$ mice confirmed increased Nos2 levels in the medial layer, which coincided with SMA-positive VSMCs, as compared to that in the aorta of their respective controls (**Fig. 5a**).

To investigate whether Nos2-derived NO mediates the aortopathy that is induced by an Adamts1 deficiency, we inoculated *Nos2*$^{+/+}$ and *Nos2*$^{-/-}$ mice with the siAdamts1-expressing lentivirus (**Fig. 5b**). *Nos2* deficiency blocked siAdamts1-induced AsAo and AbAo dilation (**Fig. 5c** and **Supplementary Fig. 5e**), elastic fiber fragmentation (**Fig. 5d** and **Supplementary Fig. 5f**) and fibrosis (**Fig. 5e**). *Nos2*$^{-/-}$ mice were normotensive and resistant to the hypotensive effects of *Adamts1* silencing (**Fig. 5f** and **Supplementary Fig. 5g**). Consistent

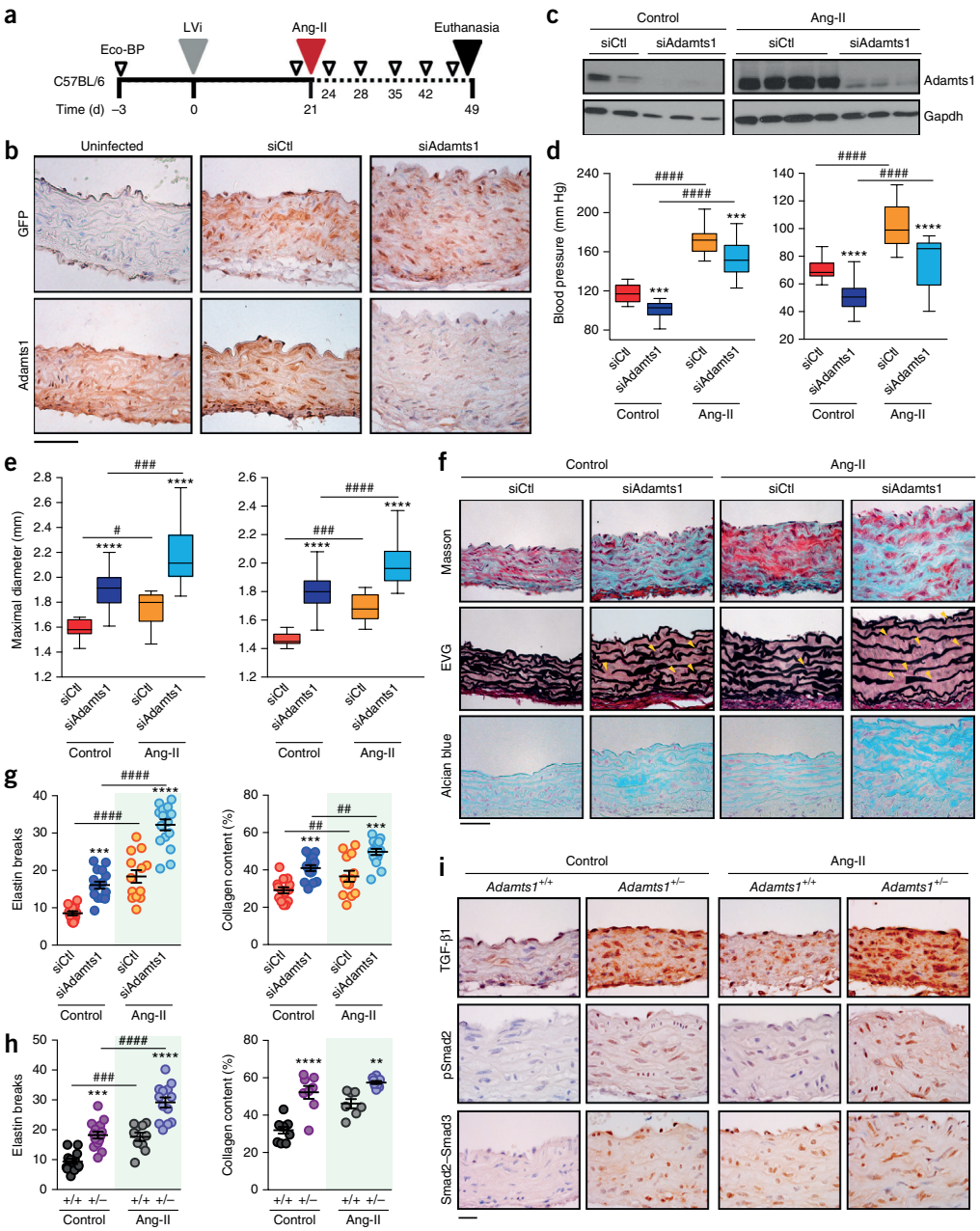

with there being a critical role for Nos2-derived NO in Adamts1-deficiency-induced aortopathy, unfixed aortic sections from siAdamts1-expressing or *Adamts1*$^{+/-}$ mice contained higher NO levels than their respective controls (**Fig. 5g**). Moreover, this siAdamts1-induced increase in aortic NO levels was not observed in *Nos2*$^{-/-}$ mice (**Fig. 5g**).

Because the kinase Akt is a mediator of Nos2 induction[27] and is activated by syndecan 4, a known proteolytic Adamts1 target[28], we investigated the contribution of Akt to Nos2 induction in Adamts1-deficient mice. The levels of phosphorylated Akt, a marker of Akt activation, were increased in protein extracts from the aorta of siAdamts1-expressing mice relative to those in siCtl-expressing mice (**Fig. 5h**). Moreover, NF-κB, a critical transcription factor for *Nos2* induction[29], was activated following *Adamts1* silencing, as indicated by increased levels of phosphorylated p65, an NF-κB subunit (**Fig. 5h**). Transduction of cultured VSMCs *in vitro* with the siAdamts1-expressing lentivirus induced Akt and NF-κB activation, as well as Akt-dependent Nos2 expression, (**Supplementary Fig. 5h–j**) and increased the levels of NO-derived metabolites and NO (**Supplementary Fig. 5k**,**l**). Finally, pharmacological inhibition of Akt activation in *Adamts1*$^{+/-}$ mice, using the mechanistic target of rapamycin (mTOR) inhibitor AZD8055, rapidly decreased aortic dilation to normal levels, inhibited NO production in the aortic wall and reduced *Nos2* levels (**Fig. 5i–l**). Taken together, these results strongly suggest that Akt activation mediates Nos2 induction in the dilated aortic wall.

A critical role for nitric oxide and Adamts1 in a mouse model of Marfan syndrome

We hypothesized that NO might mediate medial degeneration in other syndromic forms of TAAD. To determine the potential role of NO in MFS, we administered L-NAME to *Fbn1*$^{C1039G/+}$ mice, a mouse model of MFS (also referred to as MFS mice) (**Supplementary Fig. 6a**). The phenotype of *Fbn1*$^{C1039G/+}$ mice resembles that of human MFS, including aortic dilation, aneurysm and dissection, and histological features of aortic medial degeneration[18]. Twelve-week-old *Fbn1*$^{C1039G/+}$ mice showed dilation of the AsAo and AbAo (**Supplementary Fig. 6b**), which was similar to the dilation observed in Adamts1-deficient mice. L-NAME treatment rapidly decreased the AsAo and AbAo diameters to normal values (**Supplementary Fig. 6b**), augmented systolic and diastolic BP (**Supplementary Fig. 6c**), and diminished elastic fiber fragmentation (**Supplementary Fig. 6d**). There was no increase in collagen accumulation in *Fbn1*$^{C1039G/+}$ mice, and collagen content was unaffected by L-NAME treatment (**Supplementary Fig. 6e**).

Fbn1$^{C1039G/+}$ mice also had markedly elevated levels of Nos2 and NO production relative to those in the littermate controls (**Fig. 6a** and **Supplementary Fig. 7a**), whereas *Nos3* levels were unaffected (**Supplementary Fig. 7a**). To determine whether Nos2 induction in these mice had a pathogenic role, we generated *Fbn1*$^{C1039G/+}$;*Nos2*$^{-/-}$ mice and found that the AsAo and AbAo diameters in these mice were markedly smaller than those in the *Fbn1*$^{C1039G/+}$ mice (**Supplementary Fig. 7b**).

The similarities between *Adamts1*$^{+/-}$ and *Fbn1*$^{C1039G/+}$ mice that we observed suggested a link between Adamts1 and the aortic pathology of *Fbn1*$^{C1039G/+}$ mice. Immunostaining of aortic sections from *Fbn1*$^{C1039G/+}$ mice revealed reduced levels of Adamts1 relative to those in the aortic sections from littermate controls (**Fig. 6b**), which was confirmed by immunoblot analysis of protein extracts derived from aorta (**Fig. 6b**). However, *Adamts1* mRNA levels were similar in *Fbn1*$^{C1039G/+}$ mice and control littermates (**Fig. 6c**), suggesting that post-transcriptional downregulation of *Adamts1* expression occurs in these mice.

Next we assessed the contribution of ADAMTS1 and NOS2 to MFS in humans. We found that ADAMTS1 expression in the medial layer of aortic sections from patients with MFS was decreased as compared to its expression in aortic sections from organ transplant donors, regardless of sex and age of the donors (**Fig. 6d** and **Supplementary Fig. 7c**). Quantification of the ADAMTS1-positive area in immunohistochemistry-stained sections confirmed a marked decrease in ADAMTS1 expression in the samples from the patients with MFS (hereafter referred to as MFS samples) (**Fig. 6e**). Moreover, autofluorescence of elastin was barely detectable in aortic sections from patients with MFS, and the autofluorescence showed a disorganized pattern (**Fig. 6d**). NOS2 expression, as determined by immunofluorescence, was higher in the medial layer of aortic sections for six of the eight subjects with MFS than that in the control subjects (**Fig. 6d** and **Supplementary Fig. 7d**), and the NOS2-positive area in aortic

Figure 3 Knockdown of *Adamts1* rapidly induces aortic dilation, hypotension and medial degeneration independently of TGF-β activation. (**a**) Experimental design. 8-week-old C57BL/6 mice were inoculated (through the jugular vein) with siCtl- or siAdamts1-expressing lentivirus, monitored for aortic dilation and BP (Eco-BP), and euthanized at the indicated time points (open triangles) immediately after Eco-BP was performed. (**b**) *Adamts1* mRNA expression, as assessed by RT–qPCR, in extracts from the aorta of mice that were inoculated with lentivirus expressing the indicated siRNA and euthanized at the indicated time point after lentivirus inoculation (siCtl: $n = 12$; siAdamts1: $n = 3$ mice per time point at days 1–4 and day 21, $n = 10$ at 7 d, and $n = 4$ day 49 after lentivirus inoculation). mRNA amounts were normalized to those of *Gapdh*. Data are means ± s.e.m. $^{**}P < 0.01$, $^{***}P < 0.001$, $^{****}P < 0.0001$ (versus siCtl-expressing mice); by one-way ANOVA. (**c**–**f**) Systolic BP ($n = 12$ mice per group) (**c**), elastin breaks in the AsAo (siCtl: $n = 7$; siAdamts1: $n = 6$ (day 1), $n = 4$ (day 2), $n = 5$ (days 3, 4 and 7), $n = 3$ (days 14 and 21), $n = 4$ (day 49)) (**d**), maximal diameter of AsAo (left) and AbAo (right) ($n = 12$ mice per group) (**e**), and collagen content of the AsAo (siCtl: $n = 6$; siAdamts1: $n = 3$ (day 7), $n = 4$ (days 14, 21 and 49)) (**f**) at the indicated time points in mice after inoculation of siCtrl- or siAdamts1-expressing lentivirus. Data are mean ± s.e.m. $^{*}P < 0.05$, $^{**}P < 0.01$, $^{***}P < 0.001$, $^{****}P < 0.0001$ (versus siCtl at the same time point); by repeated-measurements two-way ANOVA (**c**,**e**) or one-way ANOVA (**d**,**f**). (**g**) Representative zymogram analysis of Mmp2 and Mmp9 activity in aortic extracts prepared 4 d after transduction of mice with lentivirus expressing siCtl or siAdamts1 ($n = 3$ mice per group). (**h**) Representative images of Mmp9 (red), SMA (white), and F4/80 (green) immunofluorescence, elastin autofluorescence (green) and DAPI-stained nuclei (blue) in aortic sections from mice 4 d after inoculation with siCtl-expressing or siAdamts1-expressing lentivirus. Atheroma plaques in *Apoe*$^{-/-}$ mice that were fed a high-fat diet were used as a positive control for F4/80 staining. Scale bar, 50 μm. (**i**) Experimental scheme. One group of mice received an intraperitoneal injection of a TGF-β-specific neutralizing antibody 3 d before lentivirus inoculation, and antibody injections were repeated three times per week. A second group of mice was treated with losartan by osmotic minipump delivery beginning immediately before lentivirus inoculation. Mice were monitored for aortic dilation and BP at the indicated time points (open triangles). (**j–l**) Maximal AsAo diameter (**j**) and end-of-experiment quantification of elastin breaks (**k**) and collagen content (**l**) in aortic sections in the indicated experimental groups. In **j**, number of mice per group: siCtl, $n = 8$; siCtrl, losartan, $n = 4$, siAdamts1, $n = 5$; siAdamts1, losartan, $n = 7$; and siAdamts1, anti-TGF-β, $n = 6$. In **k**,**l**, number of mice per group: siCtrl, $n = 5$; siAdamts1, $n = 4$; siAdamts1, losartan, $n = 6$; and siAdamts1, anti-TGF-β, $n = 5$. Data are mean ± s.e.m. $^{**}P < 0.001$, $^{***}P < 0.001$, $^{****}P < 0.0001$ (versus siCtl); n.s., not significant; by repeated-measurements two-way ANOVA of group means (**j**) or one-way ANOVA (**k**,**l**). In **b**,**d**,**f**, siCtl results were stable throughout the experimental period, and the data shown are means of readings at days 2, 4, 7, 14, 21 and 49.

sections was significantly greater in the MFS samples (**Fig. 6f**). Of note, aortic NOS2 expression in the MFS samples was in the VSMCs, as assessed by SMA staining (**Supplementary Fig. 7e**).

Because L-NAME treatment increases BP, probably through its inhibition of Nos3, it is unsuitable for the long-term treatment of individuals with TAA. To investigate whether drugs that target only the inducible NOS isoform might be of therapeutic interest for syndromic TAA, we tested the effects of 1400W, a potent and highly specific inhibitor of NOS2 (ref. 30). First, we found that 1400W treatment of cultured VSMCs that had been transduced with the siAdamts1-expressing lentivirus blocked production of NO and nitrites relative to that in cells that were not treated with 1400W

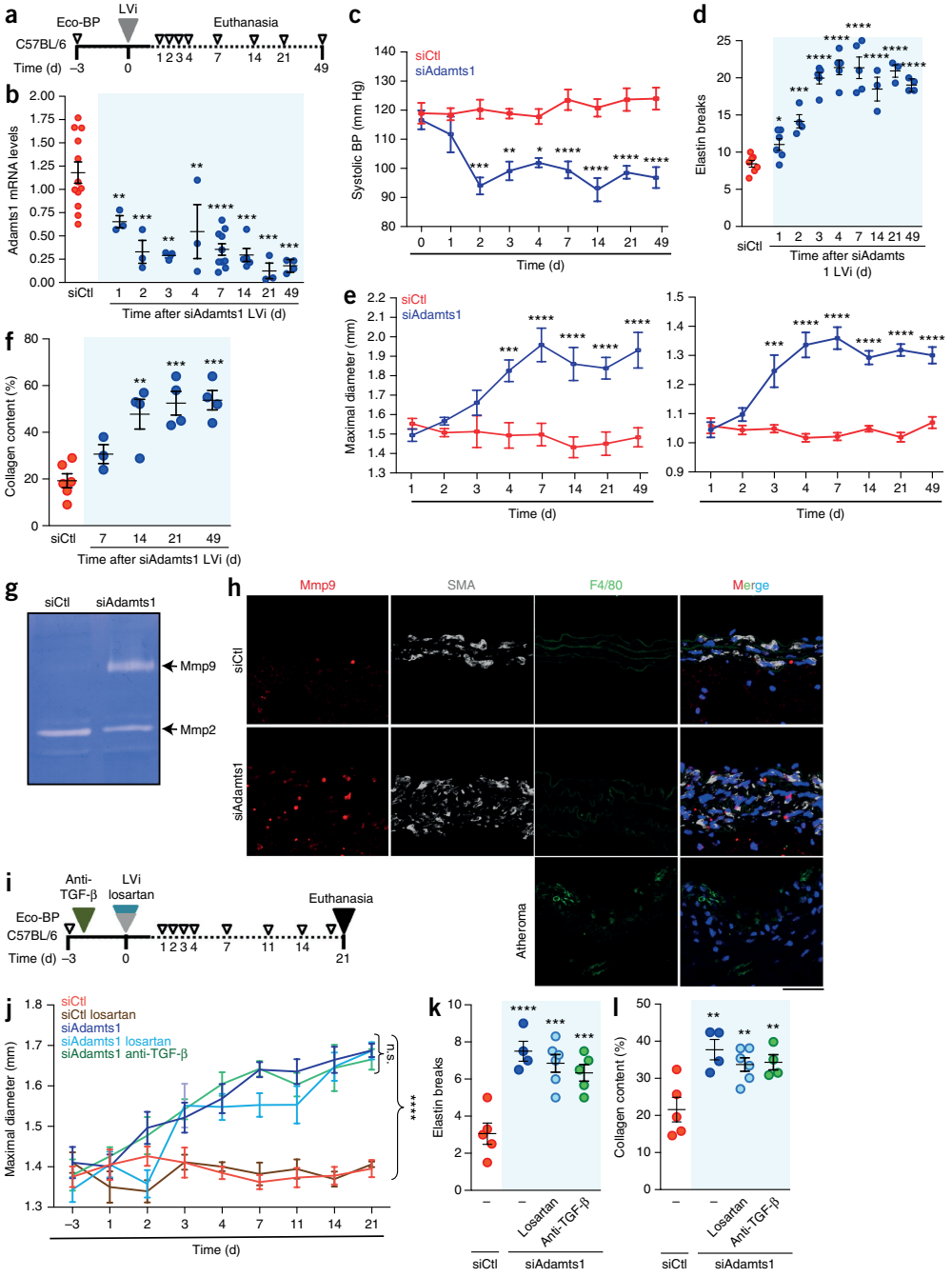

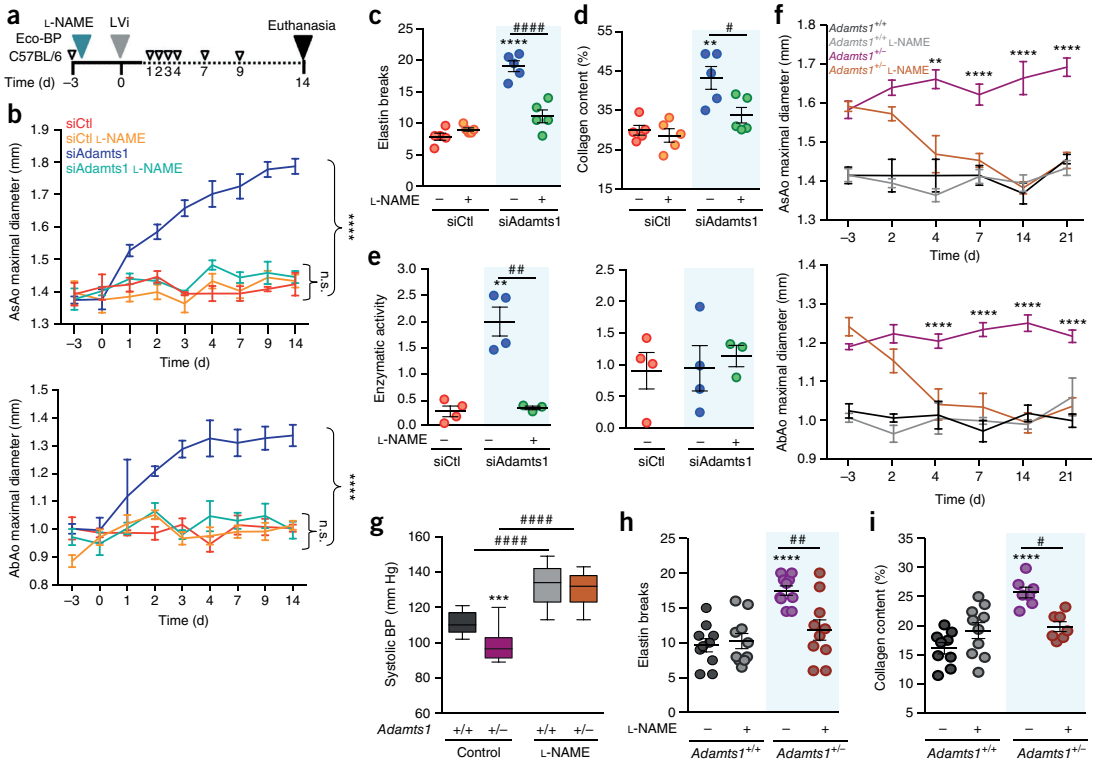

Figure 4 The aortopathy induced by *Adamts1* deficiency is mediated by NO. (**a**) Experimental design. 8-week-old C57BL/6 mice were treated with the NOS inhibitor L-NAME (in the drinking water) starting 3 d before inoculation with the siCtl- or siAdamts1-expressing lentivirus and continuing for the next 14 d. (**b**) Maximal AsAo and AbAo diameters at the indicated time points before or after lentivirus inoculation ($n = 5$ mice per group). (**c**,**d**) End-of-experiment quantification of elastin breaks (**c**) and collagen content (**d**) in aortic sections from the mice treated as indicated ($n = 5$ mice per group). (**e**) Mmp9 (left) and Mmp2 (right) activity in aortic extracts from mice that were treated as indicated (number of mice per group: siCtrl, $n = 4$; siAdamts1, $n = 4$; siAdamts1, L-NAME, $n = 3$). In **b**–**e**, data are mean ± s.e.m. $^{**}P < 0.01$ and $^{****}P < 0.0001$ (versus untreated siCtl); $^{\#}P < 0.05$, $^{\#\#}P < 0.01$, $^{\#\#\#\#}P < 0.0001$ and n.s., not significant; by repeated-measurements two-way ANOVA of group means (**b**), two-way ANOVA (**c**,**d**) or one-way ANOVA (**e**). (**f**–**i**) Maximal AsAo (top) and AbAo (bottom) diameters at the indicated time points (**f**), end-of-experiment quantification of systolic BP (**g**), elastin breaks (**h**) and collagen content (**i**) in 8-week-old *Adamts1*$^{+/+}$ (+/+) and *Adamts1*$^{+/-}$ (+/–) mice that were treated with L-NAME for 21 d or left untreated. In **f**,**g**, $n = 12$ *Adamts1*$^{+/+}$ mice, $n = 13$ L-NAME-treated *Adamts1*$^{+/+}$ mice, $n = 14$ *Adamts1*$^{+/-}$ mice, $n = 12$ L-NAME-treated *Adamts1*$^{+/-}$ mice. In **h**,**i**, $n = 9$ *Adamts1*$^{+/+}$ mice, $n = 10$ L-NAME-treated *Adamts1*$^{+/+}$ mice, $n = 7$ *Adamts1*$^{+/-}$ mice, $n = 7$ L-NAME-treated *Adamts1*$^{+/-}$ mice. Data are mean ± s.e.m., except in **g**, where data are presented as box-and-whisker plots, with 75th and 25th percentiles; bars represent maximal and minimal values. In **f**, $^{***}P < 0.001$ and $^{****}P < 0.0001$ (versus L-NAME-treated *Adamts1*$^{+/-}$ mice at each time point); by repeated-measurements two-way ANOVA. In **g**–**i**, $^{***}P < 0.001$, $^{****}P < 0.0001$ (*Adamts1*$^{+/+}$ versus *Adamts1*$^{+/-}$); $^{\#}P < 0.05$, $^{\#\#}P < 0.01$, $^{\#\#\#\#}P < 0.0001$ (L-NAME-treated versus control); by two-way ANOVA.

(**Supplementary Fig. 5k**,**l**). Next we treated 12-week-old *Adamts1*$^{+/-}$ or *Fbn1*$^{C1039G/+}$ mice for 16 weeks with 1400W. This treatment led to a rapid decrease in AsAo and AbAo diameters to normal levels, which was maintained throughout the treatment period (**Fig. 6g** and **Supplementary Fig. 8a**). The efficacy of 1400W treatment in reducing aortic dilation was confirmed by *ex vivo* measurements of the AsAo and AbAo diameters (**Supplementary Fig. 8b**). Notably, 1400W treatment did not raise BP above the normotensive values found in untreated littermate controls (**Fig. 6h** and **Supplementary Fig. 8c**) and did not have obvious detrimental effects on the health of these mice (data not shown). Histological analysis of aortic cross-sections showed that 1400W treatment led to an almost complete regression of elastic fiber fragmentation (**Fig. 6i** and **Supplementary Fig. 8d**,**e**). To determine whether NOS2 inhibition was also effective in older mice, we treated 9-month-old *Fbn1*$^{C1039G/+}$ mice with 1400W. This treatment led to a rapid decrease in aortic diameter to normal levels (**Fig. 6j** and **Supplementary Fig. 8f**), with no increase in BP (**Fig. 6k**). Taken together, these data support the idea that ADAMTS1 and NOS2 might be important mediators of the aortic pathology in human MFS and warrant evaluation of NOS2 inhibitors for the treatment of syndromic TAA.

DISCUSSION

This study identifies NO as an essential mediator of syndromic aortic disease in mouse models and suggests NO production as a possible target for intervention in human aortopathies. In addition, we show that Adamts1 is an important mediator of vascular wall homeostasis and that its expression is decreased in individuals with MFS. The resemblance of the aortopathy in *Adamts1*-deficient mice to human syndromic FTAAD suggests that ADAMTS1 downregulation in MFS may underlie the aortic phenotype of patients with MFS. The extent of aortic dilatation was similar in young *Adamts1*-deficient and in

young MFS mice, and elastic fibers were severely compromised in both mouse models. Aneurysms did not develop in young *Adamts1*-deficient or MFS mice, but administration of the hypertensive factor Ang-II to *Adamts1*-deficient mice for less than 1 month induced aneurysms in nearly 80% of mice and lethal aortic dissections in nearly 50% of mice. We suggest that the aortic dilation and medial degeneration induced by *Adamts1* deficiency resembles the early stages of human aortic diseases, whereas the exacerbated aortic pathology induced by Ang-II treatment mimics later disease stages, when aortic pathology is worsened by age-related hypertension.

Because ADAMTS1 levels are upregulated by Ang-II (ref. 10), we hypothesized that ADAMTS1 would be an important mediator of Ang-II-induced aortic disease. However, instead of having protective effects on the aortic wall, a partial Adamts1 deficiency caused pathological remodeling of the aortic wall, indicating a homeostatic role for Adamts1. Previous studies of other strains of Adamts1-deficient mice did not report vascular defects[15,31,32]. It will therefore be of interest to investigate the aortic phenotype in the previously reported strains of *Adamts1*-mutated mice and to determine whether the different genetic backgrounds in these strains (pure C57BL/6 background used in our study, as compared to the mixed genetic background used in earlier studies) account for the observed differences in lethality and fertility.

Mutations in genes encoding several members of the ADAMTS and ADAMTS-like (ADAMTSL) family that are implicated in microfibril formation have been linked to connective tissue disorders without an aortic phenotype[33]. These disorders are similar to those produced by mutation of *FBN1*, which encodes fibrillin 1, the major microfibril component of tissue[34], suggesting that interaction of ADAMTS proteins with fibrillins may be crucial to the regulation of connective tissue homeostasis. Given our results, an attractive idea is that *FBN1* mutations that are linked to MFS might disrupt FBN1 domains required for interaction with ADAMTS1; in such a scenario, loss of this interaction could destabilize ADAMTS1, thus explaining its low levels in patients with MFS and the shared features of *Adamts1*$^{+/-}$ and MFS mice.

We previously reported that lentivirus tropism depends on the route of administration[35] and that injection of lentivirus into the jugular vein yields stable and efficient transduction of the aortic wall[20]. This approach achieved long-term silencing of *Adamts1* throughout the aorta and resulted in aortic phenotypic changes and symptoms indistinguishable from those of *Adamts1*$^{+/-}$ mice. By inducing knockdown at a specific time point, we were able to define the pathological sequence leading to disease—transduction of the siAdamts1-expressing lentivirus triggered immediate hypotension and elastolysis, which was followed rapidly by aortic dilation; in contrast, activation of the TGF-β–Smad pathway did not occur until 1–2 weeks after lentiviral infection.

Although aortic medial degeneration and dilation are associated with activation of the TGF-β and Ang-II pathways in syndromic and nonsyndromic aortic disease[4,17,21,36], blockade of these pathways had no significant effects on siAdamts1-mediated aortic dilation, medial degeneration or hypotension, at least in the first 2 weeks after *Adamts1* knockdown. Our data are nonetheless compatible with a role for these pathways at later disease stages. Similarly, TGF-β neutralization failed to inhibit aneurysm progression at the early stages of a progressively severe form of MFS (in *Fbn1*$^{mgR/mgR}$ mice, which are hypomorphic for fibrillin 1 expression), but it was protective at later stages[37].

Although hypertension is considered to be a risk factor in AA, we found that L-NAME administration was able to reverse aortic dilation in *Adamts1*$^{+/-}$ and MFS mice despite its hypertensive effects. Reversal of dilation by L-NAME treatment was remarkably fast: as it was complete in 1 week. Elastic fiber integrity and collagen deposition in *Adamts1*$^{+/-}$ mice returned to normal levels 3 weeks after L-NAME administration, suggesting that NO inhibition leads to activation of mechanisms for collagen clearance from the aortic wall and induction of elastin synthesis. NO is a critical regulator of smooth muscle cell contractility; therefore, in view of the rapid dilation observed after *Adamts1* knockdown and the rapid regression of aortic diameter after treatment with NO inhibitors, we propose that aortic dilation is strongly dependent on smooth muscle cell contractility and that structural changes in the aorta are a secondary consequence of this dysregulation of cell contractility. Our results suggest that increased NO production is a primary trigger of syndromic aortic disease and that increased NO levels are also required for disease maintenance. Short-term treatment with NO donors, such as those used to treat angina, is unlikely to cause aortic damage; however, our findings indicate the need for caution in implementing long-term treatment with NO donors or with gene-therapy-augmented NOS expression.

Figure 5 Nos2 is a critical mediator of the aortopathy induced by *Adamts1* deficiency. (**a**) Representative images of Nos2 (red) and SMA (white) immunofluorescence, elastin autofluorescence (green) and DAPI-stained nuclei (blue) in aortic sections from 16-week-old *Nos2*$^{-/-}$, *Adamts1*$^{+/+}$ and *Adamts1*$^{+/-}$ mice and from WT mice that were inoculated with siCtl- or siAdamts1-expressing lentivirus (4 d after inoculation) ($n = 4$ mice per group). Scale bar, 50 µm. (**b**) Experimental design. 8-week-old WT or *Nos2*$^{-/-}$ mice were inoculated with siCtl- or siAdamts1-expressing lentivirus and monitored for aortic dilation and BP. (**c**) Maximal AsAo diameter at the indicated time points (siCtl: $n = 6$ WT mice; $n = 4$ *Nos2*$^{-/-}$ mice; siAdamts1: $n = 9$ WT mice; $n = 7$ *Nos2*$^{-/-}$ mice). (**d**,**e**) End-of-experiment quantification of elastin breaks (**d**) and collagen content (**e**) in the same groups of mice as in **c**. Each symbol represents an individual mouse. (**f**) Systolic BP at the indicated time points in the same cohorts of mice as in **c**. In **c**–**f**, data are mean ± s.e.m. In **c**,**f**, $^{****}P < 0.0001$ and n.s., not significant (versus those in siAdamts1-expressing *Nos2*$^{-/-}$ mice); by repeated-measurements two-way ANOVA of group means. In **d**,**e**, $^{**}P < 0.01$ and n.s., not significant (versus those in siCtl-expressing WT mice); by two-way ANOVA. (**g**) Representative images of NO production (red), elastin autofluorescence (green) and DAPI-stained nuclei (blue) in unfixed aortic tissue sections from WT and *Nos2*$^{-/-}$ mice that were treated as indicated 14 d after lentivirus inoculation and from 10-week-old *Adamts1*$^{+/+}$ and *Adamts1*$^{+/-}$ mice ($n = 3$ mice per group). Scale bar, 50 µm. (**h**) Representative immunoblot analysis of total and phosphorylated Akt and p65 in aortic extracts of WT mice treated with siCtl- or siAdamts1-expressing lentivirus ($n = 5$ mice per group). Each lane represents one mouse. (**i**–**l**) Maximal AsAo (left) and AbAo (right) diameters at the indicated time points (**i**), end-of-experiment systolic BP (**j**), *Nos2* mRNA levels in aortic extracts, as assessed by RT–qPCR, (**k**), and representative images of NO production (red), elastin autofluorescence (green) and DAPI-stained nuclei (blue) in unfixed aortic tissue sections (**l**) of 8-week-old *Adamts1*$^{+/+}$ and *Adamts1*$^{+/-}$ mice that received daily intraperitoneal injections of the mTOR–Akt inhibitor AZD8055 or vehicle control for 4 d. Scale bar, 50 µm. In **i**,**j**, numbers of mice per group: $n = 5$ control *Adamts1*$^{+/+}$ mice, $n = 6$ AZD8055-treated *Adamts1*$^{+/+}$ mice, $n = 4$ control *Adamts1*$^{+/-}$ mice, $n = 7$ AZD8055-treated *Adamts1*$^{+/-}$ mice; in **k**, $n = 5$ mice per group; in **l**, $n = 4$ mice per group. Data are mean ± s.e.m. except in **j**, where data are presented as box-and-whisker plots, with 75th and 25th percentiles; bars represent maximal and minimal values. $^{**}P < 0.01$ and $^{****}P < 0.0001$ (versus untreated *Adamts1*$^{+/+}$); $^{\#\#\#}P < 0.001$ (versus untreated *Adamts1*$^{+/-}$); by repeated-measurements two-way ANOVA (**i**) or two-way ANOVA (**k**).

ARTICLES

A recent report showed that gain-of-function mutations in *PRKG1*—which encodes PKG1, a downstream target of NO—are present in four families affected by TAA[38]. Increased PKG1 activity was shown to promote activation of the myosin regulatory light chain phosphatase and was, thus, predicted to decrease VSMC contractility[38]. These findings suggest that NO might also be an essential factor in nonsyndromic, familial TAAD. A critical role of the NO signaling pathway in maintaining VSMC contractility is consistent with the association of familial TAAD with mutations in other genes involved in the regulation of the VSMC contractile unit, including genes encoding aortic

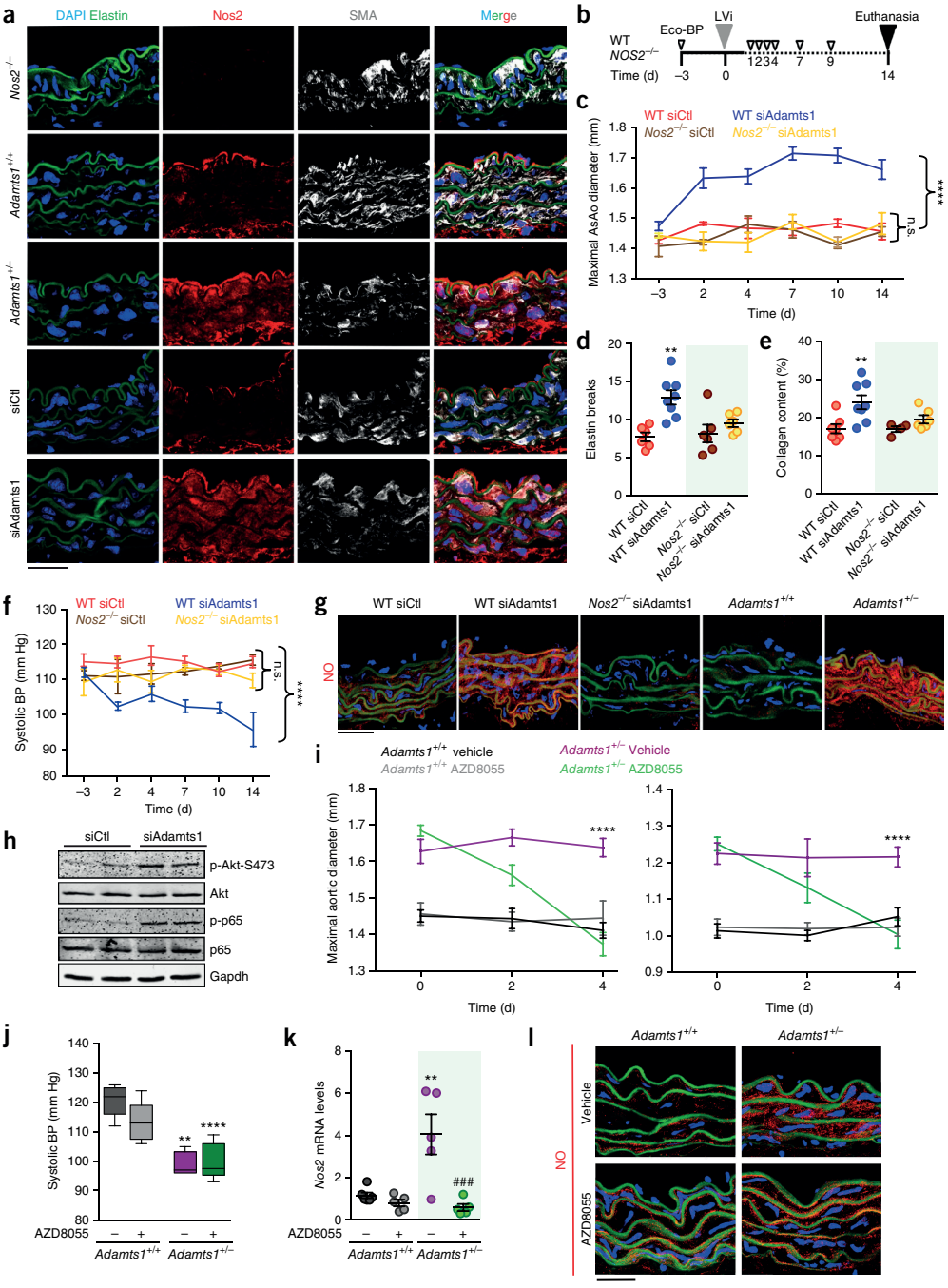

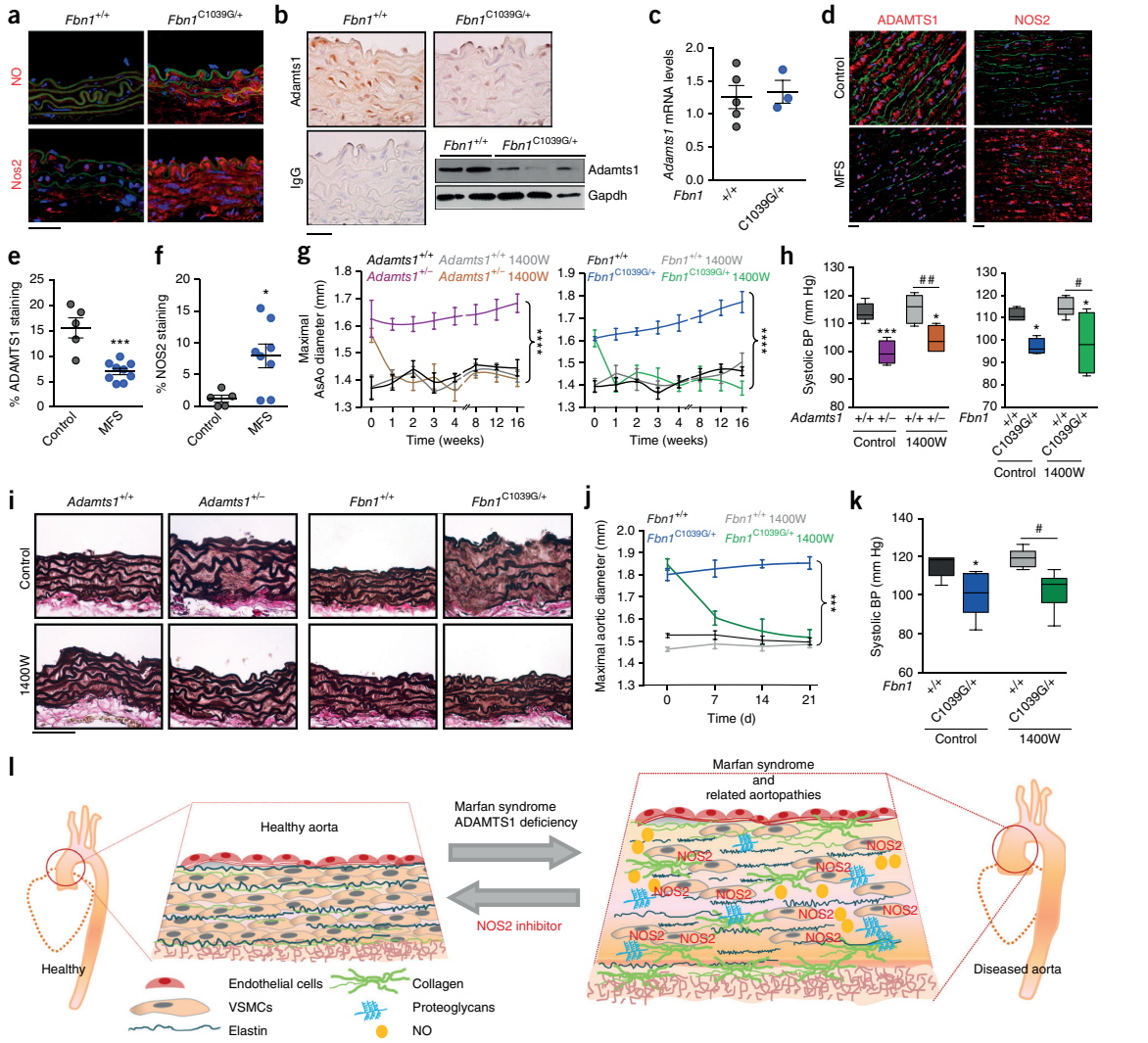

Figure 6 Adamts1 and NO have critical roles in Marfan syndrome. (**a**) Representative images of NO production (red; top), Nos2 immunofluorescence (red; bottom), elastin autofluorescence (green) and DAPI-stained nuclei (blue) in aortic sections of 16-week-old WT (left) and *Fbn1*$^{C1039G/+}$ (right) mice ($n = 3$ mice per group). (**b**) Representative images for Adamts1 expression, as assessed by immunohistochemistry, in aortic sections from WT and *Fbn1*$^{C1039G/+}$ mice ($n = 4$ mice per group) and immunoblot analysis for Adamts1 expression in aortic extracts, in which each lane represents one mouse (bottom right). IgG staining served as a negative control. Scale bar, 20 µm. (**c**) *Adamts1* mRNA levels, relative to *Gapdh* levels, in aortic extracts from WT ($n = 6$) and *Fbn1*$^{C1039G/+}$ ($n = 3$) mice, as assessed by RT–qPCR. Data are means ± s.e.m. (**d**) Representative images of ADAMTS1 immunofluorescence (red; $n = 9$ subjects per group) and NOS2 immunofluorescence (red; $n = 6$ subjects per group) in the medial layer of aortic sections from control donors or patients with MFS. Elastin autofluorescence (green) and DAPI-stained nuclei (blue) are also shown. Scale bars, 25 µm. (**e**) Percentage of ADAMTS1-positive area in immunohistochemistry-stained sections of aortas from control donors ($n = 5$) and patients with MFS ($n = 9$). (**f**) Percentage of NOS2-positive area in aortic sections from control donors ($n = 5$) and patients with MFS ($n = 8$). In **e**,**f**, data are means ± s.e.m. $^{*}P < 0.05$, $^{***}P < 0.001$; by Student's *t*-test. (**g**–**i**) Maximal AsAo diameter at the indicated time points in the groups of mice indicated ($n = 4$ mice per group) (**g**), end-of-experiment systolic BP ($n = 4$ mice per group) (**h**) and representative images of EVG staining in aortic sections (same cohorts of mice as in **g**) (**i**) from 12-week-old *Adamts1*$^{+/–}$ and *Fbn1*$^{+/C1039G}$ mice and their corresponding WT littermates after treatment with 1400W (in the drinking water) for 16 weeks. Data are means ± s.e.m. In **g**, $^{****}P < 0.0001$ and n.s., not significant (versus 1400W-treated *Adamts1*$^{+/–}$ or *Fbn1*$^{+/C1039G}$ mice); by repeated-measurements two-way ANOVA of group means. In **h**, data are presented as box-and-whisker plots, with 75th and 25th percentiles; bars represent maximal and minimal values. $^{*}P < 0.05$ and $^{***}P < 0.001$ (versus WT control); $^{\#}P < 0.05$ and $^{\#\#}P < 0.01$ (versus 1400W-treated *Adamts1*$^{+/+}$ 1400W or *Fbn1*$^{+/+}$ mice); by two-way ANOVA. Scale bar, 50 µm (**i**). (**j**,**k**) Maximal AsAo diameter at the indicated time points (**j**) and end-of-experiment systolic BP (**k**) in 36-week-old *Fbn1*$^{+/C1039G}$ mice and their WT littermates treated with 1400W in the drinking water for 21 d ($n = 5$ control or 1400W-treated WT mice; $n = 7$ control *Fbn1*$^{+/C1039G}$ mice; $n = 6$ 1400W-treated *Fbn1*$^{+/C1039G}$ mice). Data are means ± s.e.m. (**j**) or box-and-whisker plots, with 75th and 25th percentiles; bars represent maximal and minimal values (**k**). $^{***}P < 0.001$ (versus 1400W-treated *Fbn1*$^{+/C1039G}$ mice); $^{*}P < 0.05$ (versus control WT); $^{\#}P < 0.05$ (versus treated WT); by repeated-measurements two-way ANOVA of group means (**j**) or two-way ANOVA (**k**). (**l**) Model depicting the contribution of NO and NOS2 to the aortic phenotype in Marfan syndrome and the related aortopathy induced by ADAMTS1 deficiency.

smooth muscle actin (ACTA2), myosin heavy chain 11 (MYH11) and myosin light chain kinase (MYLK)[39]. It will be important to determine whether dysregulation of the NO pathway also contributes to the aortic disease associated with these mutations.

Several substrates, such as aggrecan, versican, syndecan 4, semaphorin 3C, nidogen 1, nidogen 2 and desmocollin 3, are proteolytically degraded by ADAMTS1 (ref. 40) and are therefore candidate mediators of its vascular homeostatic functions. The accumulation of any of these substrates in Adamts1-deficient tissues might contribute to the pathogenesis caused by Adamts1 insufficiency. Indeed, high levels of syndecan 4 lead to activation of Akt[28], a kinase known to activate NF-κB[41]. Akt and NF-κB are known mediators of *NOS2* induction[28,29], and we found that both Akt and NF-κB are activated early after *Adamts1* knockdown in both aortic tissue and cultured VSMCs, concomitantly with Nos2 induction. We therefore propose that Akt and NF-κB could mediate Nos2 induction elicited by Adamts1 insufficiency. Accordingly, we found that pharmacological inhibition of mTOR–Akt in *Adamts1*$^{+/-}$ mice rapidly decreased *Nos2* levels and NO production in the aortic wall and regressed aortic dilation. Although mTOR–Akt inhibitors could be considered as alternative therapeutic agents for the treatment of aortic dilation, mTOR and Akt are upstream components of many signaling pathways, including those regulating cell survival. Further analysis of the long-term effects of such inhibitors will be required before considering them as therapeutic agents in aortic diseases.

We found that Mmp9 activation and elastin fragmentation in the aorta of *Adamts1*-deficient mice were sensitive to NOS inhibition, suggesting that increased NO levels induce Mmp9-dependent elastin fragmentation and initiate medial degeneration. Although we cannot exclude the involvement of other proteinases in the elastolysis of pathological aortic dilation, Mmp9 is an important elastolytic metalloproteinase and a target of NO regulation[42,43]. Early activation of Mmp9, but not Mmp2, occurred after *Adamts1* silencing, a pattern of metalloproteinase activation characteristic of infiltrating macrophages in aortic dissection[22]. However, because we found that Mmp9 is expressed in the medial layer by VSMCs and that macrophages are almost absent from this layer, we propose that VSMCs are a major source of Mmp9 in this context. These results are consistent with previous findings showing that inflammatory cells are scarce in aortas of patients with MFS[44]. Indeed, inflammation has been documented in only a small number of cases of human TAA[45–47]. Notably, two reports that found high ADAMTS1 levels in the aorta of patients with TAA also found inflammatory cells to be present in the vessel wall[13,48], and high levels of ADAMTS1 were found in macrophages and neutrophils[48]. It thus seems likely that syndromic TAAD and inflammatory TAAD are associated with low and high ADAMTS1 levels, respectively, and are mechanistically distinct.

Previous reports implicating NO in mouse models of cerebral and abdominal AA (AAA) provide contradictory data; these discrepancies may be related to the use of pharmacological approaches versus targeted genetic-deletion approaches. For example, inhibitory or stimulatory roles for Nos2 have been reported in models of AAA[49–53]. In cerebral aneurysm, results with pharmacological inhibitors indicate that Nos2 is critical for disease development[54]; however, the incidence of cerebral aneurysm is similar in *Nos2*$^{-/-}$ and WT mice[55]. In our study, genetic analysis supports the results obtained with the pharmacological agents L-NAME and 1400W, a NOS2-specific inhibitor—*Nos2*$^{-/-}$ mice were resistant to siAdamts1-triggered aortopathy, and *Fbn1*$^{C1039G/+}$;*Nos2*$^{-/-}$ mice showed no aortic dilation. The pathological role of NO in these models is thus mediated by Nos2, whose expression is induced as early as 2 d after *Adamts1* silencing.

Although Nos2 is not normally expressed in resting cells, once induced, it remains highly active[24]. We found high levels of Nos2 protein to be a consistent feature of aortopathy, occurring in two mouse models of *Adamts1* deficiency, in MFS mice and in aortic sections of patients with MFS. Taken together, our results suggest that NOS2-mediated NO production has an essential role in the aortopathy triggered by *Adamts1* deficiency and in the pathogenesis of MFS (**Fig. 6l**). Adamts1 protein levels were decreased in MFS mice and in patients with MFS, suggesting that these aortic diseases are linked mechanistically, and that loss of Adamts1 may partially or fully explain the aortic phenotype of MFS.

The current standard treatment for MFS, β-adrenergic blockers, slow aortic dilation but do not prevent dissection[56]. Treatment with the AT1R antagonist losartan ameliorated aortic growth and controlled TGF-β pathway activation in mouse models of MFS[5], raising high expectations for MFS therapy. However, several recent clinical trials show that the β-adrenergic blocker atenolol is equally, or more, effective than losartan in reducing aortic growth in individuals with MFS[7–9,57]. Although caution should be exercised in extrapolating conclusions obtained in mouse models to human disease, the powerful and extremely fast action of NOS2 inhibition in reversing aortopathies in mouse models warrants preclinical and clinical trials with drugs that target the NO pathway for the treatment of MFS and other aortic diseases. The Nos2 inhibitor 1400W was equally effective in young and relatively old MFS mice, suggesting that Nos2 mediates not only disease initiation, but also later disease progression. Considering that NOS2 inhibitors have been safely used in clinical trials for endotoxemia, rheumatoid arthritis and migraine (https://clinicaltrials.gov/ct2/home identifiers: NCT00184990, NCT00370435 and NCT00242866), our results point to NOS2-specific inhibitors as a promising alternative for the treatment of aortic disease that could be implemented with minimal delay.

METHODS

Methods, including statements of data availability and any associated accession codes and references, are available in the online version of the paper.

Note: Any Supplementary Information and Source Data files are available in the online version of the paper.

ACKNOWLEDGMENTS

We thank B. Ibañez and G. Egea for reagents, S. Bartlett for English language editing, A.G. Arroyo, S. Lamas, J. Alegre-Cebollada and J. Ruiz-Cabello for critical reading of the manuscript and advice, and S. Pocock and J. Vazquez for advice on statistics. We also thank the CNIC histology facility, C. Velasco, A.V. Alonso and L. Flores for technical support. CNIC is supported by the Spanish Ministerio de Economía, Industria y Competitividad (MINECO) and the Pro-CNIC Foundation and is a Severo Ochoa Center of Excellence (MINECO award SEV-2015-0505). Support was also provided by grants from MINECO (grants SAF2013-45258P (M.R.C.), SAF2012-34296 (J.M.R.) and SAF2015-636333R (J.M.R.)), Fundacion La Marato (TV3 grants 20151331 (J.M.R.) and 20151330 (A.E.)), CSIC (M.R.C.), the CIBERCV of Ministerio de Sanidad (grant CB16/11/00264; J.M.R.) and the Red de Investigación Cardiovascular (RIC) of Ministerio de Sanidad (grants RD12/0042/0022 (J.M.R.), RD12/0042/0021 (A.E.), RD12/0042/0024 (M.S.), RD12/0042/0056 (J.L.J.-B.) and RD12/0042/0018 (J.F.N.)), and by a Marie Skłodowska-Curie fellowship (E.J.R.) and FPI fellowships BES 2010-034552 (J.O.) and SVP-2013-067777 (S.V.). The cost of this publication has been paid in part with FEDER funds.

AUTHOR CONTRIBUTIONS

M.R.C. and J.M.R conceived the study; J.O., N.M.-B., M.R.C. and J.M.R. designed the study and analyzed the data; J.O. and N.M.-B. performed most of the experiments, with contributions from E.J.R., S.V., L.I.C., R.A. and N.L.-V.; L.J.J.-B. supervised and analyzed the echography analysis; M.R., J.D.B., M.A.H. and J.F.N.

provided human tissue samples; L.J.J.-B., M.R., A.M.B., M.A.H., D.M., A.E., M.S., J.F.N. and J.D.B. provided experimental support and ideas for the project; M.R.C. and J.M.R. wrote the manuscript with contributions from J.O. and N.M.-B. All authors read and approved the manuscript.

COMPETING FINANCIAL INTERESTS

The authors declare no competing financial interests.

1. Dietz, H.C. TGF-β in the pathogenesis and prevention of disease: a matter of aneurysmic proportions. *J. Clin. Invest.* **120**, 403–407 (2010).
2. Gallo, E.M. *et al.* Angiotensin-II-dependent TGF-β signaling contributes to Loeys–Dietz syndrome vascular pathogenesis. *J. Clin. Invest.* **124**, 448–460 (2014).
3. Renard, M. *et al.* Novel *MYH11* and *ACTA2* mutations reveal a role for enhanced TGF-β signaling in FTAAD. *Int. J. Cardiol.* **165**, 314–321 (2013).
4. Gillis, E., Van Laer, L. & Loeys, B.L. Genetics of thoracic aortic aneurysm: at the crossroad of transforming-growth-factor-β signaling and vascular smooth muscle cell contractility. *Circ. Res.* **113**, 327–340 (2013).
5. Habashi, J.P. *et al.* Losartan, an AT1 antagonist, prevents aortic aneurysm in a mouse model of Marfan syndrome. *Science* **312**, 117–121 (2006).
6. Lim, D.S. *et al.* Angiotensin II blockade reverses myocardial fibrosis in a transgenic mouse model of human hypertrophic cardiomyopathy. *Circulation* **103**, 789–791 (2001).
7. Forteza, A. *et al.* Efficacy of losartan versus atenolol for the prevention of aortic dilation in Marfan syndrome: a randomized clinical trial. *Eur. Heart J.* **37**, 978–985 (2016).
8. Lacro, R.V. *et al.* Atenolol versus losartan in children and young adults with Marfan's syndrome. *N. Engl. J. Med.* **371**, 2061–2071 (2014).
9. Milleron, O. *et al.* Marfan Sartan: a randomized, double-blind, placebo-controlled trial. *Eur. Heart J.* **36**, 2160–2166 (2015).
10. Oller, J. *et al.* C/EBP-β and nuclear factor of activated T cells differentially regulate Adamts1 induction by stimuli associated with vascular remodeling. *Mol. Cell. Biol.* **35**, 3409–3422 (2015).
11. Luque, A., Carpizo, D.R. & Iruela-Arispe, M.L. ADAMTS1 (METH1) inhibits endothelial cell proliferation by direct binding and sequestration of VEGF165. *J. Biol. Chem.* **278**, 23656–23665 (2003).
12. Thai, S.N. & Iruela-Arispe, M.L. Expression of ADAMTS1 during murine development. *Mech. Dev.* **115**, 181–185 (2002).
13. Ren, P. *et al.* ADAMTS1 and ADAMTS4 levels are elevated in thoracic aortic aneurysms and dissections. *Ann. Thorac. Surg.* **95**, 570–577 (2013).
14. Sandy, J.D. *et al.* Versican V1 proteolysis in human aorta *in vivo* occurs at the Glu441–Ala442 bond, a site that is cleaved by recombinant ADAMTS1 and ADAMTS4. *J. Biol. Chem.* **276**, 13372–13378 (2001).
15. Mittaz, L. *et al.* Adamts1 is essential for the development and function of the urogenital system. *Biol. Reprod.* **70**, 1096–1105 (2004).
16. Cohn, R.D. *et al.* Angiotensin II type 1 receptor blockade attenuates TGF-β-induced failure of muscle regeneration in multiple myopathic states. *Nat. Med.* **13**, 204–210 (2007).
17. Neptune, E.R. *et al.* Dysregulation of TGF-β activation contributes to pathogenesis in Marfan syndrome. *Nat. Genet.* **33**, 407–411 (2003).
18. Pereira, L. *et al.* Pathogenetic sequence for aneurysm revealed in mice underexpressing fibrillin 1. *Proc. Natl. Acad. Sci. USA* **96**, 3819–3823 (1999).
19. Pyeritz, R.E. The Marfan syndrome. *Annu. Rev. Med.* **51**, 481–510 (2000).
20. Esteban, V. *et al.* Regulator of calcineurin 1 mediates pathological vascular wall remodeling. *J. Exp. Med.* **208**, 2125–2139 (2011).
21. Loeys, B.L. *et al.* A syndrome of altered cardiovascular, craniofacial, neurocognitive and skeletal development caused by mutations in *TGFBR1* or *TGFBR2*. *Nat. Genet.* **37**, 275–281 (2005).
22. Wu, Z., Ruan, Y., Chang, J., Li, B. & Ren, W. Angiotensin II is related to the acute aortic dissection complicated with lung injury through mediating the release of MMP9 from macrophages. *Am. J. Transl. Res.* **8**, 1426–1436 (2016).
23. Méndez-Barbero, N. *et al.* A major role for RCAN1 in atherosclerosis progression. *EMBO Mol. Med.* **5**, 1901–1917 (2013).
24. Förstermann, U. & Sessa, W.C. Nitric oxide synthases: regulation and function. *Eur. Heart J.* **33**, 829–837 (2012).
25. Albrecht, E.W., Stegeman, C.A., Heeringa, P., Henning, R.H. & van Goor, H. Protective role of endothelial nitric oxide synthase. *J. Pathol.* **199**, 8–17 (2003).
26. Pfeilschifter, J., Eberhardt, W. & Beck, K.F. Regulation of gene expression by nitric oxide. *Pflugers Arch.* **442**, 479–486 (2001).
27. Tang, C.-H., Lu, D.-Y., Tan, T.-W., Fu, W.-M. & Yang, R.-S. Ultrasound induces hypoxia-inducible factor 1 activation and inducible nitric oxide synthase expression through the integrin–integrin-linked kinase–Akt–mammalian target of rapamycin pathway in osteoblasts. *J. Biol. Chem.* **282**, 25406–25415 (2007).
28. Partovian, C., Ju, R., Zhuang, Z.W., Martin, K.A. & Simons, M. Syndecan 4 regulates subcellular localization of mTOR complex 2 and Akt activation in a PKC-α-dependent manner in endothelial cells. *Mol. Cell* **32**, 140–149 (2008).
29. Kleinert, H., Schwarz, P.M. & Förstermann, U. Regulation of the expression of inducible nitric oxide synthase. *Biol. Chem.* **384**, 1343–1364 (2003).
30. Garvey, E.P. *et al.* 1400W is a slow, tight-binding and highly selective inhibitor of inducible nitric oxide synthase *in vitro* and *in vivo*. *J. Biol. Chem.* **272**, 4959–4963 (1997).
31. Lee, N.V. *et al.* Fibulin 1 acts as a cofactor for the matrix metalloprotease ADAMTS1. *J. Biol. Chem.* **280**, 34796–34804 (2005).
32. Shindo, T. *et al.* ADAMTS1: a metalloproteinase–disintegrin essential for normal growth, fertility, and organ morphology and function. *J. Clin. Invest.* **105**, 1345–1352 (2000).
33. Le Goff, C. & Cormier-Daire, V. The ADAMTS(L) family and human genetic disorders. *Hum. Mol. Genet.* **20**, R163–R167 (2011).
34. Hubmacher, D. & Apte, S.S. Genetic and functional linkage between ADAMTS superfamily proteins and fibrillin 1: a novel mechanism influencing microfibril assembly and function. *Cell. Mol. Life Sci.* **68**, 3137–3148 (2011).
35. Escolano, A. *et al.* Specific calcineurin targeting in macrophages confers resistance to inflammation via MKP1 and p38. *EMBO J.* **33**, 1117–1133 (2014).
36. Chen, X., Lu, H., Rateri, D.L., Cassis, L.A. & Daugherty, A. Conundrum of angiotensin II and TGF-β interactions in aortic aneurysms. *Curr. Opin. Pharmacol.* **13**, 180–185 (2013).
37. Cook, J.R. *et al.* Dimorphic effects of transforming-growth-factor-β signaling during aortic aneurysm progression in mice suggest a combinatorial therapy for Marfan syndrome. *Arterioscler. Thromb. Vasc. Biol.* **35**, 911–917 (2015).
38. Guo, D.C. *et al.* Recurrent gain-of-function mutation in *PRKG1* causes thoracic aortic aneurysms and acute aortic dissections. *Am. J. Hum. Genet.* **93**, 398–404 (2013).
39. Karimi, A. & Milewicz, D.M. Structure of the elastin–contractile units in the thoracic aorta and how genes that cause thoracic aortic aneurysms and dissections disrupt this structure. *Can. J. Cardiol.* **32**, 26–34 (2016).
40. Kelwick, R., Desanlis, I., Wheeler, G.N. & Edwards, D.R. The ADAMTS (a disintegrin and metalloproteinase with thrombospondin motifs) family. *Genome Biol.* **16**, 113 (2015).
41. Dan, H.C. *et al.* Akt-dependent regulation of NF-κB is controlled by mTOR and raptor in association with IKK. *Genes Dev.* **22**, 1490–1500 (2008).
42. O'Sullivan, S., Medina, C., Ledwidge, M., Radomski, M.W. & Gilmer, J.F. Nitric oxide–matrix metalloproteinase 9 interactions: biological and pharmacological significance—NO and MMP9 interactions. *Biochim. Biophys. Acta* **1843**, 603–617 (2014).
43. Van Doren, S.R. Matrix metalloproteinase interactions with collagen and elastin. *Matrix Biol.* **44-46**, 224–231 (2015).
44. Segura, A.M. *et al.* Immunohistochemistry of matrix metalloproteinases and their inhibitors in thoracic aortic aneurysms and aortic valves of patients with Marfan's syndrome. *Circulation* **98**, II331–337; disc. II337–338 (1998).
45. Biddinger, A., Rocklin, M., Coselli, J. & Milewicz, D.M. Familial thoracic aortic dilatations and dissections: a case control study. *J. Vasc. Surg.* **25**, 506–511 (1997).
46. Girardi, L.N. & Coselli, J.S. Inflammatory aneurysm of the ascending aorta and aortic arch. *Ann. Thorac. Surg.* **64**, 251–253 (1997).
47. Roth, M., Lemke, P., Bohle, R.M., Klovekorn, W.P. & Bauer, E.P. Inflammatory aneurysm of the ascending thoracic aorta. *J. Thorac. Cardiovasc. Surg.* **123**, 822–824 (2002).
48. Gao, Y. *et al.* A disintegrin and metalloproteinase with thrombospondin motif 1 (ADAMTS1) expression increases in acute aortic dissection. *Sci. China Life Sci.* **59**, 59–67 (2016).
49. Johanning, J.M. *et al.* Nitric oxide in experimental aneurysm formation: early events and consequences of nitric oxide inhibition. *Ann. Vasc. Surg.* **16**, 65–72 (2002).
50. Johanning, J.M., Franklin, D.P., Han, D.C., Carey, D.J. & Elmore, J.R. Inhibition of inducible nitric oxide synthase limits nitric oxide production and experimental aneurysm expansion. *J. Vasc. Surg.* **33**, 579–586 (2001).
51. Kuhlencordt, P.J. *et al.* Accelerated atherosclerosis, aortic aneurysm formation and ischemic heart disease in apolipoprotein E and endothelial nitric oxide synthase double-knockout mice. *Circulation* **104**, 448–454 (2001).
52. Lee, J.K., Borhani, M., Ennis, T.L., Upchurch, G.R. Jr. & Thompson, R.W. Experimental abdominal aortic aneurysms in mice lacking expression of inducible nitric oxide synthase. *Arterioscler. Thromb. Vasc. Biol.* **21**, 1393–1401 (2001).
53. Zhang, J. *et al.* Inducible nitric oxide synthase is present in human abdominal aortic aneurysm and promotes oxidative vascular injury. *J. Vasc. Surg.* **38**, 360–367 (2003).
54. Fukuda, S. *et al.* Prevention of rat cerebral aneurysm formation by inhibition of nitric oxide synthase. *Circulation* **101**, 2532–2538 (2000).
55. Sadamasa, N., Nozaki, K. & Hashimoto, N. Disruption of gene for inducible nitric oxide synthase reduces progression of cerebral aneurysms. *Stroke* **34**, 2980–2984 (2003).
56. Shores, J., Berger, K.R., Murphy, E.A. & Pyeritz, R.E. Progression of aortic dilatation and the benefit of long-term β-adrenergic blockade in Marfan's syndrome. *N. Engl. J. Med.* **330**, 1335–1341 (1994).
57. De Backer, J. *et al.* Marfan syndrome and related heritable thoracic aortic aneurysms and dissections. *Curr. Pharm. Des.* **21**, 4061–4075 (2015).

ONLINE METHODS

Animal procedures. Animal procedures were approved by the CNIC Ethics Committee and by the Madrid regional authorities (ref. PROEX 80/16), and conformed to EU Directive 2010/63EU and Recommendation 2007/526/EC regarding the protection of animals used for experimental and other scientific purposes, enforced in Spanish law under Real Decreto 1201/2005. Overall mouse health was assessed by daily inspection for signs of discomfort, weight loss, or changes in behavior, mobility, and feeding or drinking habits. *Adamts1*$^{+/-}$ mice were obtained from the European Mouse Mutant Archive (EM:02291; B6;129P2-*Adamts1*^{tm1Dgen}/H) and carried a β-galactosidase (LacZ)–neomycin cassette to replace the genomic sequence (c7784) between exons 1 and 2 in the *Adamts1* target allele. *Fbn1*$^{C1039G/+}$ mice[58], which harbor a mutation in the *Fbn1* gene, and *Nos2*$^{-/-}$ mice[59] were obtained from Jackson Laboratories (JAX mice stock # 012885 and 007072, respectively). These three strains had been previously backcrossed to C57BL/6 mice for more than nine generations. All mice were genotyped by PCR of tail samples using the following primers: *Adamts1* mice (5′-GCCATCGGG GTCAGCTTTTCAAATG-3′, 5′-GGGCCAGCTCATTCCTCCCACTCAT/ GGTTGTAGTTTCGCGCTGAGTTTTG-3′); *Nos2*$^{-/-}$ mice (5′-ACATGCAGA ATGAGTACCGG-3′; 5′-TCAACATCTCCTGGTGGAAC-3′, 5′-AATATG CGAAGTGGACCTCG-3′); *Fbn1*$^{C1039G/+}$ mice (5′-CTCATCA TTTTTGGCCAGTTG-3′, 5′–GCACTTGATGCACATTCACA-3′). Wild-type littermates were used as controls unless otherwise specified. Mice were treated with Ang-II (Sigma-Aldrich) at 1 μg per kg body weight (μg/kg) per min or with losartan (Sigma-Aldrich) at 10 mg/kg/d using subcutaneous osmotic minipumps (Alzet Corp). The monoclonal pan-antibody against TGF-β1, TGF-β2 and TGF-β3 (clone 1D11; BioXcell) was injected intraperitoneally three times per week at 10 mg/kg. N_ω-nitro-L-arginine methylester hydrochloride (L-NAME, Sigma-Aldrich, 0.5 g/liter) and 1400W (Tebu-bio, 0.1 g/liter) were supplied in drinking water for the indicated periods of time, plus an additional 3 d before lentivirus inoculation. AZD8055 (Selleckchem, S1555) was dissolved in 8% DMSO in corn oil and administered daily intraperitoneally (20 mg/kg/d). *Apoe*$^{-/-}$ mice were obtained from Charles Rivers (JAX mice stock 002052). To accelerate atherosclerosis, 3-month-old mice were fed a high-fat diet (10.8% total fat, 0.75% cholesterol; S4892-E010, Ssniff Spezialdiäten, Germany) during 6 weeks.

Blood pressure measurements and *in vivo* imaging. Arterial blood pressure (BP) was measured in mouse tails using the automated BP-2000 Blood Pressure Analysis System (Visitech Systems, Apex, NC, USA). In brief, mice were trained for BP measurements every day for 1 week. After the training period, BP was measured 1 d before treatment or before lentiviral infection to determine the baseline BP values in each mouse cohort. Measurements were repeated several times during experiments. BP measurements were recorded in mice that were restrained in a tail-cuff restrainer over a warmed surface (37 °C). Fifteen consecutive systolic and diastolic BP measurements were made, and the last ten readings per mouse were recorded and averaged.

For *in vivo* ultrasound images, the aortic diameter was monitored in isoflurane-anesthetized mice (2% isoflurane) by high-frequency ultrasound with a VEVO 2100 echography device (VisualSonics, Toronto, Canada) with 30-μm resolution. Maximal internal diameters of aortic images were measured using VEVO 2100 software, version 1.5.0. All recordings were made by a cardiologist and a technician who were blinded to animal genotype and treatment. Measurements were taken before lentivirus administration or the corresponding treatments to determine the baseline diameters, and measurements were repeated several times during the experiment. In the indicated cases, after euthanization of the mice, the maximum external diameter of the AsAo was measured using a digital caliper (Ratio 6369H15).

The whole skeleton was imaged in anesthetized mice (1.5–2% isofluorane) using an X-Ray CT system integrated in a nano-PET–CT scanner (Mediso Medical Imaging Systems, Budapest). Images were acquired at 55 Kv, 500 mA/s, 360 frames per Rx rotation and pitch = 1. Skeletal three-dimensional reconstruction was performed with Medis software (Medis, the Netherlands).

Cell procedures. Primary mouse vascular smooth muscle cells (VSMCs) were isolated and grown as described[20]. All experiments were performed using cells from passages 3–7. VSMCs were infected at a multiplicity of infection (MOI) = 3 over 5 h. The medium was then replaced with fresh Dulbecco's modified Eagle's medium (DMEM) supplemented with 10% FBS, and cells were cultured for three more days, serum-starved for 48 h, and then stimulated with Ang-II for 6 h for protein assays or 4 h for mRNA expression analysis. HEK-293T and Jurkat cell lines were purchased from ATCC. All cells were *Mycoplasma* negative.

siRNA-encoding lentivirus production and infection. Lentiviruses expressing GFP and an siRNA targeting mouse *Adamts1* mRNA were purchased from ABM-GOOD. siRNA sequences were as follows: #siRNA27 (GGAAAGAATCC GCAGCTTTAGTCCACTCA); #siRNA57 (ACCGCCAGTGTCAGTTTACAT TCGGAGAG); #siRNA69 (CTTCCGAATGTGCAAAGGAAGTGAAGCCA). siCtl (GGGTGAACTCACGTCAGAA) was used as a control. Pseudotyped lentiviruses were produced by transient calcium phosphate transfection of HEK-293T cells. Supernatant containing the lentiviral particles was collected 48 h after removal of the calcium phosphate precipitate and ultracentrifuged for 2 h at 26,000 r.p.m. (Ultraclear Tubes, SW28 rotor and Optima L-100 XP Ultracentrifuge; Beckman). Viruses were suspended in cold, sterile PBS solution and titrated by transduction of Jurkat cells for 48 h. Transduction efficiency (number of GFP-expressing cells) and cell death (propidium iodide staining) were quantified by flow cytometry.

For *in vivo* transduction experiments, animals were anesthetized (with ketamine and xylazine), and a small incision was made to expose the right jugular vein[20]. Virus solution (100 μl, 10^9 particles/ml in PBS) was inoculated directly into the right jugular vein 3 weeks before Ang-II minipump implantation or 1 d before monitoring of aortic dilation. Transduction efficiency was analyzed in aortic samples by immunohistochemistry for GFP and Adamts1.

Histology. After euthanization by CO_2 inhalation, mouse aortas, kidneys and lungs were perfused with saline. Aortas and kidneys were then isolated and fixed in 10% formalin overnight at 4 °C, whereas lungs were fixed by intratracheal instillation of 10% formalin. Paraffin cross-section (5 μm) from fixed organs were stained with hematoxylin and eosin, Masson's trichrome (Masson), Alcian blue or Verhoeff elastic–van Gieson (EVG), or they were used for immunohistochemistry or immunofluorescence. Deparaffinized sections were rehydrated, boiled to retrieve antigens (10 mM citrate buffer, pH 6) and blocked for 45 min with 10% goat serum plus 2% BSA in PBS. Samples were incubated with the following antibodies for immunohistochemistry or immunofluorescence: rabbit anti-Adamts1 (1/100, sc-25581, Santa Cruz), rabbit anti-GFP (1/100, A11122, Invitrogen), rabbit anti-pSmad2 (1/50, 3108, Cell Signaling for immunohistochemistry; 1/20, 566415, Calbiochem, for immunofluorescence), rabbit anti-Smad2–Smad3 (sc-8332 1/100 Santa Cruz), rabbit anti-TGF-β1 (1/100; Abcam ab92486), rabbit anti-Nos2 (1/100, sc-650, Santa Cruz, for mice; 482728, Millipore, for human), monoclonal anti-SMA (1/500, C6198, Sigma), rat anti-F4/80 (1/50, MF48015, Invitrogen) and rabbit anti-Mmp9 (1/100, ab38898, Abcam). Specificity was determined by substituting primary antibody with unrelated IgG (Santa Cruz). For immunohistochemistry, color was developed with DAB (Vector Laboratories), and sections were counterstained with hematoxylin and mounted in DPX (Fluka). Images were acquired using a Leica DM2500 microscope with 20×, 40× or 63× HCX PL Fluotar objective lenses and Leica Application Suite V3.5.0 acquisition software. For immunofluorescence, secondary antibodies were Alexa-Fluor-546-conjugated goat anti-rabbit and Alexa-Fluor-647-conjugated goat anti-rabbit (BD Pharmigen). Sections were mounted with DAPI in Citifluor AF4 mounting medium (Aname). Images were acquired at 1024 × 1024 pixels, 8 bits, using a Leica SP5 confocal microscope with 20× or 40× oil-immersion objectives.

Collagen fibers in aortic sections were stained with a Masson–Goldner's trichrome staining kit (Merck), and elastic fibers were stained with a modified Verhoeff Van Gieson elastin stain kit (Sigma-Aldrich). Images were acquired using a Leica DM2500 microscope with 20×, 40× or 63× HCX PL Fluotar objective lenses and Leica Application Suite V3.5.0 acquisition software and processed for presentation with Photoshop and Illustrator (Adobe) according to the guidelines of this journal. Images were then analyzed with MetaMorph 6.1 software (Universal Imaging Corp., Downingtown, PA). Collagen levels were quantified by thresholding the green signal using the hue-saturation-intensity color model and determining the percentage of stained area in the entire medial layer of two

doi:10.1038/nm.4266

nonconsecutive aortic cross-sections per mouse, using 4–16 mice per experiment. The mean percentage was calculated. Elastic lamina breaks, defined as interruptions in the elastic fibers, were counted in the entire medial layer of six nonconsecutive cross-sections per mouse, using 4–16 mice per experiment, and the mean number of breaks was calculated. The exact number of mice per group is indicated in the figure legends.

Immunoblot analysis. Samples from mouse aortas were isolated, frozen in liquid nitrogen and then homogenized (MagNA lyzer, Roche). Protein extracts were obtained by lysis in ice-cold RIPA buffer (50 mM NaCl, 50 mM Tris HCl pH 8, 1% NP40, 0.1% SDS, 0.5% sodium deoxycolate) that was completed with protease, phosphatase and kinase inhibitors. For VSMCs, cells were infected and then stimulated with Ang-II, washed with ice-cold PBS and lysed in RIPA buffer.

Proteins were separated under reducing conditions on SDS–polyacrylamide gels and transferred to nitrocellulose membranes. Proteins were detected with the following primary antibodies: rabbit anti-Adamts1 (1/1,000; sc-25581 Santa Cruz), anti-Nos2 (1/1,000, sc-650 Santa Cruz), anti-p-AKT(Ser473) (1/1,000, #9271 Cell Signaling), anti-Akt (1/1,000, #9272 Cell Signaling), anti-p-p65 (1/500, #3033 Cell Signaling) and anti-p65 (1/1,000, #8242 Cell Signaling); mouse monoclonal anti-α-tubulin (1/40,000; T 6074 Sigma-Aldrich) and anti-Gapdh (1/10,000; ab8245 Abcam). Bound antibodies were detected with enhanced-chemiluminescence (ECL) detection reagent (Millipore). Uncropped immunoblots are shown in **Supplementary Figure 9**.

Real-time and quantitative PCR. Aortas were extracted after perfusion with 5 ml saline solution, and the adventitia layer was discarded. Frozen tissue was homogenized using a mortar and an automatic bead homogenizer (MagNA Lyzer, Roche). Total RNA was isolated with TRIzol (Life Technologies). Total RNA (2 µg) was reverse-transcribed at 37 °C for 50 min in a 20-µl reaction mix containing 200 U Moloney murine leukemia virus (MMLV) reverse transcriptase (Life Technologies), 100 ng random primers and 40 U RNase Inhibitor (Life Technologies). Real-time quantitative RT–PCR was performed with the following PCR primers: *Adamts1* (ACACTGGCGGTTGGCATCGT, GCCAGCCCTGGTCACCTTGC), *Tgfb1* (CGCCATCTATGAGAAAACC, GTAACGCCAGGAATTGT), *Ctgf* (GTGCC AGAACGCACACTG, CCCCGGTTACACTCCAAA), *Col1a1* (GCTCCTCTTA GGGGCCACT, CCACGTCTCACCATTGGGG), *Pai1* (GCCAGATTT ATCAT CAATGACTGGG, GGAGAGGTGCACATCTTTCTC AAAG), *Nos3* (GTTTGT CTGCGGCGATGTC, CATGCCGCCCTCTGTTG) and *Nos2* (CAGCTGGG CTGTACAAACCTT, CATTGGAAGTGAAGCGTTTCG). qPCR reactions were performed in triplicate with SYBR master mix (Applied Biosystems), according to the manufacturer's guidelines. To examine probe specificity, we conducted a post-amplification melting-curve analysis. For each reaction, only one melting-temperature (T_m) peak was produced. The amount of target mRNA in samples was estimated by the 2^{-CT} relative quantification method, using *Gapdh* for normalization. Fold ratios were calculated relative to mRNA expression levels from control animals.

Nitric oxide staining, and nitrite and nitrate quantification. NO was stained in unfixed fresh aortic sections with 4-amino-5-methylamino-2′, 7′-difluorofluorescein (DAF-FM) diacetate and in VSMCs with diaminorhodamine (DAR)-4M (Molecular Probes). Samples were incubated with 10 µmol/liter DAF-FM diacetate reagent for 1 h at room temperature and mounted in 10% glycerol in PBS. Images were acquired with a Leica SP5 microscope. Nitrites and nitrates (total NOx) were measured in conditioned medium from transduced VSMCs after 24 h using a nitric oxide quantification kit (Active Motif).

Zymography. Aortic extracts were prepared from whole aortas as described for immunoblot assays, but in the absence of DTT. Extracts (15 µg) were fractioned under nonreducing conditions on SDS–polyacrylamide gels containing 1% gelatin. Gels were washed three times in 2.5% Triton X-100 for 30 min at room temperature, incubated overnight at 37 °C in 50 mM Tris-HCl pH 7.5, 10 mM $CaCl_2$ and 200 mM NaCl, and stained with Coomasie Blue. The areas of gelatinolytic or MMP activity were visualized as transparent bands. Images were analyzed with Quantity One software (Bio-Rad).

Human samples. The study was approved by the Ethics and Clinical Research Committee of Cantabria (ref. 27/2013) and by the Ethics Committee of Ghent University Hospital (B65020111160). Ascending aortas for use as controls were obtained anonymously from multiorgan transplant donors after written informed consent was obtained from their families. During preparation of the heart for transplantation, excess ascending aortic tissue was harvested for the study. Samples from patients with Marfan syndrome were obtained during elective or emergency aortic root surgery for aortic root aneurysm–dissection. Patient clinical data were retrieved while maintaining anonymity. Tissues were immediately fixed, kept at room temperature for 48 h and embedded in paraffin.

Statistical analysis. GraphPad Prism software 6.01 was used for the analysis. The aortic-diameter data are presented as box and whiskers plots, with 75th and 25th percentiles; bars represent maximal and minimal values. Differences were analyzed by one-way, two-way or repeated-measurements two-way analysis of variance (ANOVA) and Tukey's *post hoc* test or Newman's *post hoc* test (experiments with ≥3 groups), as appropriate. For survival curves, differences were analyzed with the log-rank (Mantel–Cox) test. Statistical significance was assigned at $^{*}P < 0.05$, $^{**}P < 0.01$, $^{***}P < 0.001$ and $^{****}P < 0.0001$.

Sample size was chosen empirically based on our previous experiences in the calculation of experimental variability; no statistical method was used to predetermine sample size, and no data were excluded. The numbers of animals used are described in the corresponding figure legends. All experiments were done with at least three biological replicates. Experimental groups were balanced in terms of animal age, sex and weight. Animals were genotyped before experiments, and they were all caged together and treated in the same way. Appropriate tests were chosen according to the data distribution. Variance was comparable between groups in experiments described throughout the manuscript. Investigators were blinded to group allocation in the experiments included in **Supplementary Figure 8b**. For the rest of experiments, no randomization was used to allocate animals to experimental groups, and investigators were not blinded to group allocation during experiments or to outcome assessments.

58. Judge, D.P. *et al.* Evidence for a critical contribution of haploinsufficiency in the complex pathogenesis of Marfan syndrome. *J. Clin. Invest.* **114**, 172–181 (2004).
59. Laubach, V.E., Shesely, E.G., Smithies, O. & Sherman, P.A. Mice lacking inducible nitric oxide synthase are not resistant to lipopolysaccharide-induced death. *Proc. Natl. Acad. Sci. USA* **92**, 10688–10692 (1995).

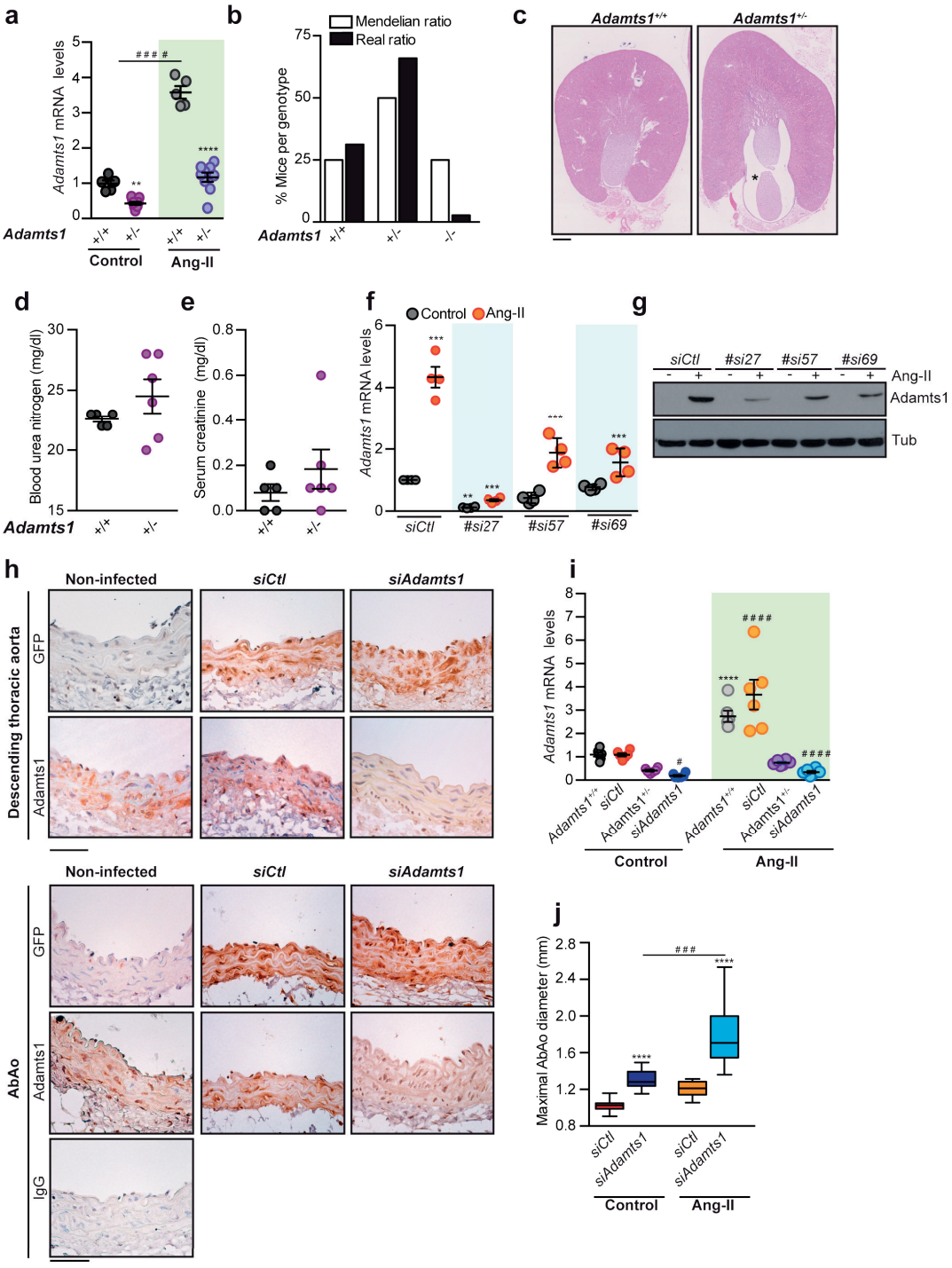

Supplementary Figure 1

Supplementary Figure 1. *Adamts1* haploinsufficiency and knockdown in the mouse. **(a)** RT-qPCR analysis of *Adamts*1 mRNA expression in 5 *Adamts1*$^{+/+}$ and 9 *Adamts1*$^{+/-}$ treated for 28 days as indicated. One-way ANOVA, *p<0.05, ***p<0.001 *Adamts1*$^{+/+}$ vs *Adamts1*$^{+/-}$ $^{###}$p<0.001 Control *Adamts1*$^{+/+}$ vs Ang-II *Adamts1*$^{+/+}$. **(b)** Percentage of *Adamts1*$^{+/+}$, *Adamts1*$^{+/-}$, and *Adamts1*$^{-/-}$ mice alive at weaning vs their expected Mendelian ratio (n=151). (**c**) Representative hematoxilin-eosin (H&E) staining of transverse kidney sections from 3-4-month-old 10 *Adamts1*$^{+/+}$ and 7 *Adamts1*$^{+/-}$ mice; *indicates hydronephrotic space. Scale bar, 500 µm. (**d**) Plasma urea and (**e**) plasma creatinine levels in 9-week-old *Adamts1*$^{+/+}$ (n=5) and *Adamts1*$^{+/-}$ (n=6) mice (mean ± SEM). **(f-g)** Vascular smooth muscle cells were transduced with lentivirus encoding Adamts1-specific siRNA (#si27, #si57, #si69) or a control siRNA (*siCtl*). Adamts1 levels were analyzed by **(f)** RT-qPCR and **(g)** immunoblot in extracts from these cells. mRNA amounts were normalized to *Gapdh* expression (mean±SEM; n=4 per group). Two-way ANOVA, **p<0.01, ***p<0.001, ****p<0.0001 vs untreated *siCtl*. Tubulin expression was used as a loading control. **(h)** Representative GFP and Adamts1 immunostaining on AbAo sections (n = 4 mice per group). IgG staining serves as a negative control. Scale bar, 50 µm. **(i)** *Adamts1* mRNA levels in aortic samples from the indicated mice and treatments (n = 6 mice per group). mRNA amounts were normalized to *Gapdh* expression (mean±SEM). Two-way ANOVA, ****p<0.0001 vs control *Adamts1*$^{+/+}$; $^{#}$p<0.05, $^{####}$p<0.0001 vs control *siCtl*. (**j**) End-of-experiment maximal aortic diameter (mean±SEM) analyzed in the same cohort of mice as Fig. 2d. One-way ANOVA, ****p<0.001 *siCtl* vs *siAdamts1*; $^{###}$p<0.001 control vs Ang-II.

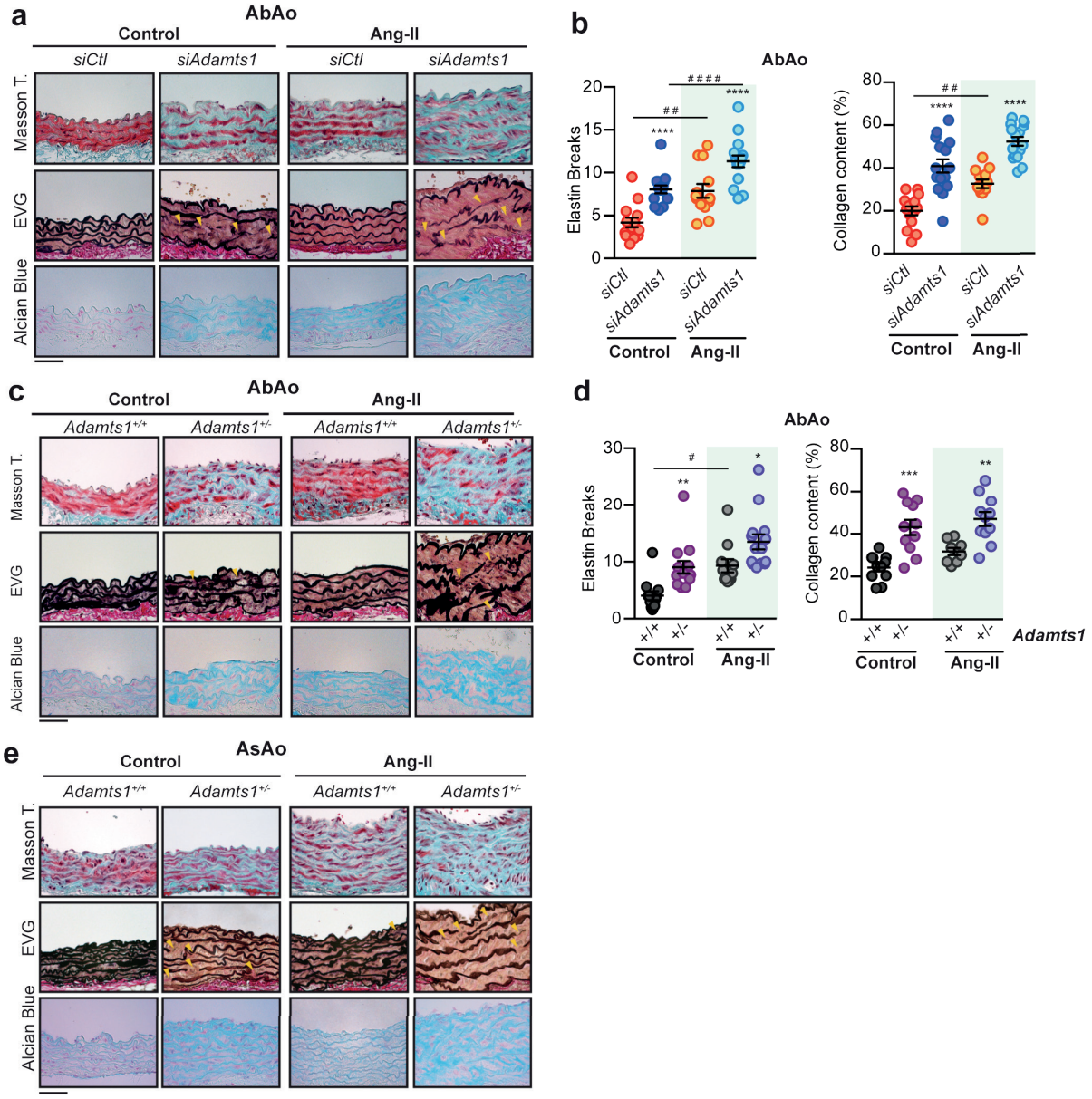

Supplementary Figure 2

Supplementary Figure 2. *Adamts1* deficiency induces aortic medial degeneration. (a) Representative Masson's trichrome (Masson T), elastin van Gieson (EVG), and alcian blue staining and (**b**) quantification of elastin breaks and collagen content in AbAo sections from the mouse cohorts shown in Figure 2g. **(c-e)** Representative Masson's trichrome (Masson T), elastin van Gieson (EVG), and alcian blue staining on (c) AbAo and (e) AsAo sections and (d) quantification of elastin breaks and collagen content in AbAo sections from the mouse cohorts shown in Figure 2h. (a,c,e) Scale bars, 50 µm. (b,d)) Two-way ANOVA, *p<0.05, **p<0.01, ****p<0.0001 *siCtl* vs *siAdamts1* or *Adamts1*$^{+/+}$ vs *Adamts1*$^{+/-;}$ $^{\#}$p<0.05, $^{\#\#}$p<0.01, $^{\#\#\#}$p<0.001, $^{\#\#\#\#}$p<0.0001 Control vs Ang-II.

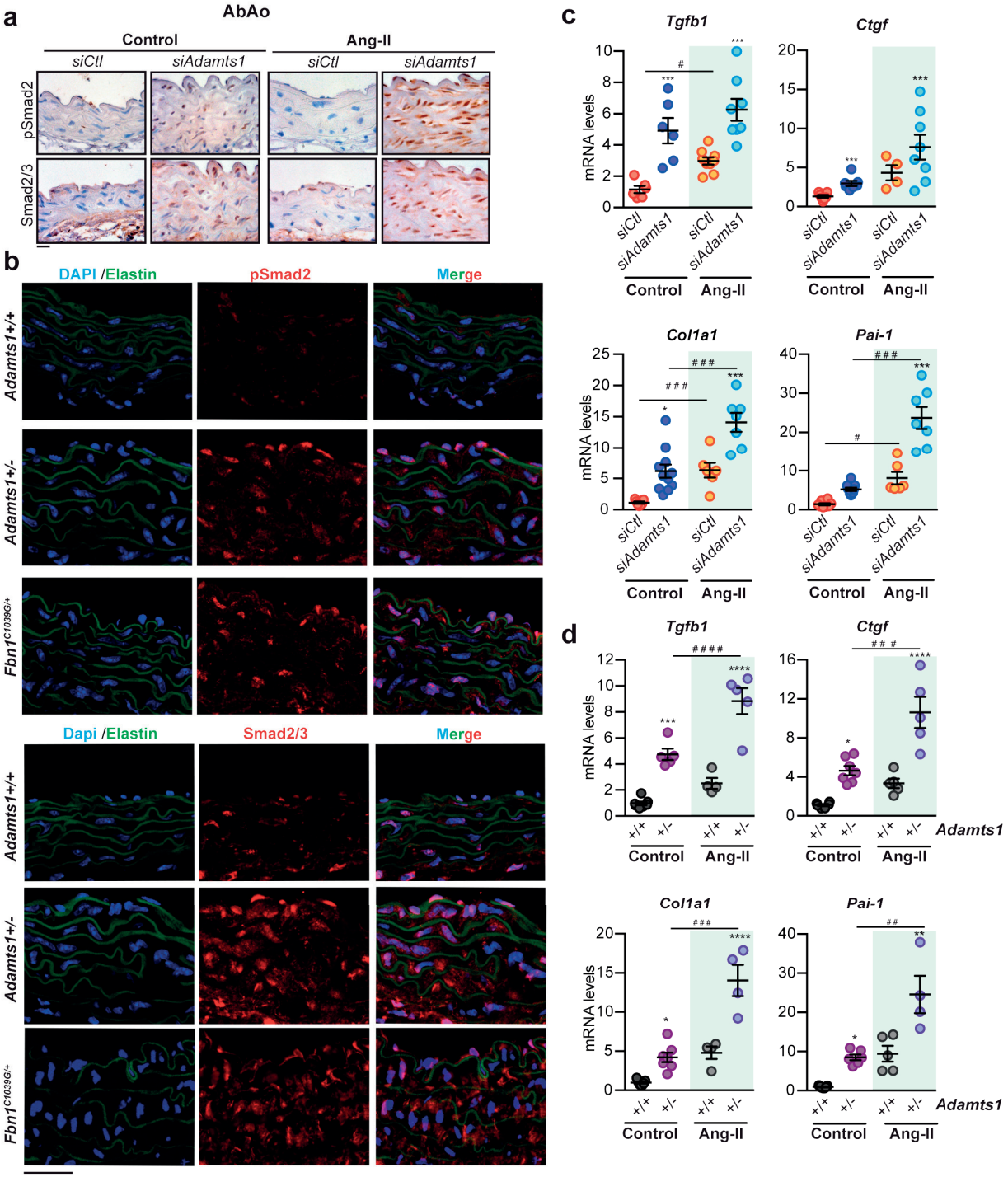

Supplementary Figure 3

Supplementary Figure 3. Activation of the TGFß pathway in the aorta of Adamts1 deficient mice. (a) Representative pSmad2 and Smad2/3 immunostaining (n = 3 mice per group) on AbAo cross sections from *siCtl*- and *siAdamts1*-transduced mice treated as indicated. Scale bar, 50 µm. (**b**) Representative images of pSmad2 or Smad2 immunofluorescence (red), elastin autofluorescence (green), and DAPI-stained nuclei (blue) in aortic sections from *Adamts1*$^{+/+}$, *Adamts1*$^{+/-}$ and *Fbn1*$^{+/C1039G}$ mice (n = 3 mice per group). Bar, 50 µm. RT-qPCR analysis of *Tgfb1*, *Ctgf*, *Col1a1*, and *Pai-1* mRNA expression in extracts from control and Ang-II-treated (**c**) *siCtl*- and *siAdamts1*-transduced mice and (**d**) *Adamts1*$^{+/+}$ and *Adamts1*$^{+/-}$ mice. Two-way ANOVA, *p<0.05, ***p<0.001, ****p<0.0001, *siCtl* vs *siAdamts1;* $^{\#}$p<0.05, $^{\#\#}$p<0.01, $^{\#\#\#}$p<0.001, $^{\#\#\#\#}$p<0.0001, Control vs Ang-II.

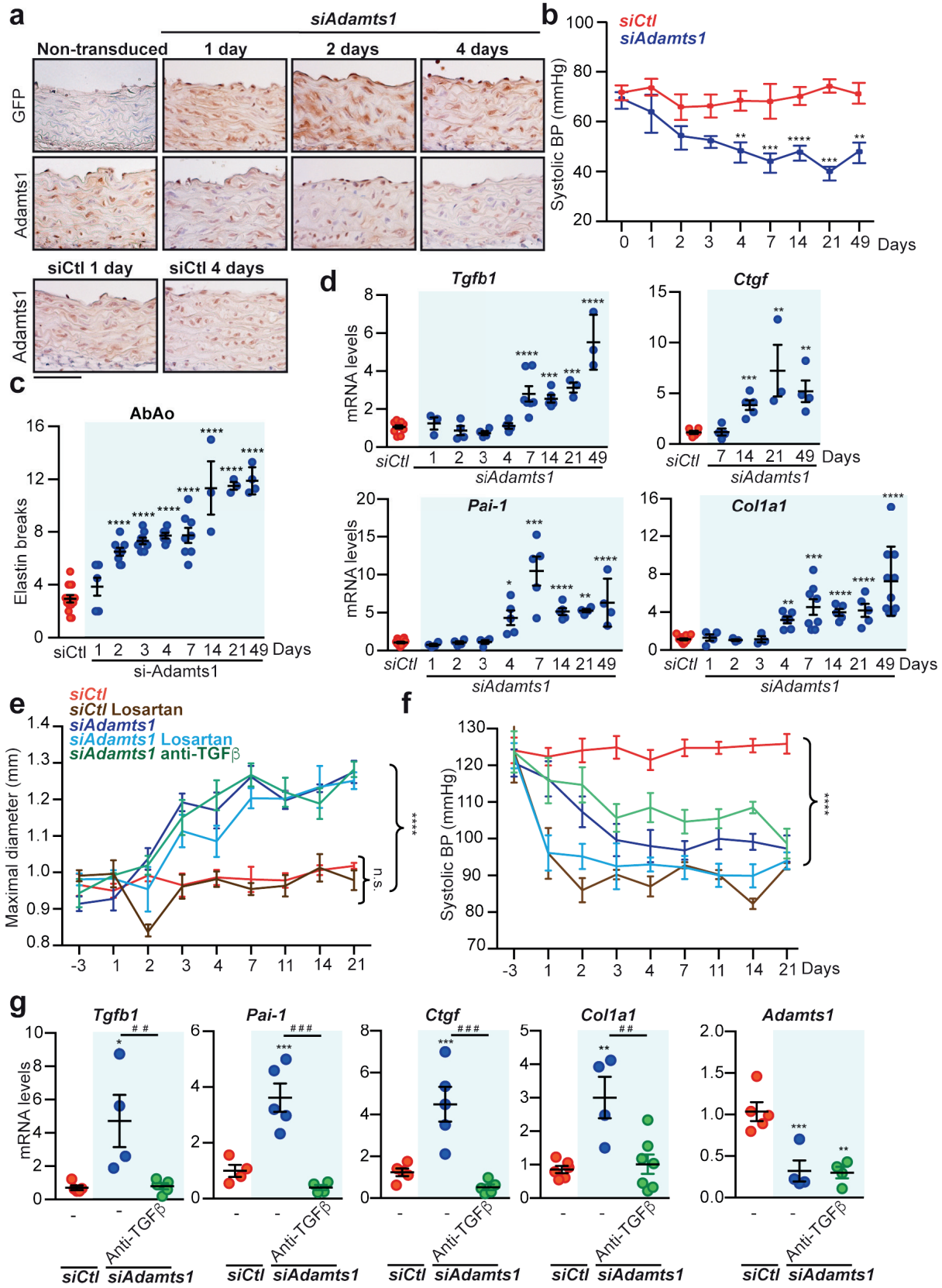

Supplementary Figure 4

Supplementary Figure 4. Aortic disease induced by *Adamts1* deficiency is fast and independent of TGFß. (a) Representative immunostaining of GFP and Adamts1 from animals in the same cohort of mice as Figures 3b-f. Scale bar 50 µm. (**b**) Diastolic BP (mean ± SEM) measured at the indicated times in *siCtl*- and *siAdamts1*-transduced mice. Repeated-measurements two-way ANOVA; **p<0.01, ***p<0.001, ****p<0.0001 vs *siCtl* at each time point. (**c**) Elastin breaks in AbAo cross sections from the same mice. (**d**) RT-qPCR analysis of *Tgfb1*, *Ctgf*, *Col1a1* and *Pai-1* expression in the same mice at the indicated times. mRNA amounts were normalized to *Gapdh* expression. One-way ANOVA; *p<0.05, **p<0.01, ***p<0.001, ****p<0.0001 vs *siCtl*. (b,c,d) Same cohort of mice as Figures 3c, 3d, and 3b, respectively. *siCtl* results in (c,d) were stable throughout the experimental period, and data are means of readings at 2, 4, 7, 14, 21, and 49 days. (**e**) Maximal AbAo diameter (mean ± SEM) and **(f)** systolic BP (mean ± SEM) at the indicated times in 8 siCtl, 4 siCtl losartan, 5 siAdamts1, 7 siAdamts1 losartan, and 6 siAdamts1 anti-TGFβ mice. Repeated measurements two-way ANOVA of group means, ****p<0.0001 vs siCtl; n.s., non-significant. (**g**) RT-qPCR analysis of *Tgfb1*, *Pai-1, Ctgf*, *Col1a1* and *Adamts1* mRNA. mRNA amounts were normalized to *Gapdh* expression. One-way ANOVA; *p<0.05, **p<0.01, ***p<0.001 vs *siCtl*; ##p<0.05, ###p<0.001.

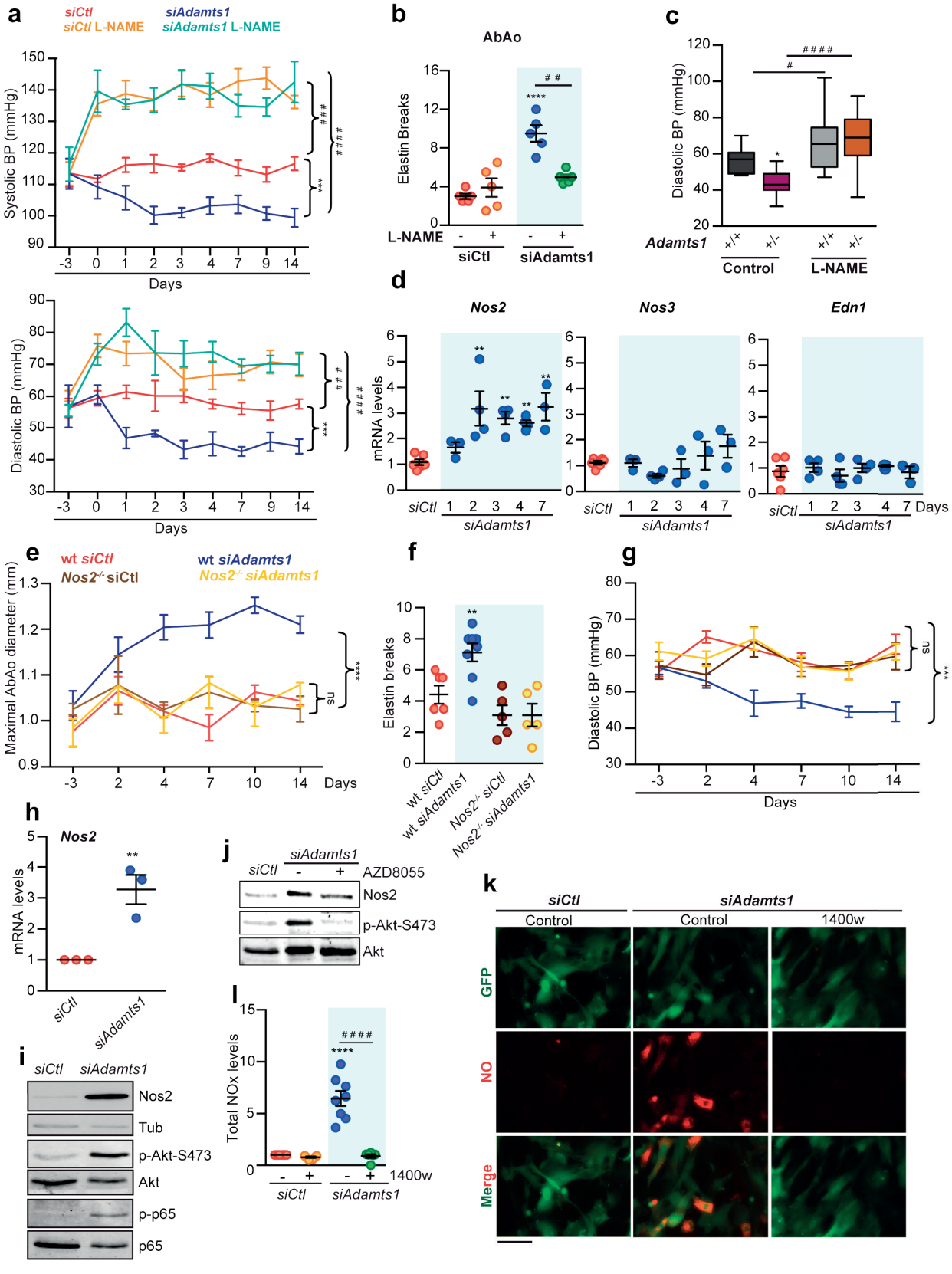

Supplementary Figure 5

Supplementary Figure 5. The Akt-Nos2 pathway mediate the aortic disease triggered by Adamts1 deficiency. (a) Systolic and diastolic BP at the indicated times in *siCtl*- and *siAdamts1*-transduced mice treated with L-NAME as indicated (mean±SEM; n=5 for each group). Repeated measurements two-way ANOVA of group means, ***p<0.001; ###p<0.001, ####p<0.0001 control vs L-NAME. End-of-experiment **(b)** quantification of elastin breaks in AbAo sections and (**c**) diastolic BP in the same cohort of mice shown in Fig. 4g-4h. (b,c) Two-way ANOVA, *p<0.05, ****p<0.0001 vs untreated *siCtl* or *Adamts1*$^{+/+}$ vs *Adamts1*$^{+/-}$; #p<0.05, ##p<0.01, ####p<0.0001, L-NAME vs untreated. **(d)** RT-qPCR analysis of *Nos2, Nos3* and *Edn1* mRNA expression at the indicated times in aortic extracts from *siCtl*- and *siAdamts1*-transduced mice. siCtl: *n* = 6; *siAdamts1*: the number of mice is shown in the figure. mRNA amounts were normalized to *Gapdh* expression. One-way ANOVA, **p<0.01 vs *siCtl*. **(e)** Maximal AbAo diameter (mean±SEM) at the indicated time points (same mouse cohort as Fig. 5c). **(f)** End-of-experiment quantification of elastin breaks (mean ± SEM) in the AbAo of 6 *siCtl*-treated WT mice, 8 *siAdamts1*-treated WT mice, 5 *siCtl*-treated *Nos2*$^{-/-}$ mice, and 5 *siAdamts1*-treated *Nos2*$^{-/-}$ mice. (**g**) Diastolic BP (mean ± SEM) (mouse cohort in Fig. 5f). (e,g) Repeated measurement two-way ANOVA of group means, ***p<0.001, ****p<0.0001 vs *Nos2*$^{-/-}$ *siAdamts1*; ns, non-significant. (f) Two-way ANOVA, **p<0.01 vs wt siCtl. (**h**) RT-qPCR analysis of *Nos2* mRNA in extracts form VSMCs transduced with *siCtl* or *siAdamts1* (mean ± SEM, n = 3 mice per group). Student's t-test, **p<0.01. (**i**) Representative immunoblot analysis of Nos2 (n = 4 per group), p-Akt-S473 (n=3 per group), Akt (n=3 per group), p-p65-S536 (n=3 per group), and p65 (n=3 per group) in extracts from VSMCs transduced with *siCtl* or *siAdamts1*. Tubulin (n=4 per group) was used as loading control. (**j**) Representative immunoblot analysis (n=3 per group) of Nos2, pAkt-S473, and Akt in extracts from VSMCs transduced with *siCtl* or *siAdamts1* and treated with the mTOR inhibitor AZD8055 as indicated. (**k**) Nitrites and Nitrates (total NOx) quantitation in conditioned media from VSMCs transduced with *siCtl* or *siAdamts1* and treated with the Nos2 inhibitor 1400w as indicated. 8 untreated and 6 treated *siCtl* mice, and 8 untreated and 6 treated *siAdamts1* mice. (**l**) Representative images (n=3 per group) of NO production (red), and GFP fluorescence (green) in unfixed VSMCs transduced with *siCtl* or *siAdamts1* and treated with the Nos2 inhibitor 1400w as indicated. Bar, 50 µm.

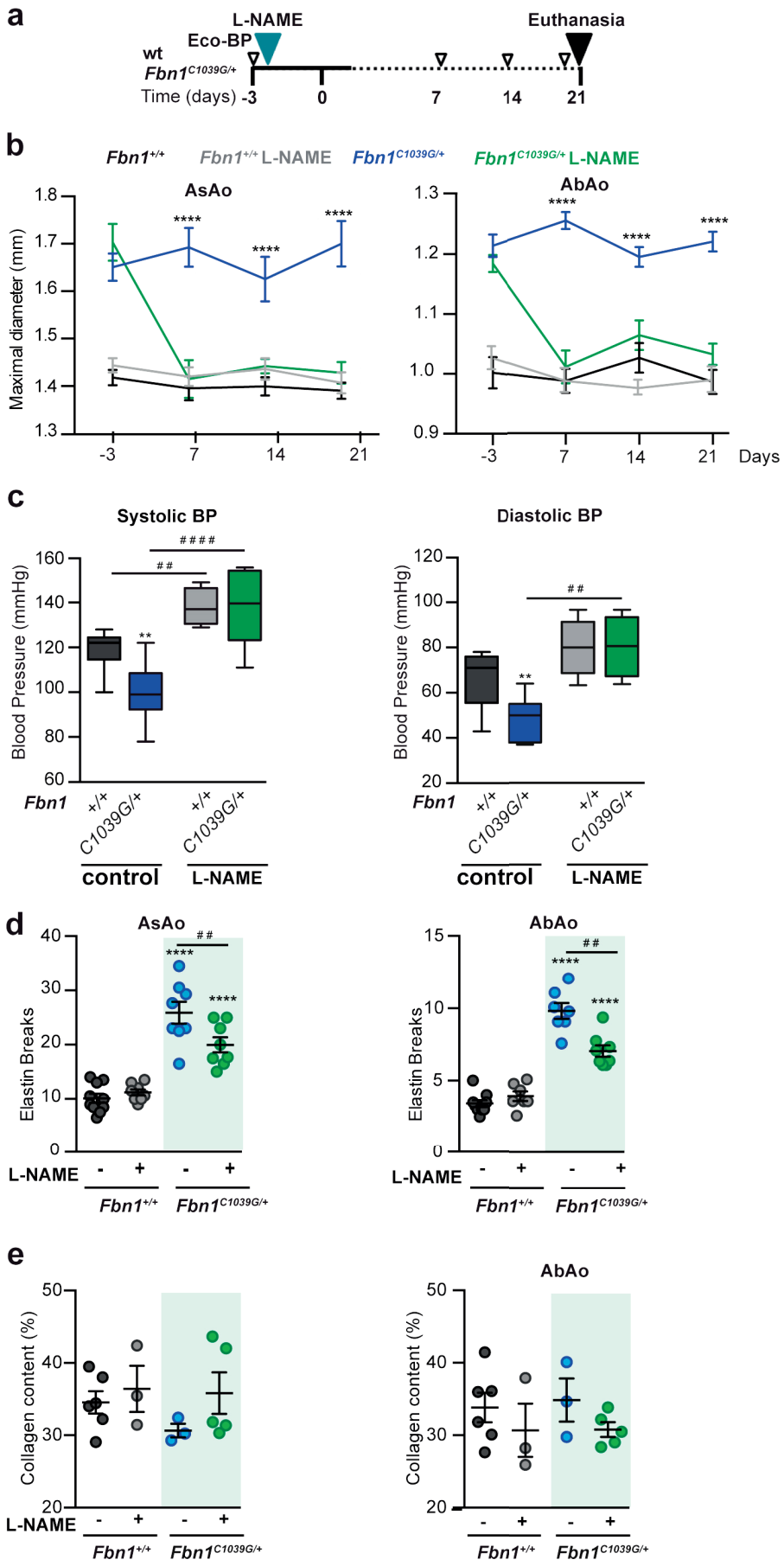

Supplementary Figure 6

Supplementary Figure 6. The L-NAME NOS inhibitor reverses aortic dilation in MFS mice despite its hypertensive effects. (a) Experimental scheme. Twelve-week-old male and female wt and *Fbn1*$^{C1039G/+}$ mice were given L-NAME in the drinking water for 21 days. Aortic dilation and BP were determined at the indicated times and before euthanasia. **(b)** Maximal AsAo and AbAo diameter (mean±SEM) at the indicated times in 9 *Fbn1*$^{+/+}$, 7 *Fbn1*$^{+/+}$ L-NAME, 8 *Fbn1*$^{C1039G/+}$, and 8 *Fbn1*$^{C1039G/+}$ L-NAME mice. Repeated measurements two-way ANOVA, ****<0.0001 vs *Fbn1*$^{C1039G/+}$ L-NAME at the same time point. End-of-experiment quantification of **(c)** systolic and diastolic BP, **(d)** elastin breaks in the AsAo and AbAo, and **(e)** collagen content in the same mice. (c and d) Same cohort of mice as in (b). (e) 6 *Fbn1*$^{+/+}$, 3 *Fbn1*$^{+/+}$ L-NAME, 3 *Fbn1*$^{C1039G/+}$, and 5 *Fbn1*$^{C1039G/+}$ L-NAME mice. (c-e) Two-way ANOVA, **p<0.01, ****p<0.0001 vs untreated *Fbn1*$^{+/+}$; ##p<0.01, ####p<0.0001 control vs L-NAME.

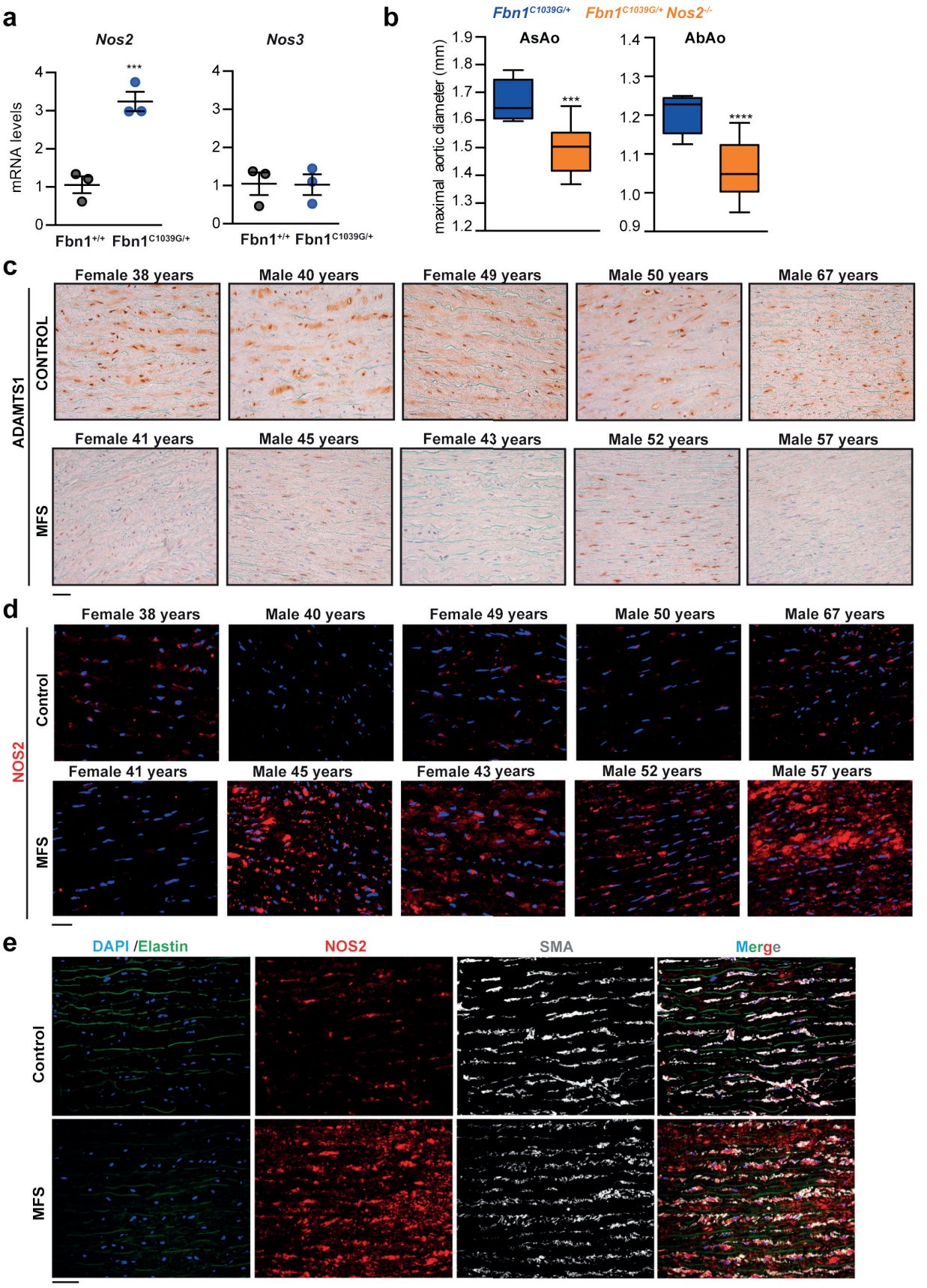

Supplementary Figure 7

Supplementary Figure 7. The ADAMTS1-NOS2 axis is deregulated in aortic samples of human MFS. (a) RT-qPCR analysis of *Nos2* and *Nos3* mRNA in aortic extracts from 3 wt and 3 *Fbn1*$^{C1039G/+}$ mice. Student's t-test, ***p<0.001. **(b)** Maximal AsAo and AbAo diameter (mean±SEM) of 8 *Fbn1*$^{C1039G/+}$ and 14 *Fbn1*$^{C1039G/+}$;*Nos2*$^{-/-}$ at 12 weeks of age. Student's t-test, ***p<0.001, ****p<0.0001. **(c)** Representative medial layer images of ADAMTS1 immunohistochemistry in aortic cross sections of human samples from 5 healthy donors and 9 MFS patients. Bar, 25 µm. **(d)** Medial layer images of NOS2 (red) immunofluorescence and DAPI-stained nuclei (blue) in sections from 5 control donors and 5 MFS patients. **(e)** Representative medial layer images of NOS2 (red) and SMA (white) immunofluorescence, elastin autofluorescence (green), and DAPI-stained nuclei (blue) in sections from 5 control donors and 8 MFS patients. Bar, 25 µm.

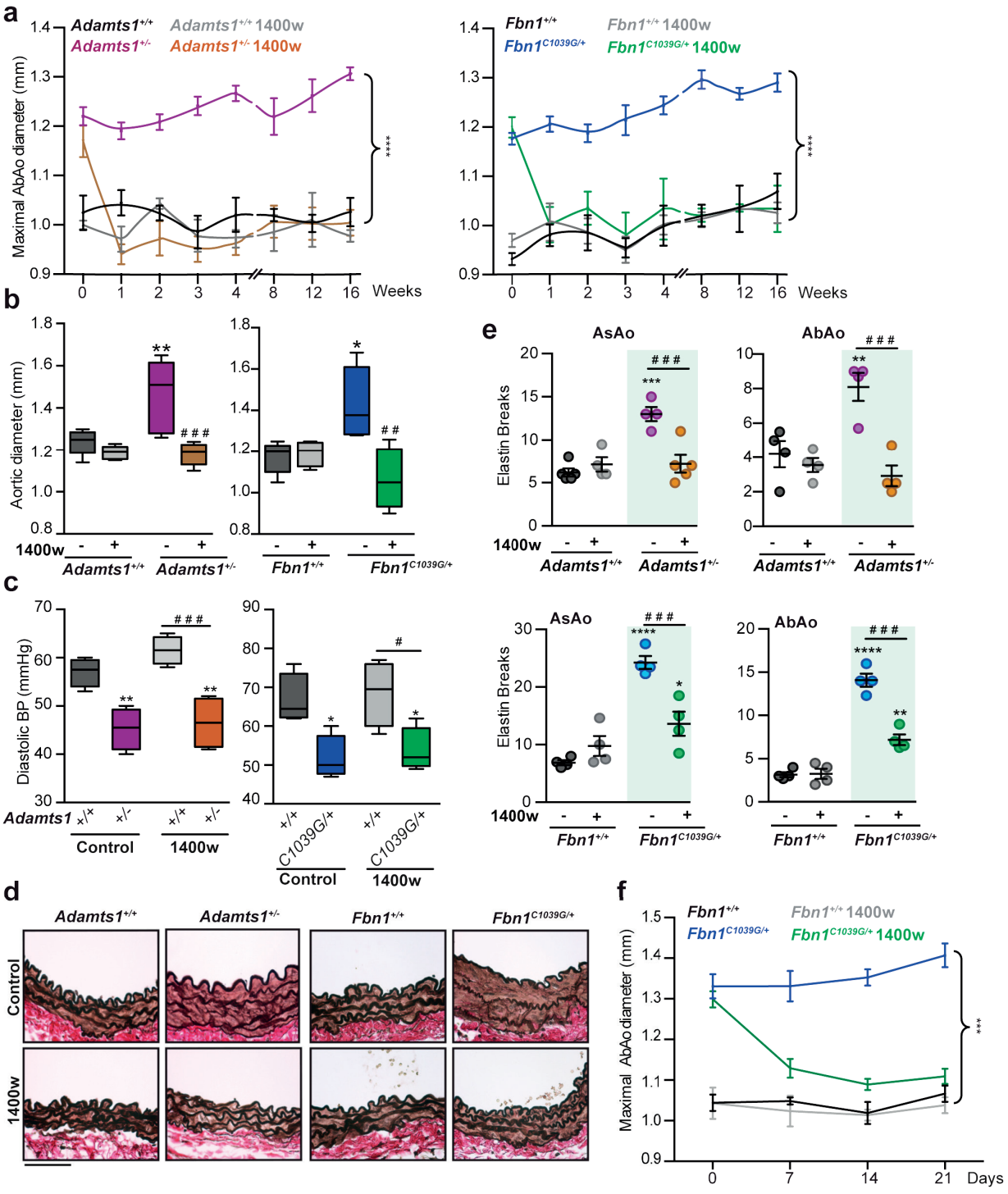

Supplementary Figure 8

Supplementary Figure 8. NOS2-specific inhibition reverses aortic pathology in Adamts1 deficient mice and in MFS model mice. (a) Maximal AbAo diameter (mean±SEM) at the indicated times in the same cohort of mice shown in Fig 6g. Repeated-measurements two-way ANOVA of group means, ****p<0.0001 vs *Adamts1*$^{+/+}$ 1400W or *Fbn1*$^{C1039G/+}$ 1400W. **(b)** End-of-experiment maximal AsAo diameter (mean±SEM) measured *ex vivo* with a digital caliper in the same animals. Two-way ANOVA, *p<0.05, **p<0.01 vs untreated wt; ##p<0.01, ###p<0.001 vs untreated *Adamts1*$^{+/+}$ or *Fbn1*$^{C1039G/+}$. **(c)** End-of-experiment quantification of diastolic BP in the same mice. Two-way ANOVA, *p<0.05, **p<0.01 vs untreated wt; #p<0.05 ###p<0.001. **(d)** Representative images from EVG staining and **(e)** quantification of elastin breaks (mean±SEM) in the same cohort of animals. Scale bar, 50μm. Two-way ANOVA, *p<0.05 **p<0.01, ***p<0.001, ****p<0.0001 vs untreated *wt*; ###p<0.001. **(f)** Maximal AbAo diameter (mean±SEM) at the indicated times in the same cohort of mice shown in Fig 6j. Repeated-measurements two-way ANOVA of group means, ***p<0.001 vs *Fbn1*$^{C1039G/+}$ 1400W.

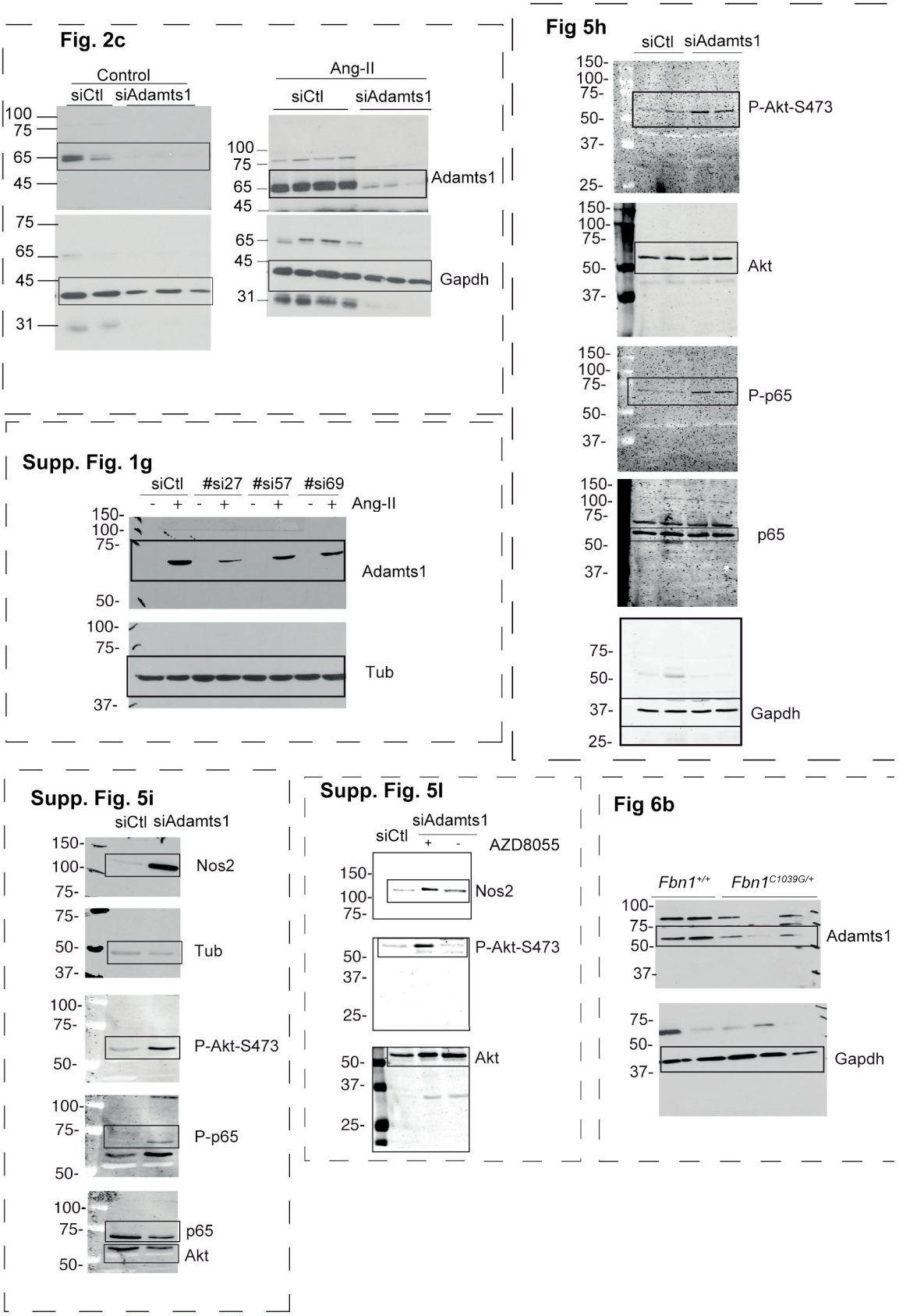

Supplementary Figure 9
Uncripped images of representative western blot images from Figures in Manuscript

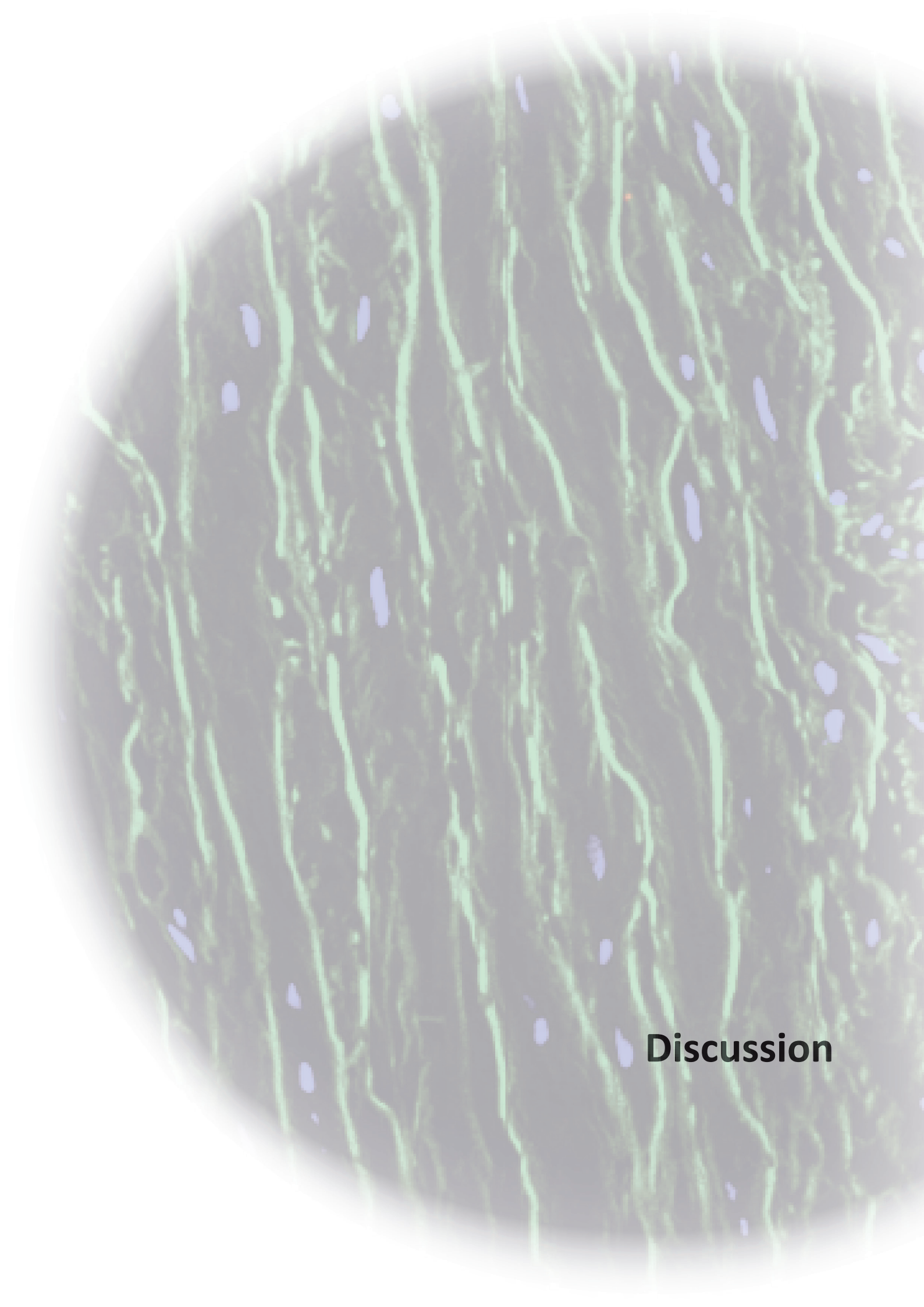

Discussion

Cardiovascular disease is the leading global cause of death, accounting for more than 17 million deaths per year, a number that is expected to grow to more than 23 million by 2030 (2015 Heart Disease and Stroke Statistics Update compiled by the AHA, CDC and NIH). The main cause underlying these pathologies is related to pathologic vascular remodeling, which eventually results in diseases such as myocardial infarction, stroke, aneurysm, congestive heart failure, atherosclerosis, coronary artery disease, peripheral vascular disease and arterial hypertension, among others.

The mediators of the arterial remodeling are not well characterized. However, the role of extracellular matrix changes in homeostasis and in vascular remodeling is well established. Thus, extracellular proteolysis is necessary to allow remodeling of the extracellular environment and cellular mobilization, in order to respond to physiological or pathological stimuli. Metalloproteases are known key factors of ECM remodeling that control maturation, degradation and assembly of the ECM components.

C/EBPβ and NFAT differentially regulate adamts1 induction by stimuli associated with vascular remodeling

Emerging evidence suggests that increased expression of the metalloproteinase Adamts1 in vascular cells and in inflammatory cells is associated with remodeling of the extracellular matrix in aortic wall diseases such as degenerative aneurysm, atherosclerosis and in pathological angiogenesis[8,153-155]. Moreover, Adamts1 expression is increased in proliferative VSMCs compared with quiescent cells[144]. In addition, previous works have reported that Adamts1 is expressed in aortic development and adult tissue[152]. Although some of these works suggested that Adamts1 might play an important role in the pathophysiology of vascular disorders, the molecular mechanisms involved in the control of *Adamts1* expression during these processes had not been established. In this work, we show that vascular expression of Adamts1 is induced by mediators of vascular remodeling, such as VEGF, Ang-II, and the pro-inflammatory cytokines IL-1β and TNF-α. We found that all of them increased Adamts1, both in ECs and in VSMCs. We have also characterized the coupling of specific signaling pathways to transcription factor activation in the regulation of *Adamts1* expression by these stimuli. Through our analysis, we have identified three major transcription factors sites within the *Adamts1* promoter that are indispensable for its up-regulation by these factors: Two novel NFAT binding sites responsible for driving Adamts1 expression in response to VEGF and a C/EBPβ binding site is necessary for Adamts1 up-regulation by IL-1β, TNF-α and Ang-II.

VEGF induces Adamts1 gene expression in a CN/NFAT dependent manner

Previous work has shown that VEGF up-regulates endothelial *Adamts1* expression in a Protein Kinase C (PKC)-dependent manner and has involved the CN-NFAT pathway in *Adamts1* gene induction by VEGF[145]. It is feasible that the increased expression of endothelial *Adamts1* triggered by VEGF requires the activation of both pathways. Accordingly, concomitant activation of CN and PKC signaling has been described during up-regulation of the endothelial proteins RCAN1.4 and Tissue Factor in activated ECs[156-158]. NFATs are transcription factors activated by CN-phosphatase activity, and are also activated by VEGF during the angiogenesis process.

In the present study we have confirmed the role for the CN-NFAT axis in the up-regulation of Adamts1 by VEGF.

To analyze this issue and to discard possible off-targets of the treatments, we have used three different methods to inhibit the CN-NFAT pathway in vascular cells: I) a pharmacological approach using Cyclosporine-A (CsA); II) transduction of ECs and VSMCs with lentiviral particles expressing the CN inhibitory peptide LxVP; III) a genetic approach using *Cnb1*-deficient mice. Moreover, we found that VEGF induces NFAT nuclear translocation *in vivo*, concomitant to Adamts1 induction in a CsA-sensitive manner. All these approaches support that CN-NFAT pathway is involved in *Adamts1* up-regulation by VEGF. Surprisingly, we have detected both, NFAT nuclear translocation and Adamts1 induction in response to VEGF, not only in the endothelial layer but also in VSMCs present in the Tunica Media. Although we cannot discard a paracrine effect on VSMCs exerted by an unidentified factor secreted by ECs, which would led to the activation of the CN/NFAT pathway and Adamts1 expression in VSMC in a secondary manner, the activation of NFAT in our system occurs briefly after VEGF administration. Furthermore, several authors have reported VEGF receptor expression in VSMCs *in vitro* and *in vivo*[159-162]. Therefore, VEGF might be also acting directly on VSMCs to promote Adamts1 expression through the CN/NFAT pathway which open the possibility that VEGF exert a crucial role of VSMCs homeostasis. Thus, VEGF pathway in VSMCs might be an important target in some vascular diseases such in the hypervascularization process in aneurysm. A detailed study of VEGF receptors expression and pathway in VSMCs should be addressed.

Our analysis of *Adamts1* promoter by luciferase assays shows two close NFAT sites. NFATs are known to activate transcription through functional co-operation with different transcription factors, however, NFAT may also bind DNA as monomers or dimers[163,164]. In fact, we have seen that Adamts1 up-regulation by VEGF requires both NFAT sites. Thus, NFAT could be operating in *Adamts1* promoter without a heterologous partner, as occurs in the case for *TNF-α* and *IL-13* promoters[164].

Adamts1 induction by Ang-II is independent of the CN/NFAT pathway activation

We have demonstrated for the first time that Ang-II induce a robust increase of the expression of Adamts1 in vascular cells *in vitro* and *in vivo*. Previously, our group has reported that Ang-II trigger the activation of the CN/NFAT pathway in vascular cells and aortic tissue[60]. Thus, we initially inferred that activation of CN/NFAT signaling could drive the transcriptional upregulation of Adamts1 by Ang-II. Indeed, we have verified that Ang-II and VEGF activate the CN-NFAT pathway in ECs. Nevertheless, the induction of *Adamts1* gene expression by Ang-II is independent to CN-NFAT pathway.

To investigate the molecular mediators involved in Adamts1 regulation by Ang-II, we have used *in silico* and luciferase analysis on *Adamts1* promoter, and found a C/EBPβ-binding site required for *Adamts1* gene expression by Ang-II. Previous reports have shown that this C/EBPβ-binding site is involved in *Adamts1* promoter induction in the progesterone receptor-mediated activation of granulosa cells[165], further supporting the relevance of C/EBPβ proteins in the regulation of *Adamts1* expression.

Adamts1 promoter contains NFAT and C/EBPβ functional binding sites

Our Chromatin Immunoprecipitation (ChIP) analysis in *Adamts1* promoter revealed the differential binding of NFATc1 upon stimulation with either VEGF or Ang-II. The involvement of specific NFAT family members in the regulation of diverse target genes has been reported and could underlie our data on the disparate role of NFAT on *Adamts1* transcriptional regulation by VEGF and Ang-II. Alternatively, differential activation kinetics or selective activation of NFATs might also account for the differential response mediated by VEGF and Ang-II. However, both factors activate all of the NFAT family members, and we cannot conclude that VEGF and Ang-II activate NFAT proteins to different extents because we have observed variability in the response to the treatments. This is probably due to variations in receptor expression among batches or passages of HUVECs. Other possibilities are that the NFAT site is occupied by other transcription factor that is released by VEGF treatment, or that an unknown factor interacts with NFAT and is differentially activated or regulated by VEGF or Ang-II.

C/EBPβ mediates the *Adamts1* induction by Ang-II, IL1β and TNF-α

Alternative translation initiation sites in the *C/EBP*β mRNA generate different protein isoforms designated as LAP (Liver-enriched Activator Protein) or LIP (Liver-enriched Inhibitor Protein). LAP contains a conserved bZIP DNA binding domain and a transactivation domain (and therefore is fully functional), whereas LIP lacks the transactivation domain and functions as a repressor. Unlike ECs, overexpression of (LIP) in VSMCs leads to a decrease in endogenous LAP expression. LIP lacks a transactivation domain that recruits the RNA-polymerase to the DNA; thus, LIP is known to impair C/EBPβ function either through competition for C/EBPβ DNA binding sites or by forming inactive heterodimers with other C/EBPs. In addition, cross talk between tyrosine kinase receptors and LAP/LIP isoforms has been described, which could act in some cases as a regulatory loop of LAP-LIP equilibrium[55-56]. Accordingly, LIP overexpression might initiate a cell-type-dependent regulatory circuit that directly or indirectly modulates LAP expression. According with the C/EBPβ and NFAT- dependent *Adamts1* up-regulation by VEGF and Ang-II, respectively, we have shown that Ang-II but not VEGF induces the phosphorylation of C/EBPβ transcription factor. Thus, it might be interesting to demonstrate target genes regulated by C/EBPβ upon Ang-II stimulation. Some of these targets might be important candidates for therapeutic intervention in cardiovascular diseases.

Cox2 and *Adamts1* promoters contain functional NFAT and C/EBPβ binding sites that are selectively regulated by VEGF and Ang-II.

We have reported that the transcriptional promoter of another target gene of VEGF and Ang-II, *Cox-2*, also contains C/EBPβ and NFAT binding sites[71]. Unlike VEGF, C/EBPβ activation is essential not only for *Adamts1* but also for *Cox-2* transcription induced by Ang-II, which is associated with functional occupancy of both C/EBPβ and NFAT-binding motifs. It is well established that the C/EBPβ and NFAT transcription factors cooperate synergistically for DNA binding and gene activation[166,167]. Because the C/EBPβ and NFAT binding sites are in close proximity in the *Cox-2* promoter[71], both factors could hypothetically cooperate

in *Cox-2* induction by Ang-II, as suggested by our functional data. In contrast, C/EBPβ could drive *Adamts1* transcription in response to Ang-II without functional cooperation with NFAT, which, would operate in a partner-independent manner upon VEGF activation. Hence, we hypothesize that cooperation with different partners might be responsible for the differential regulation of the *Adamts1* and *Cox2* promoters by the NFAT and C/EBPβ transcription factors

In summary, **the data included in the Molecular Cell Biology paper** characterize the molecular mechanisms involved in the transcriptional regulation of *Adamts1* in vascular cells by different stimuli involved in vascular wall remodeling. As the role of metalloproteinase Adamts1 in vascular homeostasis and disease remained unknown, we decided to characterize this role using different mouse models of *Adamts1* deficiency.

Nitric oxide mediates aortic disease in mice deficient in the metalloprotease Adamts1 and in a mouse model of Marfan syndrome.

To unveil the role of Adamts1 in vascular wall homeostasis and disease, we initially used an animal model, *Adamts1*-deficient mice from The European Mouse Mutant Archive (EMMA). There is considerable evidence implicating a role for Ang-II in aneurysmal formation[60]. Previously, we have described that Adamts1 levels are up-regulated by Ang-II. As Ang-II is an important inducer of aortic disease, and Adamts1 levels are up-regulated by Ang-II; we therefore hypothesized that ADAMTS1 was an important mediator of Ang-II induced aortic disease. However, partial *Adamts1* deficiency, far from protecting the aortic wall, caused its pathological remodeling, indicating a homeostatic role for Adamts1.

Induction of syndromic TAA by Adamts1 deficiency

However, we were not able to analyze in depth the aortic phenotype of *Adamts1*-null mice because their extremely high perinatal lethality. Previous works have reported impairment of the fertility of *Adatms1*$^{-/-}$ females, severe kidney defects, and severe perinatal lethality[200]. Nevertheless, these previous reports did not report any vascular defects. In contrast, our targeted-mice have a stronger phenotype because we found mild hydronephrosis in heterozygous animals, totally infertility of *Adatms1*$^{-/-}$ females and almost totally perinatal lethality in null mice. Although we have not yet investigated the cause of *Adamts1*$^{-/-}$ mice death, the aortic defects found in heterozygous mice suggest that it might be related to with cardiovascular events. The phenotypic differences between our targeted-mice and the reported previously might account for the different genetic backgrounds, because, in previous studies, a mixed background was used instead of pure C57BL/6.

We found that the kidneys of our *Adamts1*$^{+/-}$ mice had an enlarged caliceal space, indicative of hydronephrosis. However, levels of urea and creatinine in the plasma were similar in both wild type and *Adamts1*$^{+/-}$ mice, suggesting that renal function was not compromised. The presence of renal abnormalities raised the possibility that the aortic pathology induced by *Adamts1* deficiency might be syndromic. Syndromic aortic features in humans and mice, including MFS, involving alterations of both the lungs and the skeleton[168-170]. Indeed, examination of *Adamts1*$^{+/-}$ mice revealed a marked increase in distal airspace caliber, characteristic of emphysema, kyphosis (associated with increased anteroposterior and transverse

diameters of the chest) and long bones. Therefore, these data indicates that Adamts1 plays an important role in homeostasis of vascular, renal, skeletal and respiratory systems. In conclusion, *Adamts1* deficiency results in a syndromic aortopathy similar to MFS.

ADAMTS1 belongs to the ADAMTS family of secreted metalloproteases that comprises 19 members in mammals.

As summarized in the introduction, recent studies have involved several ADAMTSs and members of the structurally related ADAMTS–like (ADAMTSL) family members in microfiber formation. As microfibrils regulate bioavailability of TGFβ, a role for these genes in the regulation of TGFβ signaling has been suggested[15,125]. Moreover, it has been described that Adamts1 is able to release active-TGFβ by digestion of latent-TGFβ[171]. Indeed, mutations in ADAMTS/ADAMTSL family members have been described as causative of connective tissue disorders without aortic phenotype that yield features related to those produced by mutations in *FBN1*, the major component of tissue microfibrils[121]. This is the case of mutations in *ADAMTS10* and *ADAMTS17*, which cause the Weill-Marchesani syndrome (WMS), and mutations in *ADAMTSL2* and *ADAMTSL4*, that are involved in Geleophysic Dysplasia (GD) and *ectopia lentis*, respectively[15,121,125]. The fact that these mutations recapitulate the phenotype of diseases caused by mutations in certain residues of *FBN1* suggests that the interaction of these ADAMTS proteins with fibrilins may play a major functional regulatory role in connective tissue homeostasis. In this context, it is important to note that we have found that ADAMTS1 protein expression, but not mRNA, is strongly reduced in human and mouse samples of Marfan syndrome. In view of these results, it is tempting to speculate that ADAMTS1 (or some of its substrates) may interact with FBN1 at functional domains of FBN1 whose structural disruption by mutation results in MFS. In fact, some PGs such as Versican and Brevican, which are Adamts1 substrates, are part of the microfibers network[172]. Thus, a defective interaction between ADAMTS1 and FBN1 could result in ADAMTS1 destabilization and degradation. This would explain the low levels of ADAMTS1 that we have found in Marfan samples and that *Adamts1*$^{+/-}$ and Marfan mice share pathological features.

Knocking-Down the aortic wall via lentiviral vectors encoding siRNAs

Our group has been previously reported that the tropism of lentiviruses is dependent on the route of administration and that when systemically injected into the jugular vein, the aortic wall becomes efficiently and steadily/unceasingly transduced[33,173]. Here, by using a lentivirus encoding an *Adamts1* siRNA (Si-*Adamts1*), we achieved a long-term silencing of the protein throughout the aorta that rendered Adamts1 levels even lower than those observed in *Adamts1*$^{+/-}$ mice. Hence, this approach might be an excellent alternative to the use of genomically modified mice for the analysis of genes expressed in the vascular wall. It is much faster and easier to generate the viruses and perform the experiments than genomic editing; it can be used in mice with various genetic deficiencies or background, therefore avoiding laborious and time-consuming breeding with other genetically modified mice and/or backcrossing; and it allows the study of genes whose deletion causes embryonic lethality. In addition, *in vivo* silencing with lentiviral vectors avoids the potential misinterpretation due to phenotypes that can be indirectly induced in conventional knockout mice to compensate the absence or haploinsufficiency of a given gene during development. A potential disadvantage of the in vivo silencing by lentiviral infection is that the viruses may

infect cell others than those of the vascular wall. Although most part of the signal from transduced cells (GFP^+) is found in the vascular wall when mice are infected via intrajugular delivery, we have also detected low levels of GFP expression in liver, lung and spleen. It is thus formally possible that Adamts1 expression in cells of other tissues could be altered and indirectly affect the vascular wall. Nevertheless, it is important to note that the silencing model results in phenotypic changes and symptoms that are indistinguishable of those displayed by *Adamts1*$^{+/-}$ mice. Another important experimental benefit of silencing lentiviruses is the possibility to time gene targeting. Although conditional knock-out mice might also enable a timely controlled gene deletion, it would require the simultaneous use of several specific drivers for the three major cell types infected in the vascular wall and this, in practical terms, it would not be viable. In contrast, one single lentivirus type transduces and knocks-down gene expression in all cells of the vascular wall.

Aortic dilation induced by Adamts1 deficiency is rapid and independent of TGFβ and Ang-II pathways.

Timed knockdown might facilitate or provide a unique model for studying the mediators and the etiology of aortic disorders. Indeed, *Adamts1* silencing *in vivo* has enabled us to define sequential pathological events leading to aortic disease. Adamts1 knockdown was very fast and so was its induced phenotype, starting to occur within 1-2 days after lentivirus inoculation. The earliest effect that we have observed is a blood pressure drop that occurs as soon as the silencing is detected. Hypotension is followed immediately by elastolysis and aortic dilation (2-3 days after inoculation) whereas the TGFβ pathway is progressively activated, starting 1-2 weeks after lentiviral infection. These results therefore suggest that the onset of aortic disease is independent of the TGFβ signaling pathway. The paradigm in FTAAD field, is that both, TGFβ and Ang-II signaling pathways mediates the medial degeneration in the aortic wall, in syndromic and non-syndromic diseases[21,169]. To date, there is no published data highlighting specific mechanistic insights between mutated FBN1 and Ang-II in both MFS models and patients. However, since *FBN1* mutations determine a perturbation of ECM that protects cells from blood pressure stress, it is conceivable that, in MFS, cells sense an altered shear stress, which directly activates AT1R independently of Ang-II[174]. However, in clinical trials losartan was not more effective at reducing the rate of aortic root enlargement than the beta-blocker atenolol, and dual therapy with atenolol produced no additional benefit[65,175]. Furthermore, we have demonstrated that an efficient blockade of the TGFβ and Ang-II pathways had no significant effect in lentiviral-mediated aortic dilation or hypotension, at least during the first two weeks after virus inoculation. Similarly, blockade of the TGFβ and Ang-II pathways failed to inhibit elastic fibers fragmentation. Since TGFβ activation has been strongly associated to fibrosis, an unexpected finding was that TGFβ neutralization also failed to inhibit collagen induction and fibrosis. Together, these results strongly support the notion that Adamts1 expression is necessary for the maintenance of vascular homeostasis, and that the aortic dilation, elastolysis, fibrosis and hypotension observed in *Adamts1*-deficient mice are independent of the TGFβ and Ang-II signaling pathways, at least during the onset of the disease. Our data do not exclude that these pathways might be relevant to sustain the disease at later stages. Nowadays, it is not clear at all if the activation of TGFβ pathway is the cause or the consequence of medial degeneration. In this regard, TGFβ neutralization also failed to inhibit aneurysm progression at the early stages of a progressively severe

form of MFS (*Fbn1*$^{mgR/mgR}$ mice), but was protective at later stages[176]. Future experiments involving FBN1 silencing in vivo will help to clarify whether the sequence of molecular events that lead to the pathological symptoms of aortic disease in *Adamts1* deficient mice also occurs in this Knock-down model which represents a Marfan mouse model of aortopathy (data not shown).

The Aortopathy induced by Adamts1 deficiency is mediated by NOS2-derived nitric oxide

The extremely rapid hypotensive response of mice upon *Adamts1* silencing led us to hypothesize that NO, a major vasodilator and hypotensive agent, might be involved in the aetiology of the aortic disease. In this regard, we detected increased NOS activity in aortic sections of *si-Adamts1* mice after virus administration and found that NOS inhibition blocked aortic dilation, reduced elastolysis and ameliorated wall fibrosis in *Adamts1* silenced mice. In addition, NOS inhibition also had a therapeutic effect since it reverted aortic dilation and medial degeneration in *Adamts1*$^{+/-}$ and Marfan mice. Although hypertension is considered a risk factor in AA, we found that l-NAME administration was able to reverse aortic dilation in *Adamts1*$^{+/-}$ and MFS mice despite its hypertensive effects. Reversal of dilation by l-NAME treatment was remarkably fast: as it was complete in one week. Elastic fiber integrity and collagen deposition in *Adamts1*$^{+/-}$ mice returned to normal levels three weeks after l-NAME administration, suggesting that NO inhibition leads to activation of mechanisms for collagen clearance from the aortic wall and induction of elastin synthesis. Remarkably, using a specific NOS2 inhibitor (1400w) we observed a similar effect in both animals models, indicating a major role for NOS2 in the aortic pathology.

NO is a critical regulator of smooth muscle cell contractility. Therefore, in view of the rapid dilation observed after Adamts1 knockdown, and the rapid regression of aortic diameter exerted by NO inhibitors, we propose that the aortic dilation observed is strongly dependent on smooth muscle cell contractility, and that structural changes in the aorta may be a secondary consequence of dysregulation of the contractility. Our results suggest that increased NO production is a primary trigger of aortic disease and that increased NO levels are also required for disease maintenance. Short-term treatment with NO donors, such as those used to treat angina, is unlikely to cause aortic damage; however, our findings indicate the need for caution in implementing long-term treatment with NO donors or with gene-therapy-augmented NOS expression.

The rapid restoration of histologic features by NO inhibitors indicates that the aortic wall is highly plastic, at least in young animals. The restoration of the collagen deposition and elastin breaks occurs only three weeks after treatment with NOS inhibitors. The increase of collagen deposition in aorta might be explained as a response of the wall that increase stiffness to compensate the loss of elasticity. We have treated relatively older mice (seven-months-old), and find a similar kinetics of dilatation reversion than that observed in younger mice. However, we do not know whether this also occurs in older mice (>1.5 years old) which have a severe aortic dilation, aortic insufficiency and cardiomyopathy[177]. Future experiment will be required to clarify these issues.

A critical role for Nitric Oxide in TAAD

Recent reports are consistent with a major role for NO in FTAAD. Guo *et al.* in 2013 have shown that gain-of-function mutations in *PRKG* (which encodes *PKG1*, a downstream target of NO, are present in four families affected by TAAD[32]. Increased PKG1 activity was shown to promote activation of the myosin regulatory light chain phosphatase and Ca^{2+} pumps. Moreover, SMAD3 deficient mice, a mouse model that recapitulates the syndromic form of LDS, including early-onset osteoarthritis in humans; show an increase of NOS2 and NO levels in aortic wall. In this model, NOS2 inhibitors prevent the aortic aneurysm and dissections after Ang-II administration[179], thus suggesting that NO might be also an essential factor in FTAAD. Moreover, a critical role of the NO signaling pathway in maintaining VSMC contractility is consistent with the association of FTAAD with mutations in other genes involved in the structural and functional regulation of the VSMC contractile unit, including genes encoding aortic *Smooth Muscle Actin* (*ACTA2*), *Myosin Heavy Chain 11* (*MYH11*) and *Myosin Light Chain Kinase* (*MYLK*)[180]. It will be important to determine whether dysregulation of the NO pathway also contributes to the aortic disease associated with these mutations.

We found that both, Mmp9 activation and elastin fragmentation in the aorta of *Adamts1*-knockdown mice were sensitive to NOS inhibition, suggesting that increased NO levels induce Mmp9-dependent elastin fragmentation and initiate medial degeneration. Although we cannot exclude the involvement of other proteinases in the elastolysis of pathological aortic dilation, Mmp9 is an important elastolytic metalloproteinase and a target of NO regulation[102,103]. Early activation of Mmp9, but not Mmp2, occurred after Adamts1 silencing, a pattern of metalloproteinase activation characteristic of infiltrating macrophages in aortic dissection[181]. However, because we found that Mmp9 is expressed in the medial layer by VSMCs and that macrophages are almost absent from this layer, we propose that VSMCs are a major source of Mmp9 in this context. These results are consistent with previous findings showing that inflammatory cells are scarce in aortas of patients with MFS[14,182]. Indeed, inflammation has been documented in only a small number of cases of human TAA[183,184]. In this sense, it is important to note that degenerative and inherited aneurysms are two different diseases distinguished by their different histological properties and etiologies[185]. The most common form of degenerative aneurysm is abdominal aortic aneurysm (AAA). It is typically associated with advanced age, atherosclerosis, hypertension and diabetes. These lesions are pathologically characterized by atheromata, invasion of inflammatory cells, destructive extracellular matrix remodeling, depletion and dysfunction of VSMCs. Unlike AAA, inherited-aneurysms locate more frequently in thoracic aorta, occur in all age groups, remarkably in younger patients, are associated with hereditary influences and do not show association with cardiovascular risk factors. Pathologically, inherited forms of TAAD typically show destructive matrix remodeling with elastin fragmentation, proliferation of VSMCs and a less prominent inflammatory component without atheromata. Nevertheless, two reports that found high ADAMTS1 levels in the aorta of patients with degenerative-TAA also found inflammatory cells to be present in the vessel wall[151,186] and high levels of ADAMTS1 were found in macrophages and neutrophils[186]. It seems likely that syndromic TAAD and inflammatory TAAD are associated with low and high ADAMTS1 levels, respectively, and are mechanistically distinct.

Adamts1 substrates and medial degeneration in TAAD

Several substrates, mainly PGs such as Aggrecan, Versican, Syndecan 4, Semaphorin 3C, Nidogens Thrombospondin-1 and Desmocollin 3, are proteolytically degraded by ADAMTS1 and are therefore candidate mediators of its vascular homeostatic functions[187]. Indeed, the accumulation of PGs is a key feature of medial degeneration in FTAAD[38]. The accumulation of any of these substrates in *Adamts1*-deficient tissues might contribute to the pathogenesis caused by Adamts1 insufficiency. Indeed, high levels of Syndecan-4 lead to activation of Akt, a kinase known to activate NF-κB[188]. Akt and NF-κB are known mediators of NOS2 induction[189,190], and we found that the residue that Akt is phosphorylated by Mammalian Target of Rapamycin Comoplex-2 (mTOR2). Both, Akt and NF-κB are activated early after *Adamts1* knockdown in both aortic tissue and cultured VSMCs, concomitantly with Nos2 induction. We therefore propose that Akt and NF-κB could mediate Nos2 induction elicited by *Adamts1*-insufficiency. Consistently, we found that pharmacological inhibition of mTOR2–Akt- in *Adamts1*$^{+/-}$ mice rapidly decreased Nos2 levels and NO production in the aortic wall and regressed aortic dilation. Moreover, it has been previously described that Rapamycin, mTOR inhibitor, improves aortic phenotype in a murine model of LDS[191]. Although mTOR–Akt inhibitors could be considered as alternative therapeutic agents for the treatment of aortic dilation, mTOR and Akt are upstream components of many signaling pathways, including those regulating cell survival[192]. Therefore, they might affect other tissues and organs with putative side effects. Thus, further analysis of the long-term effects of such inhibitors will be required before considering them as therapeutic agents for chronic treatments in aortic diseases.

Roles of NOS2 and NOS3 in pathological vascular wall remodeling.

NOS2 and NOS3 have been previously involved in aortic dilation and in mouse models of cerebral and abdominal aneurysm development, but the reports have provided contradictory data when different experimental approaches (pharmacological inhibition vs genetic targeted deletion) and mouse models were used. Even contradictory data have been obtained using similar experimental approaches and mouse models. Thus, disparate reports have shown either inhibitory or stimulatory roles of Nos2 and Nos3 in AAA models[91-94,193]. In several reports, Nos3 has been considered as a vasculoprotective source of NO, whereas Nos2, produced by VSMCs and inflammatory cells, has been associated with aneurysm formation[91,93,194]. However, Nos2 deficient mice have also been reported to develop aneurysms similarly to control littermates upon elastase perfusion[94]. Likewise, contrasting results have been shown that Nos2 is critical or dispensable in studies of cerebral aneurysm, using pharmacological inhibitors, Nos2 has been reported to be critical for its development, whereas another study showed that *Nos2*$^{-/-}$ mice have similar incidence in cerebral aneurysm development than wild-type mice[195,196.] In contrast, our studies using a pharmacological inhibitor offered results that were consistent with those found employing a genetic approach. Thus, L-NAME and 1400w inhibits aortic dilation in *Adamts1*-deficient mice and *Nos2*$^{-/-}$ mice are resistant to develop aortopathy following lentiviral-mediated *Adamts1* silencing. Of note *Nos2* mRNA is induced as early as two days upon si-*Adamts1* lentiviral inoculation and *Adamts1* silencing failed to increase NO production in the aortic wall of *Nos2*$^{-/-}$ mice. It is important to note that inducible NOS2 is not

normally expressed in resting cells, but once is induced, it is continually active independently of calcium concentrations[79]. Although the precise mechanisms leading to NO production in *Adamts1* deficient mice remain to be clarified, it appears that the activation of Nos2 is a common process in diseases that occur with aortic dilation. We show here that levels of Nos2 protein in *Adamts1* silenced mice and in *Adamts1*$^{+/-}$ and Marfan mice are high, where other reports have involved Nos2 even in elastase-induced abdominal aortic dilation. More importantly, we have found that NOS2 protein levels are up-regulated in aortic sections of MFS patients. Together, the results support that the NOS2 mediated NO production plays an essential role in different aortic diseases.

NOS2 inhibitors as alternative treatments for aortic disorders

Although L-NAME is a general inhibitor of all three NOS and its chronic use causes hypertension and cardiac hypertrophy in rodents. Thus, alternatively specific NOS2 inhibitors may represent promising agents for the treatment of aortic diseases. The Nos2 inhibitor 1400W was equally effective in young and relatively old MFS mice, suggesting that Nos2 mediates not only disease initiation, but also later disease progression. Considering that NOS2 inhibitors have been safely used in clinical trials for endotoxemia, rheumatoid arthritis and migraine, our results point to NOS2-specific inhibitors as a promising alternative for the treatment of aortic disease that could be implemented with minimal delay[182]. However, it is clear that expectations derived to translate therapeutic strategies from the mouse to the human disease have to be cautiously considered, and potential future trials might be carefully designed and developed. Our results, however, encourage the use of pharmacological strategies directed to interfere with signaling components of the NO pathway in preclinical and clinical trials, including NOS inhibitors, which could be candidates for therapeutic intervention in aortic diseases and particularly in MFS patients.

In conclusion, **the data presented in the Nature Medicine paper**, identify a novel and essential pathway that is activated in the pathogenesis of MFS, and also, allows the identification and characterization of a new aorthopathy triggered by *Adamts1* deficiency. These two aortic diseases are mechanistically linked, as MFS mice and human patients display *Adamts1* deficiency. Indeed, we speculate that the aortic phenotype of MFS may be partially or completely due to *Adamts1* deficiency. Future experiments will be important to determine whether NO up-regulation is also essential in the pathogenesis of other syndromic and no syndromic diseases that occur with aortic dilation and medial degeneration, and preclinical and clinical trial will clarify whether NO inhibitors prevent and/or reverse the disease in patients.

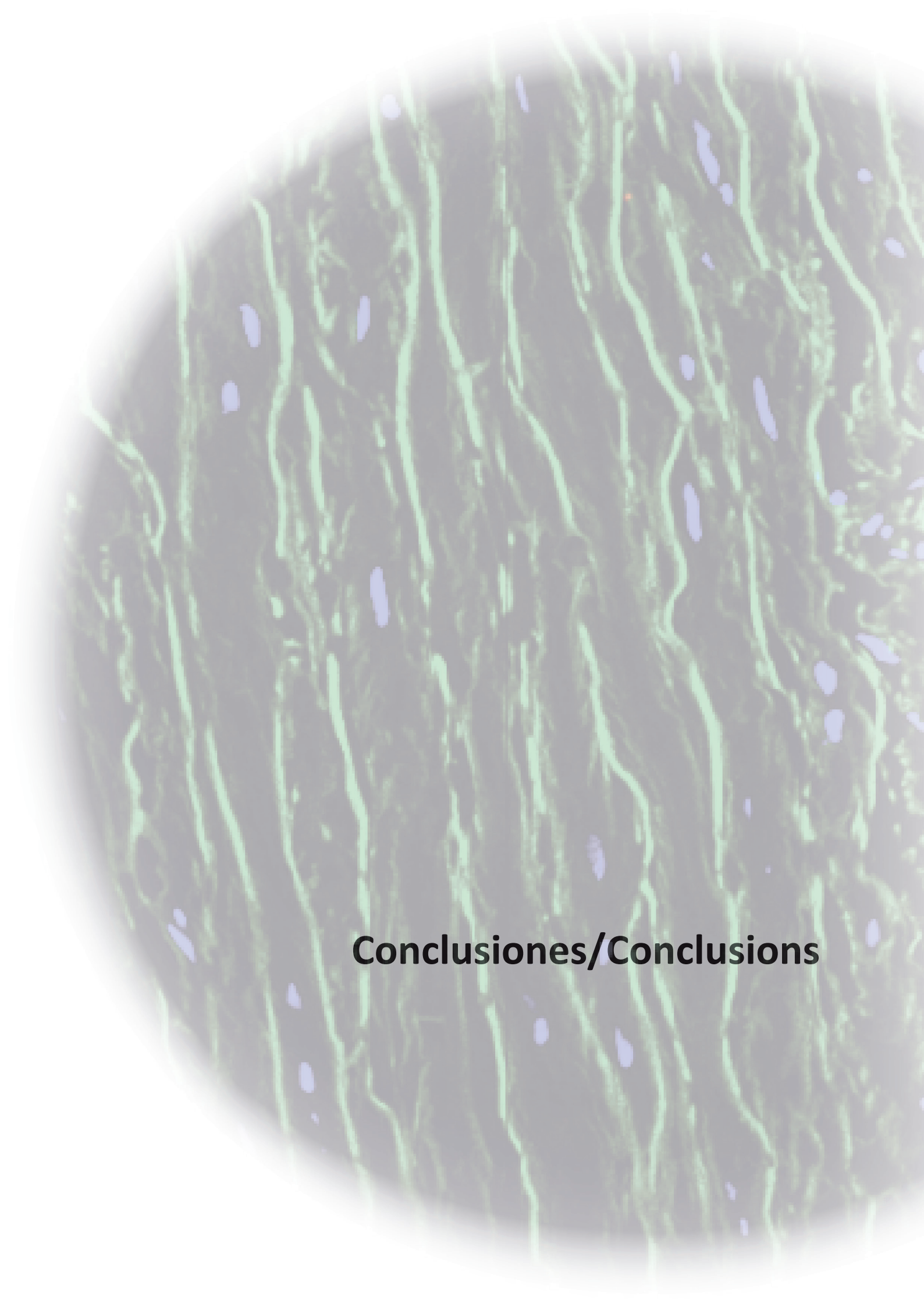

Conclusiones/Conclusions

En este trabajo de tesis hemos descrito los mediadores moleculares, de células endoteliales y células de músculo liso (VSMCs), que regulan la transcripción de *Adamts1* inducida por distintos agentes implicados en el remodelado de la pared vascular.

Por otra parte, hemos demostrado que la deficiencia en la metaloproteasa *Adamts1* produce una enfermedad aórtica en ratón debido a un aumento sostenido en la producción de NO mediado por NOS2. Estos resultados están mecanísticamente relacionados con el Síndrome de Marfan (MFS), ya que tanto la expresión reducida de Adamts1 como el incremento de NOS2 tienen lugar en pacientes como en ratones con MFS. Además la inhibición de Nos2, no solo previene, sino que también revierte la patología aórtica de los ratones Marfan.

Concretamente, estos resultados han permitido obtener las siguientes **conclusiones experimentales**:

1. VEGF, Ang-II y las citoquinas pro-inflamatorias IL-1β y TNF-α inducen la expresión de *Adamts1* en células vasculares. Diferentes vías de transducción de señales regulan la expresión de *Adamts1* independientemente del tipo celular.
2. La expresión de Adamts1 en respuesta a la estimulación con VEGF o Ang-II se regula mediante los factores de transcripción NFAT y C/EBPβ, que se unen diferencialmente al promotor de *Adamts1*. Si bien la ruta de CN-NFAT se activa tanto por VEGF como por Ang-II, solo la inducción de Adamts1 por VEGF se regula por la ruta CN-NFAT.
3. Ang-II y las citoquinas proinflamatorias IL-1β y TNF-α regulan la expresión génica de Adamts1 de manera dependiente de C/EBPβ. Estas citoquinas inducen la fosforilación de C/EBPβ y su unión al promotor de Adamts1.
4. Adamts1 es fundamental para la homeostasis en modelos de ratón, ya que su ausencia total produce alta mortalidad y su deficiencia parcial da lugar a alteraciones en el sistema vascular, óseo, pulmonar y renal.
5. Los ratones haploinsuficientes en *Adamts1* desarrollan características sindrómicas como son: dilatación aórtica, formación de aneurismas y disecciones aórticas inducidas por Ang-II, degeneración de la capa Media vascular, incremento de la longitud de los huesos de las extremidades, ensanchamiento de la caja torácica, hipercifosis, enfisema pulmonar periférico e hidronefrosis.
6. La dilatación aórtica ocurre rápidamente, solo tres días después del silenciamiento de *Adamts1*, y es independiente de las rutas de señalización de TGFβ y Ang-II.
7. La aortopatía de los ratones deficientes en *Adamts1* y la de los ratones Marfan analizados son dependientes de NO.
8. El incremento de NO observado en ratones deficientes en *Adamts1* tiene su origen en la alta expresión de NOS2 en las células de músculo liso vascular. Esta expresión es dependiente de la activación de la ruta de mTOR2/AKT.

9. En pacientes con Síndrome de Marfan, los niveles de expresión de Adamts1 en aorta están reducidos y los de NOS2 elevados. Esto también ocurre en el modelo múrido de Marfan basado en ratones *Knock-in* para *Fbn1*.
10. Inhibidores de la actividad enzimática de NOS y NOS2 disminuyen la dilatación aórtica y restablecen la estructura normal de la Túnica Media en los modelos de ratón de Marfan y en los ratones deficientes en *Adamts1*.

In this work, we have described the molecular mediators involved in the transcription of *Adamts1* in a vascular remodeling context, in endothelial cells and in Vascular Smooth Muscle Cells (VSMCs).

Moreover, we have demonstrated that *Adamts1*-deficiency in mice causes an aortic disease, due to a sustained increase in NO production mediated by NOS2. These results are mechanistically related to Marfan Syndrome (MFS), since both, in MFS and *Adamts1*-deficient mice, show a reduced expression of Adamts1 and an increased NOS2. Finally we have demonstrated that inhibition of Nos2 not only prevents, but also reverses, aortic pathology of Marfan mice.

Specifically, the results obtained suggest the following **experimental conclusions**:

1. VEGF, Ang-II and pro-inflammatory cytokines IL-1β and TNF-α induce the expression of *Adamts1* in vascular cells. Different molecular pathways regulate the expression of *Adamts1* independently of the cell type.
2. Expression of *Adamts1* in response to stimulation with VEGF or Ang-II is regulated by the transcription factors NFAT and C/EBPβ that differentially bind to the *Adamts1* promoter. Although the CN-NFAT pathway is activated by both, VEGF and Ang-II, only the induction of Adamts1 by VEGF is regulated by the CN-NFAT pathway.
3. Ang-II and the proinflammatory cytokines IL-1β and TNF-α regulate Adamts1 gene expression in a C/EBPβ-dependent manner. These cytokines induce C/EBPβ phosphorylation and its binding to the Adamts1 promoter.
4. Adamts1 is fundamental in homeostasis in mouse models, since its total absence produces high mortality and its partial deficiency results in alterations in the vasculature, lungs, bones and kidneys.
5. *Adamts1*-deficient mice develop syndromic characteristics such as: aortic dilatation, development of aneurysms and dissections induced by Ang-II, degeneration of the Tunica Media, increased length of limb bones, enlarged thoracic cage, hyperkyphosis, pulmonary distal emphysema, and hydronephrosis.
6. Aortic dilatation occurs rapidly, only three days after *Adamts1* silencing, and is independent of the TGFβ and Ang-II signaling pathways.
7. The aortopathy in *Adamts1*-deficient mice and in Marfan mice is NO-dependent.
8. The increase in NO observed in *Adamts1*-deficient mice is dependent on the high expression of NOS2 in vascular smooth muscle cells dependent on the mTOR2/AKT pathway.
9. In Marfan Syndrome patients, the levels of Adamts1 expression in the aorta are reduced and NOS2 is elevated. This also occurs in the Marfan murine model based on mutant *Fbn1 Knock-in* mice.
10. Inhibitors of the enzymatic activity of NOS and NOS2 decrease aortic dilatation and reestablish the normal structure of the Medial Layer in Marfan mice and in *Adamts1*-deficient mice.

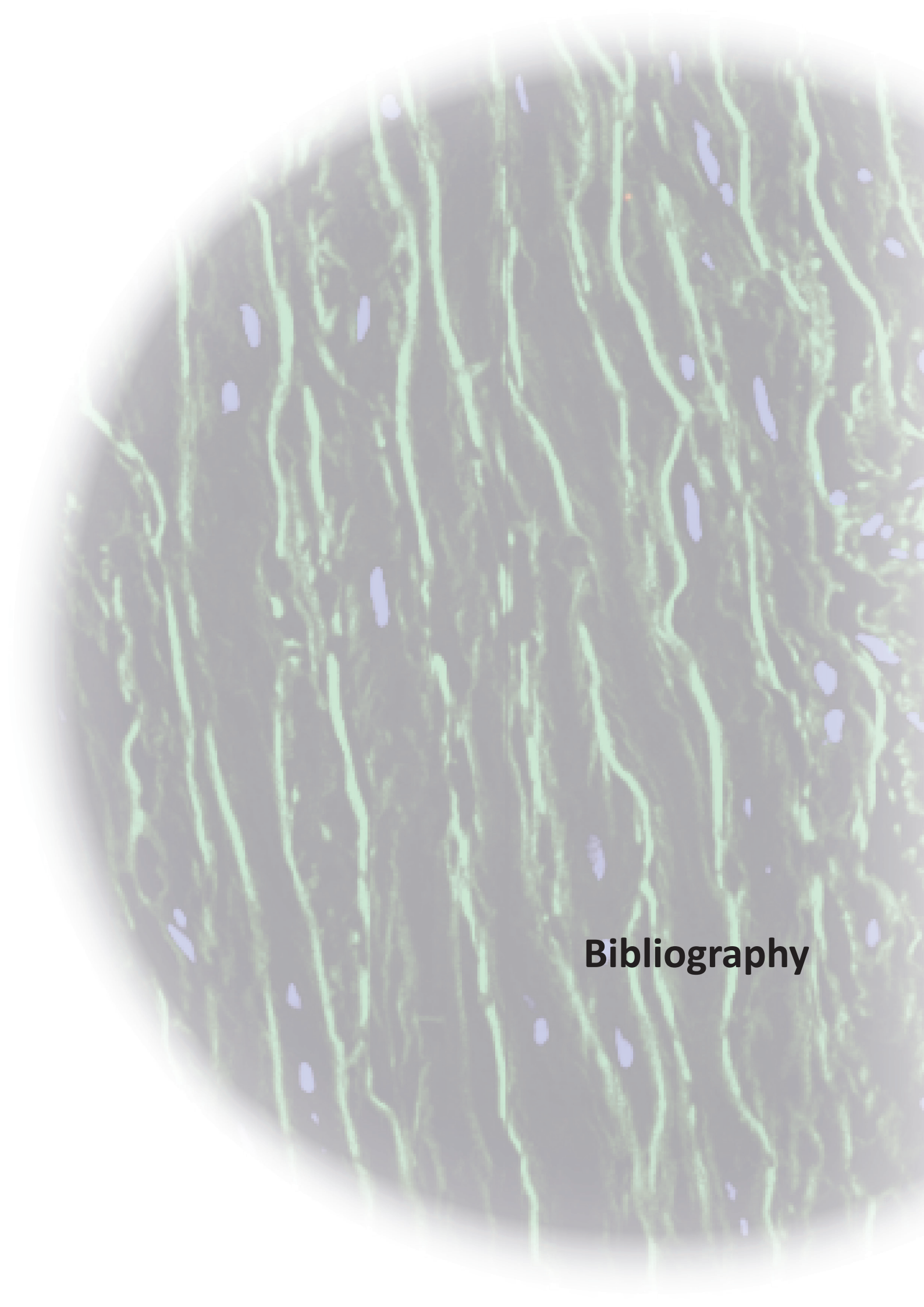

Bibliography

1. Randall, D. J., Burggren, W., French, K. & Eckert, R. Animal physiology : mechanisms and adaptations. 5th ed edn, (W. H. Freeman and Co., 2002).
2. Hill, R. W., Wyse, G. A. & Anderson, M. Animal Physiology. 3rd ed edn, (Sinauer, 2012).
3. Marieb, E. N. Essential of human anatomy & physiology. 8 ed edn, (Pearson-Benjamin Cummings, 2006).
4. Hickman, C. P., Ober, W. C. & Garrison, C. W. Integrated principles of zoology. 12th ed edn, (McGraw-Hill, 2004).
5. Paniagua Gómez-Álvarez, R. Citología e histología vegetal y animal. 4* edn, (McGraw-Hill Interamericana, 2011).
6. Baliga, R. R. et al. The role of imaging in aortic dissection and related syndromes. JACC Cardiovasc Imaging 7, 406-424, doi:10.1016/j.jcmg.2013.10.015 (2014).
7. ohnston, K. W. et al. Suggested standards for reporting on arterial aneurysms. Subcommittee on Reporting Standards for Arterial Aneurysms, Ad Hoc Committee on Reporting Standards, Society for Vascular Surgery and North American Chapter, International Society for Cardiovascular Surgery. J Vasc Surg 13, 452-458 (1991).
8. Hellenthal, F. A., Buurman, W. A., Wodzig, W. K. & Schurink, G. W. Biomarkers of abdominal aortic aneurysm progression. Part 2: inflammation. Nat Rev Cardiol 6, 543-552, doi:10.1038/nrcardio.2009.102 (2009).
9. Hellenthal, F. A., Geenen, I. L., Teijink, J. A., Heeneman, S. & Schurink, G. W. Histological features of human abdominal aortic aneurysm are not related to clinical characteristics. Cardiovasc Pathol 18, 286-293, doi:10.1016/j.carpath.2008.06.014 (2009).
10. Blanchard, J. F. Epidemiology of abdominal aortic aneurysms. Epidemiol Rev 21, 207-221 (1999).
11. Dietz, H. C. TGF-beta in the pathogenesis and prevention of disease: a matter of aneurysmic proportions. J Clin Invest 120, 403-407, doi:10.1172/JCI42014 (2010).
12. Elefteriades, J. A. & Pomianowski, P. Practical genetics of thoracic aortic aneurysm. Prog Cardiovasc Dis 56, 57-67, doi:10.1016/j.pcad.2013.06.002 (2013).
13. Gillis, E., Van Laer, L. & Loeys, B. L. Genetics of thoracic aortic aneurysm: at the crossroad of transforming growth factor-beta signaling and vascular smooth muscle cell contractility. Circ Res 113, 327-340, doi:10.1161/CIRCRESAHA.113.300675 (2013).
14. Biddinger, A., Rocklin, M., Coselli, J. & Milewicz, D. M. Familial thoracic aortic dilatations and dissections: a case control study. J Vasc Surg 25, 506-511 (1997).
15. Hoffjan, S. Genetic dissection of marfan syndrome and related connective tissue disorders: an update 2012. Mol Syndromol 3, 47-58, doi:10.1159/000339441 (2012).
16. Thatcher, S. E. TGF-beta Signaling: New Insights Into Aortic Aneurysms. EBioMedicine 12, 24-25, doi:10.1016/j.ebiom.2016.09.026 (2016).
17. van der Linde, D. et al. Aneurysm-osteoarthritis syndrome with visceral and iliac artery aneurysms. J Vasc Surg 57, 96-102, doi:10.1016/j.jvs.2012.06.107 (2013).
18. van de Laar, I. M. et al. Mutations in SMAD3 cause a syndromic form of aortic aneurysms and dissections with early-onset osteoarthritis. Nat Genet 43, 121-126, doi:10.1038/ng.744 (2011).
19. Robinson, P. N. et al. The molecular genetics of Marfan syndrome and related disorders. J Med Genet 43, 769-787, doi:10.1136/jmg.2005.039669 (2006).
20. Hu, Q. et al. Fibulin-5 mutations: mechanisms of impaired elastic fiber formation in recessive cutis laxa. Hum Mol Genet 15, 3379-3386, doi:10.1093/hmg/ddl414 (2006).
21. Loeys, B. L. et al. Aneurysm syndromes caused by mutations in the TGF-beta receptor. N Engl J Med 355, 788-798, doi:10.1056/NEJMoa055695 (2006).

22. Bolar, N., Van Laer, L. & Loeys, B. L. Marfan syndrome: from gene to therapy. Curr Opin Pediatr 24, 498-504, doi:10.1097/MOP.0b013e3283557d4c (2012).
23. El-Hamamsy, I. & Yacoub, M. H. Cellular and molecular mechanisms of thoracic aortic aneurysms. Nat Rev Cardiol 6, 771-786, doi:10.1038/nrcardio.2009.191 (2009).
24. Hucthagowder, V. et al. Fibulin-4: a novel gene for an autosomal recessive cutis laxa syndrome. Am J Hum Genet 78, 1075-1080, doi:10.1086/504304 (2006).
25. Hanada, K. et al. Perturbations of vascular homeostasis and aortic valve abnormalities in fibulin-4 deficient mice. Circ Res 100, 738-746, doi:10.1161/01.RES.0000260181.19449.95 (2007).
26. Pepin, M. G., Murray, M. L. & Byers, P. H. in GeneReviews(R) (eds R. A. Pagon et al.) (1993).
27. Cooper, T. K. et al. The haploinsufficient Col3a1 mouse as a model for vascular Ehlers-Danlos syndrome. Vet Pathol 47, 1028-1039, doi:10.1177/0300985810374842 (2010).
28. Cripe, L., Andelfinger, G., Martin, L. J., Shooner, K. & Benson, D. W. Bicuspid aortic valve is heritable. J Am Coll Cardiol 44, 138-143, doi:10.1016/j.jacc.2004.03.050 (2004).
29. Siu, S. C. & Silversides, C. K. Bicuspid aortic valve disease. J Am Coll Cardiol 55, 2789-2800, doi:10.1016/j.jacc.2009.12.068 (2010).
30. Milewicz, D. M. & Regalado, E. in GeneReviews(R) (eds R. A. Pagon et al.) (1993).
31. Milewicz, D. M. et al. De novo ACTA2 mutation causes a novel syndrome of multisystemic smooth muscle dysfunction. Am J Med Genet A 152A, 2437-2443, doi:10.1002/ajmg.a.33657 (2010).
32. Guo, D. C. et al. Recurrent gain-of-function mutation in PRKG1 causes thoracic aortic aneurysms and acute aortic dissections. Am J Hum Genet 93, 398-404, doi:10.1016/j.ajhg.2013.06.019 (2013).
33. Martin-Alonso, M. et al. Deficiency of MMP17/MT4-MMP proteolytic activity predisposes to aortic aneurysm in mice. Circ Res 117, e13-26, doi:10.1161/CIRCRESAHA.117.305108 (2015).
34. Lee, V. S. et al. Loss of function mutation in LOX causes thoracic aortic aneurysm and dissection in humans. Proc Natl Acad Sci U S A 113, 8759-8764, doi:10.1073/pnas.1601442113 (2016).
35. Meester, J. A. et al. Loss-of-function mutations in the X-linked biglycan gene cause a severe syndromic form of thoracic aortic aneurysms and dissections. Genet Med, doi:10.1038/ gim.2016.126 (2016).
36. Barbier, M. et al. MFAP5 loss-of-function mutations underscore the involvement of matrix alteration in the pathogenesis of familial thoracic aortic aneurysms and dissections. Am J Hum Genet 95, 736-743, doi:10.1016/j.ajhg.2014.10.018 (2014).
37. Regalado, E. et al. Autosomal dominant inheritance of a predisposition to thoracic aortic aneurysms and dissections and intracranial saccular aneurysms. Am J Med Genet A 155A, 2125-2130,doi:10.1002/ajmg.a.34050 (2011).
38. Milewicz, D. M. et al. Genetic basis of thoracic aortic aneurysms and dissections: focus on smooth muscle cell contractile dysfunction. Annu Rev Genomics Hum Genet 9, 283-302, doi:10.1146 /annurev.genom.8.080706.092303 (2008).
39. Renna, N. F., de Las Heras, N. & Miatello, R. M. Pathophysiology of vascular remodeling in hypertension. Int J Hypertens 2013, 808353, doi:10.1155/2013/808353 (2013).
40. Glagov, S., Weisenberg, E., Zarins, C. K., Stankunavicius, R. & Kolettis, G. J. Compensatory enlargement of human atherosclerotic coronary arteries. N Engl J Med 316, 1371-1375, doi:10.1056/NEJM198705283162204 (1987).
41. Wolf, W. C., Harley, R. A., Sluce, D., Chao, L. & Chao, J. Localization and expression of tissue kallikrein and kallistatin in human blood vessels. J Histochem Cytochem 47, 221-228 (1999).

42. Alexander, M. R. & Owens, G. K. Epigenetic control of smooth muscle cell differentiation and phenotypic switching in vascular development and disease. Annu Rev Physiol 74, 13-40, doi:10.1146/annurev-physiol-012110-142315 (2012).

43. Flamant, M. et al. Role of matrix metalloproteinases in early hypertensive vascular remodeling. Hypertension 50, 212-218, doi:10.1161/HYPERTENSIONAHA.107.089631 (2007).

44. Kuzuya, M. & Iguchi, A. Role of matrix metalloproteinases in vascular remodeling. J Atheroscler Thromb 10, 275-282 (2003).

45. Lemarie, C. A., Tharaux, P. L. & Lehoux, S. Extracellular matrix alterations in hypertensive vascular remodeling. J Mol Cell Cardiol 48, 433-439, doi:10.1016/j.yjmcc.2009.09.018 (2010).

46. van Varik, B. J. et al. Mechanisms of arterial remodeling: lessons from genetic diseases. Front Genet 3, 290, doi:10.3389/fgene.2012.00290 (2012).

47. van Varik, B. J. et al. Mechanisms of arterial remodeling: lessons from genetic diseases. Front Genet 3, 290, doi:10.3389/fgene.2012.00290 (2012).

48. Willis, A. I., Pierre-Paul, D., Sumpio, B. E. & Gahtan, V. Vascular smooth muscle cell migration: current research and clinical implications. Vasc Endovascular Surg 38, 11-23 (2004).

49. Chaudhry, S. S. et al. Fibrillin-1 regulates the bioavailability of TGFbeta1. J Cell Biol 176, 355-367, doi:10.1083/jcb.200608167 (2007).

50. Huang, F. & Chen, Y. G. Regulation of TGF-beta receptor activity. Cell Biosci 2, 9, doi:10.1186/2045-3701-2-9 (2012).

51. Gallo, E. M. et al. Angiotensin II-dependent TGF-beta signaling contributes to Loeys-Dietz syndrome vascular pathogenesis. J Clin Invest 124, 448-460, doi:10.1172/JCI69666 (2014).

52. Benke, K. et al. The role of transforming growth factor-beta in Marfan syndrome. Cardiol J 20, 227-234, doi:10.5603/CJ.2013.0066 (2013).

53. Habashi, J. P. et al. Losartan, an AT1 antagonist, prevents aortic aneurysm in a mouse model of Marfan syndrome. Science 312, 117-121, doi:10.1126/science.1124287 (2006).

54. Morissette, R. et al. Transforming growth factor-beta and inflammation in vascular (type IV) Ehlers-Danlos syndrome. Circ Cardiovasc Genet 7, 80-88, doi:10.1161/CIRCGENETICS.113.000280 (2014).

55. Hunyady, L. & Catt, K. J. Pleiotropic AT1 receptor signaling pathways mediating physiological and pathogenic actions of angiotensin II. Mol Endocrinol 20, 953-970, doi:10.1210/me.2004-0536 (2006).

56. Allen, A. M., Zhuo, J. & Mendelsohn, F. A. Localization and function of angiotensin AT1 receptors. Am J Hypertens 13, 31S-38S (2000).

57. de Gasparo, M. New basic science initiatives with the angiotensin II receptor blocker valsartan. J Renin Angiotensin Aldosterone Syst 1, S3-5, doi:10.3317/jraas.2000.052 (2000).

58. Marrero, M. B. et al. Direct stimulation of Jak/STAT pathway by the angiotensin II AT1 receptor. Nature 375, 247-250, doi:10.1038/375247a0 (1995).

59. Duff, J. L. et al. Angiotensin II signal transduction and the mitogen-activated protein kinase pathway. Cardiovasc Res 30, 511-517 (1995).

60. Touyz, R. M. & Schiffrin, E. L. Signal transduction mechanisms mediating the physiological and pathophysiological actions of angiotensin II in vascular smooth muscle cells. Pharmacol Rev 52, 639-672 (2000).

61. Esteban, V. et al. Regulator of calcineurin 1 mediates pathological vascular wall remodeling. J Exp Med 208, 2125-2139, doi:10.1084/jem.20110503 (2011).

62. Hogan, P. G., Chen, L., Nardone, J. & Rao, A. Transcriptional regulation by calcium, calcineurin, and NFAT. Genes Dev 17, 2205-2232, doi:10.1101/gad.1102703 (2003).

63. Alfranca, A., Iniguez, M. A., Fresno, M. & Redondo, J. M. Prostanoid signal transduction and gene expression in the endothelium: role in cardiovascular diseases. Cardiovasc Res 70, 446-456, doi:10.1016/j.cardiores.2005.12.020 (2006).

64. Oller, J. et al. C/EBPbeta and Nuclear Factor of Activated T Cells Differentially Regulate Adamts-1 Induction by Stimuli Associated with Vascular Remodeling. Mol Cell Biol 35, 3409-3422, doi:10.1128/MCB.00494-15 (2015).

65. Baggott, R. R. et al. Plasma membrane calcium ATPase isoform 4 inhibits vascular endothelial growth factor-mediated angiogenesis through interaction with calcineurin. Arterioscler Thromb Vasc Biol 34, 2310-2320, doi:10.1161/ATVBAHA.114.304363 (2014).

66. Lim, D. S. et al. Angiotensin II blockade reverses myocardial fibrosis in a transgenic mouse model of human hypertrophic cardiomyopathy. Circulation 103, 789-791 (2001).

67. Renard, M. et al. Novel MYH11 and ACTA2 mutations reveal a role for enhanced TGFbeta signaling in FTAAD. Int J Cardiol 165, 314-321, doi:10.1016/j.ijcard.2011.08.079 (2013).

68. Nishibe, T. et al. Expression and localization of vascular endothelial growth factor in normal abdominal aorta and abdominal aortic aneurysm. Int Angiol 29, 260-265 (2010).

69. Wolanska, M., Bankowska-Guszczyn, E., Sobolewski, K. & Kowalewski, R. Expression of VEGFs and its receptors in abdominal aortic aneurysm. Int Angiol 34, 520-528 (2015).

70. Vempati, P., Popel, A. S. & Mac Gabhann, F. Extracellular regulation of VEGF: isoforms, proteolysis, and vascular patterning. Cytokine Growth Factor Rev 25, 1-19, doi:10.1016/j.cytogfr.2013.11.002 (2014).

71. Armesilla, A. L. et al. Vascular endothelial growth factor activates nuclear factor of activated T cells in human endothelial cells: a role for tissue factor gene expression. Mol Cell Biol 19, 2032-2043 (1999).

72. Hernandez, G. L. et al. Selective inhibition of vascular endothelial growth factor-mediated angiogenesis by cyclosporin A: roles of the nuclear factor of activated T cells and cyclooxygenase 2. J Exp Med 193, 607-620 (2001).

73. Liu, D., Jia, H., Holmes, D. I., Stannard, A. & Zachary, I. Vascular endothelial growth factor-regulated gene expression in endothelial cells: KDR-mediated induction of Egr3 and the related nuclear receptors Nur77, Nurr1, and Nor1. Arterioscler Thromb Vasc Biol 23, 2002-2007, doi:10.1161/01.ATV.0000098644.03153.6F (2003).

74. Furchgott, R. F. & Zawadzki, J. V. The obligatory role of endothelial cells in the relaxation of arterial smooth muscle by acetylcholine. Nature 288, 373-376 (1980).

75. Alderton, W. K., Cooper, C. E. & Knowles, R. G. Nitric oxide synthases: structure, function and inhibition. Biochem J 357, 593-615 (2001).

76. Stuehr, D. J. Mammalian nitric oxide synthases. Biochim Biophys Acta 1411, 217-230 (1999).

77. Stuehr, D. J. & Griffith, O. W. Mammalian nitric oxide synthases. Adv Enzymol Relat Areas Mol Biol 65, 287-346 (1992).

78. Southan, G. J. & Szabo, C. Selective pharmacological inhibition of distinct nitric oxide synthase isoforms. Biochem Pharmacol 51, 383-394 (1996).

79. Pfeilschifter, J., Eberhardt, W. & Beck, K. F. Regulation of gene expression by nitric oxide. Pflugers Arch 442, 479-486 (2001).

80. Forstermann, U. & Sessa, W. C. Nitric oxide synthases: regulation and function. Eur Heart J 33, 829-837, 837a-837d, doi:10.1093/eurheartj/ehr304 (2012).

81. Chinje, E. C. & Stratford, I. J. Role of nitric oxide in growth of solid tumours: a balancing act. Essays Biochem 32, 61-72 (1997).

82. Gusarov, I., Shatalin, K., Starodubtseva, M. & Nudler, E. Endogenous nitric oxide protects bacteria against a wide spectrum of antibiotics. Science 325, 1380-1384, doi:10.1126/science.1175439(2009).

83. Xie, Q. W., Kashiwabara, Y. & Nathan, C. Role of transcription factor NF-kappa B/Rel in induction of nitric oxide synthase. J Biol Chem 269, 4705-4708 (1994).

84. Nathan, C. & Xie, Q. W. Nitric oxide synthases: roles, tolls, and controls. Cell 78, 915-918 (1994).

85. Pfeilschifter, J., Eberhardt, W. & Huwiler, A. Nitric oxide and mechanisms of redox signalling: matrix and matrix-metabolizing enzymes as prime nitric oxide targets. Eur J Pharmacol 429, 279-286 (2001).

86. Buchwalow, I. B., Schulze, W., Kostic, M. M., Wallukat, G. & Morwinski, R. Intracellular localization of inducible nitric oxide synthase in neonatal rat cardiomyocytes in culture. Acta Histochem 99, 231-240, doi:10.1016/S0065-1281(97)80046-3 (1997).

87. Buchwalow, I. B. et al. Vascular smooth muscle and nitric oxide synthase. FASEB J 16, 500-508 (2002).

88. Kyle, B. D., Hurst, S., Swayze, R. D., Sheng, J. & Braun, A. P. Specific phosphorylation sites underlie the stimulation of a large conductance, Ca(2+)-activated K(+) channel by cGMP-dependent protein kinase. FASEB J 27, 2027-2038, doi:10.1096/fj.12-223669 (2013).

89. Albrecht, E. W., Stegeman, C. A., Heeringa, P., Henning, R. H. & van Goor, H. Protective role of endothelial nitric oxide synthase. J Pathol 199, 8-17, doi:10.1002/path.1250 (2003).

90. Cooke, J. P. & Dzau, V. J. Derangements of the nitric oxide synthase pathway, L-arginine, and cardiovascular diseases. Circulation 96, 379-382 (1997).

91. Cooke, J. P. & Dzau, V. J. Nitric oxide synthase: role in the genesis of vascular disease. Annu Rev Med 48, 489-509, doi:10.1146/annurev.med.48.1.489 (1997).

92. Zhang, J. et al. Inducible nitric oxide synthase is present in human abdominal aortic aneurysm and promotes oxidative vascular injury. J Vasc Surg 38, 360-367 (2003).

93. Johanning, J. M., Franklin, D. P., Han, D. C., Carey, D. J. & Elmore, J. R. Inhibition of inducible nitric oxide synthase limits nitric oxide production and experimental aneurysm expansion. J Vasc Surg 33, 579-586, doi:10.1067/mva.2001.111805 (2001).

94. Johanning, J. M. et al. Nitric oxide in experimental aneurysm formation: early events and consequences of nitric oxide inhibition. Ann Vasc Surg 16, 65-72, doi:10.1007/s10016-001-0139-z (2002).

95. Lee, J. K., Borhani, M., Ennis, T. L., Upchurch, G. R., Jr. & Thompson, R. W. Experimental abdominal aortic aneurysms in mice lacking expression of inducible nitric oxide synthase. Arterioscler Thromb Vasc Biol 21, 1393-1401 (2001).

96. Lundberg, J. O., Weitzberg, E. & Gladwin, M. T. The nitrate-nitrite-nitric oxide pathway in physiology and therapeutics. Nat Rev Drug Discov 7, 156-167, doi:10.1038/nrd2466 (2008).

97. Yang, H. H., van Breemen, C. & Chung, A. W. Vasomotor dysfunction in the thoracic aorta of Marfan syndrome is associated with accumulation of oxidative stress. Vascul Pharmacol 52, 37-45, doi:10.1016/j.vph.2009.10.005 (2010).

98. Soto, M. E. et al. Participation of oleic acid in the formation of the aortic aneurysm in Marfan syndrome patients. Prostaglandins Other Lipid Mediat 123, 46-55, doi:10.1016/j.prostaglandins.2016.05.001 (2016).

99. Sternlicht, M. D. & Werb, Z. How matrix metalloproteinases regulate cell behavior. Annu Rev Cell Dev Biol 17, 463-516, doi:10.1146/annurev.cellbio.17.1.463 (2001).

100. Mayers, I. et al. Cardiac surgery increases the activity of matrix metalloproteinases and nitric oxide synthase in human hearts. J Thorac Cardiovasc Surg 122, 746-752, doi:10.1067/mtc.2001.116207 (2001).

101. Mayers, I. et al. Increased matrix metalloproteinase activity after canine cardiopulmonary bypass is suppressed by a nitric oxide scavenger. J Thorac Cardiovasc Surg 125, 661-668, doi:10.1067/mtc.2003.38 (2003).

102. Marcet-Palacios, M. et al. Nitric oxide and cyclic GMP increase the expression of matrix metalloproteinase-9 in vascular smooth muscle. J Pharmacol Exp Ther 307, 429-436, doi:10.1124/jpet.103.050385 (2003).

103. O'Sullivan, S., Medina, C., Ledwidge, M., Radomski, M. W. & Gilmer, J. F. Nitric oxide-matrix metaloproteinase-9 interactions: biological and pharmacological significance--NO and MMP-9 interactions. Biochim Biophys Acta 1843, 603-617, doi:10.1016/j.bbamcr.2013.12.006 (2014).

104. Van Doren, S. R. Matrix metalloproteinase interactions with collagen and elastin. Matrix biology : journal of the International Society for Matrix Biology 44-46, 224-231, doi:10.1016/j.matbio.2015.01.005 (2015).

105. Poulos, T. L. Soluble guanylate cyclase. Curr Opin Struct Biol 16, 736-743, doi:10.1016/j.sbi.2006.09.006 (2006).

106. Alberts, B., Durfort Coll, M. & Llobera i Sande, M. Biología molecular de la célula. 4{487} ed edn, (Omega, 2004).

107. Couchman, J. R., Multhaupt, H. & Sanderson, R. D. Recent Insights into Cell Surface Heparan Sulphate Proteoglycans and Cancer. F1000Res 5, doi:10.12688/f1000research.8543.1 (2016).

108. Kinsella, M. G., Bressler, S. L. & Wight, T. N. The regulated synthesis of versican, decorin, and biglycan: extracellular matrix proteoglycans that influence cellular phenotype. Crit Rev Eukaryot Gene Expr 14, 203-234 (2004).

109. Kolodgie, F. D., Burke, A. P., Wight, T. N. & Virmani, R. The accumulation of specific types of proteoglycans in eroded plaques: a role in coronary thrombosis in the absence of rupture. Curr Opin Lipidol 15, 575-582 (2004).

110. Lawrence, E. J. The clinical presentation of Ehlers-Danlos syndrome. Adv Neonatal Care 5, 301-314, doi:10.1016/j.adnc.2005.09.006 (2005).

111. Abraham, P. A., Perejda, A. J., Carnes, W. H. & Uitto, J. Marfan syndrome. Demonstration of abnormal elastin in aorta. J Clin Invest 70, 1245-1252 (1982).

112. Robinson, P. N. & Godfrey, M. The molecular genetics of Marfan syndrome and related microfibrillopathies. J Med Genet 37, 9-25 (2000).

113. Michel, J. B. Anoikis in the cardiovascular system: known and unknown extracellular mediators. Arterioscler Thromb Vasc Biol 23, 2146-2154, doi:10.1161/01.ATV.0000099882.52647.E4 (2003).

114. Carmeliet, P. et al. Urokinase-generated plasmin activates matrix metalloproteinases during aneurysm formation. Nat Genet 17, 439-444, doi:10.1038/ng1297-439 (1997).

115. Galis, Z. S., Sukhova, G. K. & Libby, P. Microscopic localization of active proteases by in situ zymography: detection of matrix metalloproteinase activity in vascular tissue. FASEB J 9, 974-980 (1995).

116. Sung, H. J. et al. Matrix metalloproteinase 9 facilitates collagen remodeling and angiogenesis for vascular constructs. Tissue Eng 11, 267-276, doi:10.1089/ten.2005.11.267 (2005).

117. Stamenkovic, I. Extracellular matrix remodelling: the role of matrix metalloproteinases. J Pathol 200, 448-464, doi:10.1002/path.1400 (2003).

118. Bosman, F. T. & Stamenkovic, I. Functional structure and composition of the extracellular matrix. J Pathol 200, 423-428, doi:10.1002/path.1437 (2003).

119. Edwards, D. R., Handsley, M. M. & Pennington, C. J. The ADAM metalloproteinases. Mol Aspects Med 29, 258-289, doi:10.1016/j.mam.2008.08.001 (2008).

120. Wight, T. N. The ADAMTS proteases, extracellular matrix, and vascular disease: waking the sleeping giant(s)! Arterioscler Thromb Vasc Biol 25, 12-14, doi:10.1161/01.ATV.0000150043.43083.aa (2005).

121. Dancevic, C. M., McCulloch, D. R. & Ward, A. C. The ADAMTS hyalectanase family: biological insights from diverse species. Biochem J 473, 2011-2022, doi:10.1042/BCJ20160148 (2016).

122. Le Goff, C. & Cormier-Daire, V. The ADAMTS(L) family and human genetic disorders. Hum Mol

Genet 20, R163-167, doi:10.1093/hmg/ddr361 (2011).

123. Vazquez, F. et al. METH-1, a human ortholog of ADAMTS-1, and METH-2 are members of a new family of proteins with angio-inhibitory activity. J Biol Chem 274, 23349-23357 (1999).

124. Porter, S., Clark, I. M., Kevorkian, L. & Edwards, D. R. The ADAMTS metalloproteinases. Biochem J 386, 15-27, doi:10.1042/BJ20040424 (2005).

125. Kelwick, R., Desanlis, I., Wheeler, G. N. & Edwards, D. R. The ADAMTS (A Disintegrin and Metalloproteinase with Thrombospondin motifs) family. Genome Biol 16, 113, doi:10.1186/s13059-015-0676-3 (2015).

126. Hubmacher, D. & Apte, S. S. ADAMTS proteins as modulators of microfibril formation and function. Matrix biology : journal of the International Society for Matrix Biology 47, 34-43, doi:10.1016/j.matbio.2015.05.004 (2015).

127. Cecchi, A. et al. Missense mutations in FBN1 exons 41 and 42 cause Weill-Marchesani syndrome with thoracic aortic disease and Marfan syndrome. Am J Med Genet A 161A, 2305-2310, doi:10.1002/ajmg.a.36044 (2013).

128. Cain, S. A., McGovern, A., Baldwin, A. K., Baldock, C. & Kielty, C. M. Fibrillin-1 mutations causing Weill-Marchesani syndrome and acromicric and geleophysic dysplasias disrupt heparan sulfate interactions. PLoS One 7, e48634, doi:10.1371/journal.pone.0048634 (2012).

129. Steinkellner, H. et al. Identification and molecular characterisation of a homozygous missense mutation in the ADAMTS10 gene in a patient with Weill-Marchesani syndrome. Eur J Hum Genet 23, 1186-1191, doi:10.1038/ejhg.2014.264 (2015).

130. Kochhar, A. et al. Similarity of geleophysic dysplasia and Weill-Marchesani syndrome. Am J Med Genet A 161A, 3130-3132, doi:10.1002/ajmg.a.36147 (2013).

131. Spranger, J., Gilbert, E. F., Arya, S., Hoganson, G. M. & Opitz, J. M. Geleophysic dysplasia. Am J Med Genet 19, 487-499, doi:10.1002/ajmg.1320190310 (1984).

132. Le Goff, C. et al. ADAMTSL2 mutations in geleophysic dysplasia demonstrate a role for ADAMTS-like proteins in TGF-beta bioavailability regulation. Nat Genet 40, 1119-1123, doi:10.1038/ng.199 (2008).

133. Bader, H. L. et al. A disintegrin-like and metalloprotease domain containing thrombospondin type 1 motif-like 5 (ADAMTSL5) is a novel fibrillin-1-, fibrillin-2-, and heparin-binding member of the ADAMTS superfamily containing a netrin-like module. Matrix biology : journal of the International Society for Matrix Biology 31, 398-411, doi:10.1016/j.matbio.2012.09.003 (2012).

134. Saito, M. et al. ADAMTSL6beta protein rescues fibrillin-1 microfibril disorder in a Marfan syndrome mouse model through the promotion of fibrillin-1 assembly. J Biol Chem 286, 38602-38613, doi:10.1074/jbc.M111.243451 (2011).

135. Li, S. W. et al. Transgenic mice with inactive alleles for procollagen N-proteinase (ADAMTS-2) develop fragile skin and male sterility. Biochem J 355, 271-278 (2001).

136. Colige, A. et al. Novel types of mutation responsible for the dermatosparactic type of Ehlers-Danlos syndrome (Type VIIC) and common polymorphisms in the ADAMTS2 gene. J Invest Dermatol 123, 656-663, doi:10.1111/j.0022-202X.2004.23406.x (2004).

137. Le Goff, C. et al. Regulation of procollagen amino-propeptide processing during mouse embryogenesis by specialization of homologous ADAMTS proteases: insights on collagen biosynthesis and dermatosparaxis. Development 133, 1587-1596, doi:10.1242/dev.02308 (2006).

138. Khan, A. O. Microcornea with myopic chorioretinal atrophy, telecanthus and posteriorly-rotated ears: a distinct clinical syndrome. Ophthalmic Genet 33, 196-199, doi:10.3109/13816810.2012.681097 (2012).

139. Ataca, D. et al. Adamts18 deletion results in distinct developmental defects and provides a model for congenital disorders of lens, lung, and female reproductive tract development. Biol Open 5, 1585-1594, doi:10.1242/bio.019711 (2016).

140. Chandra, A. et al. Expansion of ocular phenotypic features associated with mutations in ADAMTS18. JAMA Ophthalmol 132, 996-1001, doi:10.1001/jamaophthalmol.2014.940 (2014).

141. Kern, C. B. et al. Reduced versican cleavage due to Adamts9 haploinsufficiency is associated with cardiac and aortic anomalies. Matrix biology : journal of the International Society for Matrix Biology 29, 304-316, doi:10.1016/j.matbio.2010.01.005 (2010).

142. Dupuis, L. E. et al. Altered versican cleavage in ADAMTS5 deficient mice; a novel etiology of myxomatous valve disease. Dev Biol 357, 152-164, doi:10.1016/j.ydbio.2011.06.041 (2011).

143. Kuno, K., Iizasa, H., Ohno, S. & Matsushima, K. The exon/intron organization and chromosomal mapping of the mouse ADAMTS-1 gene encoding an ADAM family protein with TSP motifs. Genomics 46, 466-471, doi:10.1006/geno.1997.5064 (1997).

144. Bourd-Boittin, K. et al. Protease profiling of liver fibrosis reveals the ADAM metallopeptidase with thrombospondin type 1 motif, 1 as a central activator of transforming growth factor beta. Hepatology 54, 2173-2184, doi:10.1002/hep.24598 (2011).

145. Jonsson-Rylander, A. C. et al. Role of ADAMTS-1 in atherosclerosis: remodeling of carotid artery, immunohistochemistry, and proteolysis of versican. Arterioscler Thromb Vasc Biol 25, 180-185, doi:10.1161/01.ATV.0000150045.27127.37 (2005).

146. Xu, Z., Yu, Y. & Duh, E. J. Vascular endothelial growth factor upregulates expression of ADAMTS1 in endothelial cells through protein kinase C signaling. Invest Ophthalmol Vis Sci 47, 4059-4066, doi:10.1167/iovs.05-1528 (2006).

147. Bongrazio, M., Baumann, C., Zakrzewicz, A., Pries, A. R. & Gaehtgens, P. Evidence for modulation of genes involved in vascular adaptation by prolonged exposure of endothelial cells to shear stress. Cardiovasc Res 47, 384-393 (2000).

148. Dolan, J. M., Sim, F. J., Meng, H. & Kolega, J. Endothelial cells express a unique transcriptional profile under very high wall shear stress known to induce expansive arterial remodeling. Am J Physiol Cell Physiol 302, C1109-1118, doi:10.1152/ajpcell.00369.2011 (2012).

149. Iruela-Arispe, M. L., Carpizo, D. & Luque, A. ADAMTS1: a matrix metalloprotease with angioinhibitory properties. Ann N Y Acad Sci 995, 183-190 (2003).

150. Luque, A., Carpizo, D. R. & Iruela-Arispe, M. L. ADAMTS1/METH1 inhibits endothelial cell proliferation by direct binding and sequestration of VEGF165. J Biol Chem 278, 23656-23665, doi:10.1074/jbc.M212964200 (2003).Sandy, J. D. et al. Versican V1 proteolysis in human aorta in vivo occurs at the Glu441-Ala442 bond, a site that is cleaved by recombinant ADAMTS-1 and ADAMTS-4. J Biol Chem 276, 13372-13378, doi:10.1074/jbc.M009737200 (2001).

151. Ren, P. et al. ADAMTS-1 and ADAMTS-4 levels are elevated in thoracic aortic aneurysms and dissections. The Annals of thoracic surgery 95, 570-577, doi:10.1016/j.athoracsur.2012.10.084 (2013).

152. Thai, S. N. & Iruela-Arispe, M. L. Expression of ADAMTS1 during murine development. Mechanisms of development 115, 181-185 (2002).

153. Daugherty, A., Manning, M. W. & Cassis, L. A. Angiotensin II promotes atherosclerotic lesions and aneurysms in apolipoprotein E-deficient mice. J Clin Invest 105, 1605-1612, doi:10.1172/JCI7818 (2000).

154. Kaneko, H. et al. Role of vascular endothelial growth factor-A in development of abdominal aortic aneurysm. Cardiovasc Res 91, 358-367, doi:10.1093/cvr/cvr080 (2011).

155. Touyz, R. M. Intracellular mechanisms involved in vascular remodelling of resistance arteries in hypertension: role of angiotensin II. Exp Physiol 90, 449-455, doi:10.1113/expphysiol.2005.030080 (2005).

156. Bochkov, V. N. et al. Oxidized phospholipids stimulate tissue factor expression in human endothelial cells via activation of ERK/EGR-1 and Ca(++)/NFAT. Blood 99, 199-206 (2002).

157. Holmes, K., Chapman, E., See, V. & Cross, M. J. VEGF stimulates RCAN1.4 expression in endothelial cells via a pathway requiring Ca2+/calcineurin and protein kinase C-delta. PLoS One 5, e11435, doi:10.1371/journal.pone.0011435 (2010).

158. Yao, Y. G. & Duh, E. J. VEGF selectively induces Down syndrome critical region 1 gene expression in endothelial cells: a mechanism for feedback regulation of angiogenesis? Biochem Biophys Res Commun 321, 648-656, doi:10.1016/j.bbrc.2004.06.176 (2004).

159. Wang, H. & Keiser, J. A. Vascular endothelial growth factor upregulates the expression of matrix metalloproteinases in vascular smooth muscle cells: role of flt-1. Circ Res 83, 832-840 (1998).

160. Tedesco, M. M. et al. Analysis of in situ and ex vivo vascular endothelial growth factor receptor expression during experimental aortic aneurysm progression. Arterioscler Thromb Vasc Biol 29, 1452-1457, doi:10.1161/ATVBAHA.109.187757 (2009).

161. Lash, G. E. et al. Localization of angiogenic growth factors and their receptors in the human endometrium throughout the menstrual cycle and in recurrent miscarriage. Hum Reprod 27, 183-195, doi:10.1093/humrep/der376 (2012).

162. Ishida, A. et al. Expression of vascular endothelial growth factor receptors in smooth muscle cells. J Cell Physiol 188, 359-368, doi:10.1002/jcp.1121 (2001).

163. Martinez, G. J. et al. The transcription factor NFAT promotes exhaustion of activated CD8(+) T cells. Immunity 42, 265-278, doi:10.1016/j.immuni.2015.01.006 (2015).

164. Macian, F., Garcia-Rodriguez, C. & Rao, A. Gene expression elicited by NFAT in the presence or absence of cooperative recruitment of Fos and Jun. EMBO J 19, 4783-4795, doi:10.1093/emboj/19.17.4783 (2000).

165. Doyle, K. M., Russell, D. L., Sriraman, V. & Richards, J. S. Coordinate transcription of the ADAMTS-1 gene by luteinizing hormone and progesterone receptor. Mol Endocrinol 18, 2463-2478, doi:10.1210/me.2003-0380 (2004).

166. Zahnow, C. A. CCAAT/enhancer-binding protein beta: its role in breast cancer and associations with receptor tyrosine kinases. Expert Rev Mol Med 11, e12, doi:10.1017/S1462399409001033 (2009).

167. Tsukada, J., Yoshida, Y., Kominato, Y. & Auron, P. E. The CCAAT/enhancer (C/EBP) family of basic-leucine zipper (bZIP) transcription factors is a multifaceted highly-regulated system for gene regulation. Cytokine 54, 6-19, doi:10.1016/j.cyto.2010.12.019 (2011).

168. Pyeritz, R. E. The Marfan syndrome. Annu Rev Med 51, 481-510, doi:10.1146/annurev.med.51.1.481 (2000).

169. Neptune, E. R. et al. Dysregulation of TGF-beta activation contributes to pathogenesis in Marfan syndrome. Nat Genet 33, 407-411, doi:10.1038/ng1116 (2003).

170. Cook, J. R., Carta, L., Galatioto, J. & Ramirez, F. Cardiovascular manifestations in Marfan syndrome and related diseases; multiple genes causing similar phenotypes. Clin Genet 87, 11-20, doi:10.1111/cge.12436 (2015).

171. Laurent, M. A., Bonnier, D., Theret, N., Tuffery, P. & Moroy, G. In silico characterization of the interaction between LSKL peptide, a LAP-TGF-beta derived peptide, and ADAMTS1. Comput Biol Chem 61, 155-161, doi:10.1016/j.compbiolchem.2016.01.012 (2016).

172. Isogai, Z. et al. Versican interacts with fibrillin-1 and links extracellular microfibrils to other connective tissue networks. J Biol Chem 277, 4565-4572, doi:10.1074/jbc.M110583200 (2002).

173. Esteban, V. et al. Regulator of calcineurin 1 mediates pathological vascular wall remodeling. J Exp Med 208, 2125-2139, doi:jem.20110503 [pii]10.1084/jem.20110503.

174. Perrucci, G. L. et al. Vascular smooth muscle cells in Marfan syndrome aneurysm: the broken bricks in the aortic wall. Cell Mol Life Sci, doi:10.1007/s00018-016-2324-9 (2016).

175. Forteza, A. et al. Efficacy of losartan vs. atenolol for the prevention of aortic dilation in Marfan syndrome: a randomized clinical trial. Eur Heart J 37, 978-985, doi:10.1093/eurheartj/ehv575 (2016).

176. Cook, J. R. et al. Dimorphic effects of transforming growth factor-beta signaling during aortic aneurysm progression in mice suggest a combinatorial therapy for Marfan syndrome. Arterioscler Thromb Vasc Biol 35, 911-917, doi:10.1161/ATVBAHA.114.305150 (2015).

177. Campens, L. et al. Intrinsic cardiomyopathy in Marfan syndrome: results from in-vivo and ex-vivo studies of the Fbn1C1039G/+ model and longitudinal findings in humans. Pediatr Res 78, 256-263, doi:10.1038/pr.2015.110 (2015).

178. Soto, M. E. et al. Analysis of oxidative stress enzymes and structural and functional proteins on human aortic tissue from different aortopathies. Oxid Med Cell Longev 2014, 760694, doi:10.1155/2014/760694 (2014).

179. Tan, C. K. et al. SMAD3 deficiency promotes inflammatory aortic aneurysms in angiotensin II-infused mice via activation of iNOS. J Am Heart Assoc 2, e000269, doi:10.1161/JAHA.113.000269 (2013).

180. Karimi, A. & Milewicz, D. M. Structure of the Elastin-Contractile Units in the Thoracic Aorta and How Genes That Cause Thoracic Aortic Aneurysms and Dissections Disrupt This Structure. Can J Cardiol 32, 26-34, doi:10.1016/j.cjca.2015.11.004 (2016).

181. Wu, Z., Ruan, Y., Chang, J., Li, B. & Ren, W. Angiotensin II is related to the acute aortic dissection complicated with lung injury through mediating the release of MMP9 from macrophages. Am J Transl Res 8, 1426-1436 (2016).

182. Segura, A. M. et al. Immunohistochemistry of matrix metalloproteinases and their inhibitors in thoracic aortic aneurysms and aortic valves of patients with Marfan's syndrome. Circulation 98, II331-337; discussion II337-338 (1998).

183. Girardi, L. N. & Coselli, J. S. Inflammatory aneurysm of the ascending aorta and aortic arch. The Annals of thoracic surgery 64, 251-253 (1997).

184. Roth, M., Lemke, P., Bohle, R. M., Klovekorn, W. P. & Bauer, E. P. Inflammatory aneurysm of the ascending thoracic aorta. J Thorac Cardiovasc Surg 123, 822-824 (2002).

185. Lindsay, M. E. & Dietz, H. C. Lessons on the pathogenesis of aneurysm from heritable conditions. Nature 473, 308-316, doi:10.1038/nature10145 (2011).

186. Gao, Y. et al. A disintegrin and metalloproteinase with thrombospondin motif 1 (ADAMTS1) expression increases in acute aortic dissection. Sci China Life Sci 59, 59-67, doi:10.1007/s11427-015-4959-4 (2016).

187. Canals, F., Colome, N., Ferrer, C., Plaza-Calonge Mdel, C. & Rodriguez-Manzaneque, J. C. Identification of substrates of the extracellular protease ADAMTS1 by DIGE proteomic analysis. Proteomics 6 Suppl 1, S28-35, doi:10.1002/pmic.200500446 (2006).

188. Partovian, C., Ju, R., Zhuang, Z. W., Martin, K. A. & Simons, M. Syndecan-4 regulates subcellular localization of mTOR Complex2 and Akt activation in a PKCalpha-dependent manner in endothelial cells. Mol Cell 32, 140-149, doi:10.1016/j.molcel.2008.09.010 (2008).

189. Kleinert, H., Schwarz, P. M. & Forstermann, U. Regulation of the expression of inducible nitric oxide synthase. Biol Chem 384, 1343-1364, doi:10.1515/BC.2003.152 (2003).

190. Tang, C. H., Lu, D. Y., Tan, T. W., Fu, W. M. & Yang, R. S. Ultrasound induces hypoxia-inducible factor-1 activation and inducible nitric-oxide synthase expression through the integrin/integrin-linked kinase/Akt/mammalian target of rapamycin pathway in osteoblasts. J Biol Chem 282, 25406-25415, doi:10.1074/jbc.M701001200 (2007).

191. Li, W. et al. Tgfbr2 disruption in postnatal smooth muscle impairs aortic wall homeostasis. J Clin Invest 124, 755-767, doi:10.1172/JCI69942 (2014).

192. Hung, C. M., Garcia-Haro, L., Sparks, C. A. & Guertin, D. A. mTOR-dependent cell survival mechanisms. Cold Spring Harb Perspect Biol 4, doi:10.1101/cshperspect.a008771 (2012).

192. Liao, M. F. et al. Role of nitric oxide and inducible nitric oxide synthase in human abdominal aortic aneurysms: a preliminary study. Chin Med J (Engl) 119, 312-318 (2006).

193. Sadamasa, N., Nozaki, K. & Hashimoto, N. Disruption of gene for inducible nitric oxide synthase reduces progression of cerebral aneurysms. Stroke 34, 2980-2984, doi:10.1161/01.STR.0000102556.55600.3B (2003).

194. Fukuda, S. et al. Prevention of rat cerebral aneurysm formation by inhibition of nitric oxide synthase. Circulation 101, 2532-2538 (2000).

195. De Backer, J. et al. Marfan Syndrome and Related Heritable Thoracic Aortic Aneurysms and Dissections. Curr Pharm Des 21, 4061-4075 (2015).

196. Franken, R. et al. Beneficial Outcome of Losartan Therapy Depends on Type of FBN1 Mutation in Marfan Syndrome. Circ Cardiovasc Genet 8, 383-388, doi:10.1161/CIRCGENETICS.114.000950 (2015).

197. Franken, R. & Mulder, B. J. Aortic disease: Losartan versus atenolol in the Marfan aorta-how to treat? Nat Rev Cardiol 12, 447-448, doi:10.1038/nrcardio.2015.95 (2015).

198. Milleron, O. et al. Marfan Sartan: a randomized, double-blind, placebo-controlled trial. Eur HeartJ 36, 2160-2166, doi:10.1093/eurheartj/ehv151 (2015).

199. Lacro, R. V. et al. Atenolol versus losartan in children and young adults with Marfan's syndrome. N Engl J Med 371, 2061-2071, doi:10.1056/NEJMoa1404731 (2014).

200. Mittaz, L. et al. Adamts1 is essential for the development and function of the urogenital system. Biol. Reprod. 70, 1096–1105 (2004).

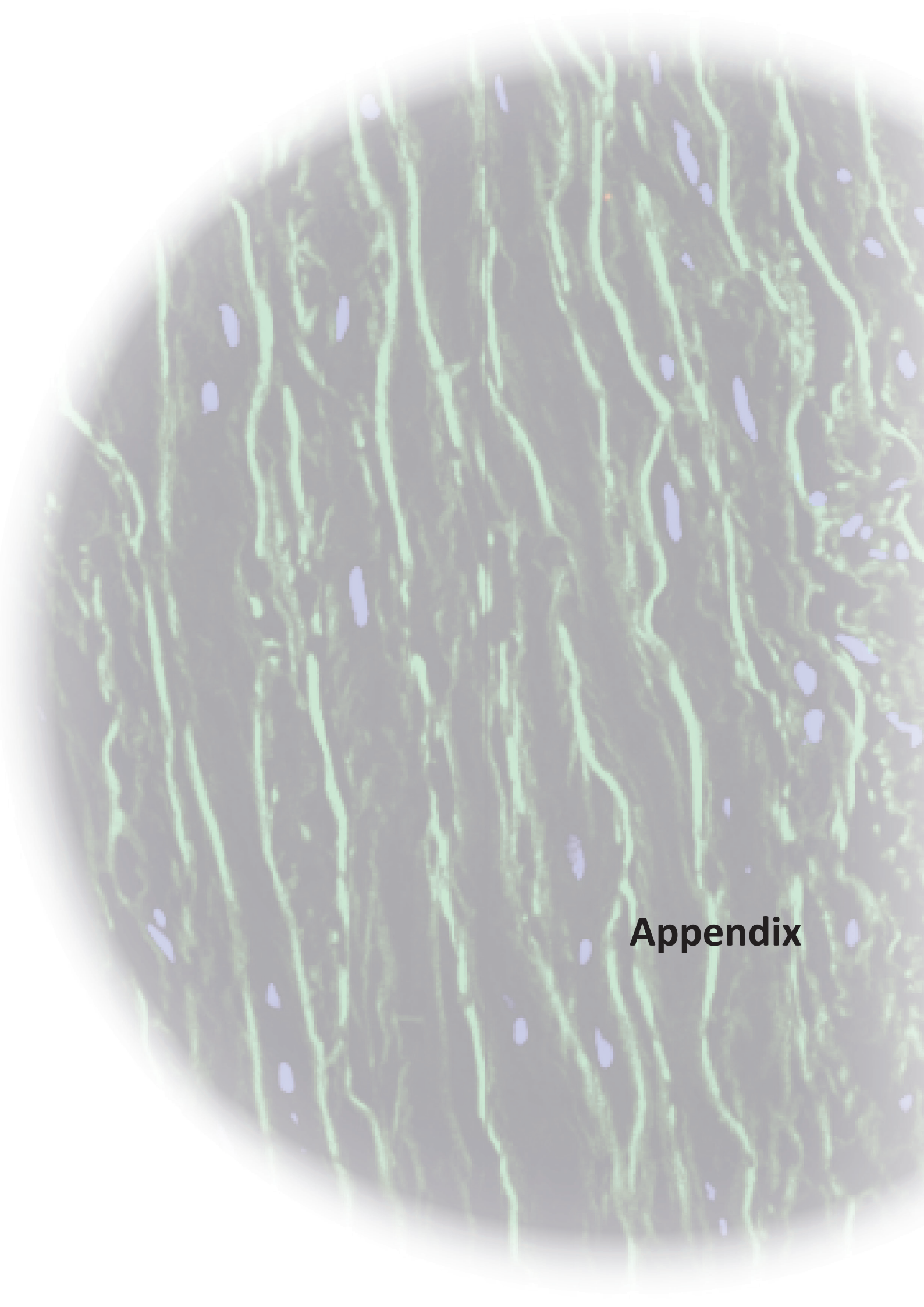

Appendix

Artículo 3: Plasma Membrane Calcium ATPase Isoform 4 Inhibits Vascular Endothelial Growth Factor–Mediated Angiogenesis Through Interaction With Calcineurin

Autores: Rhiannon R. Baggott, Arantzazu Alfranca, Dolores López-Maderuelo, Tamer M.A. Mohamed, Amelia Escolano, **Jorge Oller,** Beatriz C. Ornes, Sathishkumar Kurusamy, Farjana B. Rowther, James E. Brown, Delvac Oceandy, Elizabeth J. Cartwright, Weiguang Wang, Pablo Gómez-del Arco, Sara Martínez-Martínez, Ludwig Neyses, Juan Miguel Redondo, Angel Luis Armesilla.

Publicado en: *Arteriosclerosis, Thrombosis and Vascular Biology*, Agosto 2014.

Resumen:

La angiogénesis es la formación de nuevos capilares sanguíneos a partir de vasos preexistentes. Este proceso fisiológico es esencial para el desarrollo embrionario adecuado, el crecimiento de órganos y la reparación de tejidos. Un crecimiento anormal de los vasos sanguíneos, causado por la desregulación de este proceso, juega un papel crítico en la fisiopatología de varias enfermedades humanas. El factor de Crecimiento Endotelial Vascular (VEGF) y su receptor de tirosina-Kinasa (VEGF-R), han sido identificados como reguladores cruciales tanto de la angiogénesis fisiológica como patológica. VEGF activa a varias vías de transducción de señales intracelulares que desencadenan el proceso angiogénico. Entre ellos, se encuentra el eje de señalización de CN/NFAT. Nuestro laboratorio había descrito previamente que la vía de CN/NFAT es clave para la angiogénesis dependiente de VEGF. Además, la estimulación de VEGF en células endoteliales produce un pico transitorio en la concentración de calcio intracelular que desencadena en la activación de CN y la desfosforilación de NFAT, su posterior translocación al núcleo y unión a sitios específicos del DNA. De esta manera se produce la transcripción de genes diana clave en la angiogénesis como son el *Rcan1.4* y *Cox-2*.

Por otra parte, habíamos identificado una nueva interacción inhibitoria entre las proteínas de membrana plasmática con actividad de calcio-ATPasa (PMCA) y CN. Las proteínas PMCAs son bombas de calcio de alta afinidad que extruyen el calcio del citosol al medio extracelular. En humanos las proteínas PMCA están codificadas por 4 genes independientes denominados PMCA1 a 4. PMCA1 y 4 se expresan de manera ubicua, mientras que la expresión de PMCA2 y 3 está restringida a células y tejidos específicos. Aunque anteriormente se había descrito la unión de PMCA con CN en ECs, la importancia funcional de esta interacción en la fisiopatología endotelial era desconocida. En este trabajo demostramos que la interacción entre PMCA4 y CN altera la motilidad de las células endoteliales y la formación de vasos sanguíneos en respuesta a la estimulación de VEGF. Atribuimos que el efecto angio-inhibidor de PMCA4 a la acción bloqueadora del eje CN/NFAT y la posterior regulación negativa de *RCAN1.4* y *Cox-2*.

Aportación Personal al trabajo: He participado en parte de los experimentos de matrigel *in vivo*, y ensayos con células endoteliales *in vitro*.

Artículo 4: Plk1 regulates contraction of postmitotic smooth muscle cells and vascular homeostasis

Autores: Guillermo de Cárcer, Paulina Wachowicz, Sara Martínez-Martínez, **Jorge Oller**, Nerea Méndez-Barbero, Beatriz Escobar, Alejandra González, Tohru Takaki, Aisha El Bakkali, Juan Antonio Cámara, Luis J. Jiménez-Borreguero, Xosé Bustelo, Marta Cañamero, Francisca Mulero, María de los Ángeles Sevilla, María Jose Montero, Juan Miguel Redondo y Marcos Malumbres.

Publicado en: *Nature Medicine, AIP, accepted in principle (Decision 27 April 2017)*

Resumen:

Actualmente apenas se conoce los mecanismos moleculares involucrados en el desarrollo de aneurismas aórticos. Por otra parte, existe un gran esfuerzo en el desarrollo de fármacos para tratar tumores cuya estrategia está dirigida en inhibir la actividad enzimática de proteínas involucradas en el ciclo celular, sobre todo de kinasas. La proteína polo kinasa-1 (Plk1) es una proteína esencial que desempeña múltiples funciones en la maduración y separación del centrosoma, la replicación del DNA, la segregación cromosómica y la citocinesis. Sin embargo, los papeles de esta kinasa se han caracterizado principalmente en sistemas celulares y su relevancia fisiológica en mamíferos es desconocida. A pesar de esta falta de conocimiento, la sobreexpresión de PLK1 y su valor pronóstico en tumores humanos, ha conllevado al desarrollo de una serie de inhibidores específicos que actualmente están bajo ensayos clínicos en cáncer. Uno de estos inhibidores, el volasertib (BI6727), ha recibido recientemente la aprobación de su uso en clínica por la agencia del medicamento de Estados Unidos debido a su efecto terapéutico en Leucemia Mieloide Aguda (LMA).

En este trabajo, hemos caracterizado el fenotipo vascular en dos modelos de ratón deficientes en Plk1: en heterocigosis *(Plk1$^{+/-}$)* y en ratones deficientes de manera específica para el músculo liso (*SM-Plk1$^{Flox/Flox}$)*. En ambos modelos no hemos encontrado defectos evidentes en tejidos proliferativos pero inesperadamente, poseen alteraciones graves en la estructura arterial. De hecho, hemos observado que un gran porcentaje de los animales *Plk1$^{+/-}$* mueren en el primer año de vida debido a disecciones aórticas. Además, hemos encontrado que Plk1 se expresa en células post-mitóticas de músculo liso vascular (VSMCs). Hemos comprobado que las células deficientes químicamente o genéticamente en Plk1 poseen una activación inadecuada de RhoA, por lo tanto, hemos concluido que esta proteína posee una función crítica para la contractilidad del músculo liso vascular. Estos resultados tienen una implicación clínica relevante sobre las estrategias terapéuticas actuales con inhibidores Plk1 ya que el propio volasertib junto con angiotensina producen aneurismas y disecciones aórticas. Este efecto no deseado tendría que tenerse en cuenta en un futuro en los pacientes tratados con este fármaco.

Aportación Personal al trabajo: He participado en la caracterización fenotípica vascular de los ratones *Plk1$^{+/-}$, SM-Plk1$^{Flox/Flox}$,* y animales de tipo silvestre tratados con volasertib; tanto a nivel histológico como por imagen de ultrasonidos. Además he participado en parte del diseño de los experimentos y en la escritura del artículo.